AUTOMOTIVE FUEL ECONOMY

AND

EMISSIONS PROGRAM
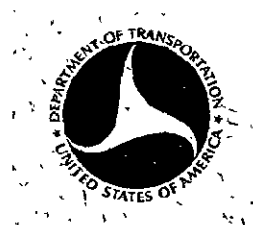
Mack W. Dowdy

Ronald L. Baisley

JUNE 1978

FINAL REPORT

THIS DOCUMENT IS AVAILABLE TO THE U.S.
PUBLIC THROUGH THE NATIONAL TECHNICAL
INFORMATION SERVICE, SPRINGFIELD,
VIRGINIA 22161

Prepared for

U.S. DEPARTMENT OF TRANSPORTATION

Office of the Secretary
Office of the Assistant Secretary for
Systems Development and Technology
Office of Systems Engineering
Washington DC 20590

By
Jet Propulsion Laboratory
California Institute of Technology
Pasadena, California
(JPL Publication 78-21)

NOTICES

This document was prepared by the Jet Propulsion Labor-
atory, California Institute of Technology, and was spon-
sored by the U. S. Department of Transportation through
their Reimbursable Agreement No. RA75-41 with NASA.

This document is disseminated under the sponsorship of
the Department of Transportation in the interest of
information exchange. The United States Government
assumes no liability for the contents or use thereof.

The United States Government does not endorse products
or manufacturers. Trade or manufacturer's names appear
herein solely because they are considered essential to
the object of this report.

1. Report No.	2. Government Accession No.	3. Recipient's Catalog No.
4. Title and Subtitle AUTOMOTIVE FUEL ECONOMY AND EMISSIONS PROGRAM		**5. Report Date** June 1978
		6. Performing Organization Code
7. Author(s) Mack W. Dowdy and Ronald L. Baisley		**8. Performing Organization Report No.** JPL Publication 78-21
9. Performing Organization Name and Address Jet Propulsion Laboratory* 4800 Oak Grove Drive Pasadena CA 91103		**10. Work Unit No. (TRAIS)**
		11. Contract or Grant No. RA 75-41
		13. Type of Report and Period Covered
12. Sponsoring Agency Name and Address U. S. Dept. of Transportation, Office of the Secretary, Office of the Assistant Secretary for Systems Development and Technology, Office of Systems Engineering, Washington DC 20590		Final Report June 1975 - Dec 1976
		14. Sponsoring Agency Code

15. Supplementary Notes

*Under contract to: U. S. Department of Transportation
Transportation Systems Center, Kendall Square
Cambridge MA 02142

16. Abstract

The purpose of this effort was to generate experimental data to support an assessment of the relationship between automobile fuel economy and emissions control systems. Tests were made at both the engine and vehicle levels. Detailed investigations were made on cold-start emissions devices, exhaust gas recirculation systems, and air injection reactor systems. Based on the results of engine tests, an alternative emission control system and modified control strategy were implemented and tested in the vehicle. With the same fuel economy and NO_x emissions as the stock vehicle, the modified vehicle reduced HC and CO emissions by about 20 percent. By removing the NO_x emissions constraint, the modified vehicle demonstrated about 12 percent better fuel economy than the stock vehicle.

17. Key Words Automobiles Fuel Economy Exhaust Emissions	18. Distribution Statement Document is available to the public through the National Technical Information Service, Springfield, Virginia 22161.

19. Security Classif. (of this report) UNCLASSIFIED	20. Security Classif. (of this page) UNCLASSIFIED	

Form DOT F 1700.7 (8-72)

CONTENTS

Preceding page blank

CONTENTS (contd)

SECTION I

INTRODUCTION

The influence of automotive engine emission controls on vehicle fuel economy has been a controversial issue since the advent of stringent Federal Emission Standards. To prevent further deterioration of the air environment, especially in urban areas, it seems likely that still more stringent controls on automobile emissions will be required in the future. Recent experience with the Arab oil embargo has dramatically shown the national need for developing alternative fuels and practicing energy conservation. These somewhat conflicting needs have placed additional emphasis on the need for a thorough understanding of the interactions between automobile fuel economy and emission control.

The primary objective of this effort was to generate experimental data to support an assessment of the relationship between automobile fuel economy and emission control systems. To provide a more complete understanding of this interaction, tests at both the engine and vehicle levels were included. The effort was concentrated on a detailed investigation of three emission control systems: cold start emissions devices, exhaust gas recirculation (EGR) systems, and air injection reactor (AIR) systems. Based on literature information, analyses and experimental data, these emission reduction techniques were evaluated to establish the potential for improving the fuel economy/emissions of the stock vehicle. Using these evaluations, an alternative emission control system was implemented, tested, and compared with the stock system.

Within the limited resources of this effort, it was not possible to obtain results for more than one vehicle; however, detailed data on one vehicle with a particular engine/emission control system does provide a foundation on which to make future projections of fuel economy.

The primary activities covered in this effort were as follows:

(1)   Vehicle selection and preparation.

(2)   Baseline engine and vehicle tests.

(3)   Evaluation of cold-start emissions devices.

(4)   Evaluation of EGR system.

(5)   Evaluation of AIR system.

(6)   Development and implementation of improved control strategies.

(7)   Completion of modified vehicle tests.

1

SECTION II

STOCK VEHICLE

SELECTION AND PREPARATION

Care was exercised in selecting a vehicle for this evaluation to insure
that the fuel economy and emissions results would be meaningful. The vehicle
selected was a 1975 Plymouth Valiant with the 6-cylinder engine. In EPA-
certified tests this vehicle/engine combination gave a fuel economy in the
Federal urban and highway driving cycles which was among the best achieved in
the 3500 lb inertia weight class as shown in Figures 1 - 3. By selecting a
vehicle from among the best fuel economy vehicles, any positive results
achieved during the program become more meaningful. A vehicle in the 3500 lb
inertia weight class was chosen since lighter vehicles seem to be the trend
of the future. The vehicle also came equipped in California with the emission
control system (exhaust catalyst, EGR, and AIR) which was necessary for this
evaluation.

Prior to the start of the break-in period, the vehicle was tuned to
factory specifications. The vehicle ran erratically and was returned to the
dealer for correction of the problem, which was identified as an EGR control
problem. Corrections were made; however, the same problem reappeared after
less than 100 miles of driving. To avoid any further delays, the EGR system
was disconnected and the break-in of the vehicle was completed. The vehicle
was driven approximately 4000 road miles with the EGR system inoperative.
Upon completion of the break-in period, the vehicle was returned to the dealer

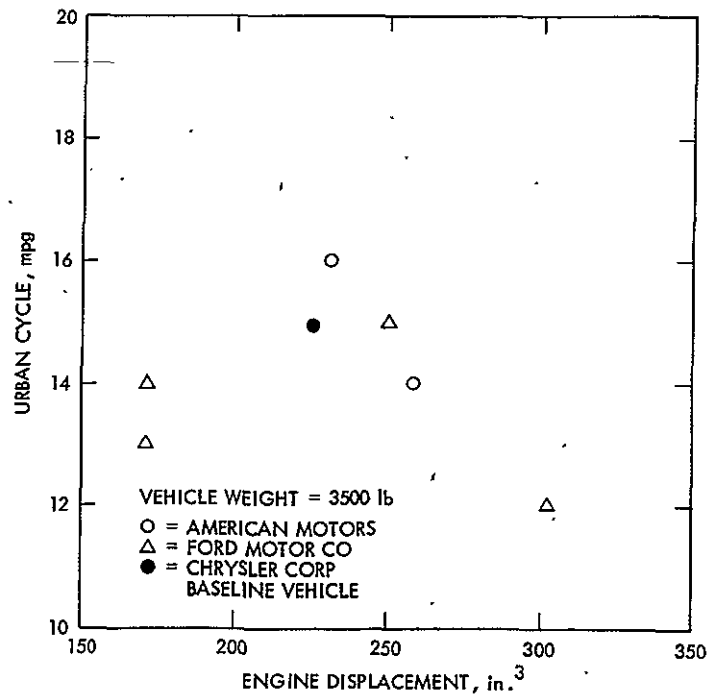Figure 1. Urban Fuel Economy for 1975 California Vehicles - Ref. 1
(Only vehicles with catalyst, EGR, and AIR are included.)
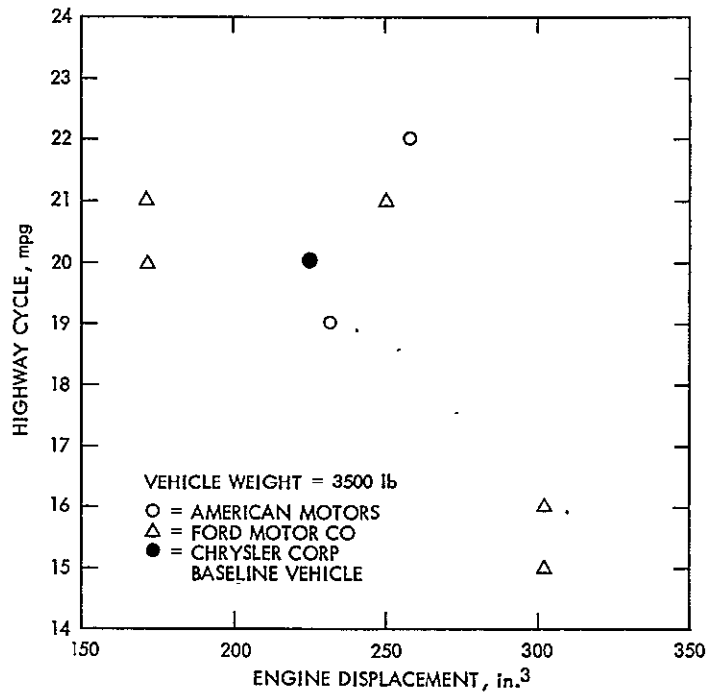
2

Figure 2.   Highway Fuel Economy for 1975 California Vehicles - Ref. 1
            (Only vehicles with catalyst, EGR, and AIR are included.)
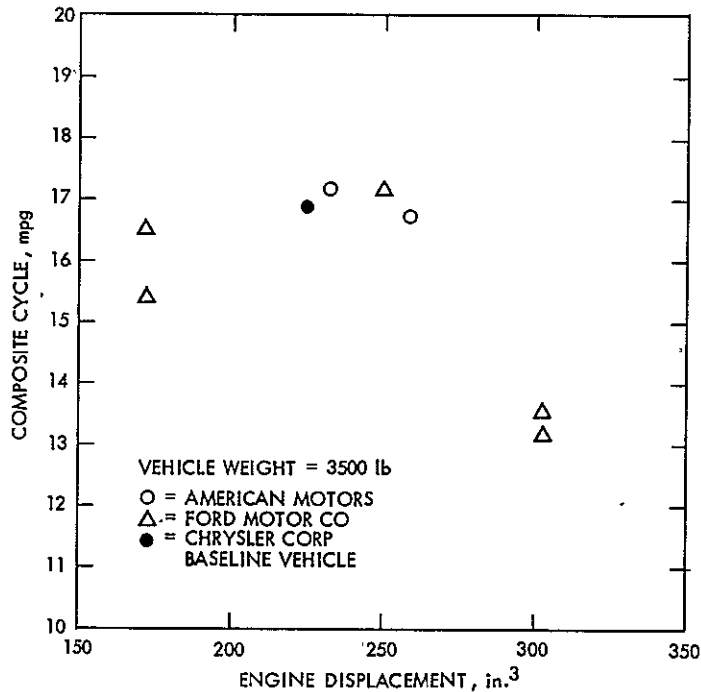

. Figure 3.   Composite Fuel Economy for 1975 California Vehicles - Ref. 1
              (Only vehicles with catalyst, EGR, and AIR are included.)

3

for another tune-up to factory specifications. Again the dealer attempted to correct the EGR control problem; however, the same problem reappeared before the baseline vehicle tests could be run. The vehicle was then taken to the Chrysler Emissions Laboratory in Santa Fe Springs, California for resolution of the EGR problem and another tune-up. This action corrected the EGR problem and permitted the start of baseline tests.

GENERAL DESCRIPTION

As described in the previous section, a 1975 Plymouth Valiant with the 6-cylinder engine was selected for evaluation. The baseline engine is a 225 cubic inch displacement (CID) engine with the slant-6 design. Factory specifications for this engine/vehicle are given in Table 1.

The stock ignition system is the standard breaker point type consisting of a coil, condenser, distributor, wiring, and spark plugs. The spark advance characteristic is determined by the 0° BTDC basic advance and the contributions of the centrifugal and vacuum advance mechanisms. The centrifugal and vacuum advance characteristics were measured on a Sun distributor machine and are given in Figure 4.

Factory-installed devices for emission control include a catalytic converter, an air injection reactor (AIR) pump, an exhaust gas recirculation (EGR) system, and a positive crankcase ventilation (PCV) system. The catalytic converter is used to oxidize the unburned hydrocarbons (HC) and carbon monoxide (CO) in the engine exhaust system. The AIR pump introduces excess air into the exhaust manifold to promote conversion of HC and CO in the catalytic converter. The EGR system recirculates a portion of the exhaust gases to a region directly

Table 1.   Stock Vehicle Specifications

|	
Vehicle	1975 Plymouth Valiant
Engine	Slant-6 (6 cylinders)
Type	In-line overhead valve
Bore	3.40 in.
Stroke	4.125 in.
Displacement	225 cu in.
Compression ratio	8.40
Advertised hp	100 @ 3600 RPM
Advertised torque	170 ft-lb @ 1600 RPM
Carburetor	Holley Model 1945 1-barrel carburetor
Fuel pump	Carter Model MS-4844S (diaphragm type)
Spark plugs	Champion BL13Y
Firing order	1-5-3-6-2-4
Emissions devices	Air injection reactor
	Exhaust gas recirculation
	Positive crankcase ventilation
	Catalytic converter
Transmission	Torque Flite
Gear ratios	First - 2.45
	Intermediate - 1.45
	High - 1.00
Rear axle ratio	2.76

4
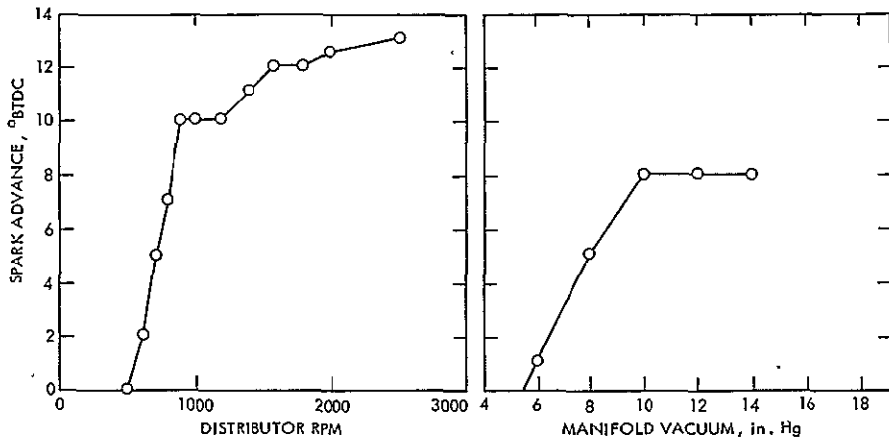
Figure 4. Spark Advance Curves for Distributor No. 3874082

below the carburetor throttle plates. These exhaust gases dilute the incoming charge, resulting in lower peak combustion temperatures and less NO_x emissions. The PCV system maintains a positive flow of crankcase blow-by gases into the engine intake system. Detailed descriptions of the emissions control system for the stock vehicle can be found in Ref. 2.

EGR SYSTEM

The Plymouth 6-cylinder engine for California automobiles uses EGR to control nitrogen oxide (NO_x) emissions. A schematic of the elements of the EGR system is shown in Figure 5. The amount of exhaust gas which flows from the exhaust manifold to the intake manifold is controlled by the position of the poppet in the EGR valve. The position of the poppet is determined by the difference in pressure between intake and exhaust manifolds and by the vacuum supplied to a vacuum diaphragm attached to the poppet. In an attempt to make EGR proportional to engine air flow, the vacuum control signal is taken from the carburetor venturi. This control signal is then amplified by a vacuum amplifier which also senses intake manifold pressure. The vacuum signal from the vacuum amplifier is supplied to the vacuum diaphragm for controlling the poppet position in the EGR valve.

Under some engine operating conditions, it is desirable to have no EGR. When the engine is idling, there is insufficient air flow to activate the EGR valve. At wide-open-throttle (WOT), conditions, manifold vacuum is dumped into the carburetor venturi vacuum signal by the dump valve in the vacuum amplifier. This limits the vacuum signal to manifold vacuum, which is quite low at WOT. The EGR valve is calibrated such that this vacuum is insufficient to open the valve, thus preventing any EGR flow at WOT. EGR is also eliminated when the coolant control exhaust gas recirculation (CCEGR) valve indicates a coolant outlet temperature less than 65°F.

The EGR delay solenoid is activated by the starter solenoid and interrupts the vacuum signal between the intake manifold and the vacuum amplifier during cranking. The EGR delay timer deactivates this EGR delay solenoid after 35 seconds of operation. The effect is to preclude EGR during cranking and for 35 seconds thereafter to assure reliable engine starting and operation immediately after starting.

5

FROM
EXHAUST
MANIFOLD

TO
INTAKE
MANIFOLD

EGR
VALVE

CARBURETOR
VENTURI

INTAKE
MANIFOLD

EGR
DELAY
SOLENOID

VACUUM
AMPLIFIER

VACUUM
DIAPHRAGM

TIME
DELAY
SWITCH

WATER
TEMPERATURE
VALVE

Figure 5.   EGR System Schematic

TO ATMOSPHERE

FROM
ATMOSPHERE

AIR
PUMP

DIVERTER
VALVE

CHECK
VALVE

AIR INJECTION
MANIFOLD

TO EACH EXHAUST PORT
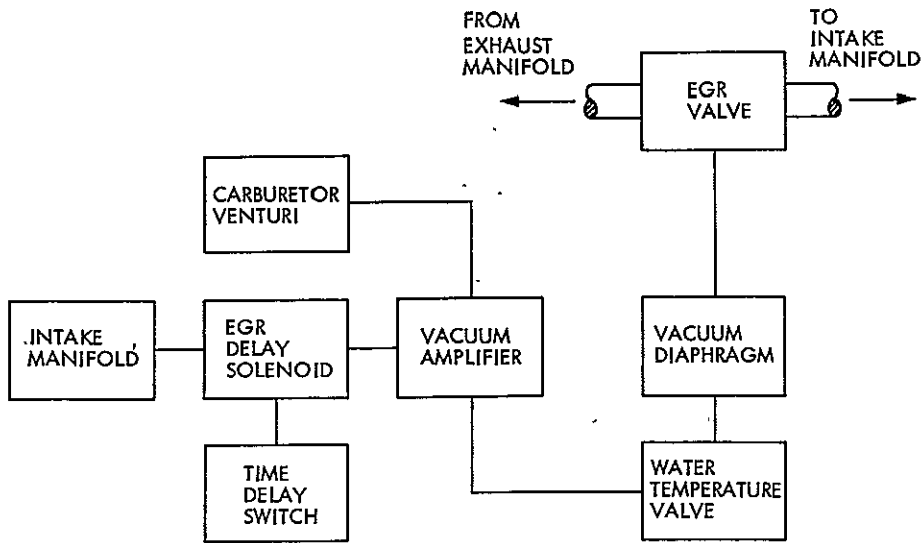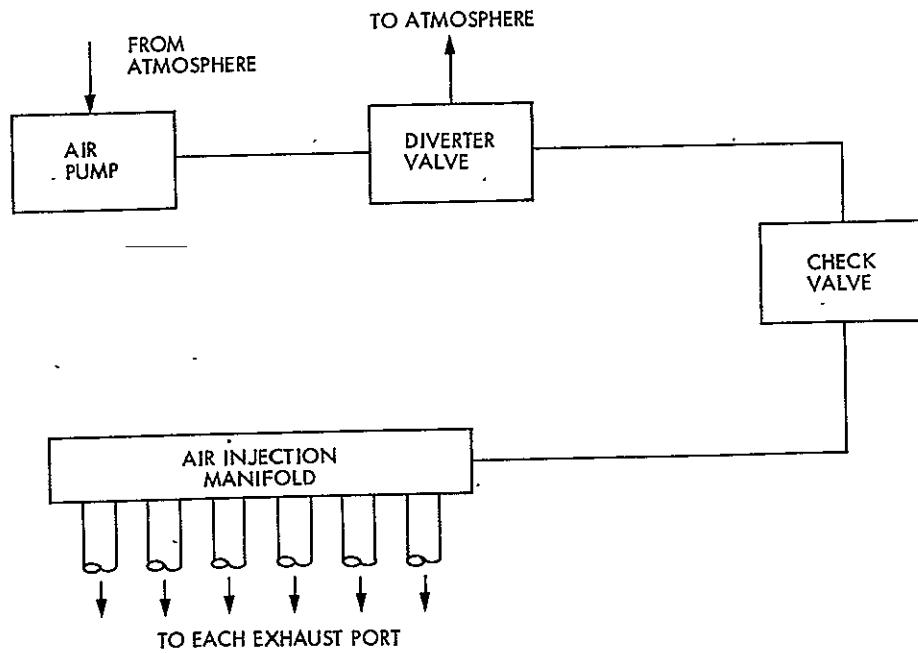
Figure 6.   AIR System Schematic

6

AIR SYSTEM

Exhaust-port air injection is used to provide excess air for oxidation of unburned hydrocarbons and carbon monoxide in the catalytic converter. A schematic of the elements of the air injection reactor (AIR) system is shown in Figure 6. The belt-driven air pump is mounted at the front of the engine with power take-off at the crankshaft pulley. Intake air passes through a centrifugal fan at the center of the pump, where foreign materials are separated from the air by centrifugal force. The pump is a self-lubricating sliding vane centrifugal compressor.

Air from the pump is delivered through a rubber hose to the air injection manifold which is cast into the cylinder head. The air injection manifold routes the compressed air to each of the exhaust ports. A check valve is located in the injection tube assembly that leads to the rear of the cylinder head. This valve has a one-way diaphragm which prevents hot exhaust gases from backing up into the rubber hose and pump.

A diverter valve located at the rear of the air pump housing diverts the output of the air pump to the atmosphere through a silencer. During sudden throttle closing, valve action prevents exhaust system backfires. Intake manifold vacuum greater than some preset value causes the diverter valve to open linearly with vacuum. A waste gate is an integral part of the diverter valve. When the air pump output pressure reaches some preset value, the waste gate allows any excess pressure to be bled off through the silencer.

CATALYTIC CONVERTER

A catalytic converter is used to oxidize hydrocarbons and carbon monoxide in the engine exhaust system. The converter consists of a stainless steel shell which contains two ceramic monolithic elements. These elements are coated with a platinum/palladium catalyst. Unleaded fuel must be used to prevent catalyst poisoning. Special heat shields are used to protect under-body and components from excessive heat.

The throttle position solenoid is activated by the electronic speed switch when engine speed is above 2000 RPM, preventing the throttle from completely closing. This minimizes unburned hydrocarbons during high speed decelerations which might otherwise overheat the converter causing the ceramic monolith to melt.

COLD-START EMISSIONS SYSTEM

The California Plymouth with the 6-cylinder engine is equipped with a number of devices which are designed to reduce exhaust emissions during engine warm-up. This cold-start emissions system includes the heated air inlet system, intake manifold hot spot, cold enrichment system, EGR system, and the evaporative control system. A block diagram of this system is shown in Figure 7.

Heated Air Inlet System

Inlet air to the carburetor is preheated to permit leaner carburetor calibration for hydrocarbon control, improve engine warm-up characteristics and minimize carburetor icing.

7

ENGINE BLOCK COOLANT

UNDER-HOOD AIR

CCIE VALVE

(OPEN WHEN T<98°F)

CONTROLLED LEAK

VACUUM DIAPHRAGM

TEMPERATURE SENSOR

UNDER-HOOD AIR

AIR CONTROL VALVE

AIR CLEANER

HEATED AIR FROM AROUND EXHAUST MANIFOLD

(MAINTAINS T AT TEMP SENSOR IN AIR CLEANER BETWEEN 80°F AND 95° F)

CHOKE

IDLE ENRICHMENT VALVE

VACUUM DIAPHRAGM

THERMOSTATIC CHOKE COIL

CARBURETOR

CONTROL SWITCH

ELECTRIC ASSIST HEATING ELEMENT

IGNITION SWITCH

INTAKE MANIFOLD

TO ENGINE

UPPER RADIATOR COOLANT

HEAT CONTROL VALVE

THERMOSTATIC COIL

HOT SPOT

TIME DELAY SWITCH

(35 SECOND DELAY AFTER ENGINE START)

TO EXHAUST MANIFOLD

FROM EXHAUST MANIFOLD

CCEGR VALVE

EGK SOLENOID VALVE

INTAKE MANIFOLD

(NORMALLY OPEN VALVE)

CLOSED FOR COOLANT T<65°F

TO INTAKE MANIFOLD

VACUUM AMPLIFIER
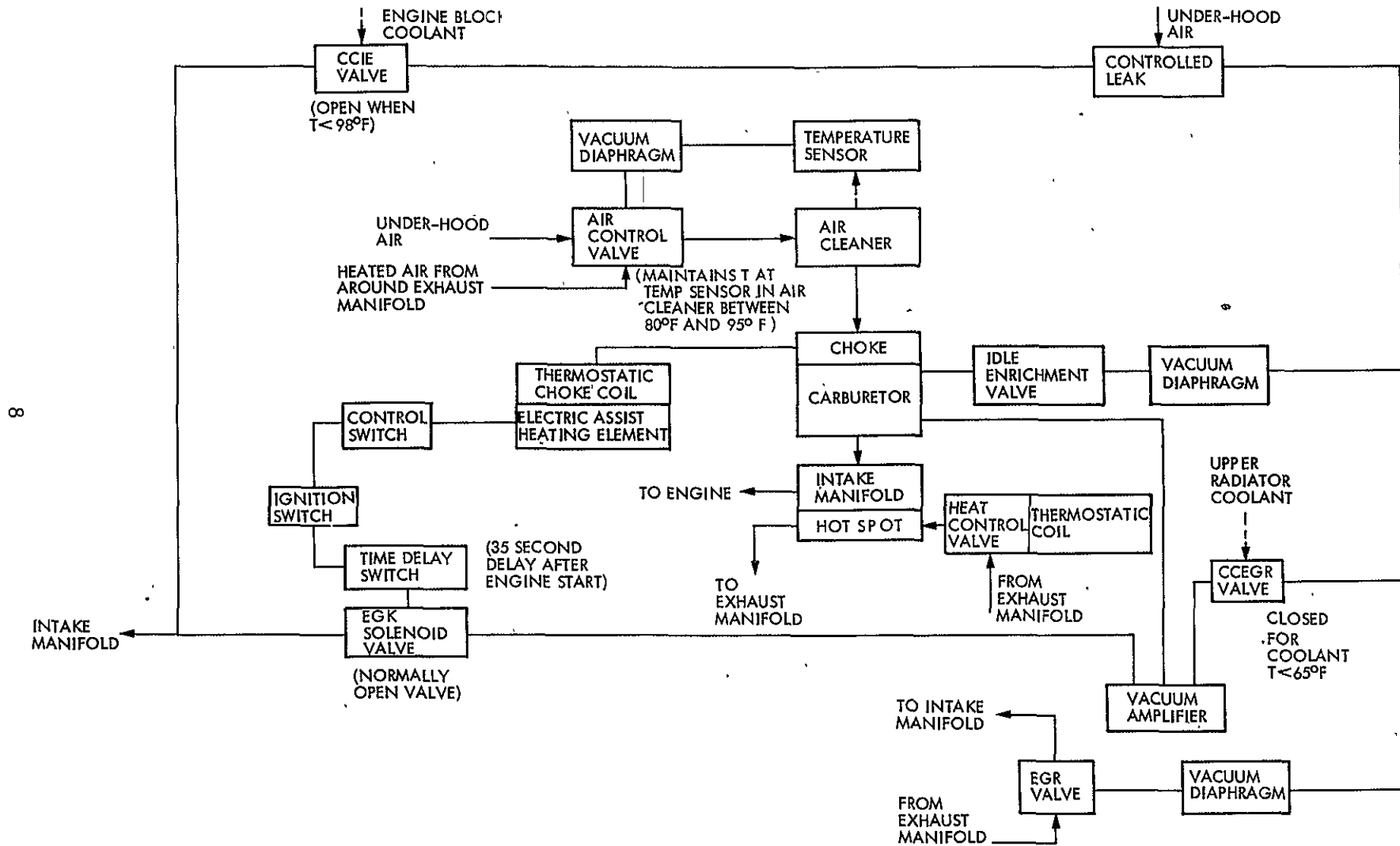
EGR VALVE

VACUUM DIAPHRAGM

FROM EXHAUST MANIFOLD

8

Figure 7. Stock Cold-Start System for 1975 6-Cylinder Plymouth

The heated air system is basically a two-circuit air flow system. When the under-hood air temperature is 10°F or lower, carburetor intake air flows between the exhaust manifold and a metal shield and picks up exhaust heat. The heated air then flows through a flexible line into the adapter on the bottom of the snorkel and into the carburetor. When the under-hood air temperature is above 90°F, the air flows directly through the snorkel.

When the under-hood air temperature is between 10°F and 90°F, air flows through both circuits after the engine has been started. The quantity of air through each circuit is controlled by a vacuum-operated heat control door in the snorkel to maintain a temperature of 85° to 95°F at the temperature sensor mounted inside the air cleaner housing.

When engine vacuum is below some preset value, a return spring over-powers the vacuum-operated heat control door and only unheated air enters the carburetor.

Intake Manifold Hot Spot

A thermostatically-controlled heat control valve is located in the exhaust manifold. During the engine warm-up period, the valve directs hot exhaust gases to the heat chamber (hot spot) in the intake manifold beneath the carburetor to help vaporize the fuel mixture.

Cold Enrichment

The cold enrichment system provides cold idle enrichment whenever the engine block coolant valve indicates that engine block temperature is below 98°F. A small vacuum-controlled diaphragm mounted near the top of the carburetor controls idle system air. When control vacuum is applied to the diaphragm, idle system air is reduced. Air losses strengthen the small vacuum signal within the idle system and fuel flow increases.

An electric assist automatic choke system is used to reduce hydrocarbon and carbon monoxide emissions during engine starting and warm-up. A single stage electric heating element located next to a bimetal spring inside the choke well assists engine heat to shorten choke duration above 68°F. Once the control switch is heated to 130°F, the choke is shut off.

EGR System

EGR is eliminated when the coolant exhaust gas recirculation valve (CCEGR valve) indicates a coolant outlet temperature less than 65°F.

The EGR delay solenoid is activated by the starter solenoid and inter-rupts the vacuum signal between the intake manifold and the vacuum amplifier during cranking. The EGR delay timer deactivates this EGR delay solenoid after 35 seconds of operation. The effect is to preclude EGR during cranking and operation immediately after starting.

Evaporative Emissions Control System

While not a cold-start device per se, operation of the evaporative emissions control system during warm-up affects the fuel/air ratio. This effect is presumed to be small.

The carburetor float bowl and fuel tank are sealed except for a vent to an activated charcoal cannister. The fuel tank vent opens when $|P| > 1/2$ psig. Any vapors formed while the car is not running are absorbed onto the surface of the charcoal.

The cannister is controlled by intake manifold vacuum such that when the engine is started, it will lower the pressure in the cannister and the hydrocarbon vapors will desorb and be burned in the engine.

BASELINE VEHICLE TESTS

After completion of the break-in period and tune-up to factory specifications, baseline chassis dynamometer tests of the vehicle were conducted at the Subaru test facility. Vehicle tests were not made on the JPL chassis dynamometer at the beginning of this effort because of facility unavailability. To avoid delays, the JPL vehicle tests were conducted after completion of the engine dynamometer tests.

The Subaru testing included three tests each for the urban and highway driving cycles. Both CVS-3 bag analysis and modal analysis of emissions were obtained for the urban cycle. Fuel economy results were obtained for both urban and highway cycles. Detailed results of these baseline vehicle tests are given in Appendix A, and are summarized in Table 2.

Table 2. Baseline Vehicle Test Results (Subaru Facility)

	1975 California Standard	Test No. 1	Test No. 2	Test No. 3	Average	EPA Certified Values
Urban Driving Cycle						
HC, g/mi	0.9	0.60	0.45	0.64	0.56	
CO, g/mi	9.0	3.47	3.70	4.02	3.73	
NO_x, g/mi	2.0	0.92	0.98	1.07	0.99	
Fuel Economy, mpg		14.90	14.57	14.79	14.75	15
Highway Driving Cycle						
Fuel Economy, mpg		20.11	19.92	19.92	19.98	20
Composite Cycle						
Fuel Economy, mpg		16.87	16.57	16.75	16.73	17

Fuel economy values for both the urban and highway driving cycles are based on the carbon balance techniques of Ref. 3. Urban driving cycle mileages have been computed using the following equation.

$$1975 \text{ FTP mpg} = \frac{26895}{0.866 \text{ (g HC in bags 1, 2, and 3)}}$$ (1)

$$+ \ 0.429 \text{ (g CO in bags 1, 2, and 3)},$$

$$+ \ 0.273 \text{ (g } CO_2 \text{ in bags 1, 2, and 3)}$$

Emissions values needed in this calculation were based on "weighted" bag results according to the following equation:

$$\text{(g emissions in bags 1, 2, and 3)} = 0.43 \text{ (g emissions in bag 1)} \qquad (2)$$

$$+ \ 0.57 \text{ (g emissions in bag 3)}$$

$$+ \ 0.57 \text{ (g emissions in bag 3)}$$

$$+ \ \text{(g emissions in bag 2)}$$

This weighting is in agreement with that specified in the Federal Register, Ref. 4. Composite fuel economy results were computed by assuming 55 percent urban driving and 45 percent highway driving. This is in accordance with Ref. 5.

Based on these results, the DOT vehicle is felt to be representative of this engine/vehicle combination since the fuel economy data agree with EPA certified results. The baseline emissions for the DOT vehicle (0.56 g/mi HC, 3.73 g/mi CO, 0.99 g/mi NO_x) compare favorably with the typical values given on the window sticker for the 225 CID engine (0.4 g/mi HC, 3.6 g/mi CO, 1.9 g/mi NO_x).

The modal analysis of emissions which was used in the baseline tests is based on dividing the 1371-second urban driving cycle into 66 modes for emissions evaluations. The modes are selected to represent primarily one of four kinds of vehicle operation: idle, acceleration, deceleration or constant speed driving. The identification of this modal breakdown of the urban driving cycle is given in Table 3. A measure of the HC, CO, and NO_x emissions is recorded for each mode of the test. By adding the emissions from each mode, an estimate of the emissions over any portion of the driving cycle can be obtained.

Although the modal emissions results provide some information about the distribution of emissions during the driving cycle, the emissions obtained from the modal analysis differ considerably from bag results as shown in Table 4. The modal emissions tend to be much lower than the bag results especially for bag 1 and bag 3, which collect the emissions from the first 505 seconds of the driving cycle.

In automobiles which use oxidation catalyst for emission control, it is expected that a large fraction of the total HC and CO emissions occur during the cold-start part of the cycle while the catalyst is below its operating

11

Table 3. Modal Breakdown of Urban Driving Cycle (Ref. 4).

MODE TYPES: I = Idle
             A = Accelerate
             C = Cruise
             D = Decelerate

Mode	Mode Type	Time(s)	Accumulated Time(s)	Mode	Mode Type	Time(s)	Accumulated Time(s)
1	I	20	20	34	A	19	717
2	A	9	29	35	D	14	731
3	C	33	62	36	A	18	749
4	C	61	113	37	D	20	769
5	D	12	125	38	A	17	786
6	I	38	163	39	C	69	845
7	A	41	204	40	C	61	906
8	C	45	249	41	C	44	950
9	C	50	299	42	D	10	960
10	D	33	332	43	A	16	976
11	I	19	351	44	C	34	1,010
12	A	18	369	45	D	16	1,026
13	C	18	387	46	I	30	1,056
14	D	15	402	47	A	17	1,073
15	I	5	407	48	D	30	1,103
16	A	11	418	49	A	21	1,124
17	D	15	433	50	C	18	1,142
18	I	19	452	51	D	12	1,154
19	A	16	468	52	I	16	1,170
20	C	12	497	53	A	9	1,179
21	D	12	509	54	D	20	1,199
22	I	6	515	55	I	1	1,200
23	A	15	530	56	A	16	1,216
24	C	16	546	57	C	17	1,233
25	D	11	557	58	D	12	1,245
26	I	15	572	59	I	8	1,253
27	A	7	579	60	A	26	1,279
28	C	35	614	61	C	24	1,303
29	D	11	625	62	D	11	1,314
30	I	24	649	63	I	23	1,337
31	A	14	663	64	A	13	1,350
32	D	21	684	65	D	11	1,361
33	I	14	698	66	I	10	1,371

temperature. The HC and CO emissions reductions which would result from the elimination of the cold-start contributions to these emissions are illustrated in Table 5 for the baseline vehicle tests. The potential emissions are calculated by replacing the bag 1 values with the bag 3 values. From these calculations it is seen that a 40 percent reduction in HC emissions and an 84 percent reduction in CO emissions are possible by eliminating cold-start emissions. Similar calculations using modal emissions data indicate that a 36 percent reduction in HC emissions and a 77 percent reduction in CO emissions are possible as shown in Table 6.

Table 4. Comparison of Modal and Bag Emissions Results
(Chassis Dynamometer Tests at Subaru Facility)

Test No.	Type Data	Emissions (g)								
		Bag 1			Bag 2			Bag 3		
		HC	CO	NO_x	HC	CO	NO_x	HC	CO	NO_x
1	Bag	6.30	52.65	3.15	0.45	1.2	3.6	2.4	3.75	3.45
	Modal	3.0	27.5	2.5	0.5	1.0	2.6	0.9	2.4	2.5
2	Bag	4.2	56.93	3.38	0.53	1.35	3.75	1.8	3.45	3.83
	Modal	2.7	26.9	2.4	0.7	0.7	2.5	1.0	2.2	2.5
3	Bag	7.88	64.95	3.45	0.38	0.6	4.2	1.8	2.85	4.13
	Modal	2.9	24.2	2.5	0.5	0.8	2.7	0.8	1.8	2.8

Table 5. Cold-Start Emissions Improvement Potential
(Chassis Dynamometer Tests at Subaru Facility)

Test No.	Bag Values (g)						Actual (g/mi)		Potential (g/mi)		Percent Improvement	
	1		2		3							
	HC	CO	HC	CO	HC	CO	HC	CO	HC	CO	HC	CO
1	6.30	52.65	0.45	1.2	2.4	3.75	0.60	3.46	0.38	0.66	36.7	81.0
2	4.2	56.93	0.53	1.35	1.8	3.45	0.45	3.71	0.31	0.64	31.1	82.7
3	7.88	64.95	0.38	0.60	1.8	2.85	0.64	4.02	0.29	0.46	54.7	88.5
Average Percentage Improvement											40.8	84.1

Table 6. Cold-Start Emissions Improvement Potential Based on Modal Emissions
Data (Chassis Dynamometer Tests at Subaru Facility)

Test No.	Integrated Modal Values (g)						Actual (g/mi)		Potential (g/mi)		Percent Improvement	
	1		2		3							
	HC	CO	HC	CO	HC	CO	HC	CO	HC	CO	HC	CO
1	3.0	27.5	0.5	1.0	0.9	2.4	0.31	1.89	0.19	0.45	38.7	76.2
2	2.7	26.9	0.7	0.7	1.0	2.2	0.32	1.80	0.23	0.39	28.1	78.3
3	2.9	24.2	0.5	0.8	0.8	1.8	0.29	1.63	0.17	0.35	41.4	78.5
Average Percentage Improvement											36.1	77.7

Measurements of the time distribution of emissions during the urban driving cycle, obtained from accumulated emissions during the first 505 seconds of the driving cycle, are given in Figures 8, 9, and 10 for both the cold transient (bag 1) and hot transient (bag 3) tests. These plots again show the much higher HC and CO emissions which occur during the cold-start operation. The NO_x emissions for the cold and hot tests are very similar, as expected.

For the cold transient test, each emissions value is shown normalized with respect to its total emissions for the test in Figure 11. Using this plot and Table 3, it is seen that 90 percent of the HC emissions in the cold transient bag are collected during the first 5 minutes, while 90 percent of the CO emissions come in the first 3 - 4 minutes.

BASELINE ENGINE TESTS

To provide a good base from which to evaluate potential improvements in the stock emission control systems, a complete engine mapping of the stock engine was conducted on a water brake dynamometer. Forty engine operating conditions were selected to cover the operating map. These points are shown in Figure 12. For these baseline tests, emissions measurements were made both upstream and downstream of the catalytic converter. Exhaust gas temperatures were measured near the exhaust valve for each cylinder. EGR flow rate was calculated using the air calibration data from cold-flow bench tests of the EGR valve. AIR flow rate was based on AIR pump calibration data. Calibration curves for the EGR valve and AIR pump are included in Appendix B.

A listing of the primary results of the stock baseline tests is given in Table 7. The fuel-to-air ratio is one of the key parameters which influences both fuel economy and exhaust emissions. This parameter is expressed in terms of equivalence ratio which is defined as follows:

$$\phi = \frac{\dot{M}_G}{\dot{M}_A \, \zeta_S} \tag{3}$$

where

ϕ = fuel/air equivalence ratio

$\dot{M}_G$ = gasoline flow rate

$\dot{M}_A$ = air flow rate

ζ_S = stoichiometric fuel-to-air ratio

The variation of equivalence ratio with manifold pressure for the baseline data is given in Figure 13. The results for all engine speeds are shown on the same plot, which accounts for some of the data scatter about the curve. The stock carburetor is calibrated at an equivalence ratio of about 0.95 over the mid-range with enrichments ($\phi > 1.0$) at both light loads and wide-open-throttle (WOT) conditions.
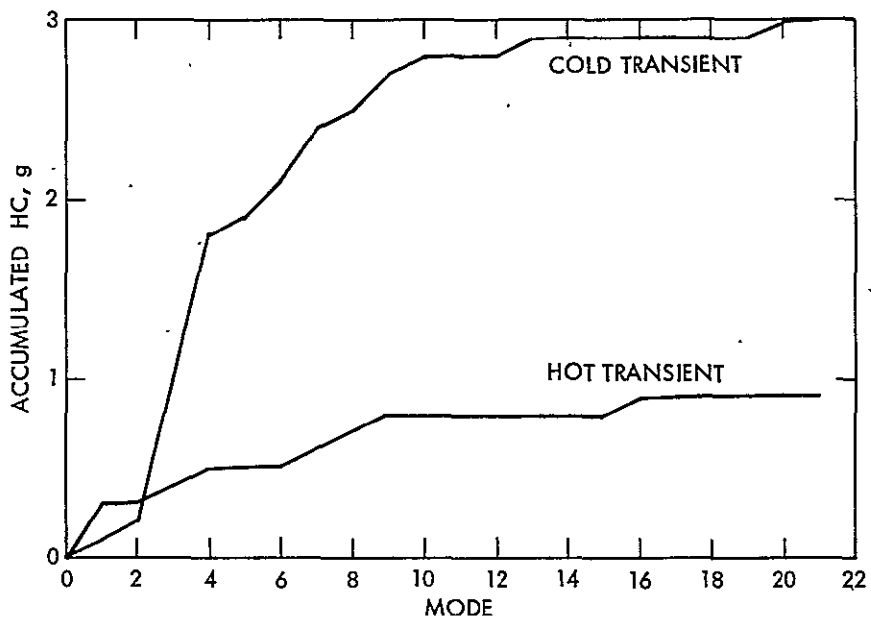
14

Figure 8. Transient Mode HC Emissions for Baseline
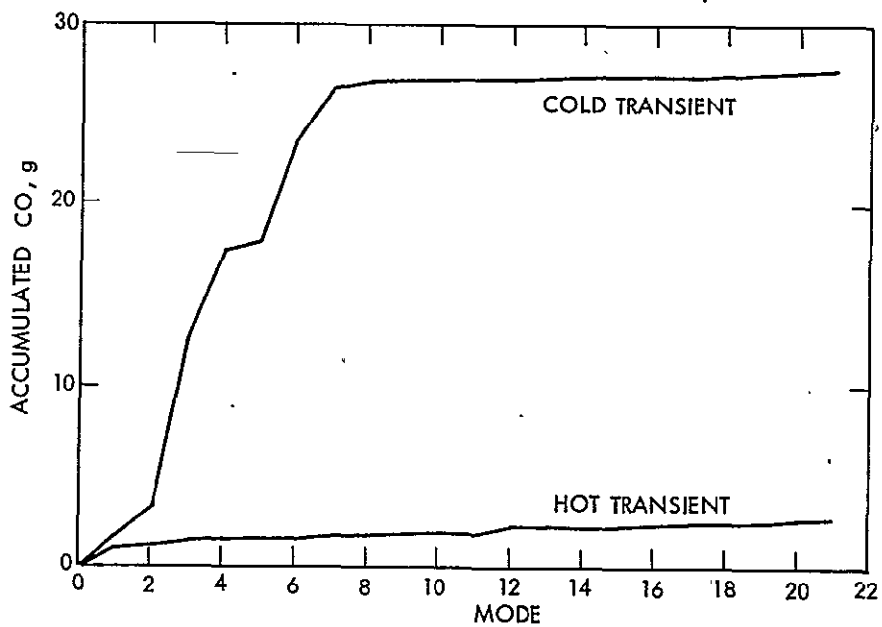Vehicle Over Urban Driving Cycle

Figure 9. Transient Mode CO Emissions for Baseline
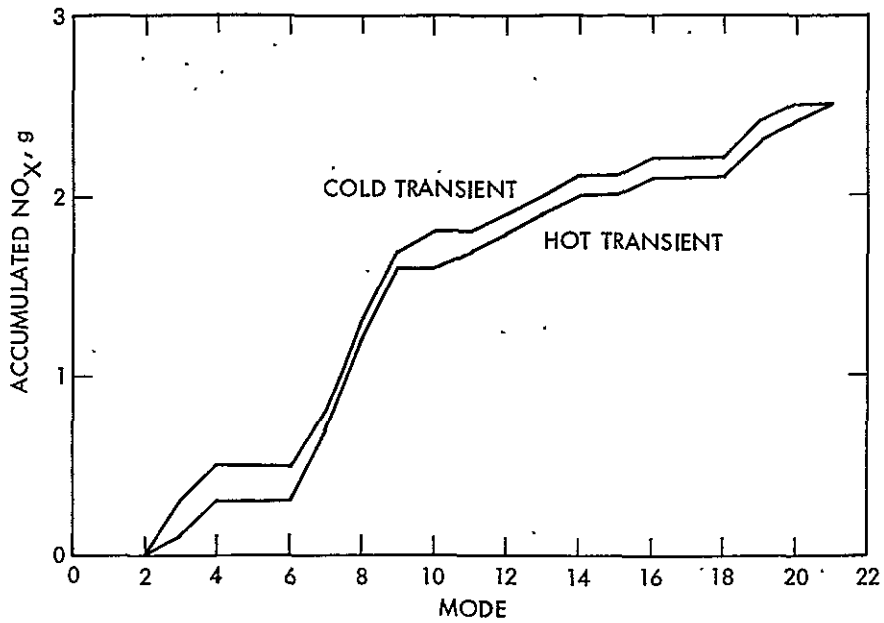Vehicle Over Urban Driving Cycle

Figure 10. Transient Mode NO_x Emissions for Baseline
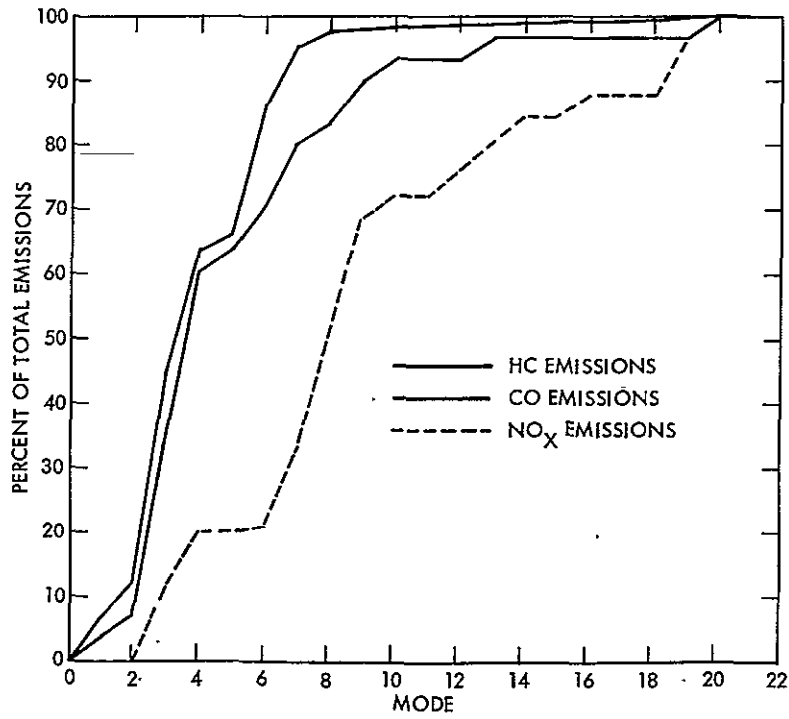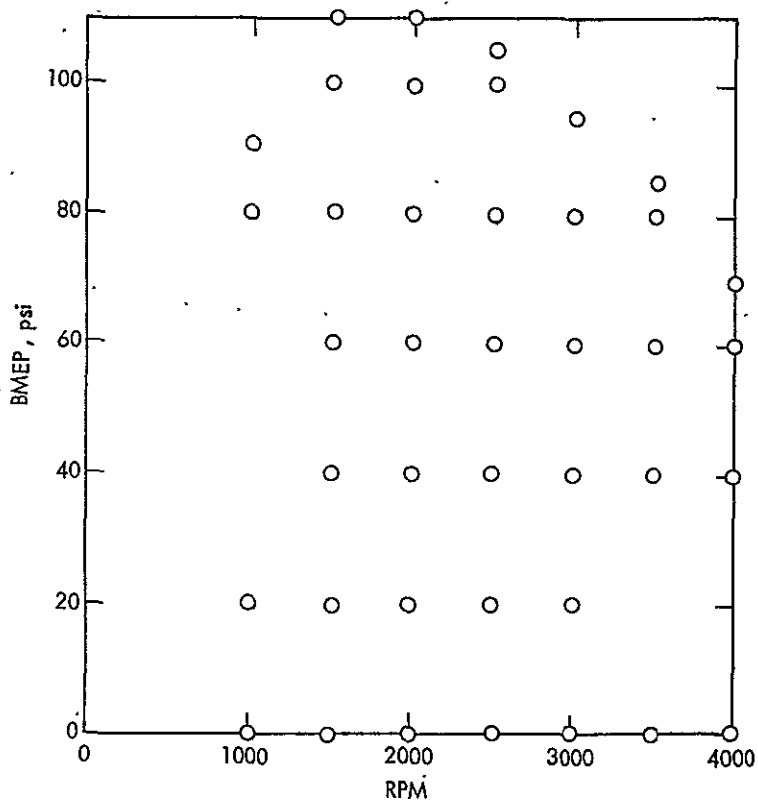Vehicle Over Urban Driving Cycle

Figure 11. Normalized Emissions for Baseline Vehicle
Over Transient Mode of Urban Driving Cycle

Figure 12. Operating Conditions Used for Baseline
Tests of Stock Engine

It is convenient to define two new effective equivalence ratios which aid in understanding the emissions results. The dilution effect of EGR is included in the following effective equivalence ratio, ϕ_E.

$$\phi_E = \frac{\dot{M}_G}{\left(\dot{M}_A + \dot{M}_{EGR}\right)\zeta_S} \tag{4}$$

where

ϕ_E = effective equivalence ratio

$\dot{M}_G$ = gasoline flow rate

$\dot{M}_A$ = air flow rate

$\dot{M}_{EGR}$ = EGR flow rate

ζ_S = stoichiometric fuel-to-air ratio

17

Table 7. Stock Baseline Engine Data

Sequence No.	RPM	BMEP (psi)	$\dot{m}_{gaso}$ (lbm/h)	$\dot{m}_{air}$ (lbm/h)	% A.I.R.	% EGR	P_{man} ("Hg vac)	Spark Advance (°BTDC)	Average T_{exh} (°F)	ϕ	ϕ_A	ϕ_E	BSFC (lbm/bhp-h)	Emissions Data*	BSNO$_x$ (g/bhp-h)	BSHC (g/bhp-h)	BSCO (g/bhp-h)	η_{HC}	η_{CO}
144.06	1035	0.0	5.70	62.2	40	16	17.88	4.2	1249	1.324	0.772	1.088		U					
145.06	1031	0.0	5.68	62.2										D					
144.09	993	20.1	5.07	74.4	35	15	15.90	17.3	977	0.986	0.626	0.834	0.895	U	3.14	3.64	29.26		
145.09	993	20.1	5.08	74.4										D	3.51	1.72	0.90	52.8	96.9
146.39	1070	88.8	16.78	221.2	5	0	0.47	4.1		1.096	1.039	1.096	0.622	U	4.56	1.26	130.03		
147.39	1070	88.8	16.78	221.2										D	2.83	0.14	41.22	88.9	68.3
146.42	1037	83.3	15.03	197.1	7	1	1.84	1.9		1.102	1.019	1.092	0.613	U	4.11	1.19	100.55		
147.42	1037	83.3	15.03	197.1										D	2.74	0.16	17.36	86.6	82.7
142.03	1476	2.0	6.20	63.6	42	18	20.12	24.2	1217	1.408	0.780	1.135		U					
143.03	1476	2.0	6.20	63.6										D				75.5	
142.06	1501	19.7	7.86	108.8	31	24	14.29	35.5	1067	1.044	0.703	0.781	0.933	U	2.75	6.09	16.22		
143.06	1501	19.7	7.86	108.8										D	3.30	0.91	0.21	85.1	98.7
142.09	1502	40.1	10.85	164.0	24	24	7.76	29.0	1106	0.956	0.721	0.712	0.634	U	2.25	6.14	9.36		
143.09	1502	40.1	10.85	164.0										D	2.63	0.78	0.35	87.3	96.3
142.12	1450	60.0	14.29	212.6	18	17	3.02	18.5	1181	0.971	0.789	0.796	0.578	U	3.24	2.25	5.03		
143.12	1450	60.0	14.29	212.6										D	3.86	0.29	0.27	87.1	94.6
142.15	1542	79.9	18.93	240.2	16	17	1.87	20.6	1168	1.139	0.941	0.932	0.540	U	1.97	2.25	95.25		
143.15	1542	79.9	18.93	240.2										D	1.94	0.22	1.74	90.2	98.2
142.18	1564	100.8	19.66	295.4	13	0	2.53	21.2	1206	0.962	0.826	0.962	0.439	U	18.49	1.24	6.46		
143.18	1546	100.8	19.66	295.4										D	20.19	0.21		83.1	
142.21	1513	111.9	24.20	307.1	11	0	0.82	19.9	1178	1.139	1.008	1.139	0.503	U	7.34	1.82	113.00		
143.21	1513	111.9	24.20	307.1										D	5.16	0.30	43.34	83.5	61.7
146.18	1995	2.0	7.73	86.6	41	15	19.95	37.4	1214	1.290	0.735	1.088		U					
147.18	1995	2.0	7.73	86.6										D					
146.21	2036	20.3	11.31	174.6	26	31	11.43	37.8	1117	0.937	0.681	0.638	0.964	U	2.62	23.38	21.71		
147.21	2036	20.3	11.31	174.6										D	3.27	3.77	0.69	83.9	96.8
146.24	2041	40.2	16.11	258.0	19	19	5.79	23.2	1254	0.902	0.719	0.720	0.691	U	3.11	4.42	10.48		
147.24	2041	40.2	16.11	258.0										D	3.66	0.62	0.32	86.0	97.0
146.27	2036	59.8	19.59	298.8	17	16	3.42	21.4	1278	0.947	0.778	0.789	0.566	U	4.83	0.95	7.65		
147.27	2036	59.8	19.59	298.8										D	5.48	0.12	0.20	87.4	97.4
146.30	2060	79.6	22.71	348.0	15	3	4.21	21.9	1290	0.943	0.795	0.912	0.487	U	15.53	0.61	5.48		
147.30	2060	79.6	22.71	348.0										D	16.96	0.09	0.17	85.3	96.9
146.33	1981	99.7	26.23	375.6	14	0	2.45	21.7	1304	1.010	0.864	1.007	0.468	U	17.03	0.47	18.61		
147.33	1981	99.7	26.23	375.6										D	18.28	0.08	0.50	83.0	97.3
146.36	2019	107.0	31.54	399.1	12	0	1.31	22.1	1292	1.142	0.992	1.140	0.514	U	7.40	0.78	96.06		
147.36	2019	107.0	31.54	399.1										D	6.05	0.20	47.06	74.4	51.0
144.12	2516	0.0	9.49	147.6	34	34	16.63	40.8	1152	0.930	0.604	0.601		U					
145.12	2516	0.0	9.49	147.6										D					
144.16	2512	20.5	13.78	211.0	26	29	12.20	40.5	1195	0.944	0.691	0.654	0.942	U	3.58	9.52	19.63		
145.16	2512	20.5	13.78	211.0										D	4.19	1.59	0.59	83.3	97.0
144.18	2490	39.8	17.94	271.0	21	23	8.64	35.8	1237	0.957	0.748	0.728	0.638	U	5.32	2.09	10.61		
145.18	2490	39.8	17.94	271.0										D	5.90	0.29	0.28	86.1	97.4
144.21	2485	59.8	23.56	363.5	16	14	3.80	24.7	1345	0.937	0.781	0.795	0.558	U	6.61	0.43	6.33		

Table 7.   Stock Baseline Engine Data (Contd)

Sequence No.	RPM	BMEP (psi)	$\dot{m}_{gaso}$ (lbm/h)	$\dot{m}_{air}$ (lbm/h)	% A.I.R.	% EGR	P_{man} ("Hg vac)	Spark Advance (°BTDC)	Average T_{exh} (°F)	ϕ	ϕ_A	ϕ_E	BSFC (lbm/bhp-h)	Emissions Data*	BSNO$_x$ (g/bhp-h)	BSHC (g/bhp-h)	BSCO (g/bhp-h)	η_{HC}	η_{CO}
145.21	2485	59.8	23.56	363.5										D	7.21	0.05	0.17	88.4	97.3
144.24	2548	79.6	28.26	436.3	13	3	4.08	25.6	1370	0.936	0.808	0.905	0.490	U	17.61	0.28	4.69		
145.24	2548	79.6	28.26	436.3										D	18.63	0.04	0.15	85.7	96.8
144.27	2525	99.7	35.58	481.1	11	1	2.37	25.7	1414	1.069	0.947	1.060	0.497	U	13.58	0.18	33.07		
145.27	2525	99.7	35.58	481.1										D	12.37	0.03	4.00	83.3	87.9
144.30	2503	103.4	38.13	483.2	11	1	1.86	25.3	1390	1.141	1.013	1.134	0.519	U	7.39	0.51	92.33		
145.30	2503	103.4	38.13	483.2										D	7.12	0.31	71.54	39.2	22.6
144.33	2958	0.7	11.67	180.4	32	35	16.01	42.3	1219	0.935	0.624	0.596		U					
145.33	2958	0.7	11.67	180.4										D					
146.03	3033	20.4	16.90	263.9	24	27	12.03	42.5	1272	0.925	0.692	0.659	0.961	U	5.75	7.73	19.27		
147.03	3033	20.4	16.90	263.9										D	6.62	1.17	0.57	84.9	97.0
146.06	3044	39.8	22.03	344.0	19	20	8.66	37.6	1328	0.926	0.741	0.728	0.641	U	7.46	1.12	7.81		
147.06	3044	39.8	22.03	344.0										D	8.30	0.14	0.22	87.5	97.2
146.09	3021	59.8	29.87	468.5	13	8	4.90	24.4	1460	0.922	0.792	0.846	0.582	U	10.23	0.19	4.53		
147.09	3021	59.8	29.87	468.5										D	11.04	0.02	0.13	89.5	97.1
146.12	3059	79.6	35.15	535.2	11	2	3.76	28.3	1482	0.949	0.839	0.930	0.508	U	18.78	0.16	5.11		
147.12	3059	79.6	35.15	535.2										D	19.66	0.02	0.14	87.5	97.3
146.15	2985	96.6	45.27	564.2	9	1	2.56	28.7	1465	1.160	1.050	1.147	0.553	U	7.78	0.57	105.02		
147.15	2985	96.6	45.27	564.2										D	7.72	0.44	93.06	22.8	11.4
148.06	3503	0.6	14.19	214.8	32	30	15.48	41.9	1304	0.955	0.657	0.640		U					
149.06	3503	0.6	14.19	214.8										D					
148.09	3567	39.7	26.61	411.1	18	18	8.24	34.9	1391	0.936	0.761	0.756	0.662	U	11.07	0.56	7.23		
149.09	3567	39.7	26.61	411.1										D	11.06	0.07	0.19	87.5	97.4
148.12	3541	59.9	35.27	541.7	7	13	4.83	25.3	1511	0.941	0.814	0.874	0.586	U	15.47	0.17	4.66		
149.12	3541	59.9	35.27	541.7										D	15.69	0.02	0.14	88.2	97.0
148.15	3500	79.6	41.58	606.3	1	11	3.42	25.5	1551	0.991	0.878	0.976	0.525	U	22.67	0.10			
149.15	3500	79.6	41.58	606.3										D	22.83	0.02	0.26	80.0	
148.18	3554	85.9	50.34	621.5	2	10	3.18	25.5	1518	1.171	1.041	1.152	0.581	U	8.83				
149.18	3554	85.9	50.34	621.5										D	8.45				
150.06	4086	1.7	18.39	254.3	28	20	15.01	43.4	1425	1.045	0.733	0.825	9.203	U					
151.06	4086	1.7	18.39	254.3										D					
150.09	4037	40.3	34.16	532.9	15	15	5.20	26.0	1543	0.927	0.783	0.783	0.739	U	8.92	0.19	6.62		
151.09	4037	40.3	34.16	532.9										D	9.16	0.02	0.22	89.5	96.7
150.12	4045	60.1	41.23	617.4	12	5	4.14	26.3	1584	0.965	0.839	0.918	0.597	U	18.53	0.07	5.31		
151.12	4045	60.1	41.23	617.4										D	18.93	0.01	0.20	85.7	96.2
150.16	4071	72.9	52.17	647.2	12	2	3.47	26.7	1571	1.165	1.022	1.141	0.619	U	9.65	0.50	118.02		
151.16	4071	72.9	52.17	647.2										D	8.29	0.50	128.54	0.0	0.0

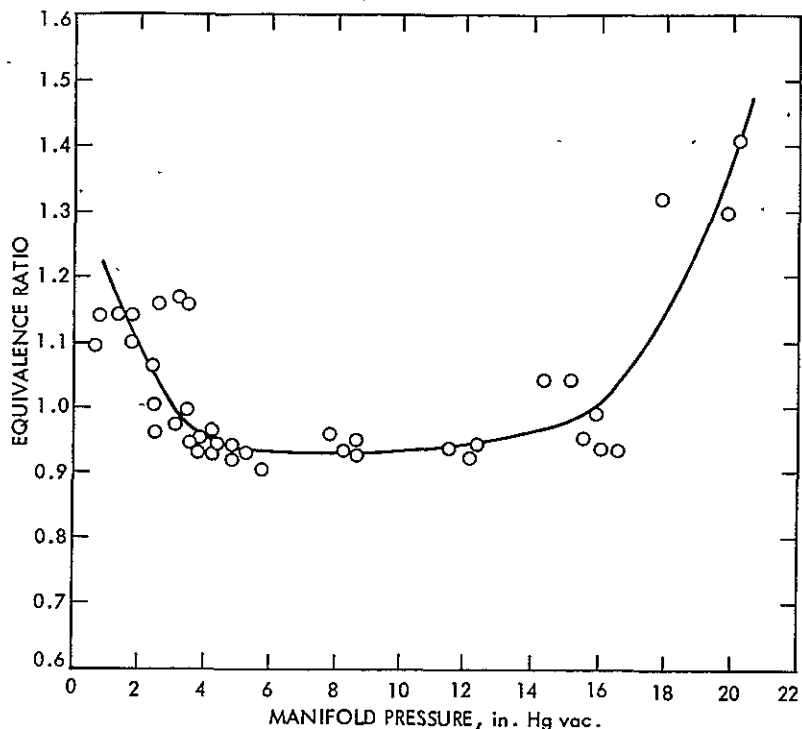*U = Upstream of catalytic converter; D = downstream of catalytic converter.

Figure 13. Stock Carburetor Calibration

The additional air supplied by the AIR pump is included in the following effective equivalence ratio, ϕ_A.

$$\phi_A = \frac{\dot{M}_G}{\left(\dot{M}_A + \dot{M}_{AIR}\right)\zeta_S} \tag{5}$$

where

ϕ_A = effective equivalence ratio

$\dot{M}_G$ = gasoline flow rate

$\dot{M}_A$ = air flow rate

$\dot{M}_{AIR}$ = AIR flow rate

ζ_S = stoichiometric fuel-to-air ratio

To simplify the presentation of material and the discussion of the results, detailed results for only one engine RPM are presented in the main body of this report. Similar results are included in Appendix C. Comparisons of the variations of the equivalence ratios (ϕ, ϕ_A and ϕ_E) with BMEP are given in Figure 14 for 2000 RPM.

20
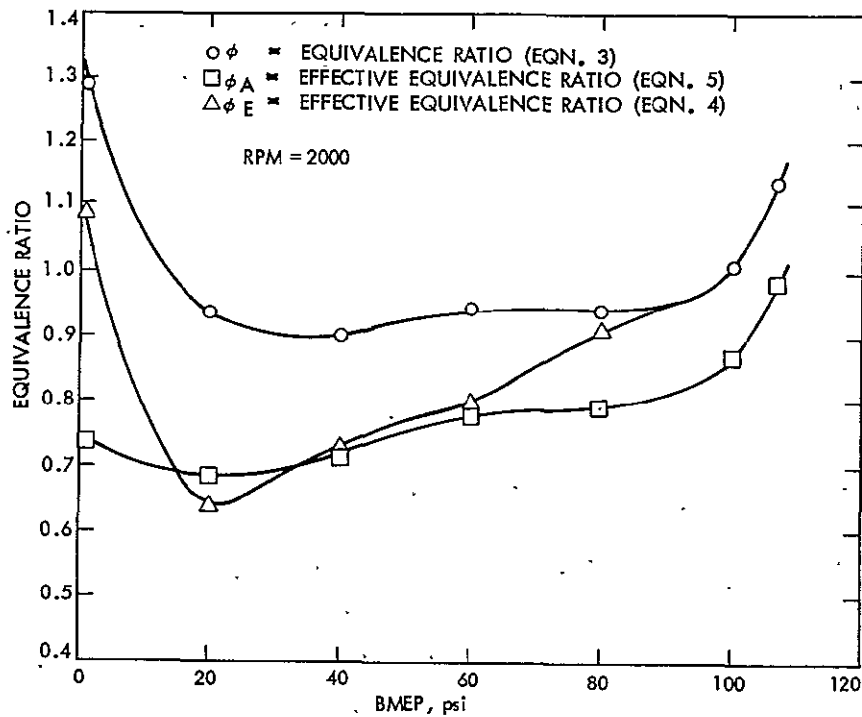
Figure 14. Equivalence Ratio Versus BMEP for Stock Engine

Spark advance data is given as a function of manifold pressure in Figure 15 for 2000 RPM. The data is seen to be consistent with the spark advance characteristic based on a bench test of the distributor. The distributor vacuum advance mechanism acts to retard the spark timing as the throttle approaches the WOT conditions.

The effect of load on fuel consumption is illustrated in Figure 16. As the load is increased, BSFC decreases to a minimum value of about 0.47 lbm/bhp-h for BMEP = 90 psi before increasing again at the WOT condition.

The NO_x emissions data for the stock engine is shown in Figure 17 plotted as a function of the effective equivalence ratio, ϕ_E. The effective equivalence ratio includes the dilution effect of the EGR flow rate. As shown in this data, the peak NO_x emissions occur for a ϕ_E of about 0.9. The plot includes data for all engine speed and load conditions. The data also includes a wide range of spark advance conditions with respect to minimum best torque (MBT) timing. Since all of these factors affect the amount of NO_x produced in the combustion process, it is not surprising to see such a wide variation in the NO_x data.

The EGR schedule for the stock engine is shown in Figure 18 for 2000 RPM. For this engine speed the percent EGR increases to a maximum of about 30 percent at a BMEP = 20 psi and then decreases as the load is further increased. The EGR is significantly reduced above a BMEP = 60 psi and becomes zero for a BMEP = 100 psi. The effect of EGR on the manifold pressure is shown in Figure 19. Above a BMEP = 60 psi the manifold pressure is relatively

21
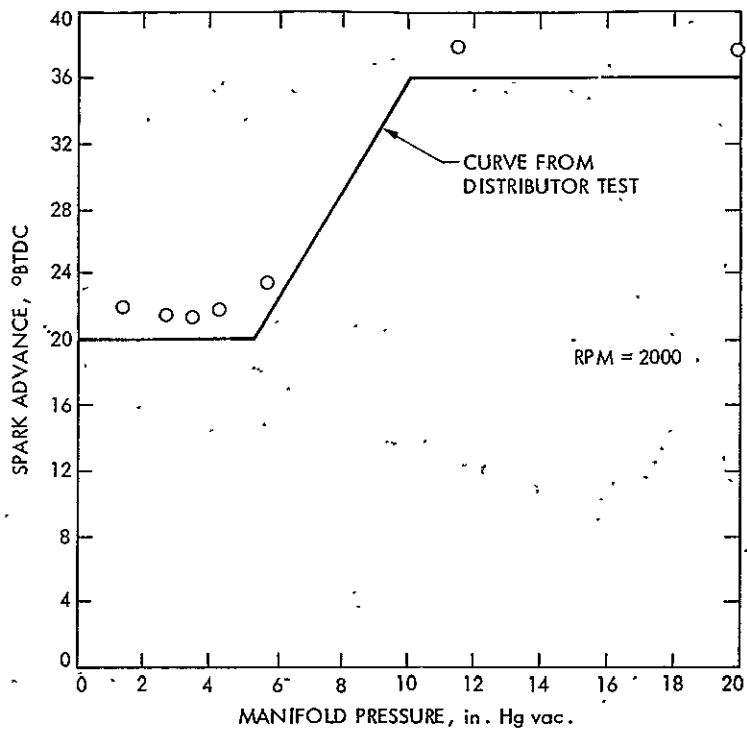
Figure 15. Spark Advance Versus Manifold Pressure for Stock Vehicle
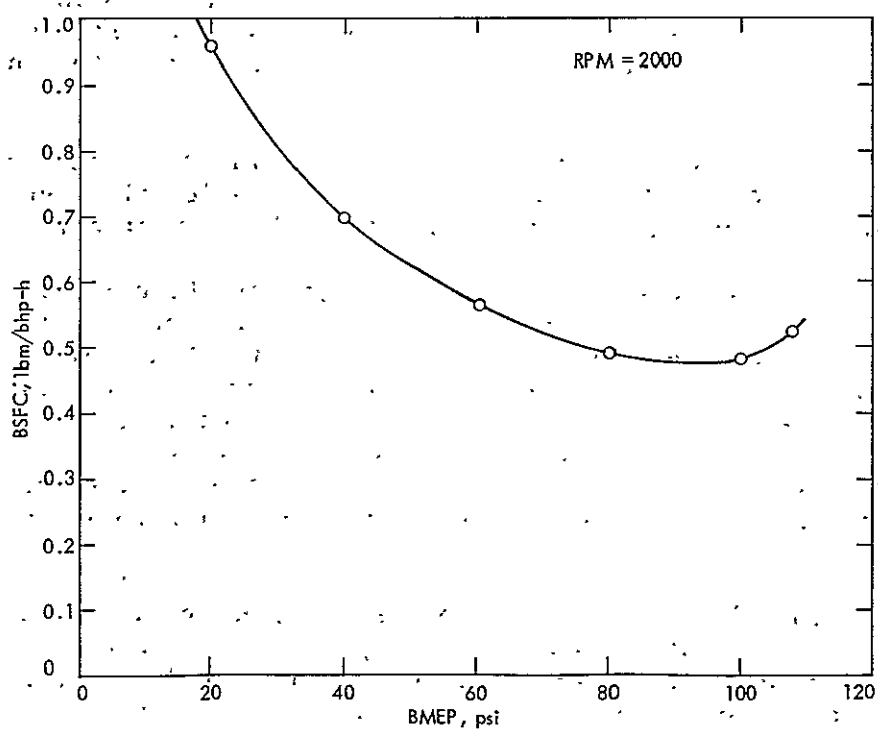
Figure 16. Fuel Consumption Versus BMEP for Stock Engine

22

NOTE: DATA ARE FOR ALL
SPEED AND LOAD
CONDITIONS.
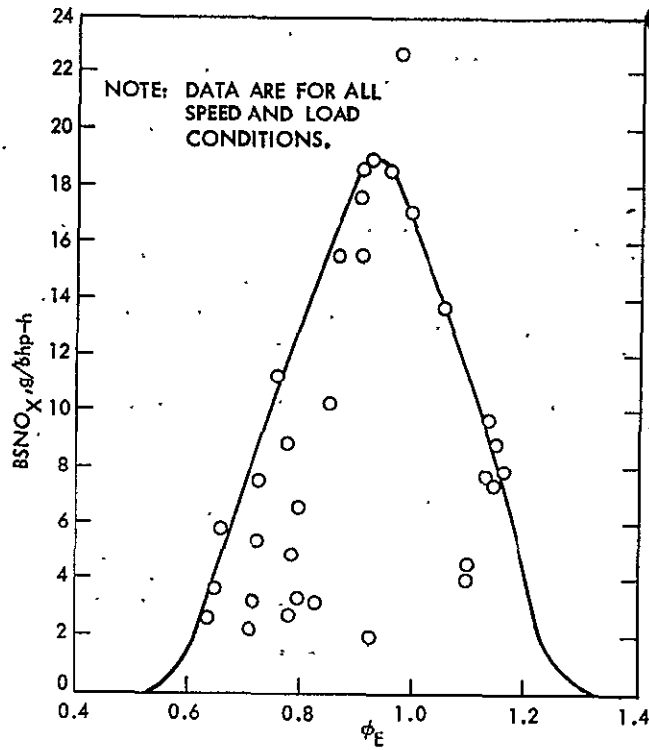
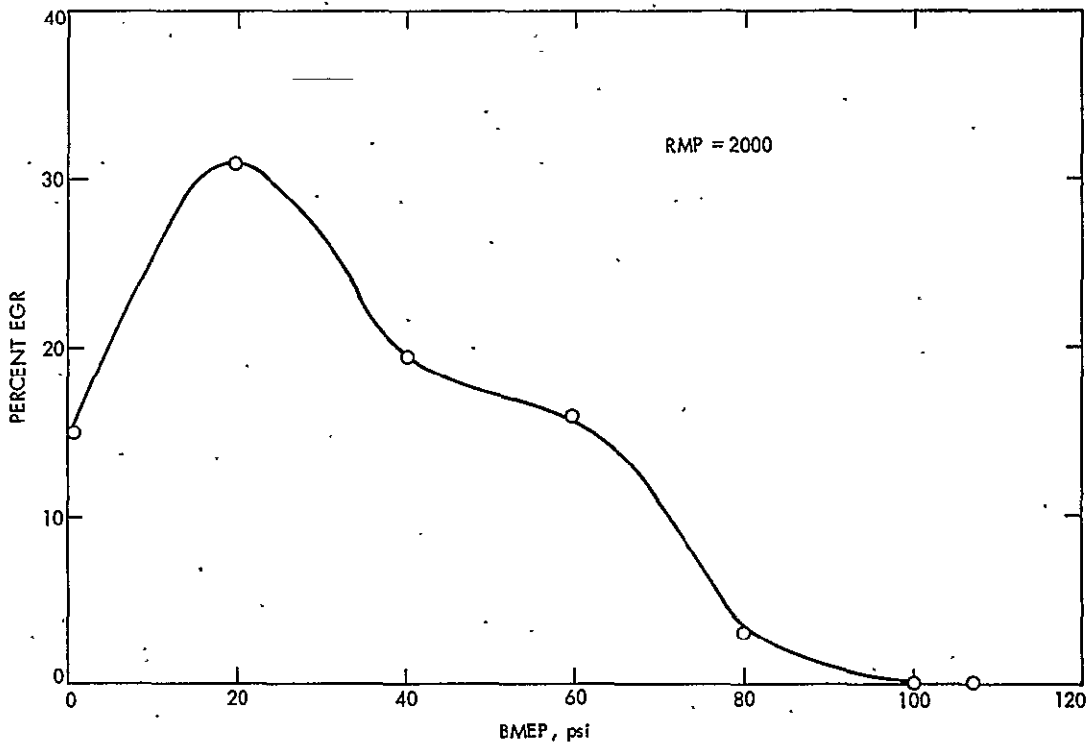Figure 17. NO_x Emissions Versus Equivalence Ratio for Stock Engine

RMP = 2000
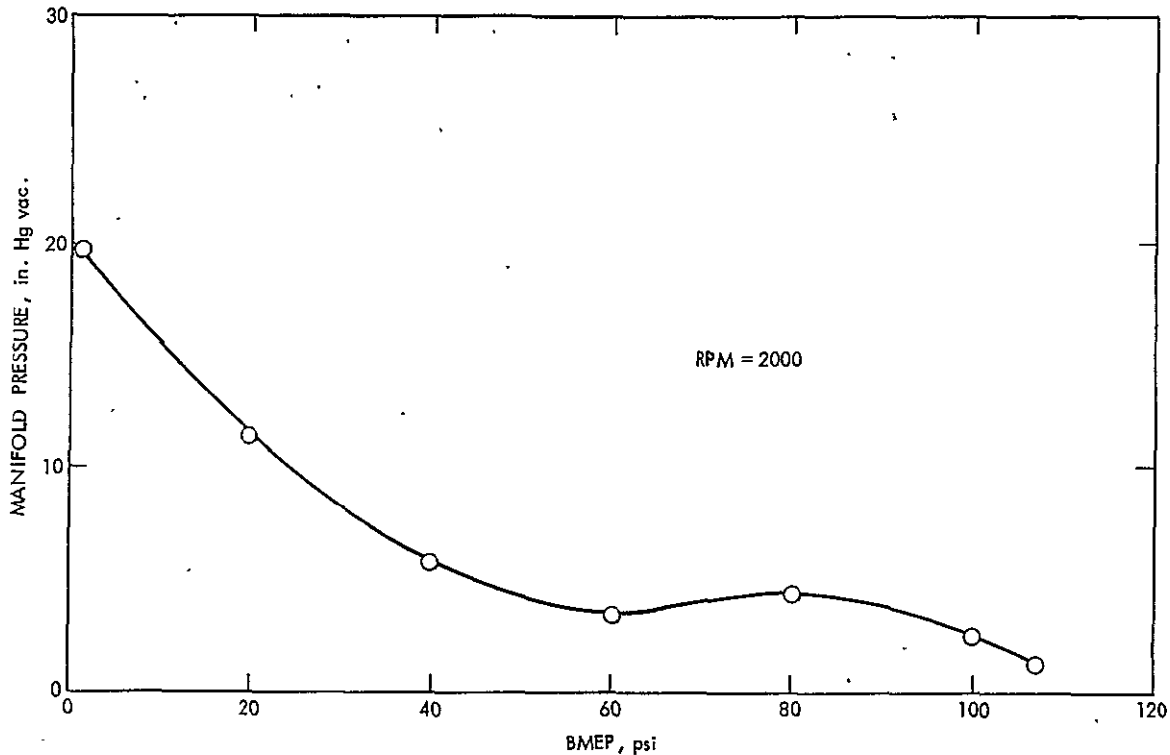
Figure 18. Percent EGR Versus BMEP for Stock Engine

23

Figure 19. Manifold Pressures Versus BMEP for Stock Engine

constant, indicating a balance between the increase in primary air flow and the decrease in EGR flow.

A comparison of the HC emissions measured both upstream and downstream of the catalytic converter is given in Figure 20 for 2000 RPM. Both upstream and downstream characteristics show similar variation with load. The specific HC emissions reach a low in the mid-load range and increase for light loads and at WOT conditions. An indication of the effectiveness of the catalytic converter in reducing HC emissions is shown in Figure 21. This curve shows HC conversion efficiency plotted versus the effective equivalence ratio, ϕ_A. This effective equivalence ratio includes the AIR flow and should be a good indicator of the oxygen which is available for the oxidation of the unburned HC emissions in the catalytic converter. This curve shows that good HC conversion efficiencies are obtained with the stock vehicle when there is adequate oxygen available in the catalytic converter ($\phi_A < 1$). Most stock operating conditions yield HC conversion efficiencies of 80 to 90 percent.

A comparison of the CO emissions measured both upstream and downstream of the catalytic converter is shown in Figure 22 for 2000 RPM. In this case, the downstream CO emissions are very low for all load conditions except WOT. The CO conversion efficiency is plotted versus the effective equivalence ratio, ϕ_A, in Figure 23. Again, good conversion efficiencies ($N_{CO} > 90$ percent) are obtained when there is adequate oxygen available in the catalytic converter ($\phi_A < 1$).
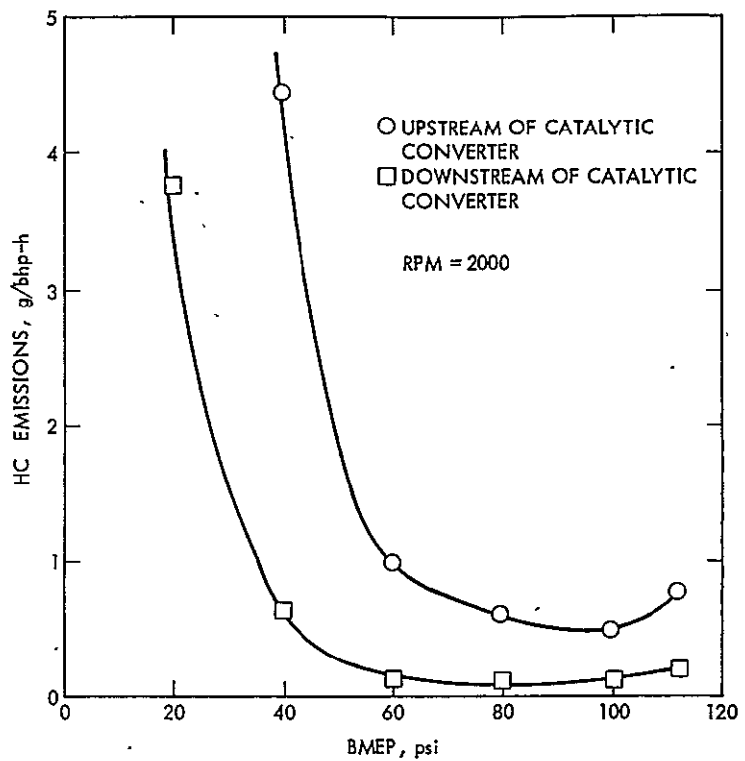
Figure 20.   HC Emissions Versus BMEP for Stock Engine
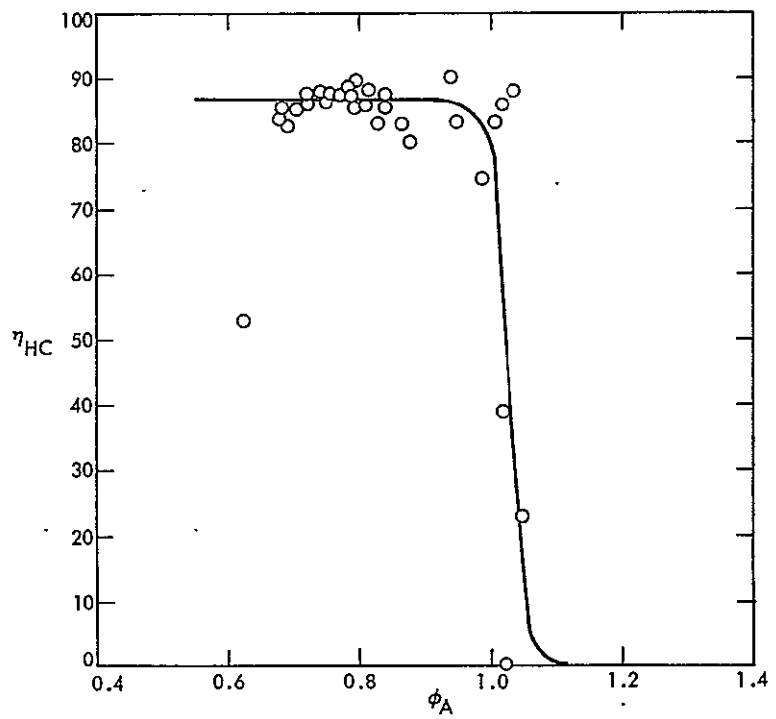

Figure 21.   HC Conversion Efficiency Versus Equivalence
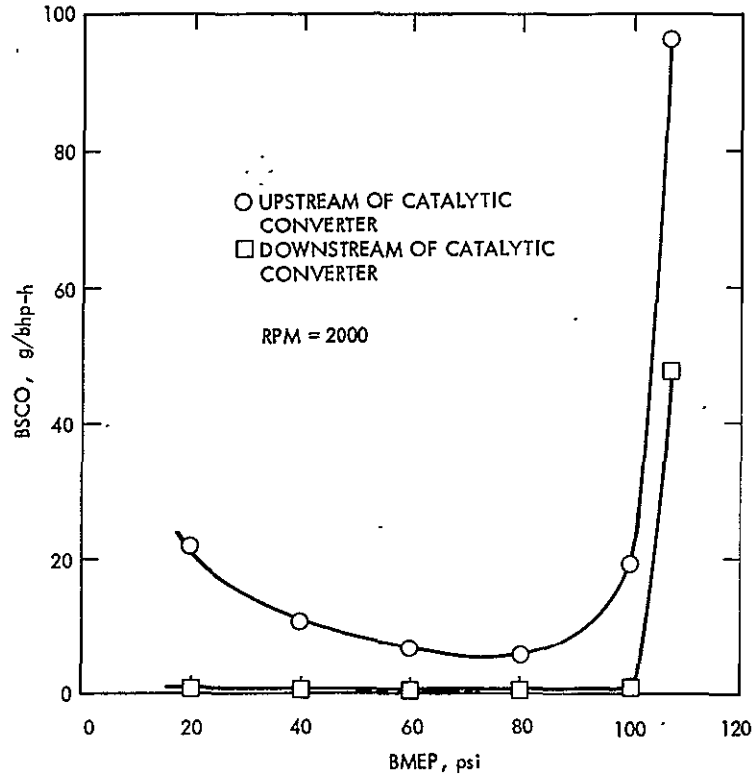   Ratio for Stock Engine

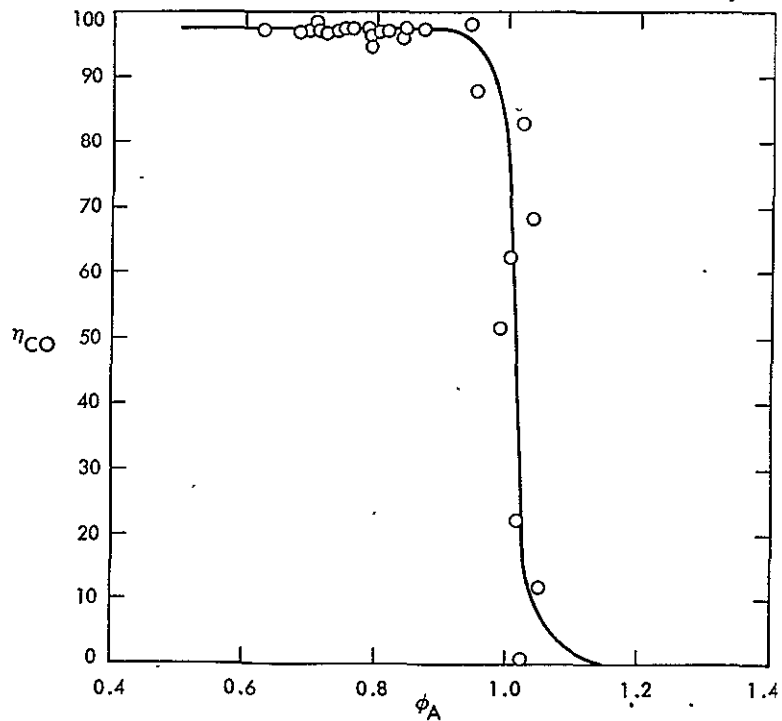25

Figure 22.   CO Emissions Versus BMEP for Stock Engine

Figure 23.   CO Conversion Efficiency Versus Equivalence
Ratio for Stock Engine

26

Spark advance is plotted versus load for 2000 RPM in Figure 24. The spark is retarded for the higher loads. Retarding the spark leads to higher exhaust temperatures as shown in Figure 25. Average exhaust temperatures range from 1100°F to about 1300°F near WOT operating conditions.
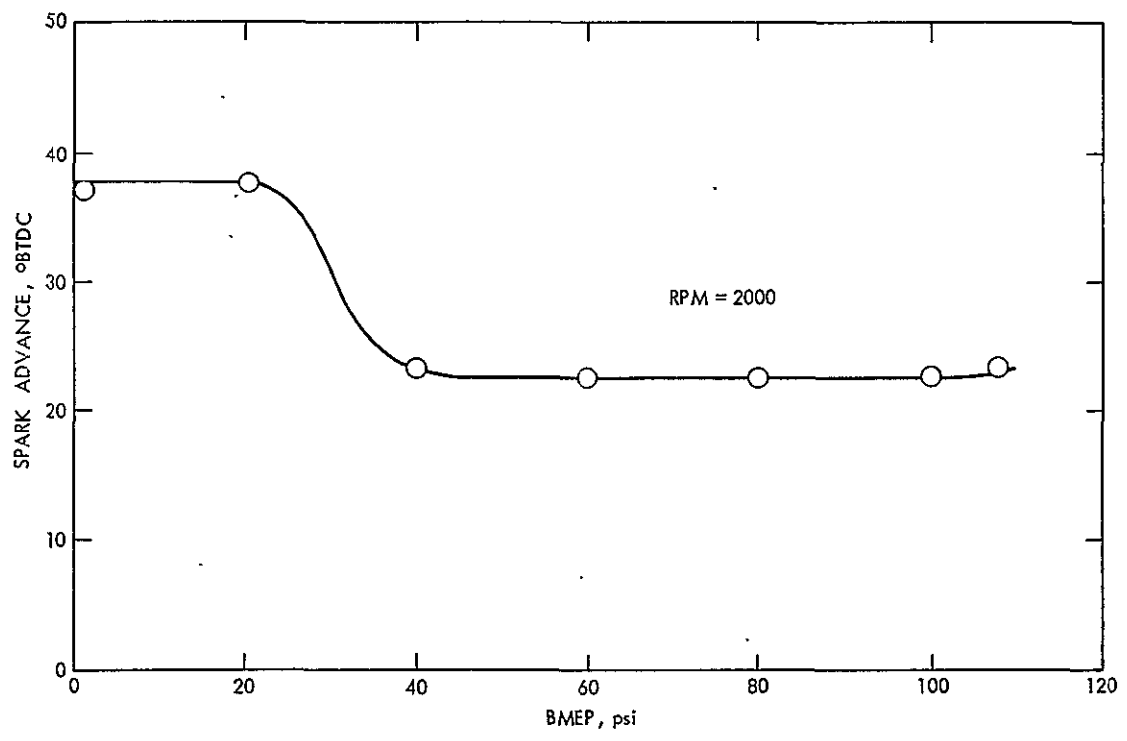
Figure 24. Spark Advance Versus BMEP for Stock Engine
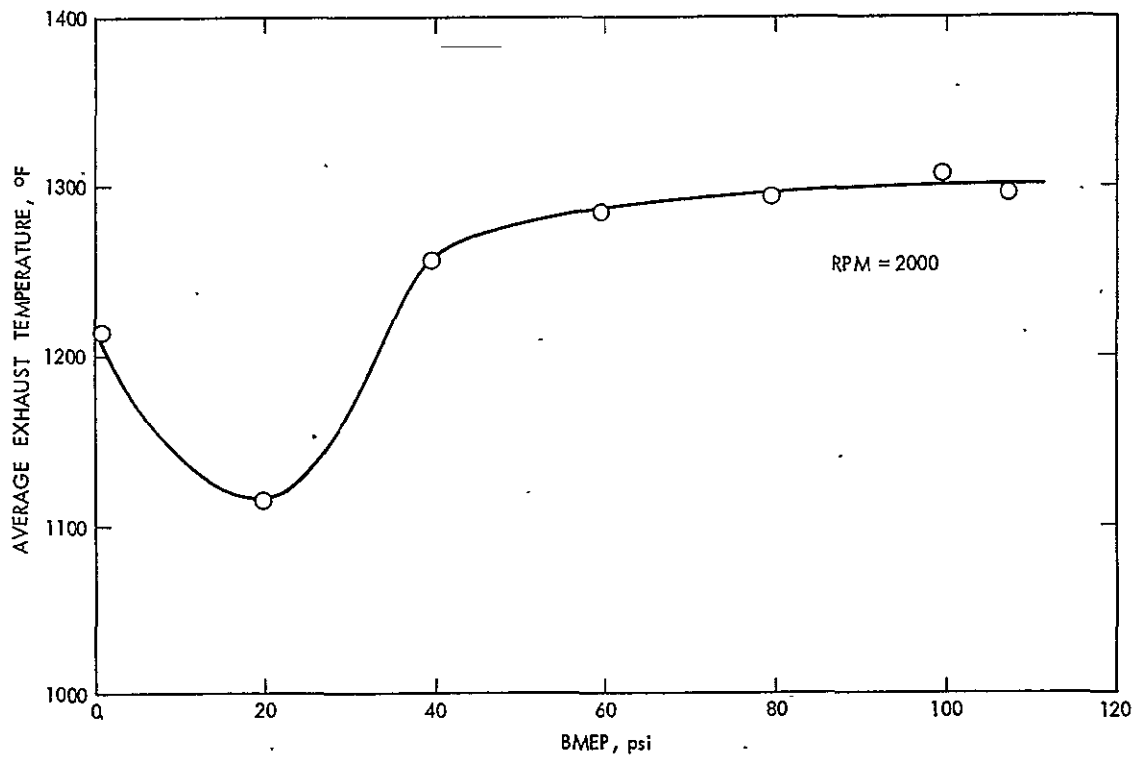
Figure 25. Average Exhaust Temperature Versus BMEP for Stock Engine

27

COLD-START EMISSIONS

BACKGROUND INFORMATION

Automobile manufacturers successfully met the 1975 California emissions standards, which were 0.9 g/mi HC, 9.0 g/mi CO, and 2.0 g/mi NO_x over the urban driving cycle. In general, these emissions levels were met by using exhaust gas recirculation (EGR) and spark retard for NO_x control, and catalytic converters for HC/CO control. The more stringent 1978 California emissions standards are 0.4 g/mi HC, 9.0 g/mi CO, and 1.5 g/mi NO_x over the urban driving cycle. In general, these standards are being met using similar emissions control techniques, except for the few production vehicles which are using the three-way catalyst approach. To maintain or improve air quality it will be necessary to impose even more stringent emissions standards in future years. In light of the recent energy crisis, it is imperative that these tighter emissions standards be met with little or no fuel economy penalty. The most stringent standards currently being proposed are the 0.41 g/mi HC, 3.4 g/mi CO, and 0.4 g/mi NO_x levels. To meet these standards will require significant improvements over existing production systems.

Although catalytic converters have demonstrated their effectiveness for controlling HC/CO emissions once they reach steady-state operating temperature, HC and CO emissions are still a problem during cold engine starting and warm-up conditions. For most automobiles equipped with catalytic converters, over 50 percent of the total HC/CO emissions are produced during the first several minutes of the urban driving cycle test while the engine is still cold. Thus, improved cold-start emissions devices and techniques potentially offer large payoffs in meeting stricter HC/CO standards.

The cold-start emissions problem is an especially difficult one since the system must provide effective control of HC/CO emissions only a few seconds after cranking a cold engine. The system must impose no severe driveability penalties, and it must have adequate durability. This problem is further complicated by the fact that some measures which are needed for NO_x emissions control and good fuel economy are detrimental to HC/CO emissions control.

This work included an evaluation of current production cold-start emissions systems (including the baseline vehicle system) as well as advanced systems which have been proposed to reduce cold-start emissions. Based on these evaluations, a modified cold-start system was implemented and tested.

Most of the candidate cold-start approaches which have been identified can be grouped under three categories: mixture control, combustion effects, and aftertreatment methods. Techniques which have been considered for improving mixture control include fuel atomization, fuel vaporization, closed-loop control, modified choke operation, and better intake manifold design. In approaches involving the combustion process, spark retard, EGR shut-off, and improved combustion chamber design have been shown to improve cold-start emissions performance. Aftertreatment methods which have been considered include exhaust port liners, air injection, thermal reactors, start catalysts, charcoal canisters, and fast warm-up of present catalyst systems.

Mixture Control

Good mixture control requires the delivery of a uniform distribution of homogeneous charges to the engine cylinders. Good equivalence ratio (ϕ) distribution must be maintained on both a cylinder-to-cylinder and cycle-to-cycle basis. Although the need for charge homogeneity and good ϕ distribution exists for all engine conditions, the requirement is more important during a cold start and warm-up of the engine, when engine heat is not readily available for charge preparation. The choking which is necessary in a cold start for good driveability increases the HC/CO emitted by the engine. These emissions cannot be adequately handled by the catalytic converter until it reaches its light-off temperature.

Many techniques show some promise of improving the quality of the fuel/ air mixture being delivered to the cylinders during a cold start. The best results will probably be achieved through the use of a combination of the approaches discussed here.

Atomization: The purpose of all atomization approaches is to disperse finely atomized fuel droplets into an airstream to produce a homogeneous charge. Many techniques (Ref. 6) have been developed for accomplishing this atomization. In an automotive application the atomized fuel droplets must remain suspended in the airstream as the mixture is distributed to the cylinders through the intake manifold. The impingement of fuel droplets on intake manifold walls and flow obstacles such as the throttle plate produces liquid-fuel films which hinder good distribution. Fuel droplet impingement is more severe during a cold start since the cold intake manifold is ineffective at vaporizing the fuel film.

Studies (Ref. 6) indicate that atomization to fuel droplet sizes of 10-20 microns is required to provide adequate droplet suspension in automobile intake systems. This level of fuel atomization, coupled with a low-impact intake manifold which is heated to improve fuel vaporization, should help minimize the liquid-fuel film. Manifold design will be discussed in a later section. Good atomization should reduce the need for ϕ enrichment (choking) during cold-start operation, and lessened choking should reduce HC/CO emissions.

Most atomization methods can be grouped according to the technique used to atomize the liquid: two-fluid atomization, pressure atomization, ultrasonic atomization, spinning-disc atomization, or electrostatic atomization. Some devices use combinations of these approaches to promote better fuel atomization.

The two-fluid atomization technique is based on atomizing the liquid fuel by the action of air on the liquid. In this method the droplet size produced decreases with increasing velocity of the atomizing air. To achieve droplet sizes in the desired 10-20 micron range requires air atomization velocities of about 500 ft/sec. Most conventional carburetors use venturi-type atomizers based on the two-fluid technique. Because of the wide range of air flow rates required by an engine, fixed-venturi carburetors tend to provide good fuel atomization only near their maximum flow rates. Some carefully designed multiple barrel carburetors (Refs. 7, 8) have been successful at achieving good fuel atomization over a broader operating range.

The new variable-throat sonic carburetor being developed by Dresser Industries (Refs. 9, 10) achieves its fuel atomization primarily by the two-fluid technique. The carburetor operates in the choked condition for manifold pressures of less than about 3 inches Hg, a level which maintains high air velocities for good atomization for most operating conditions. Fuel is supplied upstream of the throat so that fluid droplets pass through the high velocity throat region to be broken up. The airstream attains supersonic velocities just downstream of the throat and then passes through a normal shock wave to return to subsonic velocities. Further atomization of the fuel droplets occurs as they pass through this normal shock wave. In this system no downstream throttle plate is required since airflow is controlled by moving the fuel supply bar to adjust the carburetor throat area. The removal of the downstream throttle plate should help minimize the impingement of fuel droplets in the intake system.

The Hartmann-whistle atomizer (Ref. 11), currently under development for automotive use, is another two-fluid atomization technique. In this system a secondary flow of high-velocity air is supplied along with the fuel to a small resonating cavity which produces ultrasonic waves to aid in atomizing the fuel. This fuel/air mixture is then mixed with the primary engine air in a highly turbulent plenum. The air throttle is located upstream of the atomizer unit, an arrangement which should help reduce fuel impingement in the intake system.

Pressure atomization is based on the use of fuel pressure as the driving force for atomization. The most widely used form of this approach employs a swirl-type nozzle which produces a hollow, conically-shaped fuel spray. With this technique it is difficult to get droplet sizes less than 50 microns. This fact places certain limitations on its use in the automobile application. It would also require the use of a pressurized fuel supply.

In ultrasonic atomization, liquid fuel flows over a vibrating surface and is atomized by forces generated in the fluid by mechanical agitation. Fuel droplet size decreases with increasing agitation frequency, but the atomizing capacity per unit of atomizing surface falls off with increasing frequency. An ultrasonic atomizer operating at 100 kHz could deliver the desired 10-20 micron fuel droplets; however, this is near the upper frequency limit for good flow capacity.

In the spinning-disc atomization technique, droplets of fuel are thrown from the edge of a high-speed rotating disc into an airstream for atomization. Fuel droplet size decreases with increasing disc radius and disc RPM. At a disc speed of 45,000 RPM, a 2-inch-radius disc should be capable of providing 10-20 micron fuel droplets.

Electrostatic atomization is based on subjecting the free surface of fuel to an intense electric field. Although this technique shows promise, more research is required before it is ready for automotive application.

Vaporization: Because of intake manifold geometry and inadequate fuel atomization, engines frequently operate with liquid gasoline flowing along intake manifold walls. The presence of this liquid film in the intake system leads to large variations in ϕ between cylinders (Refs. 6, 12, 13). Some basic studies of mixture preparation (Refs. 13, 14, 15) have been carried out

using prevaporized fuel in premixed fuel/air mixtures to examine the benefits of good mixture control. In all cases the vaporized fuel system gave an improved cylinder-to-cylinder ϕ distribution; however, fuel vaporization alone is not adequate to eliminate maldistribution (Refs. 13, 16). Good mixing of the vaporized fuel with the airstream is still extremely important in achieving good distribution. In warmed-up engines, fuel vaporization consistently reduces CO emissions; however, in some cases only slight reductions in HC emissions are observed (Ref. 14). It is expected that significant reductions in HC/CO emissions during engine warm-up operation are possible through fuel vaporization.

Preheating all or part of the intake mixture has been used as a means of improving engine warm-up characteristics and aiding fuel vaporization during a cold start. Most current production vehicles have preheat systems which take energy from the exhaust manifold to increase the temperature of the inducted air. The systems are thermostatically controlled so that they operate only during engine warm-up. The preheating results in a loss in volumetric efficiency, but since it is used only during the warm-up mode, the loss is acceptable.

Some effort has been made to develop practical ways of implementing the fuel vaporization technique for mixture control. One such approach uses a heat pipe (Ref. 17) (Vapipe) which provides heat transfer from the exhaust gases to the intake fuel/air mixture. The fuel is vaporized as the fuel/air mixture passes over the tubes which form the condenser section of the heat pipe. Although Vapipe was developed for one specific engine, test results indicate significant improvements in economy and emissions, with good driveability. Some (Ref. 10) have expressed doubts that the Vapipe system could be used to reduce cold-start emissions because of the time required to bring the heat pipe to full operating temperature. It has been demonstrated (Ref. 17) that existing designs of the Vapipe can be brought from 32°F to full operating temperature within 1 minute. It is expected that, with further development, start-up time can be reduced.

Other systems (Refs. 10, 11, 18) transfer heat directly from the exhaust gas to a portion of the intake manifold to promote fuel vaporization. One system under development by Ethyl Corporation (Ref. 6) passes the entire primary fuel/air mixture through a small sheet metal box (hot-box) which is completely surrounded by the exhaust gas in the exhaust crossover area. During engine warm-up a thermostatically-controlled valve directs the exhaust gases through the crossover area. The valve reduces flow through the crossover once the engine is warm. Tests of this hot-box manifold have demonstrated good cylinder-to-cylinder ϕ distribution.

Most production vehicles utilize exhaust gases to heat a hot spot in the intake manifold during engine warm-up operation. This hot spot is usually located at a point where fuel impingement on the manifold wall is probably due to manifold geometry. Continuing work is being done in improving the effectiveness of the hot spot to develop an early-fuel-evaporation (EFE) system (Ref. 18). The objective of an EFE system is to achieve good fuel vaporization

20 seconds after an engine start so that the choke can be removed early, to reduce cold-start emissions. The three principal requirements in designing an EFE system are

(1) Use a heating surface with a low thermal mass to achieve fast temperature rise.

(2) Vaporize the fuel without heating the air.

(3) Maintain fuel contact with heating surface until vaporized.

Both exhaust gases and electrical energy (Ref. 19) have been used in experiments on advanced EFE systems. The results of these experiments have shown a considerable reduction in cold-start CO emissions, but only a slight reduction in cold-start HC emissions.

Closed-Loop Control: In recent years it has become increasingly important to provide better control of engine variables to as to meet the emissions constraints with increasing fuel economy. Some advanced emissions control devices, such as the three-way catalyst system, require very precise control of engine equivalence ratio for acceptable performance. The need for more flexible, precise control of engines has led to increased interest in the use of electronic controls on automobiles.

In the 1975 model year an electronic spark control system is being used with a lean-burn engine (Ref. 20) to achieve emissions control without the use of add-on devices. This system instantaneously senses engine condition, analyzes these inputs to determine the needed action, and produces the actuating signals needed to accomplish this action. The input signals used are (1) engine condition when started, (2) engine RPM, (3) intake manifold pressure, (4) throttle position, (5) rate of change of throttle position, (6) intake air temperature, and (7) coolant temperature. These inputs are used to determine the signal needed by the electronic distributor to fire the spark plugs at the optimum time for all engine conditions.

An active feedback control system which automatically selects the ϕ and spark advance for minimum fuel consumption is currently under development (Ref. 21). The controls adjust ϕ and spark advance to maximize output power, regardless of what caused the ϕ and spark advance to be off-optimum. For a fixed gasoline flow, optimizing for maximum power also results in best fuel economy. Although this particular system is set up for a lean-burn engine application, similar type closed-loop control systems could be developed using other control strategies. A more flexible means of controlling ϕ and spark advance during engine warm-up would no doubt result in better fuel economy and reduced emissions.

In the use of thermal manifold reactors for emissions control, tests (Ref. 22) indicate a significant improvement in CO emissions control when a modulated secondary air system is used. The secondary air is controlled to maintain a constant tailpipe air/fuel ratio by sensing engine RPM and intake manifold pressure. Carbon monoxide emissions are reduced for both cold-start and warmed-up engine operation.

Closed-loop controls have been used in tests of the three-way catalyst emissions control systems (Ref. 23). In three-way or dual catalyst systems, it is necessary to maintain $\phi = 1.0$ within very close tolerances for proper catalyst effectiveness. In these tests an oxygen sensor in the exhaust manifold was used to control the fuel injection system. The durability of the oxygen sensor and the catalyst systems used in this approach have not been proven at this time.

Modified Choke Operation: When a cold engine is being started, much of the fuel delivered by the carburetor impinges on the cold walls of the intake manifold because of inadequate atomization and vaporization. To insure an adequate fuel supply to the cylinders, a choke is used to restrict the flow of air and supply a rich mixture during warm-up. As the engines warms up, the choke is opened by a thermostatically-controlled valve.

With the current HC/CO emissions standards, it has become necessary to lean the choke calibrations in order to minimize HC/CO emissions during warm-up. It is also desirable to minimize the time that the choke stays on. Some production vehicles use an electric heating element to assist the engine heat in shortening choke duration. Even with these choke modifications, approximately 50 percent of the HC/CO emissions produced during the urban driving cycle occur during engine warm-up.

Much work is being done on early-fuel-evaporation systems (Ref. 18) which would make a quick choke possible. Significant modifications in choke operation must await implementation of improved early-fuel-evaporation systems.

Intake System Design: Some of the methods of mixture control which have been discussed are closely related to intake system design. Studies (Ref. 6) have indicated that it is desirable to have an intake system which is free of obstacles such as throttle plates. Many times intake manifold geometry is determined by the space available, which leads to the use of nonoptimum shapes. Most current automobiles have the throttle plate downstream of the carburetor and have at least one sharp bend in the intake manifold, leading to fuel impingement and poor distribution. Some advanced carburetor designs (Ref. 9) have air throttles upstream of the fuel introduction point, and this results in less fuel impingement.

To alleviate the problem of fuel impingement in the intake manifold, much effort (Refs. 11, 18) is being made to improve the design of intake manifold hot spots and to develop more advanced early-fuel-evaporation systems. These systems are especially important during cold-start operation when the intake manifold is cold.

Another promising design under development is the three-barrel carburetor and dual induction manifold system (Ref. 7). The three-barrel carburetor has a small primary venturi for idle and light-load operation with two secondary barrels to provide full power. This carburetor gives better fuel atomization over a range of engine operating conditions. The dual manifold system uses high velocities for good mixing and increased evaporation. A small diameter manifold supplied by the primary barrel of the three-barrel carburetor supplies mixtures to the engine during idle and light-load operation. A separate large diameter manifold supplied by the two secondary barrels of the carburetor is used for full power.

33

Combustion Methods

Once the fuel/air mixture has been prepared in the engine intake system, the HC/CO emissions which leave the engine are determined by the combustion chamber geometry and the combustion process itself. The amount of exhaust gas recirculation (EGR) used and the spark timing strategy have first-order effects on the emissions characteristics of the engine. Other engine factors such as combustion chamber shape, crevice volume, and valve overlap can also be important aspects of an engine design. Discussion in the following sections will be limited to consideration of EGR and spark timing effects.

Spark Control: Many aftertreatment techniques for control of HC/CO emissions require that the exhaust system be warmed up before they become effective. During cold-start operation it is important to minimize the time required for this warm-up process. Spark retard during engine warm-up has been used effectively to increase exhaust temperatures (Ref. 19). When used in conjunction with air-injected reactors, this increased exhaust temperature helps promote thermal reaction of HC/CO by warming up the system much faster. When spark retard is used with catalyst systems, the higher exhaust temperatures speed catalyst warm-up and lead to high catalyst conversion efficiencies earlier after engine starting. The amount and duration of the spark retard required depend on each particular application. An anti-stall device is used to deactivate the system when manifold vacuum falls below a set value to minimize stalling and improve driveability during engine warm-up.

In addition to having an effect on the HC/CO conversion efficiency of catalysts and thermal reactors during engine warm-up, spark retard also affects the amount of HC emissions which leave the combustion chamber. Spark retard causes more of the combustion process to occur during the expansion stroke, and this reduces the HC emissions due to the decreased surface/volume during combustion (Ref. 24). Spark retard has little effect on CO emissions except at very retarded timing where there is insufficient time to complete CO oxidation.

EGR Shut-Off: Exhaust gas recirculation has been used effectively as a means of controlling NO_x emissions; however, there are several reasons why it is not desirable during cold-start operation. First, EGR adversely affects vehicle driveability, which is already somewhat impaired with a cold engine. Secondly, EGR dilutes the mixture, and this yields lower combustion temperatures and aggravates HC emissions (Ref. 25). In some applications a time delay switch is used to deactivate the EGR during the warm-up period of a cold start.

Aftertreatment Methods

Hydrocarbon and carbon monoxide emissions that are produced in an engine can be reduced by various aftertreatment techniques. The most important aftertreatment device in current use is the oxidation catalyst. Although oxidation catalysts have demonstrated their effectiveness for controlling HC/CO emissions once they reach steady-state operating temperature, HC/CO emissions still pose a problem during engine starting and warm-up operation.

In general, aftertreatment methods attempt to promote additional HC/CO oxidation in the exhaust system. Factors which are needed for effective

oxidation are an excess of oxidizing agent (air), a high exhaust temperature, sufficient residence time, and perhaps the presence of catalytic material. The requirements for a high exhaust temperature and/or a warm catalyst bed make these methods less effective for controlling cold-start HC/CO emissions.

Aftertreatment methods which have been considered include exhaust port liners, air injection, thermal reactors, start catalysts, charcoal canisters, and fast warm-up of present catalyst systems. These techniques are discussed briefly in the following sections.

Exhaust Port Liners: Insulating exhaust ports and exhaust manifolds with internal liners is a simple and effective way to maintain high temperatures in the exhaust system. This is especially important during cold-start operation, when the exhaust system (including the exhaust catalyst) is cold. The insulation provided by the exhaust system liners reduces the thermal energy loss of the exhaust products during the first few minutes of engine operation. This has the effect of decreasing the catalyst warm-up time. Tests (Ref. 8) have shown that the addition of exhaust port liners reduces HC emissions by 10-20 percent. Insulating the exhaust pipes and increasing the exhaust manifold volume by 2-1/2 times resulted in an additional 20-40 percent reduction in HC emissions.

One potential drawback of this approach may occur under steady-state operation. Under high speed/load conditions, the increased exhaust temperatures may lead to reduced catalyst life. It is not clear how much hotter catalyst bed temperatures will run in this case since the increased exhaust temperatures will cause additional HC reaction to occur upstream of the catalyst bed.

Air Injection: Many current vehicles, especially those sold in California, use air injection into the exhaust manifold as a means of supplying the excess air needed for HC/CO oxidation. Although simple in principle, controlling the air injection flow rate to get maximum effectiveness in oxidizing hydrocarbons and carbon monoxide presents a difficult problem. As previously mentioned, high exhaust temperatures and a sufficient residence time are also required for effective oxidation to take place.

Single-cylinder engine and vehicle studies (Ref. 26) have demonstrated that the temperature, composition, and residence time of the exhaust gas-air mixture are the basic factors which determine the effectiveness of air injection and the type of oxidation process which occurs in the exhaust system. Both luminous and nonluminous oxidation have been observed. These basic factors are affected by engine spark timing and equivalence ratio, insulation and size of the exhaust manifolds, flow rate and temperature of the injected air, and the warm-up characteristics of the air injection system.

It was found that the lowest HC/CO emissions obtained with air injection were achieved in the luminous oxidation regime (equivalence ratios between 1.05 and 1.30). In the past this fact has led to the use of rich carburetor calibrations to help with emissions control. Efforts have been made to extend the luminous oxidation regime to lower equivalence ratios to get better fuel economy while maintaining the desirable emissions control characteristics.

The optimum air flow requirements for HC and CO emissions reduction were about the same in the luminous oxidation regime; however, the optimum air flow requirement for CO was four to five times greater than the optimum air flow requirement for HC when in the nonluminous oxidation regime ($\phi<1.05$). Since carburetors typically have nonlinear calibrations, it is usually necessary to optimize the air injection flow rate to obtain either the lowest HC or CO emissions. At any rate, some compromise is required in setting up a control strategy. Modulated air injection systems have shown advantages in controlling HC/CO emissions by maintaining a constant tailpipe air/fuel ratio.

The desire to achieve better efficiencies from air-injected reactors at leaner equivalence ratios has led to studies (Ref. 27) of ways to improve the mixing of the injected air with the exhaust gas. It was found that improved mixing of the secondary air and exhaust gas can substantially increase the HC/CO conversion efficiency.

Although air injection can be very effective in oxidizing HC and CO in the engine exhaust under favorable temperature and composition conditions, its cold-start performance is limited by the warm-up characteristics of the exhaust system. Air injection alone cannot be used for cold-start emissions control; it must be combined with other techniques such as exhaust port and manifold insulation, spark retard, etc. if it is to be effective.

Thermal Reactors: Thermal reactors are exhaust system elements that attempt to maintain a high exhaust temperature in the presence of air for sufficient time to oxidize the HC/CO in the exhaust. Studies (Ref. 26) have shown that thermal reactors are better at reducing HC/CO emissions when engines are operated in the rich regime ($1.05 <\phi< 1.30$). This results in a significant fuel economy penalty for systems using the thermal reactor. The recent interest in fuel economy has led to an increased interest in lean-burning thermal reactors (Ref. 28).

Not much information is available on the operating characteristics of lean-burning thermal reactors. A lean-burning reactor will be temperature limited to slightly above the exhaust temperature. Additional work is required to help understand the important influences and how to separate their effects to optimize lean-burning reactor systems.

The large reactor volumes required to get the needed residence time make thermal reactors produce relatively large quantities of cold-start emissions. This fact makes good insulation and a low thermal mass almost mandatory for thermal reactor systems.

Charcoal Canisters: Charcoal is available in numerous types and in various mesh sizes. Charcoal is used commercially for scrubbing organic vapors of all types, e.g., halides, carbonyls, aromatics, paraffins, etc., from gaseous streams prior to venting. Many of the processes in use reclaim the adsorbed organic species after the charcoal bed becomes saturated (which is indicated by the "breakthrough" of the organic species downstream from the bed). The common procedure for removing the organic compounds requires heating of the charcoal and usually this is accompanied by steam, for which charcoal has very little affinity. To maintain the greatest working adsorptive capacity of the charcoal, it is desirable to be able to clean off as much of

36

the adsorbed species at as low a temperature as possible without suffering degradation of the adsorbed species after the charcoal has become saturated. It is important to note that charcoal operating under dynamic conditions has different adsorptive properties than under static conditions. In determining the effectiveness of a charcoal adsorber, the properties of the gaseous stream passing through the charcoal - its temperature, pressure, velocity, moisture content, and concentration of the gases to be adsorbed - are as important as the type and size of charcoal, its moisture content and reactivity.

A charcoal canister on an engine exhaust would be required to function under conditions involving all of the above parameters which apply to a dynamic system. However, two additional problems arise: continuous and high moisture content of the gaseous stream and the range of temperatures encountered during engine warm-up. The effect of the first would be to desorb all adsorbed hydrocarbons. The desorption would be a function of the rate of increase in steam temperature, the amount and activity of charcoal used, and the concentration of hydrocarbons. Increasing temperature can cause serious deterioration of the charcoal's adsorbing surface; oxidation, and possibly combustion, will take place at the higher temperatures (~750°F). The charcoal used in this application must meet special requirements; it must

    (1)   Not oxidize readily at lower temperatures (660-750°F is acceptable).

    (2)   Have high affinity for saturated, unsaturated, and oxygenated hydrocarbons.

    (3)   Be in a form which will create little backpressure in the exhaust system.

    (4)   Have a high working capacity (i.e., adsorption, desorption).

In addition, the ideal system would necessarily have excellent high temperature valves to allow bypassing the carbon canister after engine warm-up. Provision should also be made to permit flushing the canister back into the exhaust system upstream of the catalyst bed. The length of time during which the exhaust could be diverted through the canister before hydrocarbon breakthrough and oxidation of the carbon occur would depend on the size of the carbon bed, concentration of hydrocarbons, adsorptive character of the carbon, oxidation point of the carbon, rate of increase in temperature, and steam content of the exhaust gas. Any degradation of the charcoal or deposition of polymers on metal particulates will change the working ability of the charcoal and could destroy it. It must be stressed that this system is merely a storage system for hydrocarbons and does not oxidize hydrocarbons nor does it store carbon monoxide. The removal of carbon monoxide during cold starts is not affected by the use of charcoal canisters.

Exhaust Catalysts: Improvements in reducing the cold-start hydrocarbon concentrations by dual and three-way catalyst systems can be achieved by many

of the same methods. The various avenues available for improving cold-start catalytic activity include

(1) More active oxidation catalysts which "light-off" at lower temperatures (300-400°F).

(2) Catalyst beds electrically heated for faster activation.

(3) More heat resistant catalysts, located closer to or in the exhaust manifold either alone or in conjunction with either of the two catalyst systems.

(4) Secondary catalysts used only for cold-start periods and which are more active than the primary catalysts that are located in the exhaust system.

Any increase in activity in the catalytic oxidation at lower temperatures must not reduce the maximum temperature durability of the catalyst. An increase in operating temperature range is presently being pursued by industry; however, the most recent advances in this area are proprietary.

It must be emphasized that at the lower light-off temperatures achievable by these two catalyst systems, the ability to start the engine richer and thereby aid in shortening the start-up time with the dual catalyst is not now applicable to the three-way catalyst. However, if a bypass of the signal from the oxygen sensor in the three-way catalyst system were available during start-up, richer conditions might then be applied to it also. The extent to which decreasing the air/fuel ratio results in a gain in shorter light-off time and lower hydrocarbon concentrations during cold start is not known at this time.

Electrical heating of the catalyst to improve its cold-start performance is not a new concept, but some novel approaches make this method worthy of further investigation. Use of a non-noble metal for current conduction to heat the exhaust gases prior to entry into the oxidation catalyst is one scheme which looks promising. Another possibility is to use a semiconductor as the catalyst support and heat the catalyst directly by passing the current through the support.

The use of a secondary, "fast-start" catalyst for cold starts has the advantage that, being located close to the exhaust manifold, the catalyst heats up faster. However, a disadvantage of this system is that valves are needed in the exhaust system to direct the flow through the secondary catalyst until the exhaust reaches the temperature at which the primary catalyst can oxidize the hydrocarbons. Its capability for removing cold-start hydrocarbons should, however, be examined.

In general, the improvement of the catalyst in order to reduce cold-start hydrocarbon emissions offers several viable alternatives and at the same time reduces carbon monoxide concentration.

MODIFIED COLD-START SYSTEM

The cold-start system on the baseline Plymouth vehicle is discussed in Section II. Other production cold-start systems have been analyzed, as have proposed advanced systems for controlling cold-start emissions. Based on these evaluations, a modified cold-start system was selected for implementation and testing on the vehicle. Modifications were made in mixture preparation, exhaust energy flow, catalyst performance, and choke operation. A block diagram of the modified cold-start system is given in Figure 26.

Intake manifold changes were made to improve the effectiveness of the manifold hot spot. In the stock configuration the hot spot is located directly under the carburetor and is heated by exhaust gases directed to the hot spot plenum by a thermostatically-controlled heat control valve in the exhaust manifold. The incoming fuel/air mixture impinges directly on the hot spot area before making a 90-degree turn into the manifold runners. The exhaust gas recirculation (EGR) entrance tube is located in the center of the hot spot and directs the EGR into the intake manifold in a direction opposite to that of the incoming fuel/air mixture. The stock manifold is quite massive in the hot spot area, which results in a slow warm-up. To augment this method of heating the hot spot, an electrically-heated coil was installed in the hot spot area in the floor of the manifold. This supplies additional energy for fuel vaporization until the exhaust gases have time to heat the floor of the intake manifold.

The EGR shutoff control was studied through a series of sensitivity tests to determine the best emissions performance. The amount and duration of choke operation was also examined during engine warm-up. A more flexible method of control for spark advance was implemented to permit an evaluation of alternate cold-start spark advance strategies.

Improvements in catalyst effectiveness during cold-start operation were accomplished by providing for a fast warm-up of the existing stock catalyst unit and installing a start catalyst to be used only during engine starting and warm-up. These two approaches permitted an evaluation of the relative merits of these alternatives. Flow through the start catalyst was controlled by a damper valve which responds to the bed temperature in the start catalyst unit. This provides protection against overheating of the start catalyst.

The stock catalyst unit contains two ceramic monolithic elements which are coated with a catalytic agent consisting of a mixture of palladium and platinum. This catalyst unit was modified to permit the installation of an additional heated monolithic element to decrease the catalyst warm-up time. This auxiliary heating was accomplished electrically with the energy being supplied by an external power supply.

EGR COLD-START CONTROL

The baseline emission control system has a means for preventing operation of the EGR system during the warm-up period after a cold start. As previously discussed, this is desirable for several reasons. EGR adversely affects driveability, which, with a cold engine, is already impaired. The addition of EGR to the fuel/air mixture lowers combustion temperatures and leads to higher HC emissions.

39
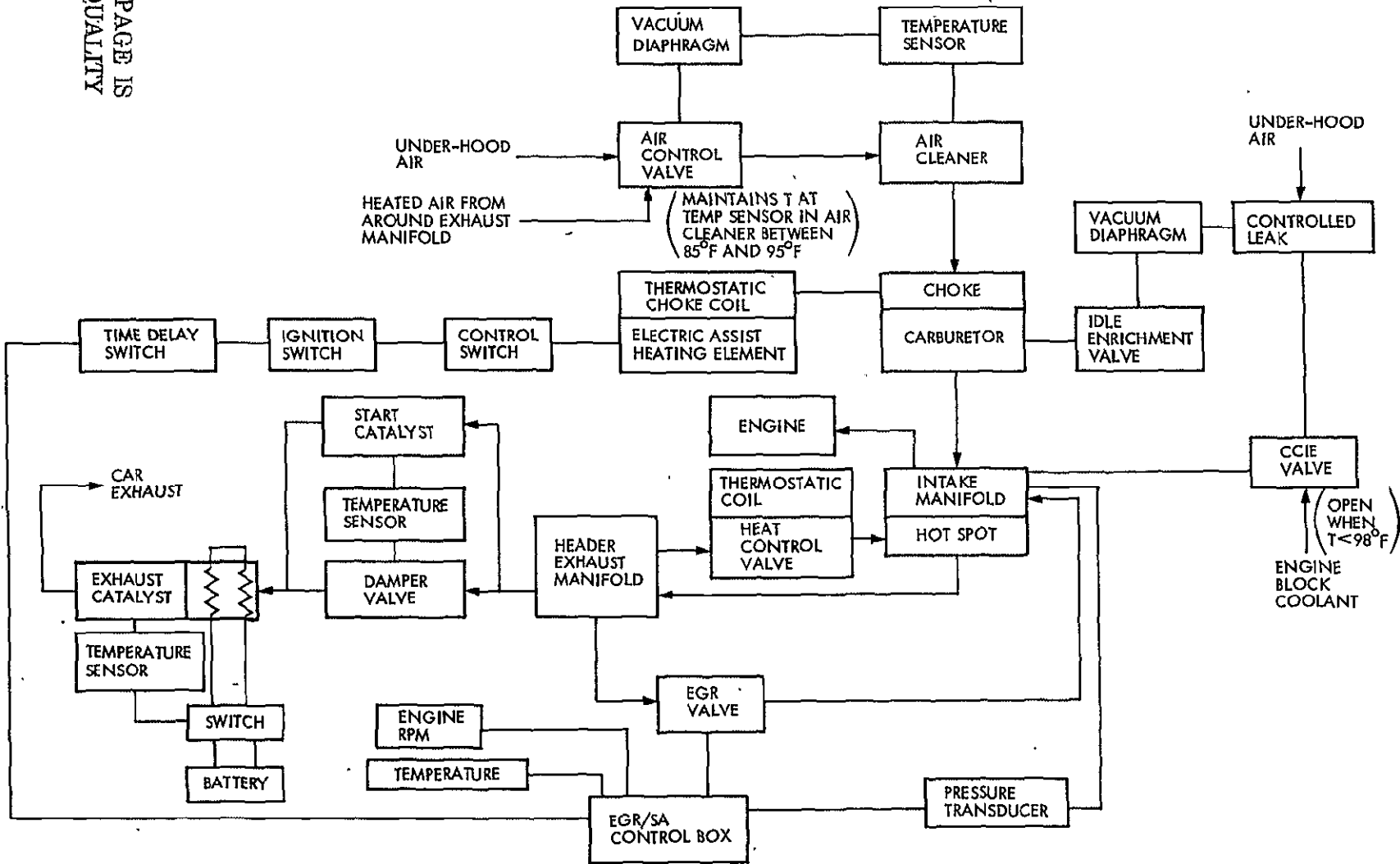
Figure 26. Modified Cold-Start System for 6-Cylinder 1975 Plymouth

In the baseline system, an EGR delay solenoid is energized by the starter solenoid and closes the line between the intake manifold and the vacuum amplifier. A time delay switch deactivates the EGR delay solenoid after about 30 seconds of engine operation. When the delay solenoid is deactivated, manifold pressure is supplied to the vacuum amplifier which in turn provides a control signal to the EGR valve.

Four tests were made to examine the effect of the EGR delay time on cold-start emissions. In the urban driving cycle, the engine remains at idle for about 20 seconds before accelerating up the first ramp of the cycle. The stock time delay of about 30 seconds permits the vehicle to start the first acceleration ramp without EGR. This helps minimize any driveability problems during this initial acceleration and also provides some engine warm-up before starting EGR flow. EGR flow is needed before any heavy accelerations to help control NO_x emissions. The sensitivity tests covered delay times from 30 seconds to 120 seconds.

Results of the sensitivity tests are given in Table 8. Emissions are expressed in grams per phase. Comparisons of the total HC and CO emissions for the cold transient portion of the urban driving cycle (first 505 seconds) are given in Figure 27. Two sets of baseline data are provided for comparison with the results for the modified control strategies. The vehicle baseline data represents an average of the data from three full urban driving cycle tests made at the Subaru test facility. The second baseline shown is a result of testing the stock engine/transmission at JPL on the eddy current (EC) dynamometer at the time the sensitivity tests were being made. The results indicate little or no improvement in cold-start emissions with an increase in EGR delay time. Indeed, the 90- and 120-second delay times result in higher HC and CO emissions than the stock baseline. For the 60-second delay time, HC emissions are slightly lower than the baseline values, but CO emissions are higher. The data from these tests does not support any change in the stock EGR delay time.

Continuous mode data was taken during the driving cycle tests to aid in understanding system operation. Some samples of this data are presented here. All plots show data for the first 130 seconds of the driving cycle since this period is of prime interest for cold-start emissions. The vehicle speed trace is shown in Figure 28. Time starts when the engine is cranked. Note the 20-second idle time before accelerating up the first ramp.

Comparison plots are shown for the tests with EGR delay times of 30, 90, and 120 seconds. The control pressure for the EGR valve is shown in Figure 29. This parameter remains at zero until the time delay switch deactivates the EGR delay solenoid to start EGR operation. This plot shows that the proper EGR switching was accomplished in these tests. Choke operation is shown in Figure 30. The 80 percent position for the choke corresponds to the wide-open choke case. The choke was removed after the first 90 seconds of the run in all three tests. The test data for the EGR delay time of 90 seconds indicates more choking of the engine during the first 20-30 seconds of the test. This would tend to aggravate the HC emissions problem for this test and could be one of the reasons for the higher HC emissions in bag 1 as shown in Table 8. The catalyst bed temperature is given in Figure 31. The catalyst bed temperature reaches its operating temperature faster for the stock EGR delay time. This factor acts to negate any decrease in HC emissions

41
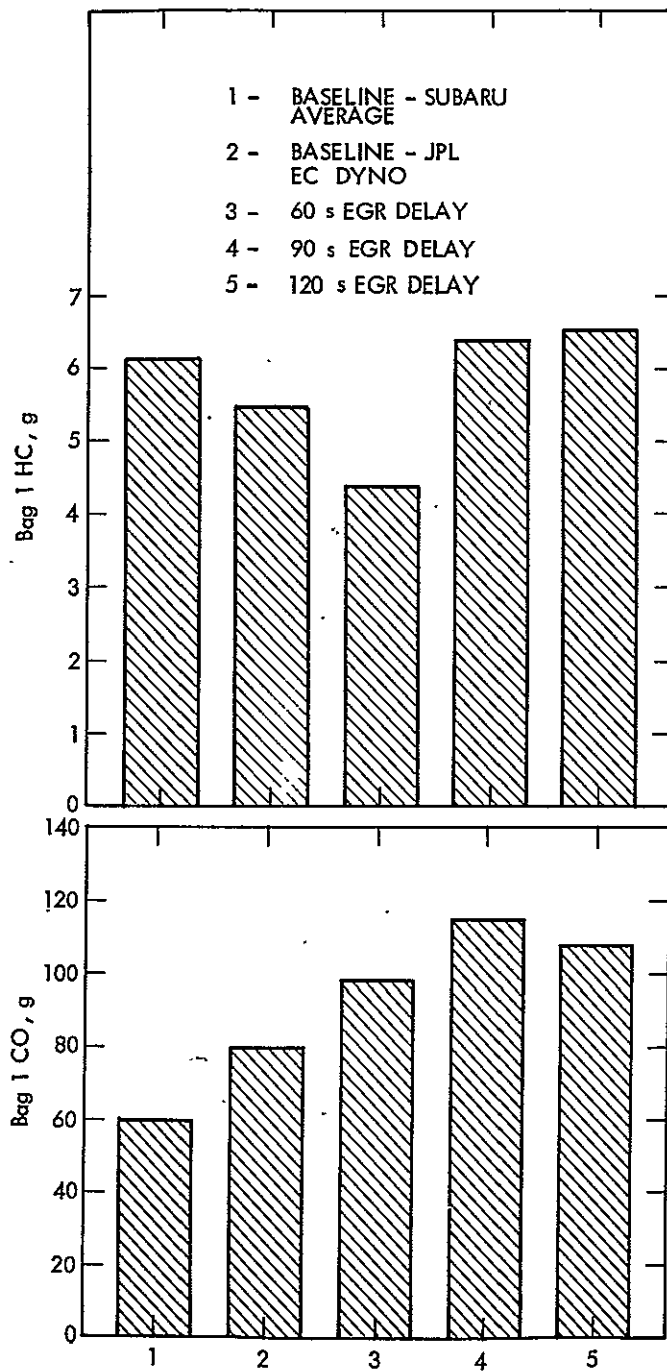
Figure 27. Effect of EGR Shut-Off on Cold-Start Emissions
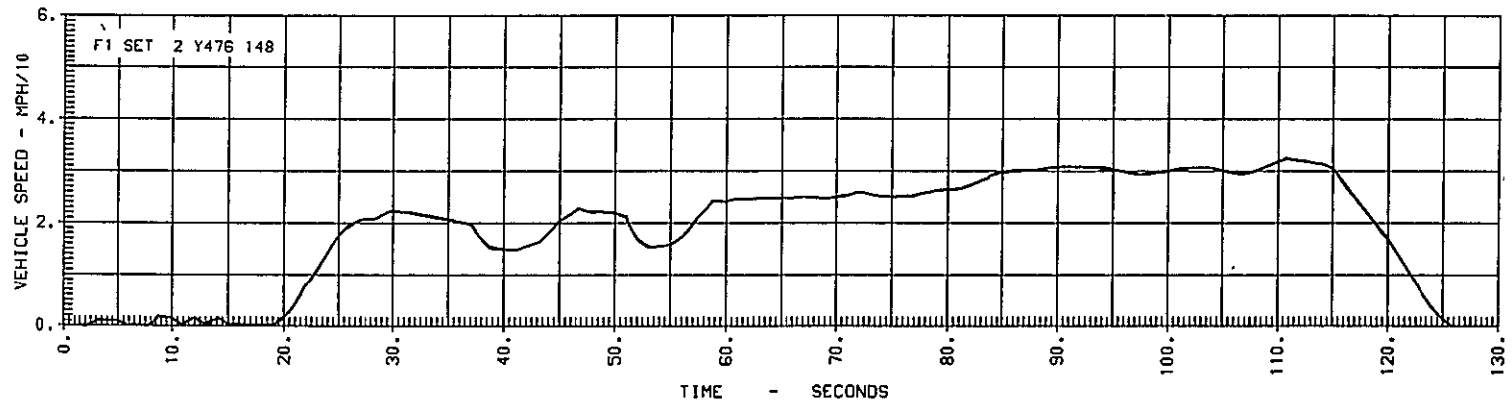
Figure 28. Vehicle Speed Versus Time For Urban Driving Cycle
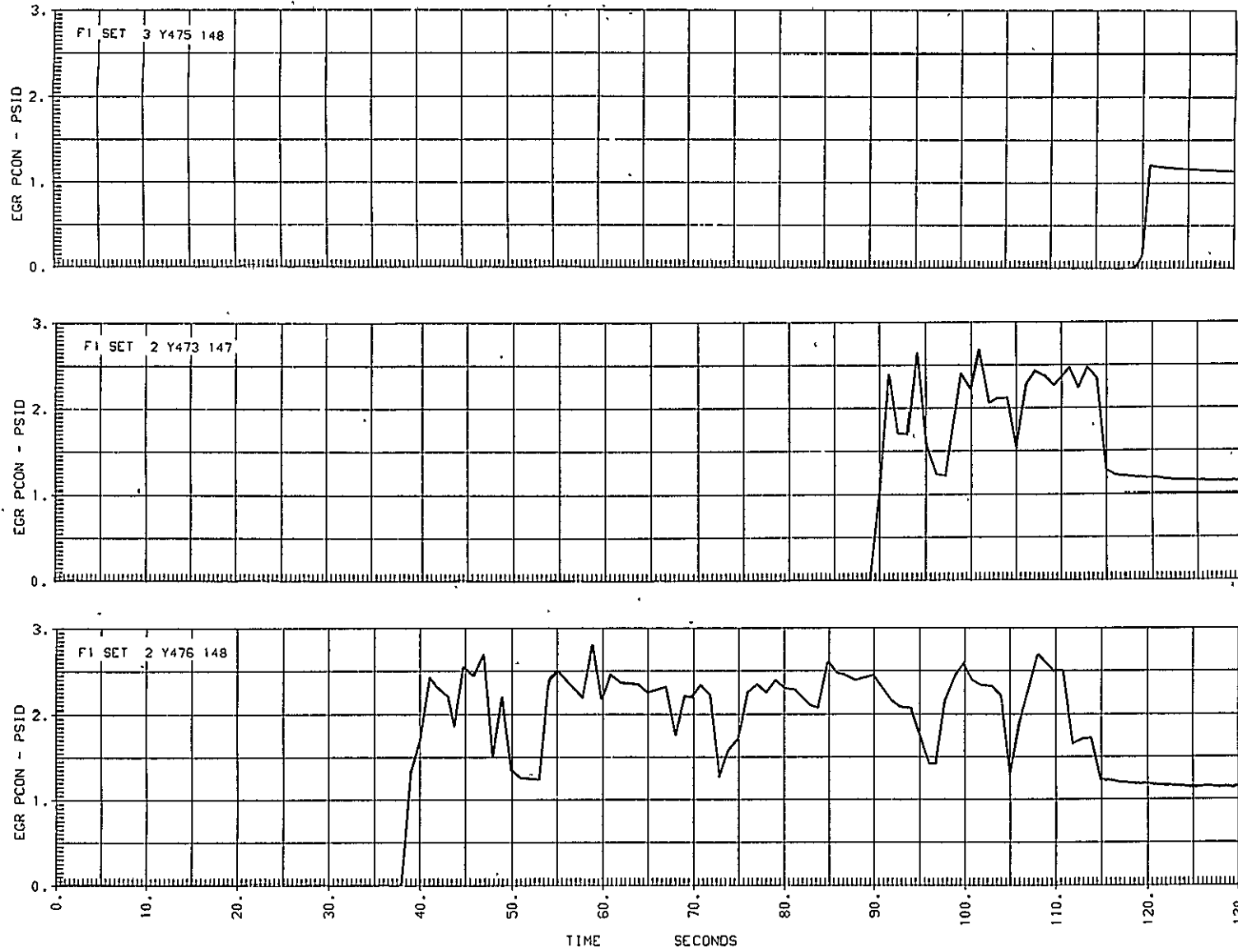
Figure 29.   Control Pressure for EGR Valve

44

45
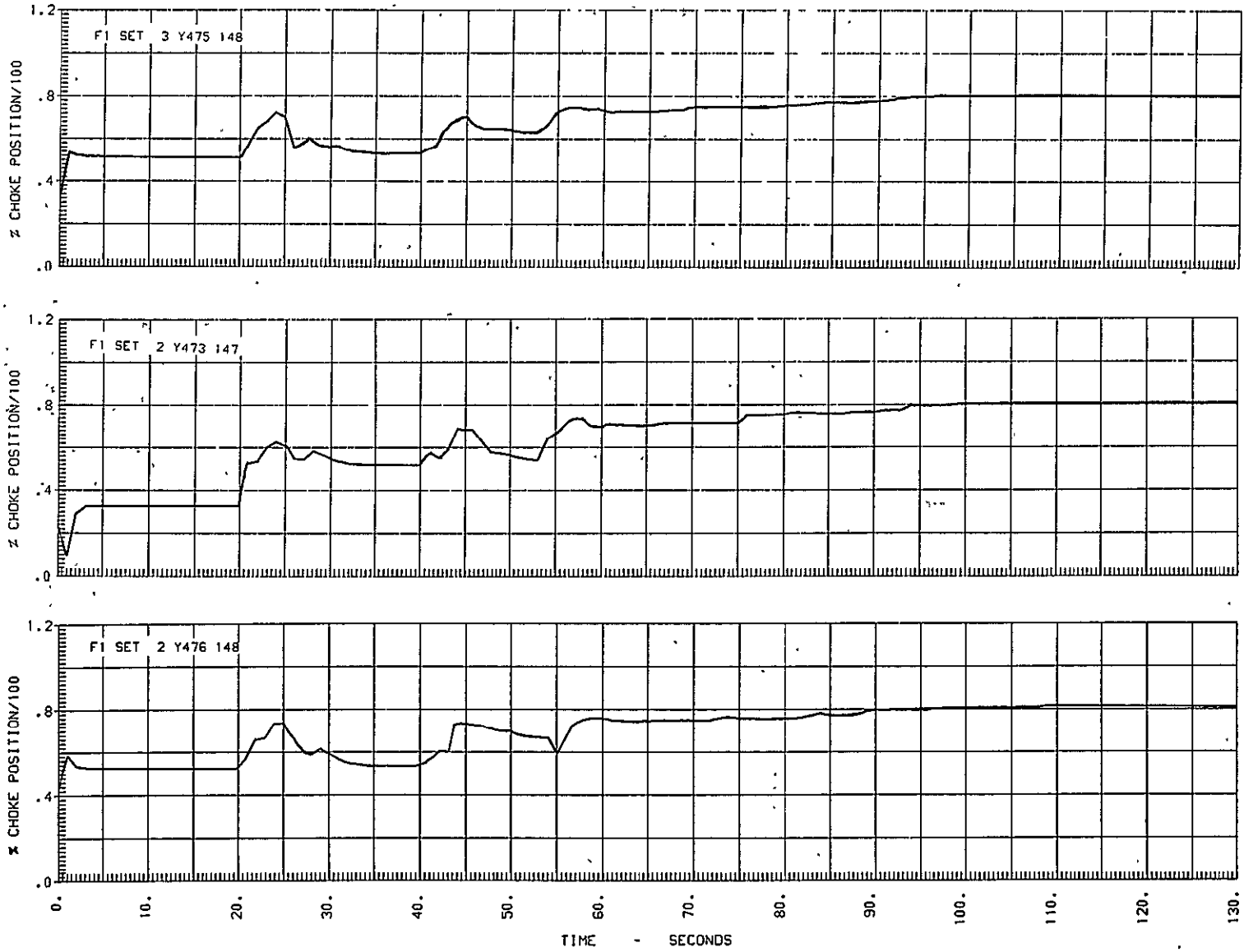
Figure 30. Choke Characteristics

F1 SET 3 Y475 148

F1 SET 2 Y473 147

F1 SET 2 Y476 148

TIME — SECONDS
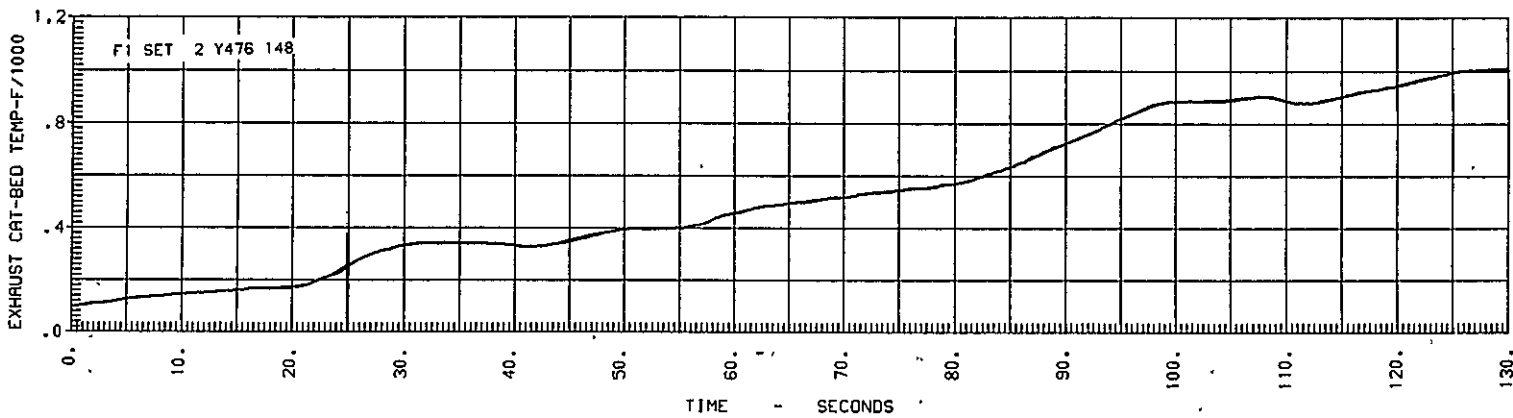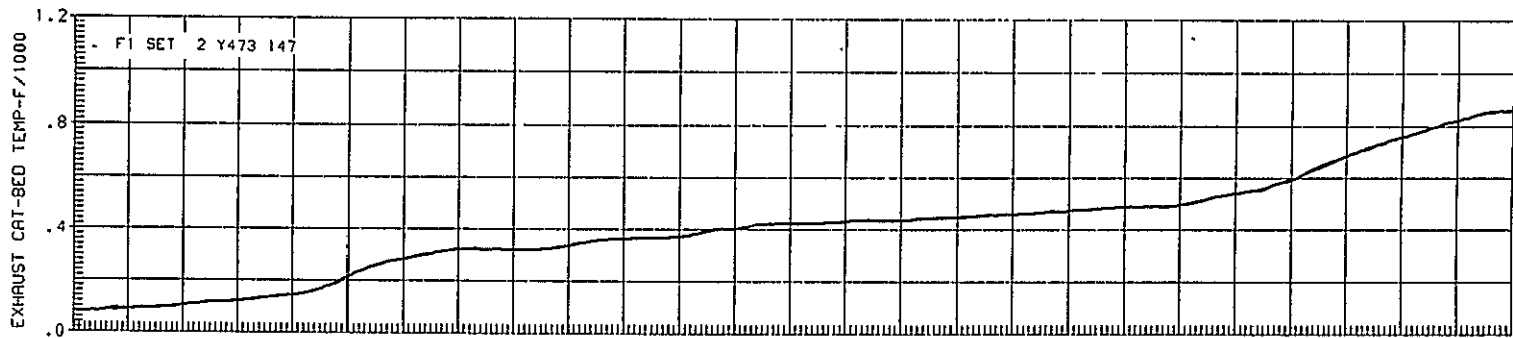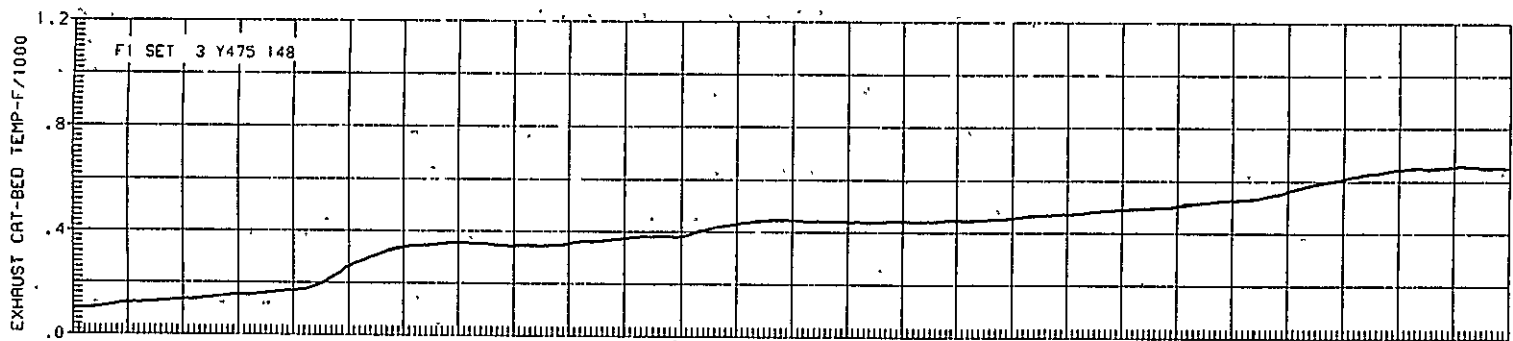
Figure 31. Catalyst Bed Temperature

Table 8. Cold-Start Emissions Tests: EGR Shut-Off Results
for Cold 505 Federal Urban Driving Cycle

Day	Tape	Phase	NO_x(g)	CO(g)	HC(g)	Comments
6148	Y476	g/bag 1	0.54	55.95	3.60	Stock system. EGR system
		g/bag 2	1.92	22.38	1.37	becomes operational at 29
		g/bag 3	0.94	1.42	0.45	seconds into the run.
		TOTAL g/bag	3.4	79.75	5.42	
6147	Y472	g/bag 1	0.73	76.29	3.23	EGR system turned on at
		g/bag 2	2.45	16.52	0.95	60 seconds into the run.
		g/bag 3	1.28	3.65	0.20	
		TOTAL g/bag	4.46	96.46	4.38	
6147	Y473	g/bag 1	0.80	94.50	4.49	EGR system turned on at
		g/bag 2	2.22	18.85	1.38	90 seconds into the run.
		g/bag 3	1.16	2.45	0.51	
		TOTAL g/bag	4.18	114.9	6.38	
6148	Y475	g/bag 1	1.14	77.13	3.79	EGR system turned on at
		g/bag 2	2.13	28.31	2.17	120 seconds into the run.
		g/bag 3	1.05	2.22	0.54	
		TOTAL g/bag	4.32	107.66	6.5	

from the engine achieved with an increased EGR delay time. Hydrocarbon emissions measured downstream of the catalyst are shown in Figure 32.

INTAKE MANIFOLD HOT SPOT MODIFICATION

The baseline engine has a hot spot area in the intake manifold to improve vaporization of the incoming fuel when the engine is cold. After leaving the carburetor, the fuel-air mixture is directed vertically downward into the intake manifold. The flow then impinges directly on the hot spot in the floor of the manifold, turns 90 degrees and then flows through the manifold runners into the cylinders. The hot spot area of the intake manifold is heated from below by exhaust gases. A thermostatically-controlled heat control valve in the exhaust manifold directs hot exhaust gases to the hot spot area during engine warm-up operation.

With a cold engine, it is necessary to provide an adequate gasoline vapor/air ratio to the cylinders for good engine operation. Because of liquid condensation on the cold walls of the intake manifold, this vapor/air ratio may be considerably less than the fuel/air ratio of the mixture leaving the carburetor. With the stock hot spot region, it is still necessary to apply the choke with a cold engine to provide an adequate vapor/air ratio for the engine. The choke causes a much richer gasoline/air mixture to be produced by the carburetor. Changes in choke control strategy must be considered jointly with improvements in the effectiveness of the intake manifold hot spot.

47
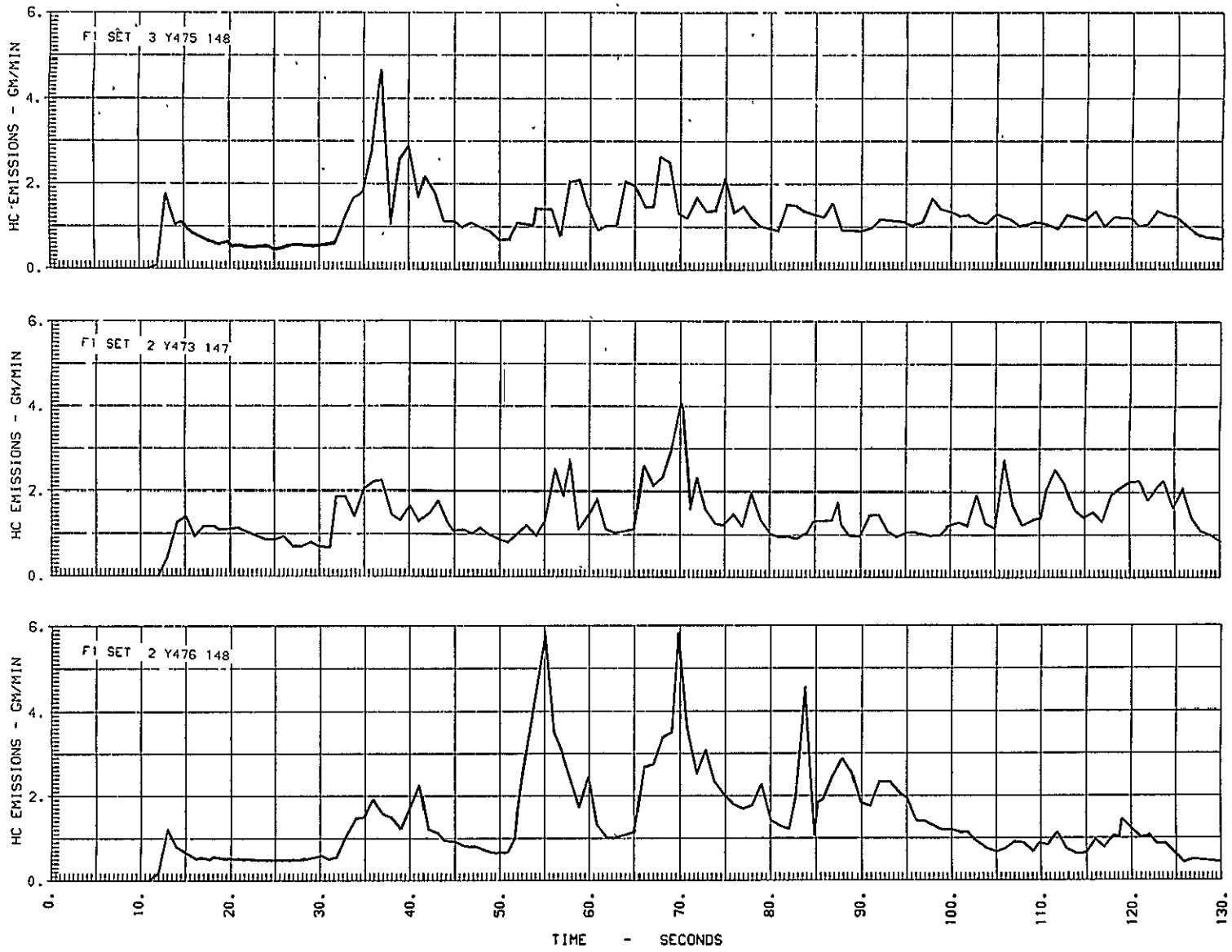
Figure 32. Hydrocarbon Emission Characteristics

Three tests were made to determine the effect of an improved hot spot on cold-start emissions. To supplement the stock hot spot system, a coil of electrical resistance wire was placed near the floor of the intake manifold over the hot spot area. Electrical leads were brought out through the carburetor mounting flange to be hooked up to the electrical power supply. Temperature of the electrical coil was monitored by a thermocouple in contact with the coil. Once the coil temperature reached 200°F, the control circuit adjusted the electrical power to maintain this temperature throughout the test.

The results for the three tests are given in Table 9. Emissions are expressed in grams per phase. Comparisons of the HC and CO emissions for the cold transient part of the urban driving cycle are given in Figure 33. Again two sets of baseline data are shown for comparison: the vehicle results from the tests at the Subaru facility and the JPL engine/transmission results from the EC dynamometer. In each of the tests with the modified configuration using the electrically heated coil, the coil temperature reached the 200°F set-point after about 210 seconds into the driving cycle run. These two tests were different in that one used the stock choke control·strategy and the other used no choke. The emissions results for the stock choke case were not better than the baseline results, with the CO emissions being somewhat worse. The stock choke strategy – which results in a richer vapor/air mixture being supplied to the engine – probably offset any improvement in fuel vaporization. The emissions results for the same modified configuration with no choke are considerably better. Both HC and CO emissions are reduced; however, vehicle driveability was less acceptable. To achieve the best results, it would be necessary to tailor the choke control strategy to provide adequate vehicle driveability and minimize system interaction problems.

Continuous mode data was taken for the tests with the electrically-heated hot spot. Comparative choke position data are given in Figure 34. In the third test (Tape W746) the choke was held open manually after the first 30 seconds of the test. This permitted the choke to operate normally until the vehicle had successfully started up the first acceleration ramp. For this ·test, the wide-open choke corresponds to 100 percent choke position. In the other two tests, the wide-open choke is achieved with an 80 percent choke position. In the second test (Tape W745), more choking is used than in the stock case, and it remains in effect longer.

Catalyst bed temperatures are shown plotted in Figure 35. The data indicate that the catalyst warm-up was at least as fast in the tests with the electrically-heated hot spot tests as in those with the stock system. Hydrocarbon emissions profiles are given in Figure 36. There is a delay of about 10-12 seconds in the continuous mode emissions trace for flow time and system response time. This delay is a result of the length of the sample lines between the engine exhaust system and the emissions instruments.

START CATALYST

The stock baseline emission control system has an oxidizing catalyst for the conversion of HC and CO emissions from the engine. As is shown in Section II, the stock catalyst unit achieves high conversion efficiencies for both HC and CO under warmed-up conditions. Under cold-start conditions, the

49

Table 9. Cold-Start Emissions Tests: Electrically Heated Hot
Spot Results for Cold 505 Federal Urban Driving Cycle

Day	Tape	Phase	$NO_x(g)$	CO(g)	HC(g)	Comments
6148	Y476	g/bag 1	0.54	55.95	3.6	Stock system
		g/bag 2	1.92	22.38	1.37	
		g/bag 3	0.94	1.42	0.45	
		TOTAL g/bag	3.4	79.75	5.42	
6166	W745	g/bag 1	0.36	87.42	4.77	Heating element set for
		g/bag 2	2.45	4.84	0.75	200°F, turned on at start
		g/bag 3	1.10	2.61	0.34	of test, and reached 200°F
		TOTAL g/bag	3.91	94.87	5.86	after about 210 seconds into the run. Stock choke.
6166	W746	g/bag 1	0.47	45.77	3.14	Heating element set for
		g/bag 2	2.34	2.95	0.72	200°F, turned on at start
		g/bag 3	1.12	1.90	0.32	of test, and reached 200°F
		TOTAL g/bag	3.93	50.62	4.18	after about 210 seconds into the run. Choke was held open manually.

engine produces greater quantities of emissions, but the catalyst operates at
lowered conversion efficiency until it reaches its light-off temperature
(about 500-600°F).

Several methods can be used to improve the performance of the oxidation
catalyst in cold-start operation. The standard catalyst unit could be located
closer to the exhaust manifold for a faster warm-up. The closer location
would lead to higher peak temperatures in the catalyst bed and reduced cata-
lyst activity. An alternative technique for reducing catalyst warm-up time
is to provide supplemental heating of the catalyst bed for faster activation.
The use of an electrically heated element for this purpose is discussed in the
next section. Another method is the addition of a cold-start catalyst (CSC)
unit in addition to the standard catalyst unit. The CSC unit would be used
only during engine warm-up operation.

A series of tests was performed using a separate CSC unit mounted as
shown in Figure 37. Flow through the CSC unit was regulated by a damper valve.
The configuration was designed to keep the distance between the exhaust mani-
fold and the standard catalyst unit the same as in the stock vehicle. This
insured that the standard catalyst would not overheat during engine operation.
The standard catalyst unit has two monolith elements (oval cross-section) with
a platinum/palladium (Pt/Pd) ratio of 2/1 and a total precious metal loading
of 25 g/ft³. The catalyst material is mounted on a cordierite base. The CSC
unit was mounted closer to the exhaust manifold, for faster warm-up. The CSC
unit contained one monolith element (circular cross-section). Tests were
made with both the standard catalyst material and a more active oxidation
catalyst with a Pt/Pd ratio of 1/1 and a total precious metal loading of
165 g/ft³ mounted on a cordierite base. The damper valve was controlled to
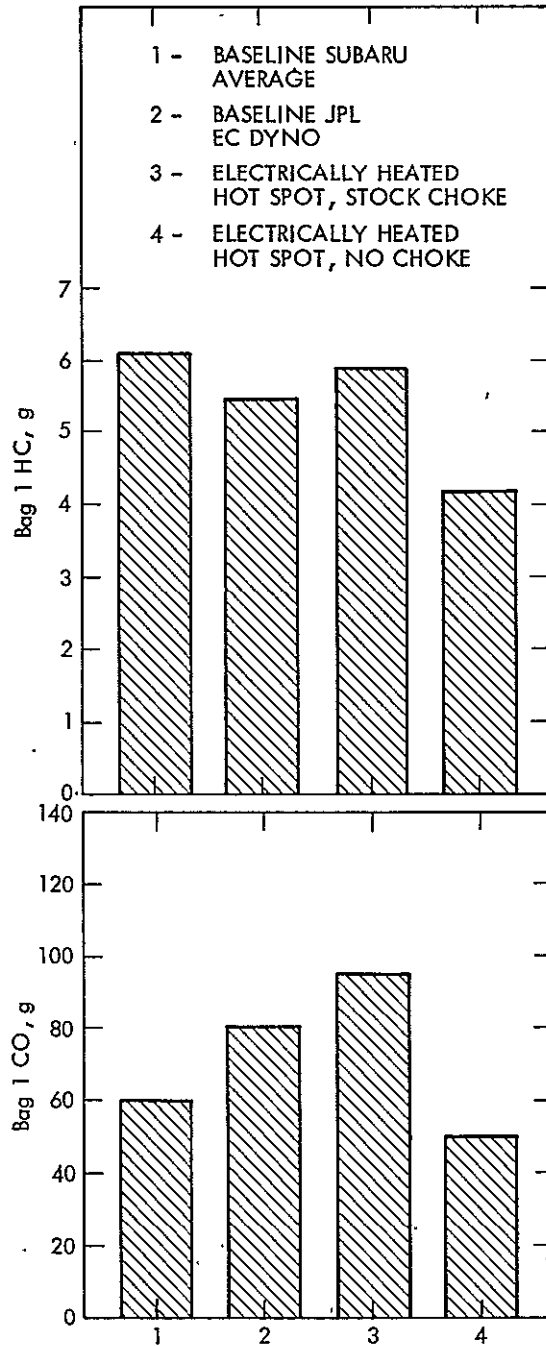
Figure 33. Effect of Electrically Heated Hot Spot on Cold-Start Emissions
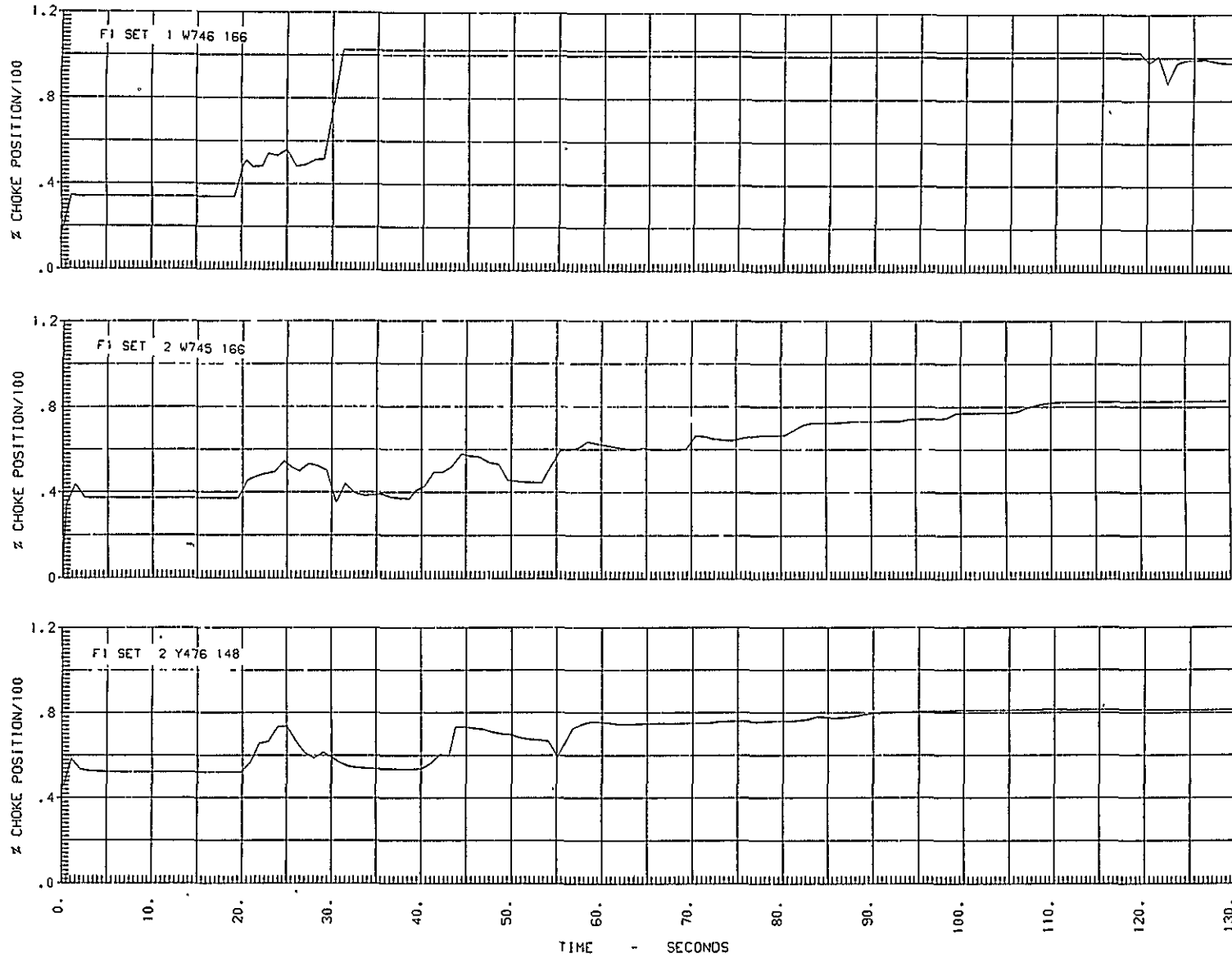
Figure 34. Choke Characteristics
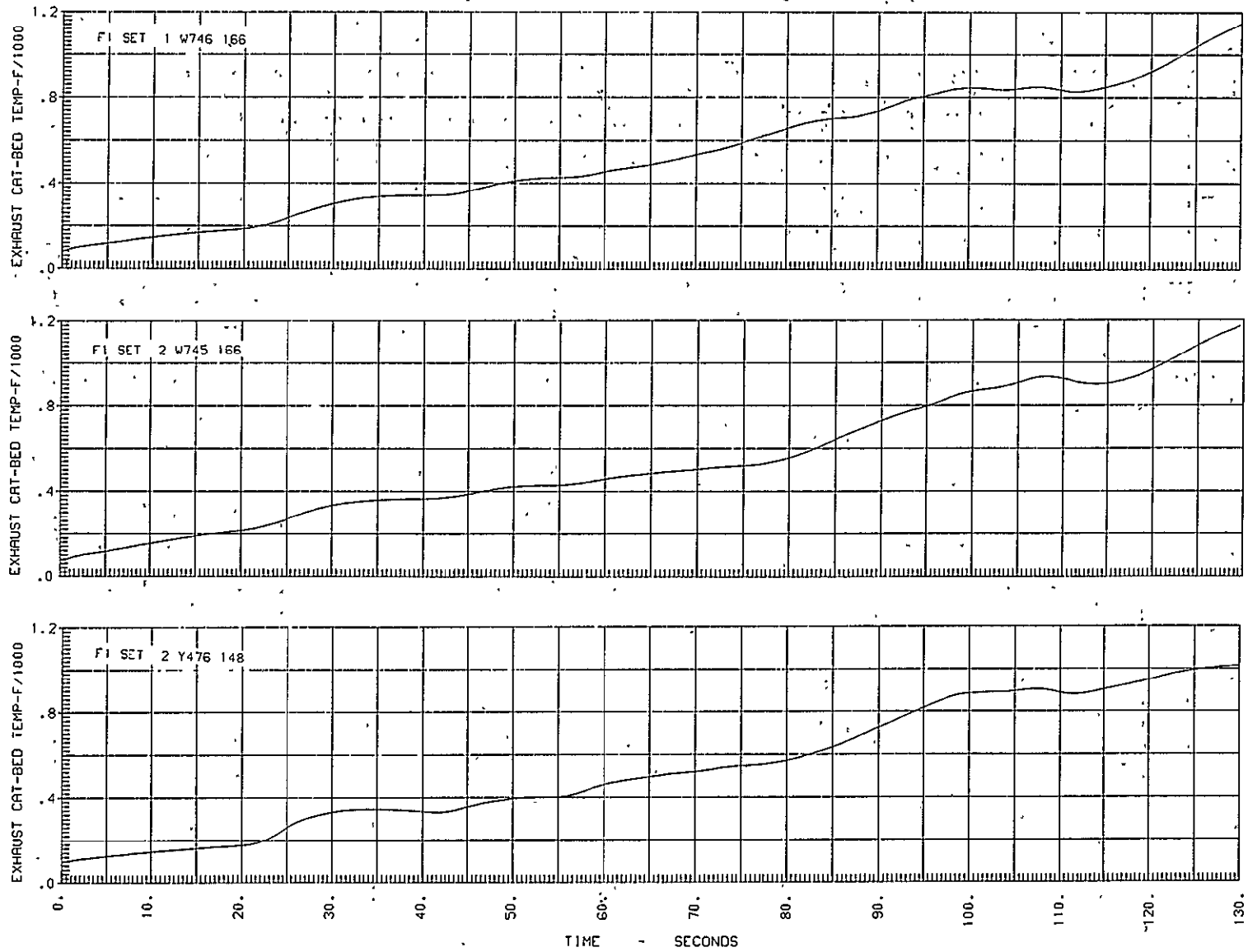
Figure 35. Catalyst Bed Temperature

53
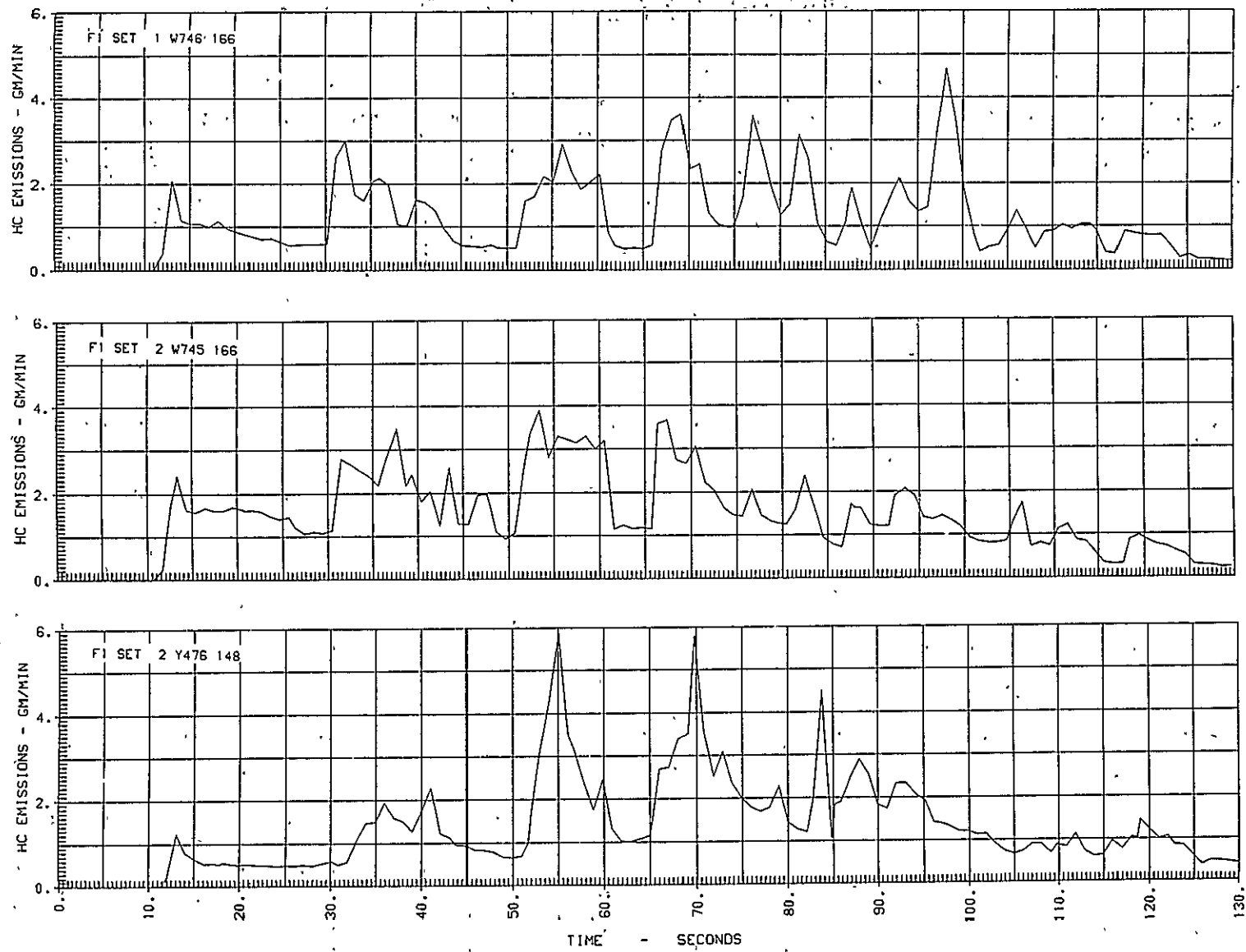
Figure 36. Hydrocarbon Emission Characteristics

DAMPER
VALVE

EXHAUST
MANIFOLD

SECTION A-A

SECTION B-B

A

STANDARD
CATALYST UNIT

A

B

B

COLD START CATALYST (CSC) UNIT
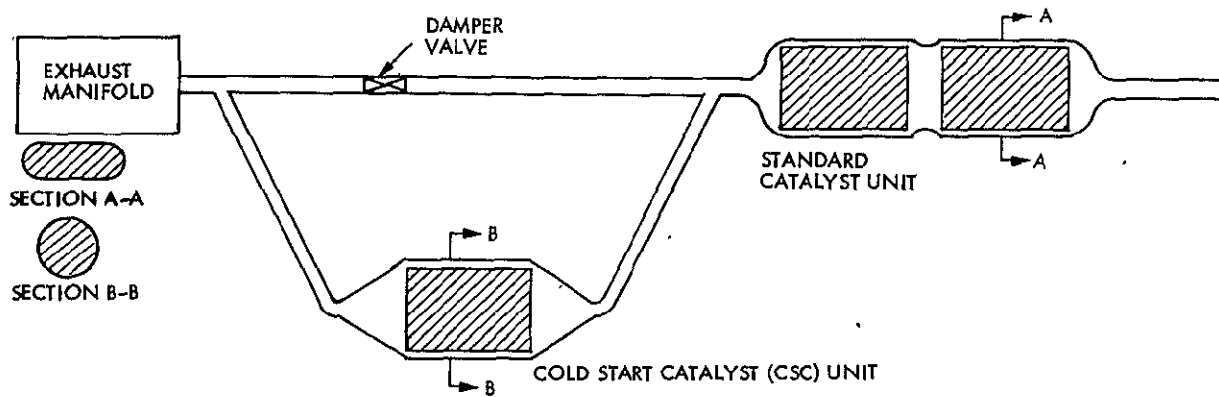
UNIT	CATALYST	PRECIOUS METAL LOADING
STANDARD	$Pt/Pd \approx 2/1$	25 g/ft^3
COLD START	$Pt/Pd = 1/1$	165 g/ft^3

Figure 37.   Exhaust Configuration for Cold-Start Catalyst Tests

bypass the CSC unit when CSC bed temperature reached 800-850°F, to prevent damage to the catalyst material.

The results for the three tests are given in Table 10. Emissions are expressed in grams per phase. Comparisons of the HC and CO emisisons for the cold transient portion of the urban driving cycle are given in Figure 38. Again two sets of baseline data are shown for comparison: the vehicle results from the tests at the Subaru facility and the JPL engine/transmission results from the EC dynamometer. The baseline test on the EC dynamometer was made with the modified exhaust configuration; however, the damper valve was set to bypass the CSC unit for the entire test.

In each of the tests with the CSC unit, exhaust gas flow was directed through the CSC unit until the catalyst bed temperature reached 800-850°F; the diverter valve was then switched to bypass the CSC unit for the remainder of the test. In the first CSC test, standard catalyst material was used; however, a more active catalyst material was used in the second test. The test results show some nominal reduction of HC and CO emissions when compared with the EC dynamometer baseline. In the configuration tested, the standard catalyst unit had not reached its light-off temperature when the diverter valve was switched to bypass the CSC unit at about 50 seconds into the test.

SUPPLEMENTAL HEATING OF CATALYST UNIT

The HC and CO conversion efficiencies of the standard catalyst unit are not good until the catalyst bed reaches its light-off temperature (about 500-600°F). The addition of some supplemental heating to the catalyst unit should reduce this warm-up time. The hardware used in evaluating the supplemental heating technique consisted of a standard catalyst unit which had been modified to accept an electrically-heated element as shown in Figure 39.

The standard catalyst unit was lengthened 1 inch to accommodate the heater element. The heated element was a silicon carbide monolith with a Pt/Pd ratio of 1/1 and a total precious metal loading of 56 g/ft^3. The element was oval in cross-section with a 1-inch thickness. To provide better heating of the entire catalyst unit, the heater element was located upstream of the two standard monolith elements. Two flat rectangular electrodes were placed on the flat sides of the heater element to provide the maximum flow path for electrical current flow. The element, with electrodes, was wrapped first with fibrefrax insulation and then with stainless wire mesh. The element was then placed in the extended catalyst container. Electrical leads were run from the electrodes, through insulated openings in the container, and to the electrical power supply.

Tests of the electrically-heated catalyst unit were not made on the EC dynamometer. This modification was included as a part of the final series of vehicle tests. These results are discussed in Section VI.

Table 10. Cold-Start Emissions Tests: Start Catalyst Results
for Cold 505 Federal Urban Driving Cycle

Day	Tape	Phase	NO_x(g)	CO(g)	HC(g)	Comments
6194 -	Ø037	g/bag 1 g/bag 2 g/bag 3 TOTAL g/bag	0.31 1.62 0.63 2.56	83.09 5.63 4.75 93.47	6.21 1.08 0.46 7.75	Stock system without cold-start catalyst (CSC) unit installed.
6190	Ø032	g/bag 1 g/bag 2 g/bag 3 TOTAL g/bag	0.39 1.57 0.60 2.56	68.16 11.45 5.29 84.90	3.70 1.95 0.54 6.19	Cold-start catalyst unit installed using stock catalyst material. Valving switched to by-pass CSC when CSC bed temperature reached 850°F at about 40 seconds into the run.
6191	Ø035	g/bag 1 g/bag 2 g/bag 3 TOTAL g/bag	0.26 2.02 0.60 2.88	61.97 7.43 4.44 73.84	3.63 2.28 0.50 6.41	Cold-start catalyst unit installed using start catalyst material. Valving switched to by-pass CSC when CSC bed temperature reached 800°F at about 52 seconds into the run.
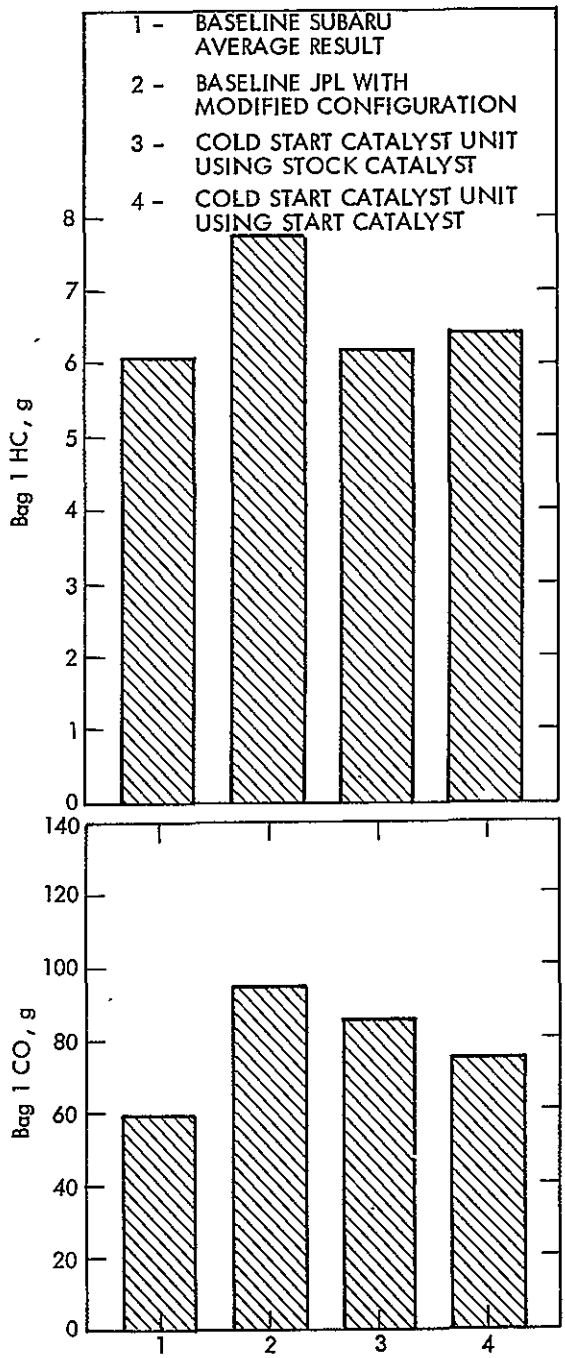
Figure 38. Effect of Start Catalyst on Cold-Start Emissions

ELECTRICALLY-HEATED CATALYST ELEMENT

CASE

FLAT RECTANGULAR ELECTRODES

STAINLESS WIRE MESH

FIBREFRAX INSULATION

CATALYST ELEMENT

STANDARD CATALYST ELEMENTS

ELEMENT	CATALYST	PRECIOUS METAL LOADING
STANDARD	Pt/Pd = 2/1	25 g/ft^3
HEATED	Pt/Pd = 1/1	56 g/ft^3
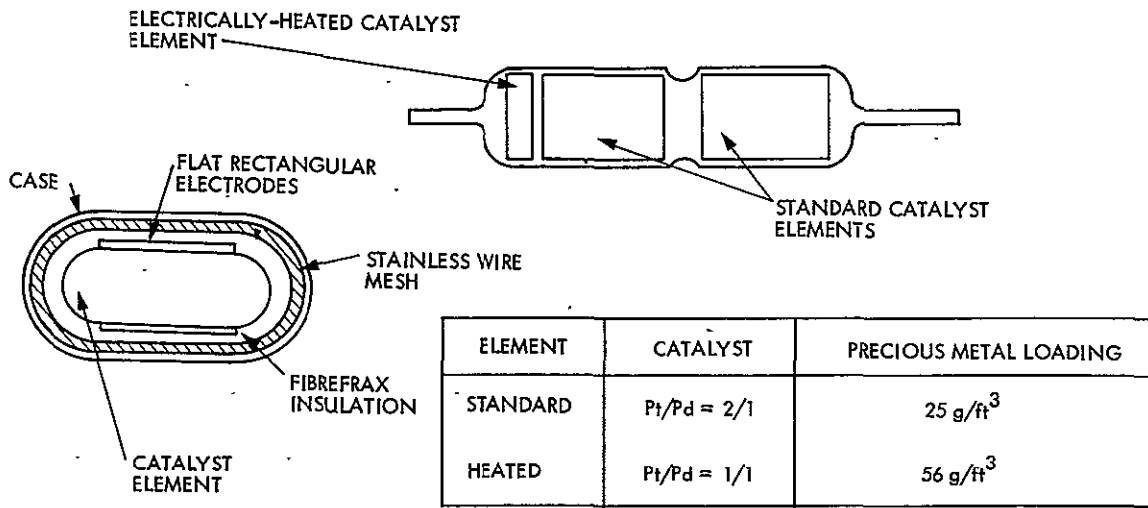
Figure 39. Configuration for Electrically-Heated Catalyst Element

SECTION IV

EGR EVALUATION

BACKGROUND INFORMATION

Studies (Refs. 29, 30, 31) have shown that NO_x exhaust emissions are directly related to peak cylinder temperatures and residence times spent above the threshold temperature for NO_x formation. The amount of NO_x emissions formed is also dependent on the concentrations of oxygen and nitrogen available for reaction. To suppress the formation of oxides of nitrogen in the combustion chamber, several techniques have been used, including spark retard and the addition of diluents to the intake mixture. Recently, considerable success in controlling NO_x emissions has been achieved using three-way catalyst systems for exhaust aftertreatment (Refs. 32, 33, 34).

The addition of diluents to the incoming fuel/air mixture helps to reduce NO_x emissions by absorbing some of the energy released by the combustion process. This decreases peak temperatures and reduces the time when conditions are favorable for NO_x formation. The desirable properties of such a diluent are nonreactivity, relative to the intake mixture, and a high heat capacity (Refs. 29, 35). Exhaust gases, water, and excess air have all been studied as possible charge diluents. Injecting water, usually in the intake port, is undesirable because it requires a storage tank and care must be taken to prevent freezing in cold environments. The use of excess air reduces cylinder temperatures and is the basis of the lean burn concept which has been studied elsewhere (Ref. 36) and will not be discussed here.

Exhaust gas recirculation (EGR) has been widely used for NO_x emissions control since exhaust gases are readily available, EGR is relatively simple to implement, and EGR is an effective controller of NO_x emissions (Ref. 37). Large reductions of NO_x emissions can be achieved with small amounts of EGR. However, EGR influences other engine characteristics such as HC emissions, vehicle driveability, and fuel economy. The EGR installation and control strategy must provide the proper balance among these important factors.

Recirculated exhaust gases act to suppress NO_x emissions by diluting the intake mixture. When in the combustion chamber, the EGR absorbs some of the energy released during combustion and thus limits peak temperatures. This reduction in peak temperature affects other areas of engine operation. When engine power and spark advance are held fixed, an increase in EGR results in an increase in fuel consumption since combustion is slowed and extends further into the expansion portion of the cycle. Gumbleton (Ref. 38) has shown that with proper engine adjustments the use of EGR can result in a reduction in fuel consumption.

The use of EGR has an adverse effect on HC emissions. This results partially from the decreased temperature in the combustion chamber, which leads to larger quench zones and more unburned hydrocarbons. This effect has been demonstrated in vehicle tests by Gumbleton (Ref..38). For large amounts of EGR, hydrocarbon emissions show a steep rise as the combusion process begins to degrade. This point coincides with a significant reduction

in vehicle driveability. Thus, there are definite limits on the amount of EGR that can be used to control NO_x emission without sacrificing HC emission control and driveability.

Various techniques have been used to implement the recirculation of exhaust gases. Freedman and Nicholson (Ref. 39) discuss the control of EGR through valve timing. In their work, exhaust gas residuals were increased through the use of increased valve overlap and a variable cam timing mechanism. As improved control of EGR was needed, new EGR systems with the capability for more accurately metering EGR flow rate were developed. Thompson (Ref. 40) describes the development of the EGR system for Buick.

Many EGR control schemes have been investigated. The system on the Plymouth baseline vehicle for this study uses an EGR valve, controlled by a vacuum amplifier, to meter exhaust gases through an external flow passage from the exhaust manifold to the intake manifold. This approach is discussed in more detail in Section II. Other designs have incorporated the EGR valve in the intake manifold to connect the exhaust crossover flow passage with the intake plenum. The use of microprocessors on engines will permit more complex control algorithms to be implemented. EGR valves, and thus EGR flow, can be controlled as specified functions of intake manifold pressure, exhaust manifold pressure, engine RPM, etc.

TEST SETUP DESCRIPTION

Considerable success has been achieved through the use of exhaust gas recirculation (EGR) as a means for controlling nitrogen oxide (NO_x) emissions. The EGR tests on this project were structured to provide insight into the relationship between fuel economy and emission for the EGR emission control approach. Since some combination of EGR and spark advance control is generally used for control of NO_x emissions, a series of sensitivity tests were made while varying both EGR flow rate and spark advance. The sensitivity tests were made at steady-state operating conditions on a water brake dynamometer.

To facilitate the engine testing, the stock controls for both EGR and spark advance were made inoperative. With both the vacuum and centrifugal advance mechanisms of the distributor not operating, the spark advance was adjusted by mechanically moving the distributor with a pneumatic actuator. The vacuum supply to the EGR valve was disconnected and the poppet in the EGR valve was positioned mechanically using a pneumatic actuator. EGR flow rate was calculated using air calibration data from cold-flow bench tests of the EGR valve. All cold-start emissions devices and the air injection reactor (AIR) system were operating in the stock manner during the sensitivity tests. Since all of the sensitivity tests were run with the engine in a fully warmed-up condition, the cold-start emissions devices should have had no influence on the test results. The stock AIR system had an effect on the results since it determined the excess air available for HC and CO conversions in the catalytic converter.

SENSITIVITY TESTS

Eleven engine operating conditions were selected for evaluation in the EGR/spark advance sensitivity tests. The test conditions were selected to give adequate coverage of the region used most frequently when driving the urban driving cycle. This is appropriate for developing an EGR/spark advance control strategy since vehicle emissions results are determined from the urban driving cycle test. The selected test conditions are shown in Figure 40.

Measurements of fuel consumption and HC, CO, and NO_x emissions were taken for each operating condition. Exhaust emissions were measured both upstream and downstream of the oxidation catalyst. Engine equivalence ratio and AIR flow rate were used to determine the excess air available in the oxidation catalyst.

To simplify the presentation of material and the discussion of the results, detailed results for only one engine operating condition are presented in the main body of this report. The operating condition chosen is 2000 RPM and 40 BMEP which is typical for level-road-load conditions at about 50 MPH. Similar data and plots for the remaining engine conditions are included in Appendix D. In all plots, comparisons are made with the stock engine results previously discussed. A summary of the sensitivity data is given in Table 11.

The effect of EGR and spark advance on the brake specific fuel consumption is shown in Figure 41. For each EGR flow rate, a preliminary real-time plot of engine thermal efficiency versus spark advance was made to determine the minimum best torque (MBT) spark advance. In general, tests were made for
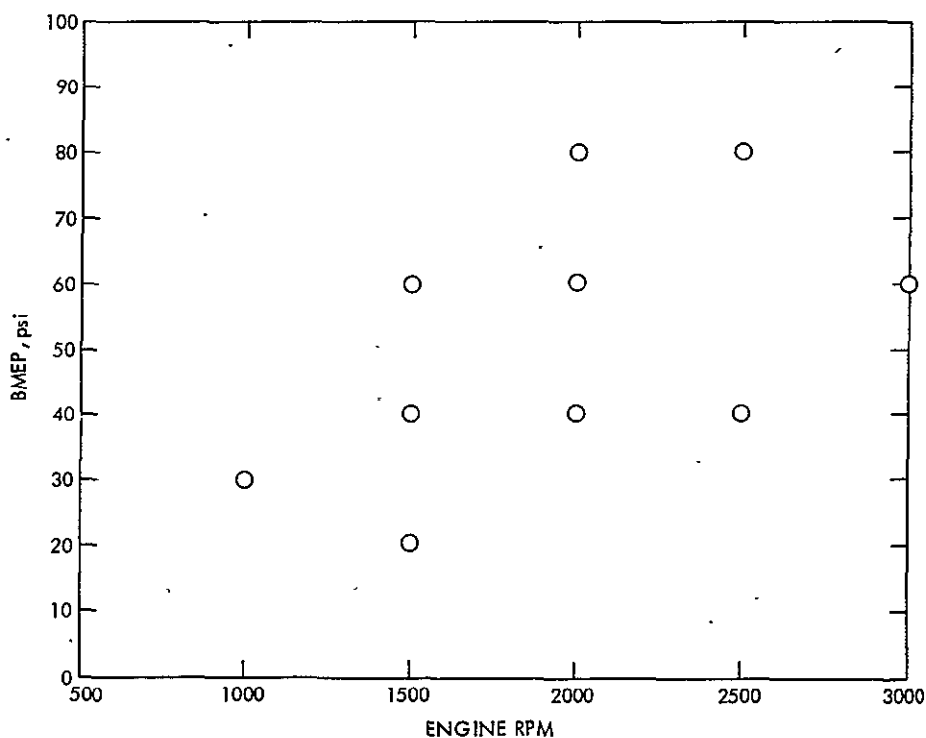
Figure 40.   Operating Conditions Used for
EGR/Spark Advance Sensitivity Tests

62

Table 11. EGR/Spark Advance Sensitivity Data for 2000 RPM and 40.1 BMEP

Sequence Number	$\phi_{Eff.}$	Spark Advance (°BTDC)	Percent EGR	BSFC (1bm/bhp-h)	Emissions Data*	$BSNO_x$ (g/bhp-h)	BSHC (g/bhp-h)	BSCO (g/bhp-h)	Average T_{exh} (°F)
2103.10	0.935	35.4	1	0.593	D	24.09	0.27	0.26	1190
2103.12	0.890	34.3	1	0.581	U	24.82	0.14	2.50	1190
2103.14	0.901	25.2	1	0.596	D	16.55	0.91	0.69	1238
2103.16	0.898	25.4	1	0.594	U	17.36	1.01	8.44	1240
2103.18	0.931	15.2	0	0.685	D	11.45	0.08	0.22	323
2103.20	0.937	15.2	0	0.685	U	11.30	0.65	6.65	1322
2103.22	0.790	45.1	14	0.572	D	12.85	0.28	0.23	1133
2103.24	0.796	45.1	14	0.570	U	14.32	1.91	6.37	1135
2103.26	0.818	35.5	12	0.593	D	9.31	0.25	0.24	1175
2103.28	0.817	34.3	12	0.594	U	9.71	1.62	6.63	1177
2103.30	0.849	25.7	9	0.632	D	7.14	0.16	0.25	1241
2103.32	0.855	25.6	8	0.626	U	7.19	1.13	8.56	1242
2103.34	0.726	50.1	25	0.602	D	5.06	0.75	0.46	1119
2103.36	0.725	50.3	25	0.602	U	5.11	5.17	7.21	1122
2119.01	0.745	39.9	23	0.626	D	3.79	0.62	0.47	1165
2119.04	0.741	40.1	23	0.623	U	3.88	4.42	7.51	1168
2119.06	0.761	29.9	21	0.666	D	3.17	0.68	0.46	1223
2119.08	0.756	30.3	21	0.664	U	3.20	4.10	7.13	1231

*U - upstream of catalytic converter; D - downstream of catalytic converter.
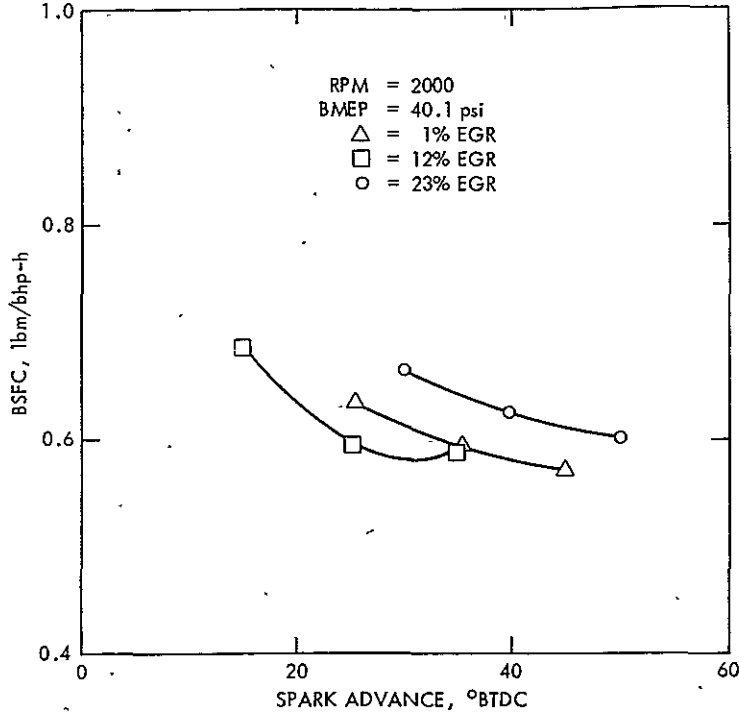
Figure 41. Fuel Consumption Versus Spark Advance for EGR/Spark Advance Tests

MBT, MBT-10° and MBT-20° spark advance settings at each EGR flow rate. The curves show that BSFC decreases to a minimum as the spark advance is increased to the MBT value. For this particular engine operating condition, the minimum BSFC is achieved with about 12 percent EGR. To include the effect of EGR, the following effective equivalence ratio can be defined.

$$\phi_E' = \frac{\dot{M}_g}{(\dot{M}_A + \dot{M}_{EGR})\zeta_s}$$

where

ϕ_E = effective equivalence ratio

$\dot{M}_G$ = gasoline flow rate

$\dot{M}_A$ = primary air flow rate

$\dot{M}_{EGR}$ = EGR flow rate

ζ_s = stoichiometric fuel-to-air ratio

Thus, the minimum BSFC occurs at an effective equivalence ratio of about 0.8. This result is consistent with the fact that the most efficient lean operating condition in a typical conventional engine occurs at equivalence ratios between 0.8 and 0.85.

The effect of EGR and spark advance on the brake specific NO_x ($BSNO_x$) emissions is shown in Figure 42. For a given EGR flow rate, increasing the spark advance results in an increase in NO_x emissions. EGR is seen to be a very effective means for reducing NO_x emissions. This effect is shown clearly in Figure 43 where NO_x emissions are plotted versus effective equivalence ratio.

The trade-off between BSFC and $BSNO_x$ emission for this operating condition is illustrated in Figure 44. For a given EGR flow rate, an increase in spark advance, up to the MBT value, results in a decrease in fuel consumption; however, this improvement in engine efficiency is accompanied by an increase in NO_x emissions. The characteristics are similar for each of the EGR flow rates tested. Comparisons with the stock data for this operating condition indicated that substantial reductions in fuel consumption could be achieved at the expense of higher NO_x emissions.

The relationship between BSHC emissions and $BSNO_x$ emission is shown in Figure 45. The emissions data plotted here are based on exhaust samples taken downstream of the oxidation catalyst. Dashed lines are drawn through conditions yielding the same specific fuel consumption. For each EGR flow rate, the data points with MBT spark timing are shown with solid symbols. For MBT spark timing, increases in EGR flow rate result in less NO_x emissions; however, HC emissions increase substantially. Within the range of this data, retarding the spark timing from its MBT value reduces both NO_x and HC emissions; however, fuel consumption is increased. Comparisons with the stock data indicate that large reductions in HC emissions could be achieved with the same fuel consumption and only slightly increased NO_x emissions for this operating condition.

The increase in HC emissions with increasing EGR flow rate could be the result of either an increase in HC emissions from the engine or a decrease in HC conversion efficiency in the catalytic converter. For all the data shown, the average HC conversion efficiency is 85 percent and the average CO conversion efficiency is 95 percent. These values are about equal to the conversion efficiencies for the stock data points for this operating condition. For high conversion efficiencies, the catalytic converter must have an excess of air and an adequate operating temperature ($\sim$800°F). The engine equivalence ratio for this data is less than stoichiometric ($\phi\sim$0.95) indicating than an excess of oxygen is available for the catalytic converter. Additional air is introduced by the AIR system. To include the effect of AIR, the following effective equivalence ratio is defined.

$$\phi_A \approx \frac{\dot{M}_G}{(\dot{M}_A + \dot{M}_{AIR})\zeta_s}$$
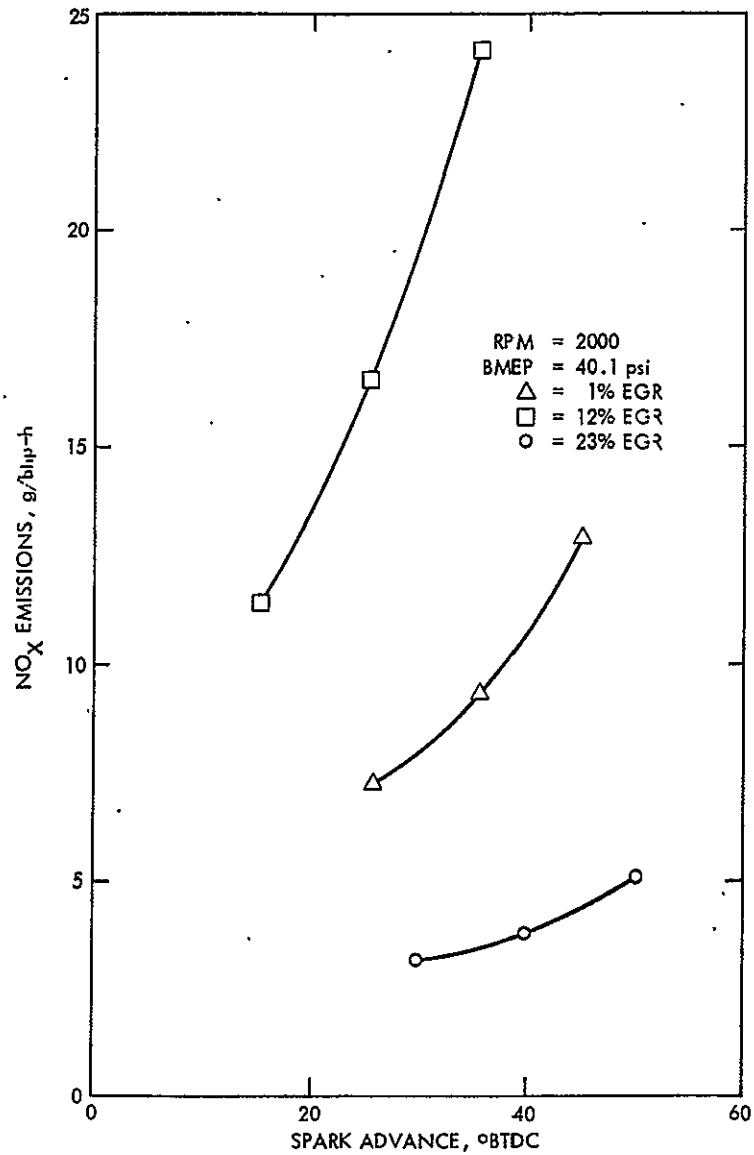
Figure 42. NO_x Emissions Versus Spark Advance for
EGR/Spark Advance Sensitivity Tests

66
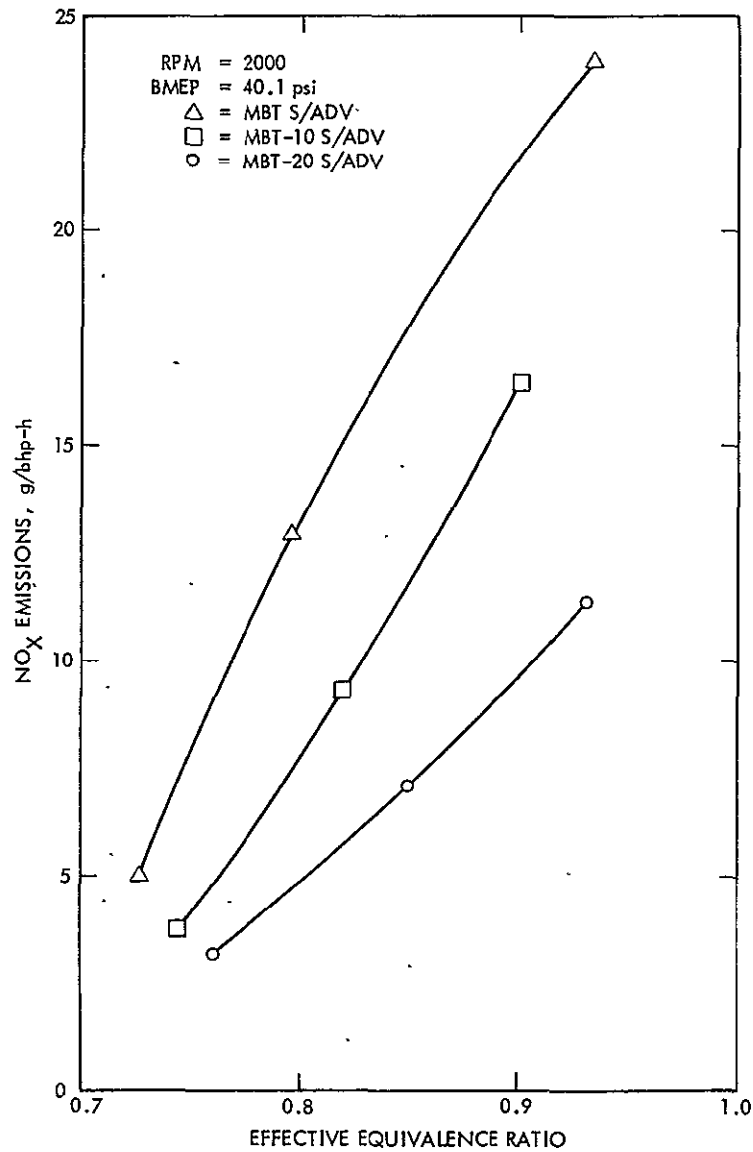
Figure 43. NO_x Emissions Versus Effective Equivalence Ratio for EGR/Spark Advance Sensitivity Tests
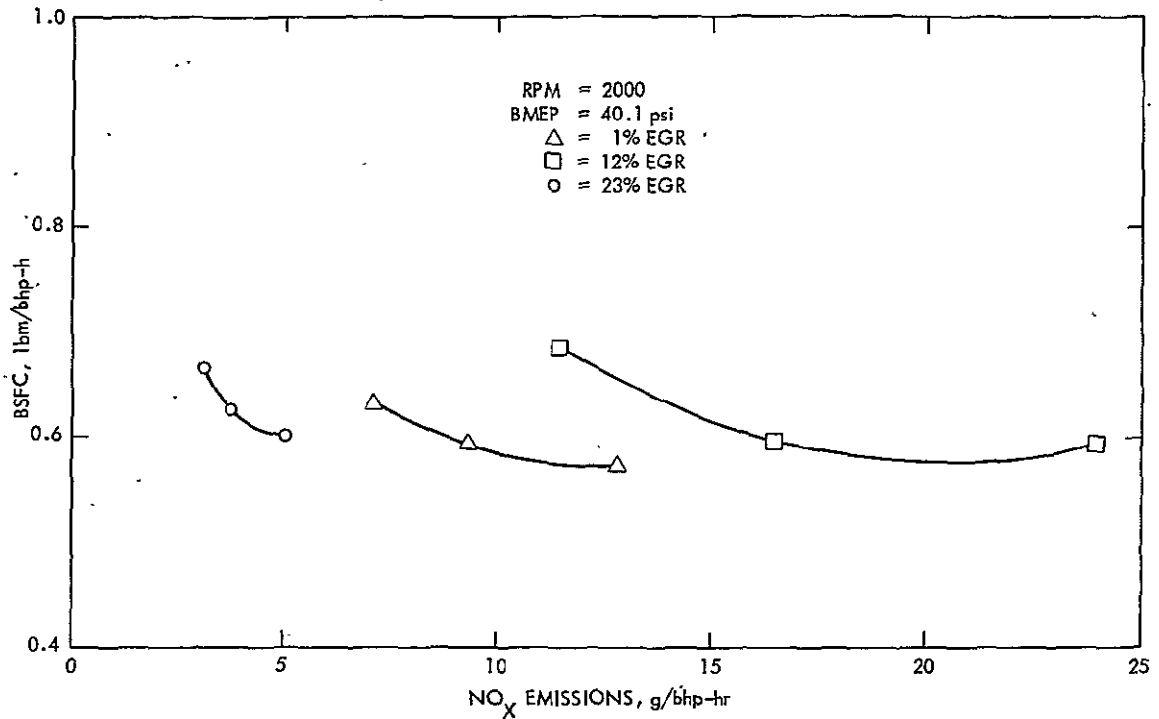
Figure 44. Fuel Consumption Versus NO_x Emissions for
EGR/Spark Advance Sensitivity Tests
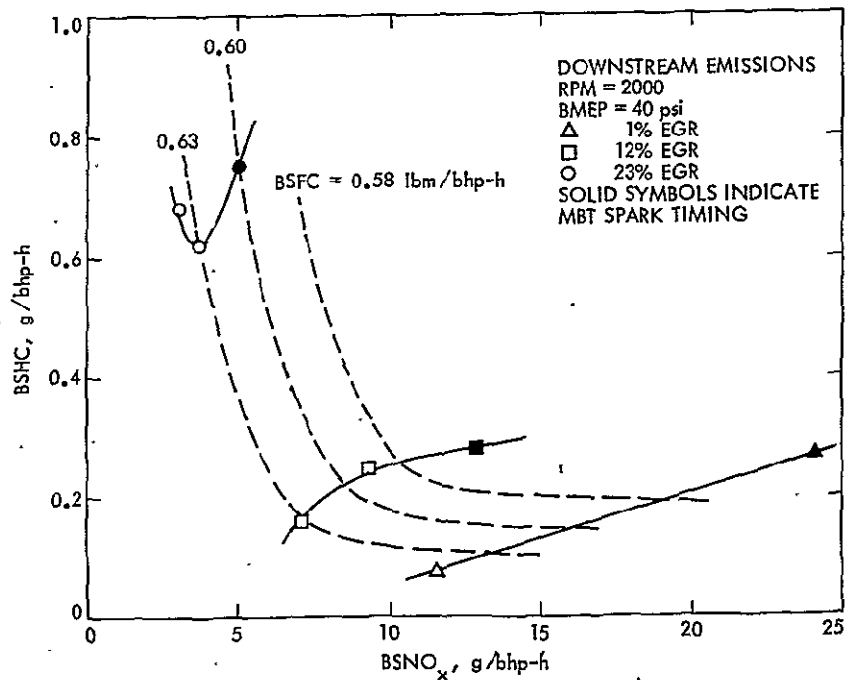
Figure 45. HC Emissions Versus NO_x Emissions for
EGR/Spark Advance Sensitivity Tests

where
ϕ_A = effective equivalence ratio

$\dot{M}_G$ = gasoline flow rate

$\dot{M}_A$ = air flow rate

$\dot{M}_{AIR}$ = AIR flow rate

ζ_S = stoichiometric fuel-to-air ratio

For this data, the effective equivalence ratio is in the range from 0.7 to 0.8 indicating plenty of excess oxygen for the catalytic converter.

Average exhaust gas temperatures are shown in Figure 46. The average exhaust temperature is computed by averaging the exhaust gas temperatures from the six individual cylinders. These temperatures are measured in the exhaust manifold near the exhaust valves. For each test condition, the average exhaust temperature exceeded 1100°F. Although the exhaust gas temperatures at the entrance to the catalytic converter are lower (850°F to 1050°F), they are still well above the temperature required for high conversion efficiencies. The average exhaust gas temperature increases as the spark timing is retarded from its MBT value; however, the amount of EGR flow rate has little effect for this data.
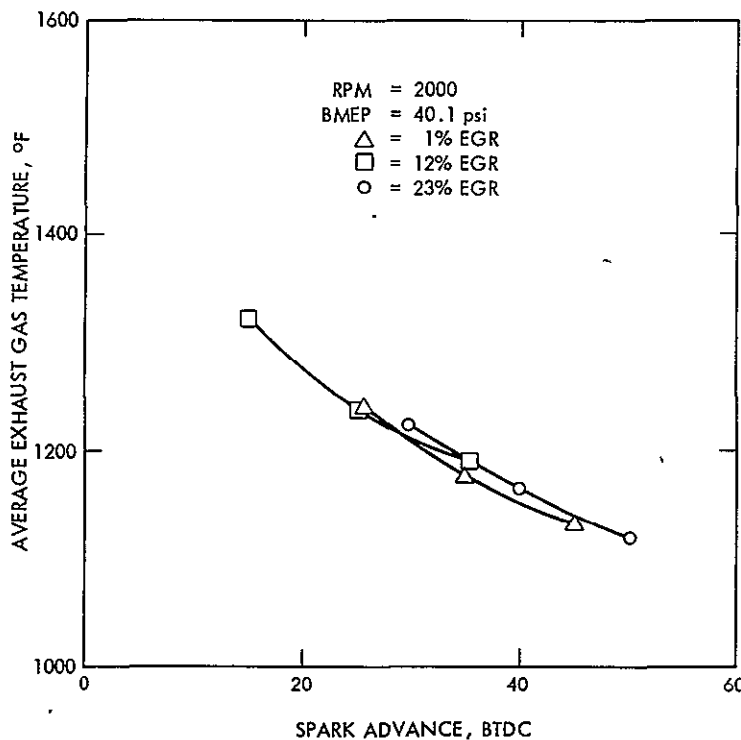
Figure 46. Exhaust Gas Temperature Versus Spark Advance for EGR/Spark Advance Sensitivity Tests

CONTROL STRATEGY SELECTION

The overall objective of this part of the activity was to select EGR/ spark advance strategies which would yield better fuel economy and/or exhaust emissions than the stock system. Data from the EGR/spark advance sensitivity tests described in the previous section were used to establish the control strategies. For each strategy, one data point was selected for each of the 10 engine operating conditions used in the sensitivity tests. These 10 data points were used as a basis for developing the control functions needed to implement the strategies. A total of 8 strategies were developed and tested. The data points used as a basis for these 8 control strategies are given in Table 12.

The general approach was to first run a case with zero EGR flow rate and MBT spark timing (Strategy No. 1). This was followed by several cases where the data points were selected to bring the NO_x emissions down to a level comparable to the stock vehicle while minimizing the adverse effects on fuel consumption and HC emissions (Strategies Nos. 2, 3, and 4). Test results for each strategy were examined before proceeding to the next case. Since implementation of the strategies was not always done as accurately as desired, several alternative functional representations of one set of data were examined to see which approach gave the best results (Strategies Nos. 5, 6, 7, and 8).

It was decided that EGR flow rate and spark advance would be made a function of engine RPM, manifold pressure, and exhaust pressure since these parameters could be easily used as inputs to the control module. Strategy No. 6 will be used for discussion in this part of the report; information on the other strategies is included in Appendix E.

The data points which were used as a basis for Strategy No. 6 are given in Table 13. The position of the poppet in the EGR valve is expressed in percent of full travel. The EGR poppet position is shown plotted as a function of exhaust pressure in Figure 47. The following functional representation is shown to provide an adequate representation of the data for this strategy.

$$D_P = \begin{cases} 0 & \text{for} \quad P > 14.3 \text{ psia} \\ (0.365 P_{exh} - 5.094) & \text{for } 14.3 \text{ psia} < P_{exh} < 14.7 < \text{psia} \\ 0.139 & \text{for} \quad P_{exh} > 14.7 \text{ psia} \end{cases} \quad (8)$$

where D_P = EGR poppet displacement, in.

P_{exh} = exhaust pressure, psia

Functional representations for the other control strategies are given in Table 14. Spark advance is shown plotted versus manifold pressure in Figure 48. The following function represents the line through the data and is seen to adequately represent this strategy.

Table 12. Data for EGR/Spark Advance Strategies

Operating Conditions		Sequence Numbers for Data Used in EGR/Spark Advance Strategy							
RPM	BMEP	1	2	3	4	5	6	7	8
750	0	114.26	114.26	114.26	115.02	115.02	115.02	115.02	115.02
1000	30	115.10	115.37	115.37	115.43	115.43	115.43	115.43	115.43
1500	20	115.11	159.45	116.16	116.40	116.40	116.40	116.40	116.40
1500	40	159.08	159.30	159.33	159.36	159.36	159.36	159.36	159.36
1500	60	110.32	112.8	112.14	112.20	112.20	112.20	112.20	112.20
2000	40	103.14	103.34	119.01	119.06	119.06	119.06	119.06	119.06
2000	60	93.04	94.12	161.15	161.15	161.15	161.15	161.15	161.15
2000	80	109.1	110.20	110.26	110.26	110.26	110.26	110.26	110.26
2500	40	107.01	108.20	108.26	108.26	108.26	108.26	108.26	108.26
2500	80	119.10	120.11	120.11	120.17	120.17	120.17	120.17	120.17
3000	60	112.26	112.43	112.49	114.14	114.14	114.14	114.14	114.14

Table 13. Engine Dynamometer Data Used for Implementation of EGR/Spark Advance Strategy No. 6

Sequence Number	RPM	BMEP (psi)	Spark Advance (°BTDC)	Percent EGR	Percent* Position	P_{man} (in. Hg vac)	P_{exh} (psia)
115.43	1000	30	20	22	11	9.8	14.28
106.40	1500	20	29	47	15	8.3	14.48
159.36	1500	40	32	25	72	6.6	14.45
112.30	1500	60	26	18	76	4.0	14.85
119.06	2000	40	30	21	72	7.1	14.78
161.15	2000	60	21	16	98	3.3	15.19
110.26	2000	80	21	12	75	1.2	16.03
108.26	2500	40	35	20	75	8.5	15.03
120.17	2500	80	15	-4	9	1.8	17.90
114.14	3000	60	17	12	69	2.1	17.50
115.02	750	0	25		14	13.5	14.05

*Refers to percent of full poppet travel in EGR valve.

Figure 47. EGR Strategy No. 6

$$SA = \begin{cases} 20 & \text{for } P_{man} < 7 \text{ psia} \\ (10P - 50) & \text{for } 7 \text{ psia} < P < 8 \text{ psia} \\ 30 & \text{for } 8 \text{ psia} < P < 11 \text{ psia} \\ (96 - 6\,P_{man}) & \text{for } P_{man} > 11 \text{ psia} \end{cases} \qquad (9)$$

where   SA = spark advance, ^{o}BTDC

P_{man} = manifold pressure, psia

Functional representations for the other spark advance control strategies are given in Table 15.

CONTROL STRATEGY IMPLEMENTATION

Implementation of the EGR/spark advance strategies discussed in the previous section required consideration of several important factors. Requirements were established to aid in the selection of the control system method to be used. The control system was required to yield a reasonable reproduction of the mathematical modes of the EGR and spark advance strategies. Good repeatability without system adjustment was needed for the transient driving cycle testing. Since several different strategies were to be implemented, ease of reprogramming from one model to another was an essential

72

Table 14. Summary of EGR Strategies

Strategy No.	EGR Strategy Description
1	$D_p = 0.0$
2	$D_p = f_1(RPM)\ f_2(P_{man})\ f_3(P_{exh})$ where $f_1 = \begin{cases} 0 \text{ for RPM} < 1000 \\ (0.002\ RPM - 2) \text{ for } 1000 < RPM < 1500 \\ 1 \text{ for RPM} > 1500 \end{cases}$ $f_2 = \begin{cases} 0 \text{ for } P_{man} < 6 \text{ psia} \\ (0.0311\ P_{man} - 0.1865) \text{ for } 6 < P_{man} < 11.5 \text{ psia} \\ 0.171 \text{ for } P_{man} > 11.5 \text{ psia} \end{cases}$ $f_3 = \begin{cases} 0 \text{ for } P_{exh} > 16 \text{ psia} \\ 1 \text{ for } P_{exh} < 16 \text{ psia} \end{cases}$
3	Same as Strategy No. 2
4	$D_p = \begin{cases} 0.019 \text{ for RPM} < 1200 \\ 0.019 \text{ for RPM} > 1200 \text{ and } P_{man} < 7 \text{ psia} \\ (0.0412\ P_{man} - 0.2694) \text{ for RPM} > 1200 \text{ and } 7 < P_{man} < 10 \text{ psia} \\ 0.1425 \text{ for RPM} > 1200 \text{ and } P_{man} > 10 \text{ psia} \end{cases}$
5	$D_p = \begin{cases} 0.019 \text{ for RPM} < 1200 \\ 0.019 \text{ for RPM} > 1200 \text{ and } P_{man} < 7 \text{ psia} \\ (0.0570\ P_{man} - 0.38) \text{ for RPM} > 1200 \text{ and } 7 < P_{man} < 10 \text{ psia} \\ 0.190 \text{ for RPM} > 1200 \text{ and } P_{man} > 10 \text{ psia} \end{cases}$
6	$D_p = \begin{cases} 0 \text{ for } P_{exh} < 14.3 \text{ psia} \\ (0.356\ P_{exh} - 5.094) \text{ for } 14.3 < P_{exh} < 14.7 \text{ psia} \\ 0.139 \text{ for } P_{exh} > 14.7 \text{ psia} \end{cases}$
7	Same as Strategy No. 6
8	$D_p = \begin{cases} 0 \text{ for } P_{exh} < 14.3 \text{ psia} \\ (0.38\ P_{exh} - 5.434) \text{ for } 14.3 < P_{exh} < 14.8 \text{ psia} \\ 0.10 \text{ for } P_{exh} > 14.8 \text{ psia} \end{cases}$
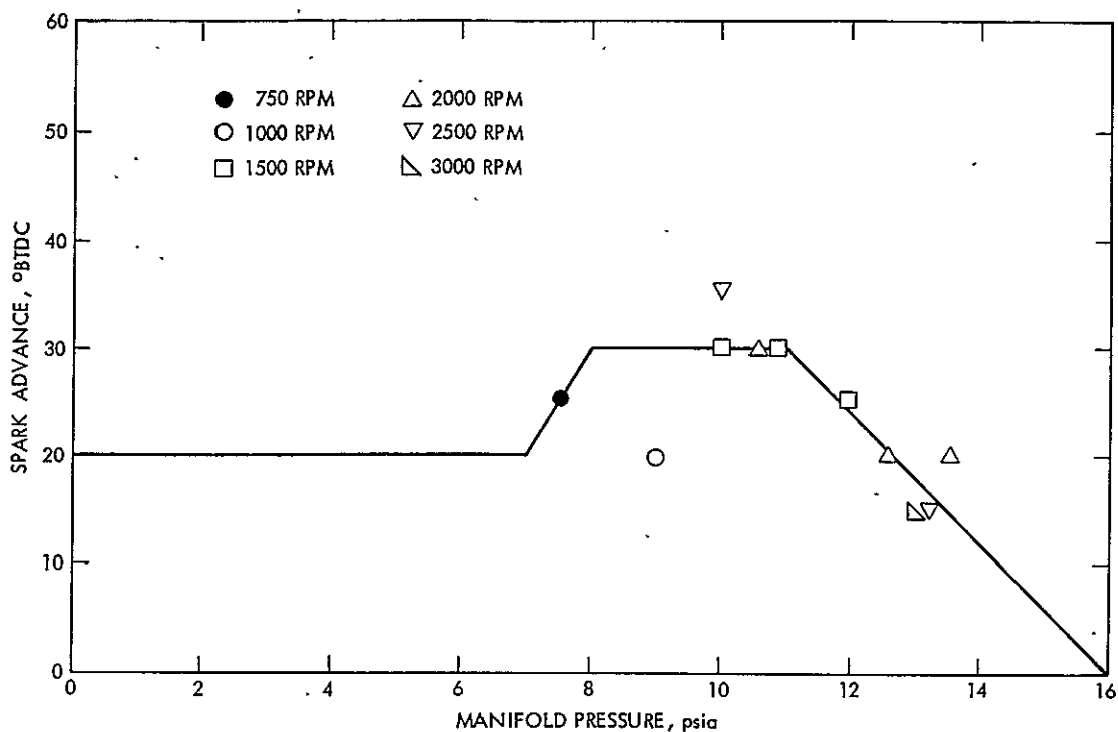
Figure 48. Spark Advance Strategy No. 6

requirement for the control system. The system had to conveniently interface with the test engine both to obtain the measured input parameters and to supply output control signals.

Hardware Description

Based on the above system requirements, it was decided to use electro-pneumatic pressure transducers for interfacing with measured parameters, to represent the mathematical model with electronic analog logic, and to use electromechanical devices to implement the controlled functions in the engine.

Design and fabrication of the control system was accomplished using current technology and available hardware. Wherever possible, equipment existing in the JPL automotive facility was utilized to minimize impacts upon cost and schedule. The Integrated Data Acquisition Control (IDAC) system, which normally handles the data processing and storage for the automotive test facility, provided the required analog voltage to the control system logic.

The mathematical models were implemented primarily by means of standard plug-in analog modules manufactured by Moore Industries. These standard modules, which conveniently interface with each other, were capable of representing the majority of the required mathematical functions. By utilizing several of these standard modules as a group and supplementing them with a few custom modules, an electronic analog of the various EGR/spark advance mathematical models was developed. With the plug-in modules and dial-set potentiometers, the control system could easily be modified and/or reset to represent various control strategies with good accuracy.

74

Table 15. Summary of Spark Advance Strategies

Strategy No.	Spark Advance Strategy Description
1	$SA = \begin{cases} 18 + 0.01 \text{ RPM} & \text{for RPM} < 1700 \\ 35 & \text{for RPM} > 1700 \end{cases}$
2	$SA = \begin{cases} 20 & \text{for } P_{man} < 5 \text{ psia} \\ (8.67\ P_{man} - 23.35) & \text{for } 5 < P_{man} < 8 \text{ psia} \\ 46 & \text{for } 8 < P_{man} < 11 \text{ psia} \\ (141.37 - 8.67\ P_{man}) & \text{for } P_{man} > 11 \text{ psia} \end{cases}$
3	$SA = \begin{cases} 20 & \text{for } P_{man} < 4 \text{ psia} \\ (6.67\ P_{man} - 6.67) & \text{for } 4 < P_{man} < 7 \text{ psia} \\ 40 & \text{for } 7 < P_{man} < 10 \text{ psia} \\ (90 - 5\ P_{man}) & \text{for } P_{man} > 10 \text{ psia} \end{cases}$
4	$SA = \begin{cases} 20 & \text{for } P_{man} < 7 \text{ psia} \\ (10\ P_{man} - 50) & \text{for } 7 < P_{man} < 8 \text{ psia} \\ 30 & \text{for } 8 < P_{man} < 11 \text{ psia} \\ (96 - 6\ P_{man}) & \text{for } P_{man} > 11 \text{ psia} \end{cases}$
5	Same as Strategy No. 4
6	Same as Strategy No. 4
7	Same as Strategy No. 3
8	Same as Strategy No. 4

As an output from the control logic, current signals are supplied to electropneumatic transducers. These transducers convert electrical signals to variable pneumatic control pressures which, when applied through pneumatic actuators, provide a means of mechanically moving the distributor for spark control and the EGR valve poppet for variable EGR flow rate. A block diagram of this system is shown in Figure 49.

Spark Advance Controls

For a detailed description of the operation of the control system, the Spark Advance Strategy No. 6 in Table 15 is used for illustration purposes. This strategy curve, shown in Figure 48, is composed of straight line segments, two ramps bounded by upper and lower limits. Details of the control logic implementation are illustrated in Figure 50. A description of the analog logic follows.
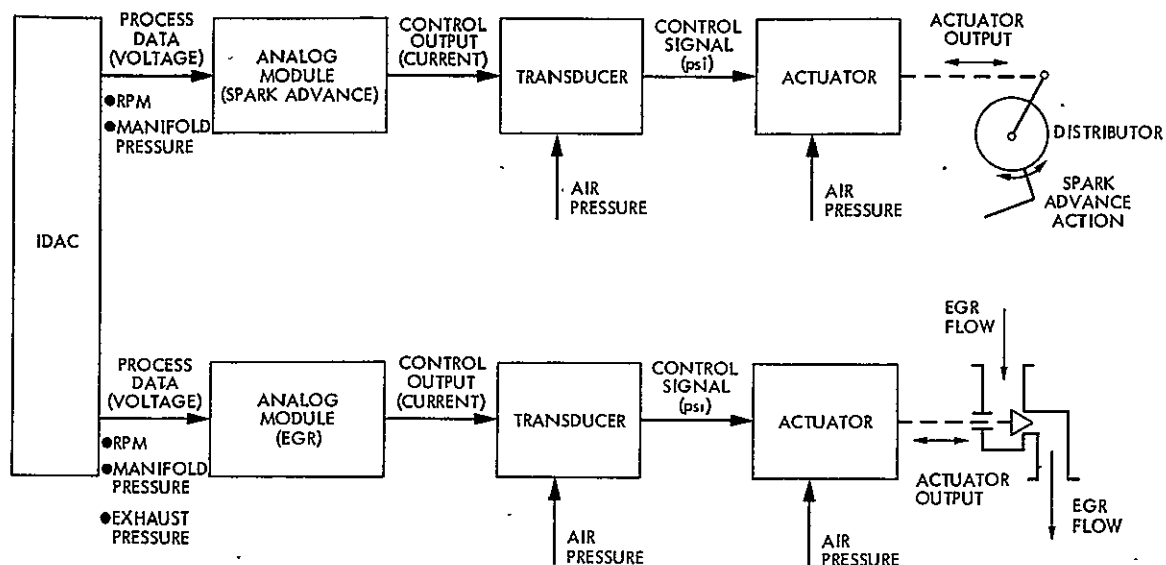
Figure 49. Block Diagram for Spark Advance and
EGR Control System

An analog of manifold pressure, generated by a pressure transducer and processed in IDAC, is supplied to the Voltage Interface Module as a DC voltage with a range of 0-9 volts. This module provides two functions. First, it re-ranges the signal to a nominal 1-5 volt range, providing compatibility with the balance of the logic elements. Secondly, it provides a means for both gain and offset adjustments through resettable controls, thus allowing the slope and Y-axis intercept for the up-ramp to be adjusted. Module gain is adjusted to provide: Δ(spark advance, degrees) = Δ $(P_{manifold}, psia)/10$. Module offset is adjusted to yield a spark advance of -50 degrees for a manifold pressure of 0 psia.

Output from the Voltage Interface Module (V2) interfaces with the High Select Amplitude Discriminator Module and the Inverse Output Voltage Module. The High Select Amplitude Discriminator Module provides a resettable adjustment of the lower limit for spark advance, i.e., an adjustment for constant spark advance at values of manifold pressure less than a specific value. This module, after comparing the input voltages V2 and V3 (an adjustable reference voltage), selects the higher of the two, and provides an output voltage (V4) proportional to the selected input. In operation, as the manifold pressure drops, V2 will also drop, but V3 will remain constant since it is fixed at a level corresponding to the selected lower limit spark advance. Output voltage V4 will track V2 until V2 falls below V3, at which time V4 will be set equal to V3 and will remain at this value until V2 exceeds V3. This module thus provides a lower limit on V4 which is set to correspond to a spark advance of 20 degrees for this strategy.

The output from the Voltage Interface Module (V2) is also supplied to the Inverse Output Voltage Module. This module generates the negative slope portion of the spark advance curve. Through the use of resettable controls,

76
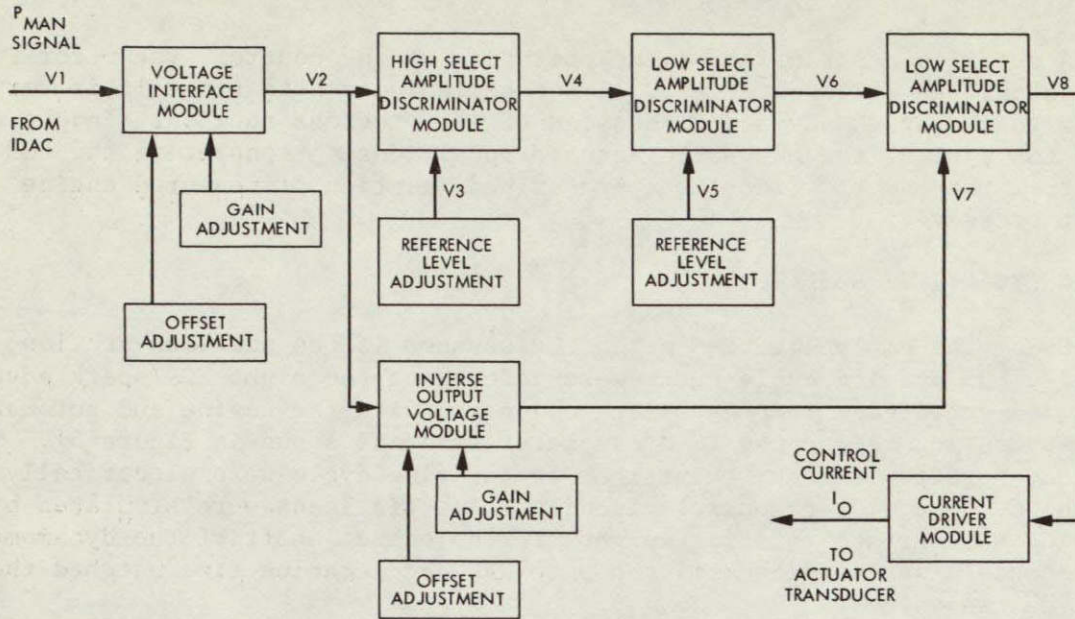
Figure 50. Typical Spark Advance Logic

gain and offset adjustments can be made, thus allowing the slope and Y-axis intercept for the down-ramp to be adjusted. Module gain is adjusted to provide: Δ(spark advance, degrees) = $-\Delta(P_{manifold}, psia)/6$. Module offset is adjusted to yield a spark advance of 96 degrees for a manifold pressure of 0 psia.

Output from this module (V7) is compared with V6 in the Second Low Discriminator Module. This module provides the transfer from upper limit on spark advance to the negative-sloping segment of the spark advance curve generated by the Inverse Output Voltage Module. In operation, as the manifold pressure increases, the output from the Inverse Output Voltage Module (V7) decreases. At the same time, the output from first Low Select Discriminator Module (V6) is set at a value corresponding to V5. Output from this module (V8) will track lower of the two values of V6 or V7. This provides the negative sloping portion of the curve for this spark advance strategy. This output voltage (V8) is converted to a proportional output current by the Current Driver Module. This module converts the nominal 1-5 volt signal to a 4-20 milliampere signal to provide the required compatibility with the balance of the system.

Mechanical actuation of the distributor is the final link to spark advance control of the engine. This actuation is accomplished with a pneumatic positioning actuator, whose position output is proportional to a varying pneumatic pressure, nominally 3-15 psi. This varying pressure is generated by a electropneumatic pressure transducer whose output pressure excursions are proportional to input signal variations.

77

EGR Controls

A detailed description of the operation of the control system for implementing the EGR strategies will not be included here since it is very similar to the spark advance discussion of the previous section. In the case of the EGR system, the pneumatic actuator positions the poppet in the EGR valve to control the EGR flow rate as a prescribed function of measured engine exhaust pressure.

DRIVING CYCLE TEST RESULTS

Using the implementation methods discussed in the previous section, Federal urban driving cycle tests were made using the eight EGR/spark advance strategies selected. The tests were conducted with the engine and automatic transmission mounted on the EC dynamometer stand as shown in Figure 51. The road load horsepower requirements for the driving cycle were electrically fed into the EC dynamometer control circuits. Inertia loads were simulated by attaching appropriate rotating weights to the output shaft of the dynamometer. Inertia wheels were added until the 0-60 MPH acceleration time matched the stock vehicle values.
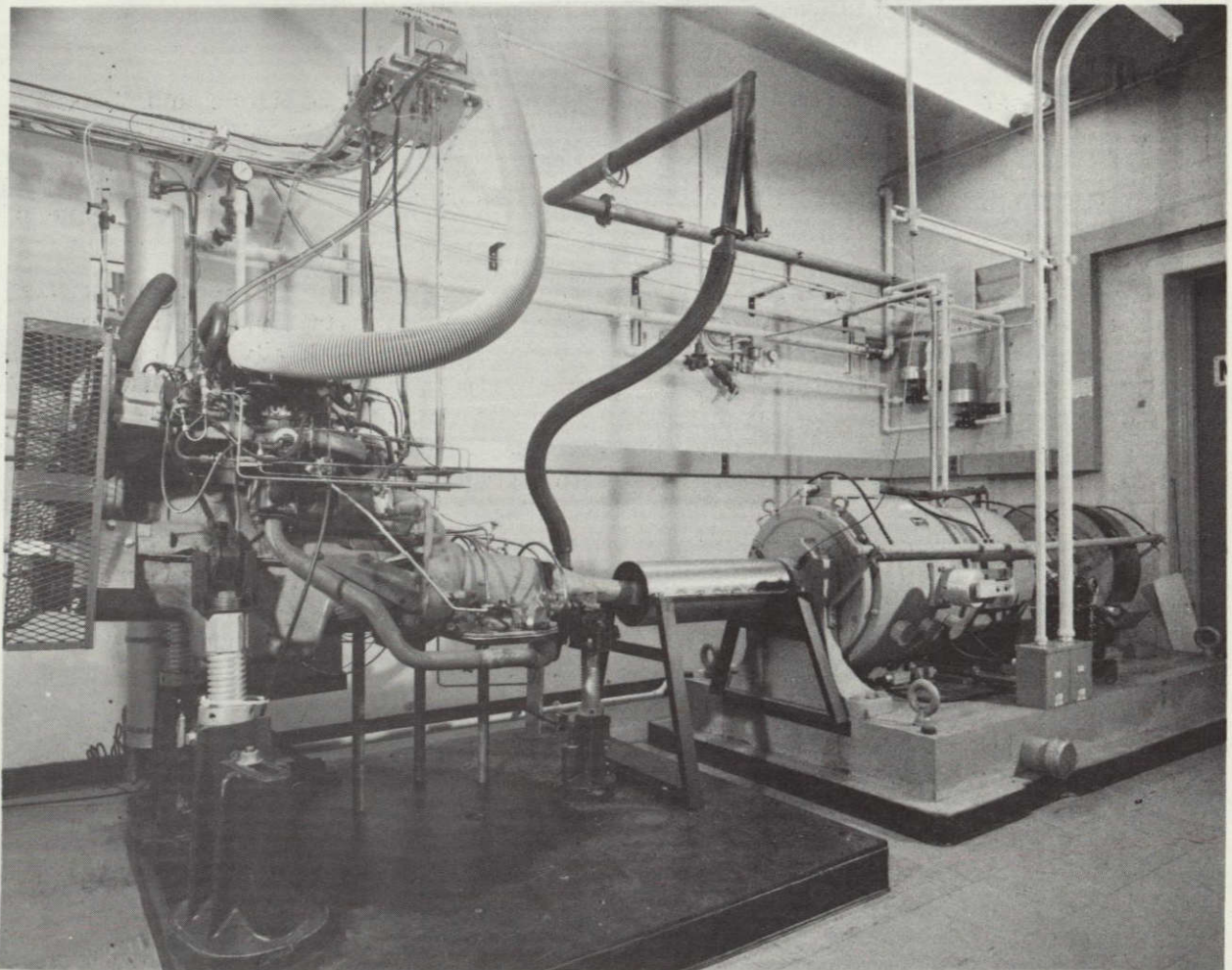
Figure 51. Eddy Current (EC) Dynamometer Test Setup

78

The complete cold-start 1975 Federal Test Procedure (FTP) was used for each of the control strategy tests. Both Constant Volume Sample (CVS) and continuous mode emissions data was recorded. The cold-start emissions devices and the AIR pump were operated in their stock condition for these tests.

Results of the EGR/spark advance strategy tests are given in Table 16 along with the stock test results. The trade-off between fuel economy and NO_x emissions is illustrated in Figure 52. The best fuel economy was achieved using Control Strategy No. 1 (zero EGR and MBT spark timing) which yielded about 16 percent better MPG than the stock system. However, the NO_x emissions from this strategy were very high, being about 4 times the stock value. At the same NO_x emissions level as the stock system, several strategies were able to show about 7-11 percent better fuel economy than stock. When HC emissions are considered, Control Strategy No. 6 appears to be best as shown in Figure 53. This strategy gave HC and NO_x emissions levels equivalent to the stock system and provided about 7 percent better fuel economy.

Since the completion of this activity, considerable effort has been directed toward determining an optimum engine calibration that maximizes fuel economy over the urban driving cycle subject to a set of emissions constraints (Refs. 41, 42). Use of these new techniques greatly reduces the testing required to optimize an engine.

Table 16. EGR/Spark Advance Control Strategy Tests
Federal Urban Driving Cycle Results

Day	Tape	Strategy	MPG	NO_x(g/mi)	CO(g/mi)	HC(g/mi)
6146	Y468	Stock	14.58	0.80	5.65	1.02
6113	W667	1	16.97	3.18	11.12	0.74
6124	Y133	2	15.51	1.32	16.62	1.32
6126	Y136	3	15.28	1.20	20.48	1.74
6126	Y137	4	16.25	1.00	13.44	2.08
6127	N921	5	15.65	0.74	14.80	2.08
6132	N926	6	15.61	0.81	9.72	1.06
6133	N927	7	14.48	1.08	6.21	1.38
6133	N928	8	14.47	1.09	10.50	1.17
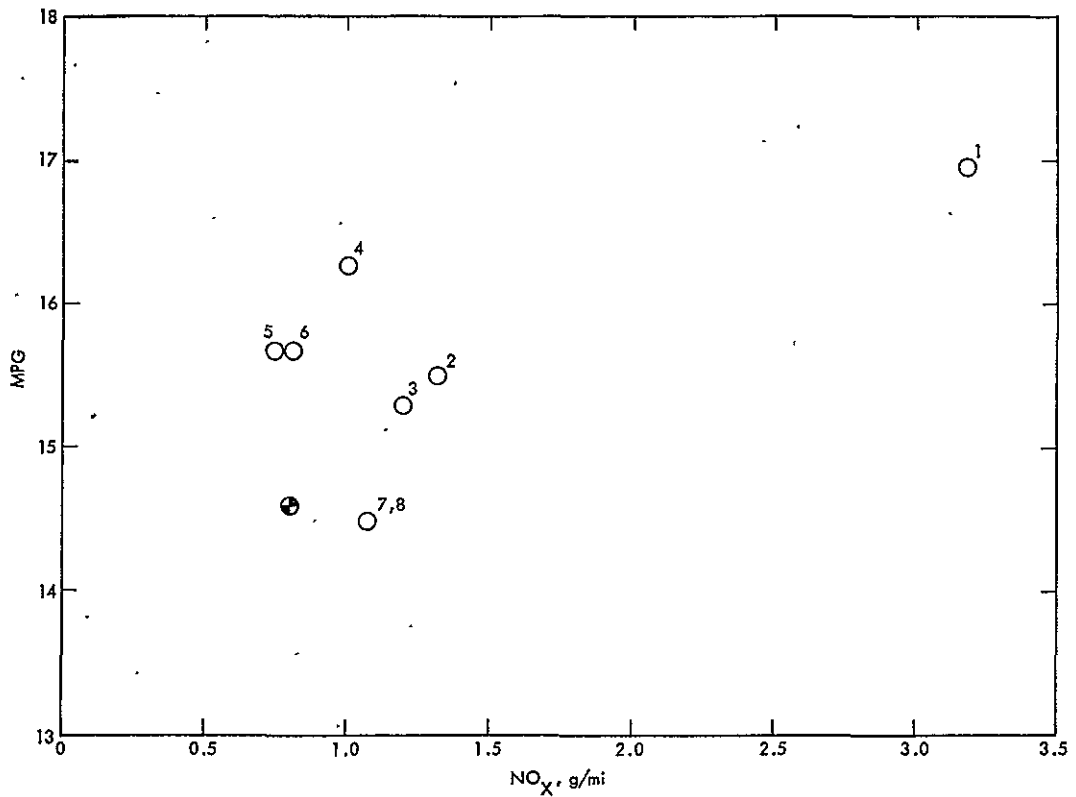
Figure 52. Urban Driving Cycle Results for EGR/Spark
Advance Strategies – NO_x Versus MPG
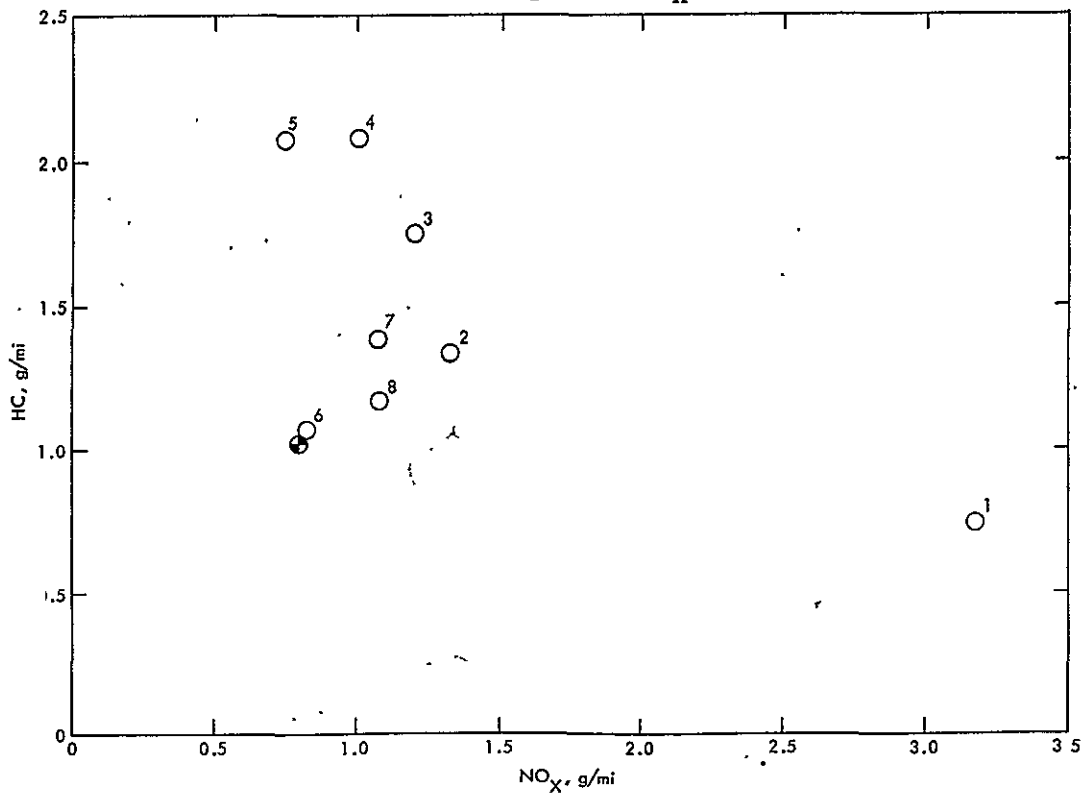
Figure 53. Urban Driving Cycle Results for EGR/Spark
Advance Strategies – NO_x Versus HC

SECTION V

AIR EVALUATION

BACKGROUND INFORMATION

Many of the techniques used to control NO_x emissions aggravate the HC/
CO emissions problem. When primary combustion is carried out under rich con-
ditions ($\phi>1$), considerable HC and CO are present in the exhaust due to a lack
of sufficient oxygen to complete the oxidation reactions. Also, the use of
large quantities of EGR tends to result in more HC emissions in the exhaust.
Techniques commonly used to control HC/CO emissions from the engine are thermal
reactors and catalytic converters. In either case, it is necessary that
sufficient oxygen be present in the exhaust for the oxidation reactions to go
to completion. This excess oxygen can be achieved by running the engine lean
($\phi<1$) or by supplying additional air to the exhaust stream from the engine.
The system used to provide additional air to the exhaust is called an air
injection reactor (AIR) system.

Much of the early work on AIR systems was directed toward its use with
thermal reactors rather than catalytic converters. In this case, developing
an AIR system for an engine requires some tailoring of the reactivity and con-
centration of the exhaust species. The species' reactivities and concentra-
tions are important since both affect the conversion rate of HC and CO.

The composition of the exhaust stream, including HC and CO, varies con-
siderably under different engine operating conditions. In particular, HC
emissions levels are a function of air-to-fuel ratio, mixture uniformity,
engine load, surface-to-volume ratio of combustion chamber, spark advance, and
engine operating temperatures. CO emissions are primarily a function of air-
to-fuel ratio. Since both HC and CO emissions increase with engine speed, it
would be desirable to match air injection with engine RPM.

It would require a complex control scheme to adequately match AIR flow
to the emissions concentration in the exhaust; however, it is not clear that
such a complex system is desirable. The fact that HC and CO are both reducing
agents is probably one of the few things they have in common. They are
different chemically, and they occur at different stages of the combustion
reaction. Brownson and Stebar. (Ref. 43), in their research aimed at determin-
ing the optimum injection rates, found that the best AIR flow is not the same
for HC and CO. The AIR flow requirements for optimum HC and CO reduction
were the same for air-to-fuel ratios between 10 and 14.5; however, for air-to-
fuel ratios leaner than 14.5, the CO requirement for AIR flow was 4 to 5 times
greater than the HC requirement. The abrupt change in AIR requirement for
optimum CO reduction corresponded to a change in oxidation mechanism.
Luminous oxidation was observed for air-to-fuel ratios richer than 14.5, while
luminosity was not observed in leaner mixtures.

The reactivity of the species in the exhaust is another important influ-
encing factor. Regardless of the excess air present, the HC and CO will not
oxidize if the reaction rates are too low. Perhaps the strongest effect on
reaction rates is exerted by the exhaust manifold temperature. Lower bulk

temperatures lead to slower conversion rates. High conversion rates are important because the gases are in the exhaust pipe for a short time. In systems with a catalytic converter, the residence time in the catalyst unit is important. Other factors which are important in this case include catalyst activity, catalyst bed temperature, and exhaust concentrations.

Exhaust manifold volume and insulation have a strong influence on HC and CO emissions. Larger exhaust manifolds provide more residence time for the exhaust gases to complete the oxidizing reactions. The addition of insulation to the exhaust system increases exhaust gas temperature, and this increases the reactivity of the constituents.

The development of the General Motors AIR system is discussed by Steinhagen, et al. (Ref. 44) and Thompson (Ref. 45). These papers cover the practical aspects of making an AIR system work. The basic hardware needed for an AIR system are an air pump, a power supply for the pump, and plumbing to carry the air from the pump to the exhaust port or manifold. Practical application of the AIR system has shown the need for several additional hardware elements. An air bleed valve is required to prevent backfiring during a sudden closing of the throttle. This solution keeps the engine firing at all times, and prevents excess fuel from igniting in the exhaust system. A pressure relief valve on the AIR pump is required to give good engine operation at high speeds and loads. The relief valve prevents high back pressures from developing due to the increased flow from the AIR pump and it also reduces exhaust system temperatures which can become too high with the rich mixtures needed for maximum power. A third feature needed in the AIR system is a check valve in the supply line from the pump to the exhaust manifold. This prevents backflow into the AIR pump and supply line in the event of a failure in the pump drive. In vehicles using an AIR pump, other engine changes are normally made to improve the effectiveness in controlling exhaust emissions.

Alternative methods of adding air to the exhaust gases have been studied One such technique, called Pulsair (Ref. 46), uses the exhaust pressure fluctuations to induct the fresh air rather than an AIR pump. The advantages of this approach are that it does not affect net engine power, and it is potentially less complex than the AIR pump system.

Various control techniques have been studied to more nearly optimize the air flow into the exhaust stream. Poyniak and Siewert (Ref. 47) studied a control system which tailored the air injection rate to the engine speed and load to produce a constant exhaust air-to-fuel ratio.

Under the proper conditions, air injection into the exhaust port or manifold will oxidize a large amount of the HC and CO in the exhaust. The effectiveness of the AIR system in reducing emissions is greatly enhanced when used in conjunction with a thermal reactor or catalytic converter.

TEST SETUP DESCRIPTION

Some success in controlling HC and CO emissions has been achieved by using an AIR system to provide additional air to the exhaust stream, especially in systems using a thermal reactor or catalytic converter. The baseline

vehicle for this activity has a catalytic converter to aid in controlling HC and CO emissions. The AIR tests on this project were structured to provide information about the relationship between emissions and the AIR emission control approach. A series of sensitivity tests were made while varying the flow rate from the AIR system. These tests were made at steady-state conditions on a water brake dynamometer.

For the sensitivity tests, the EGR system, the spark advance, and all cold-start emissions devices were operated in a stock manner. Since all of these tests were run with the engine in a fully warmed-up condition, the cold-start emissions devices should have had no influence on the test results. Rather than attempt to incorporate a variable speed drive for the AIR pump, facility air was used to supply the air for injection into the exhaust system. To keep approximately the same parasitic loss on the engine, the AIR pump continued to be driven by the engine during these tests. Air flow was measured using a laminar flow element, and then supplied to the stock hose leading to the AIR distribution manifold in the engine block.

SENSITIVITY TESTS

Eleven operating conditions were selected for evaluation in the AIR sensitivity tests. The test conditions were selected to give adequate coverage of the region of the operating map which is most frequently used in driving the urban driving cycle. This is appropriate for developing an AIR control strategy since vehicle emissions results are based on the urban driving cycle test. The selected test conditions are shown in Figure 54.
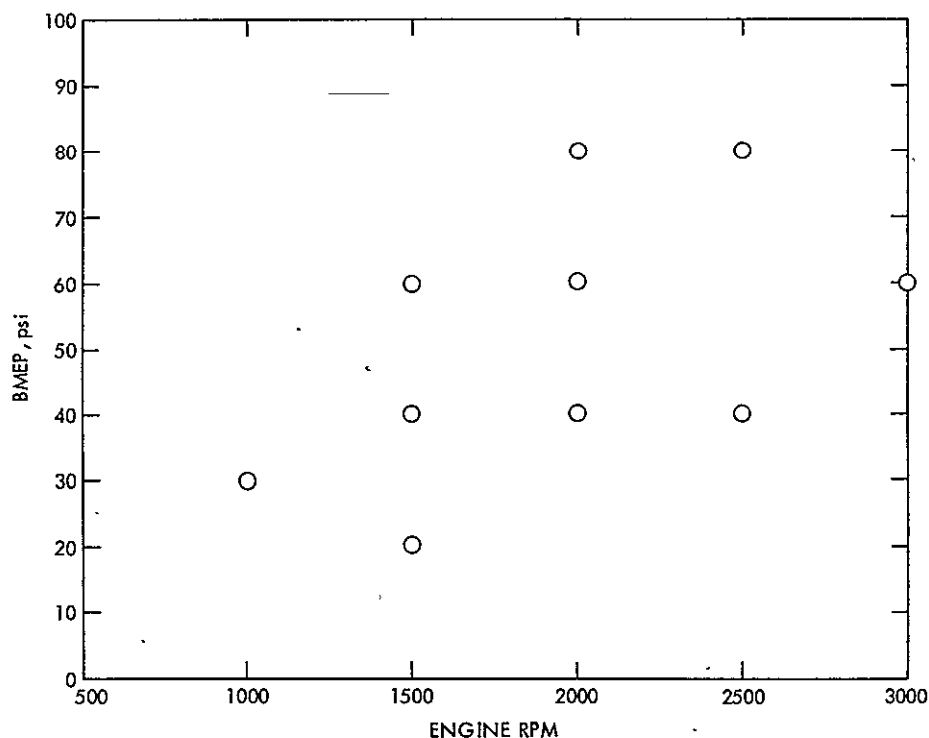
Figure 54. Operating Conditions Used for AIR Sensitivity Tests

Measurements of fuel consumption and HC, CO, and NO_x emissions were taken for each engine operating condition. Exhaust emissions were measured both upstream and downstream of the oxidation catalyst. Engine equivalence ratio and AIR flow rate were used to determine the excess air available in the oxidation catalyst.

To simplify the presentation of material and the discussion of the results, detailed results for only two engine operating conditions are presented in the main body of the report. These two conditions represent a case where the primary combustion is rich ($\phi>1$) and a case where the primary combustion is lean ($\phi<1$). Similar data and plots for the remaining test conditions are included in Appendix F.

The operating condition selected to represent the lean primary combustion case is 2000 RPM and 40 BMEP. Sensitivity test results for this operating condition are given in Table 17. The equivalence ratio for this test condition is 0.90 indicating that about 10 percent excess air is available in the exhaust to promote further oxidation of HC and CO in the exhaust manifold or in the oxidation catalyst. HC emissions, both upstream and downstream of the oxidation catalyst, are shown plotted versus percent AIR in Figure 55. The catalyst is effective in reducing HC emissions for all AIR flow rates. This is a result of the lean calibration ($\phi = 0.90$) of the engine at this operating condition. Note that the minimum upstream HC emissions occur for about 6 percent AIR flow added to the exhaust. The corresponding plot of CO emissions versus percent AIR is given in Figure 56. Again the catalyst is effective in reducing CO emissions for all AIR flow rates. In this case, however, the minimum upstream CO emissions occur for about 30 percent AIR flow. Thus, the AIR flow required to minimize upstream CO emissions is 5 times as large as the flow required to minimize upstream HC emissions. This result is consistent with the findings of Brownson and Stebar (Ref. 43) for primary combustion leaner than stoichiometric. Average exhaust temperature is shown in Figure 57. Exhaust temperature decreases as more AIR flow is added to the exhaust stream. For this engine operating condition, the catalyst conversion efficiencies for HC and CO are very high and are essentially independent of AIR flow rate since all test points have excess air.

The operating condition representing the rich primary combustion case is 1000 RPM and 30 BMEP. Sensitivity test results for this operating condition are given in Table 18. The equivalence ratio in this case is 1.04. HC emissions, both upstream and downstream of the catalytic converter, are shown plotted versus percent AIR in Figure 58. The catalyst becomes more effective at reducing HC emissions for AIR flows greater than 10 percent. Note that the minimum upstream HC emissions occur for about 30 percent AIR flow. A plot of CO emissions is given in Figure 59. Again the catalyst is more effective for AIR flows greater than 10 percent. Minimum CO emissions occur for about 30 percent AIR flow, which is the AIR flow for minimum HC emissions. This result is again consistent with the findings of Brownson and Stebar (Ref. 43) for primary combustion richer than stoichiometric. HC and CO conversion efficiencies are shown plotted versus the effective equivalance ratio ϕ_A, in Figures 60 and 61, respectively. With excess air, the conversion efficiency of CO levels out at about 95 percent, while the conversion efficiency of HC reaches about 64 percent. When the effective

84

Table 17. AIR Sensitivity Test Results for RPM = 2000 and BMEP = 40 psi

Sequence No.	RPM	BMEP (psi)	$\dot{m}_{gaso}$ (lbm/h)	$\dot{m}_{air}$ (lbm/h)	% A.I.R.	% EGR	Spark Advance (°BTDC)	Average T_{exh} (°F)	ϕ	ϕ_A	ϕ_E	BSFC (lbm/bhp-h)	Emissions Data*	$BSNO_x$ (g/bhp-h)	BSHC (g/bhp-h)	BSCO (g/bhp-h)	$\dot{m}_{A.I.R.}$ (lbm/h)	$\dot{m}_{EGR}$ (lbm/h)	η_{HC}	η_{CO}
3152.36	2052	39.9	15.39	238.8	0.0	19.5	29.2	1293	0.931	0.931	0.740	0.661	U	2.35	5.82	26.29	0.1	61.7		
3154.36	2052	39.9	15.39	238.8	0.0	19.5	29.2	1293	0.931	0.931	0.740	0.661	D	2.42	0.57	1.04	0.1	61.7	90.2	96.0
3152.33	2035	40.0	15.47	237.4	7.6	19.8	29.2	1265	0.942	0.867	0.746	0.670	U	2.87	5.33	21.16	20.8	62.4		
3154.33	2035	40.0	15.47	237.4	7.6	19.8	29.2	1265	0.942	0.867	0.746	0.670	D	3.05	0.57	0.52	20.8	62.4	89.3	97.5
3152.30	1952	40.6	14.85	227.8	14.4	20.0	28.6	1227	0.943	0.800	0.745	0.661	U	3.19	6.02	17.07	40.9	60.7		
3154.30	1952	40.6	14.86	227.8	14.4	20.0	28.6	1227	0.943	0.800	0.745	0.661	D	3.40	0.72	0.44	40.9	60.7	88.0	97.4
3152.27	1964	40.1	14.87	227.1	20.2	20.6	28.8	1199	0.947	0.746	0.742	0.665	U	3.55	5.80	14.96	61.2	62.7		
3154.27	1964	40.1	14.87	227.1	20.2	20.6	28.8	1199	0.947	0.746	0.742	0.665	D	3.82	0.81	0.41	61.2	62.7	86.0	97.3
3152.24	1978	40.2	14.83	227.6	25.1	21.0	28.9	1171	0.942	0.695	0.734	0.657	U	3.88	5.95	11.96	81.4	64.5		
3154.24	1978	40.2	14.83	227.6	25.1	21.0	28.9	1171	0.942	0.695	0.734	0.657	D	4.24	0.93	0.37	81.4	64.5	84.4	96.9
3152.21	2024	40.3	15.48	234.0	28.9	21.3	28.9	1152	0.956	0.668	0.742	0.668	U	4.21	5.94	10.39	101.4	67.6		
3154.21	2024	40.3	15.48	234.0	28.9	21.3	28.9	1152	0.956	0.668	0.742	0.668	D	4.51	1.04	0.36	101.4	67.6	82.5	96.5

*U = Upstream of catalytic converter; D = downstream of catalytic converter.
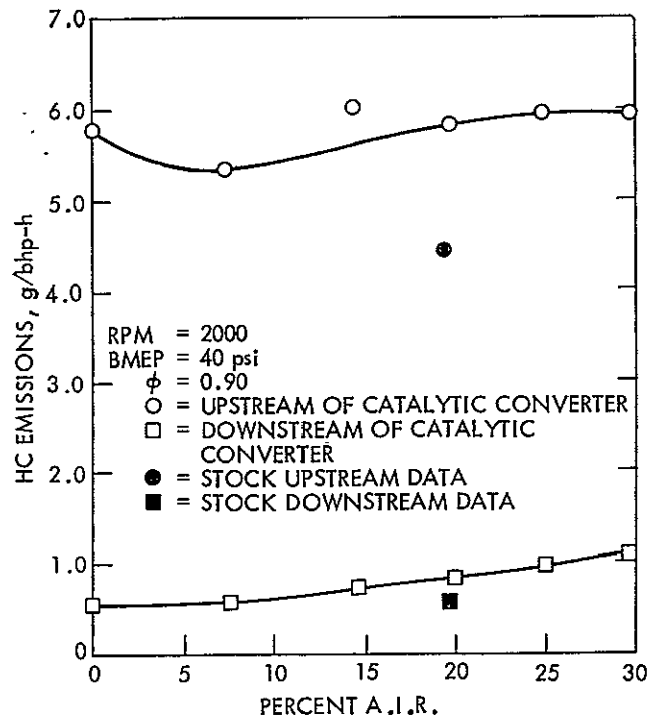
Figure 55. HC Emissions for AIR Sensitivity Test
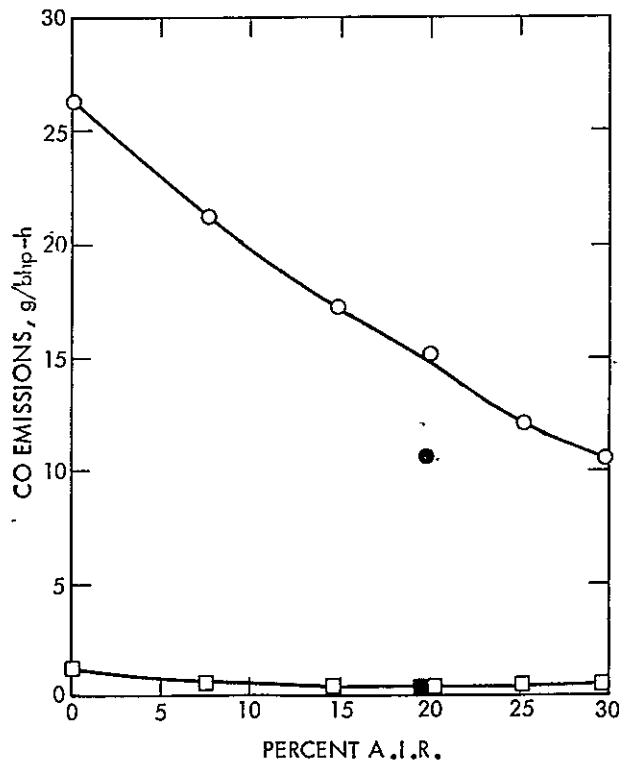
Figure 56. CO Emissions for AIR Sensitivity Test
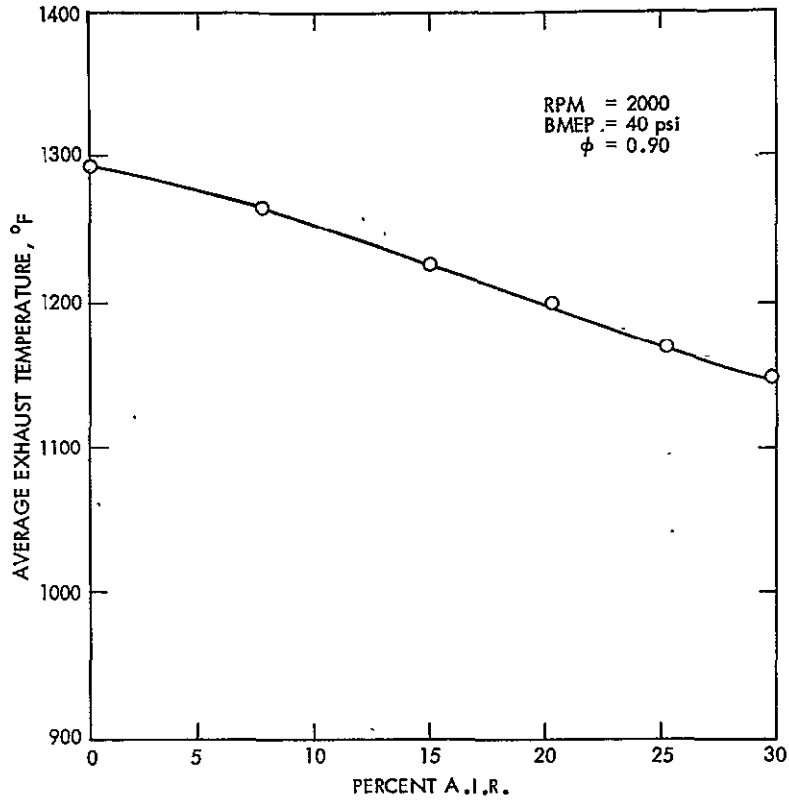
Figure 57. Average Exhaust Temperature
for AIR Sensitivity Test
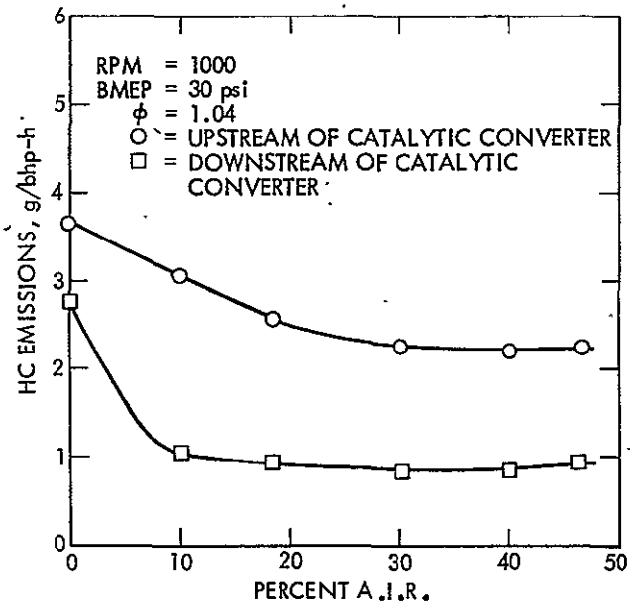
Figure 58. HC Emissions for AIR
Sensitivity Test

Table 18. AIR Sensitivity Test Results for RPM = 1000 and BMEP = 30 psi

Sequence No.	RPM	BMEP (psi)	$\dot{m}_{gaso}$ (lbm/h)	$\dot{m}_{air}$ (lbm/h)	% A.I.R.	% EGR	Spark Advance (°BTDC)	Average T_{exh} (°F)	ϕ	ϕ_A	ϕ_E	BSFC (lbm/bhp-h)	Emissions Data*	BSNO$_x$ (g/bhp-h)	BSHC (g/bhp-h)	BSCO (g/bhp-h)	$\dot{m}_{A.I.R.}$ (lbm/h)	$\dot{m}_{EGR}$ (lbm/h)	η_{HC}	η_{CO}
3130.44	1012	30.8	6.20	86.1	0.1	11.7	20.3	1034	1.040	1.038	0.911	0.700	U	5.16	3.67	18.73	0.1	12.2		
3130.08	1010	31.0	6.22	86.7	0.1	11.5	20.3	1033	1.037	1.036	0.910	0.701	D	4.14	2.76	9.36	0.1	12.1	24.8	50.0
3130.41	1017	30.9	6.21	86.2	10.2	11.8	20.1	1027	1.041	0.928	0.911	0.695	U	5.74	3.09	13.86	10.6	12.3		
3130.11	1011	30.9	6.18	86.6	9.8	11.6	20.1	1027	1.031	0.824	0.904	0.697	D	4.82	1.04	0.80	10.2	12.2	66.3	94.2
3130.38	1024	30.9	6.17	86.3	18.5	11.9	20.5	1014	1.034	0.833	0.903	0.687	U	6.36	2.57	10.71	20.9	12.5		
3130.19	1019	30.8	6.25	86.5	18.7	11.7	20.2	1015	1.043	0.838	0.913	0.702	D	5.56	0.94	0.56	21.4	12.4	63.4	94.8
3130.35	1028	30.9	6.19	86.1	30.7	12.2	20.6	971	1.040	0.705	0.905	0.687	U	7.30	2.27	6.29	40.9	12.8		
3130.20	1026	30.9	6.14	86.6	30.2	12.0	20.8	973	1.025	0.701	0.895	0.683	D	5.81	0.85	0.47	40.2	12.6	62.6	92.5
3130.32	1034	30.9	6.13	86.4	39.5	12.4	20.7	918	1.025	0.605	0.890	0.675	U	7.88	2.24	14.28	60.3	13.2		
3130.23	1032	30.9	6.12	86.6	40.2	12.4	20.7	915	1.023	0.595	0.888	0.677	D	6.49	0.84	0.40	62.3	13.1	62.5	97.1
3130.29	1030	30.9	6.19	86.3	46.4	12.6	20.5	865	1.036	0.538	0.897	0.683	U	8.71	2.24	12.42	80.2	13.4		
3130.26	1036	30.9	6.18	86.4	46.3	12.7	21.0	866	1.034	0.538	0.895	0.681	D	7.80	0.91	0.39	79.8	13.4	59.4	96.9

*U = Upstream of catalytic converter; D = downstream of catalytic converter.
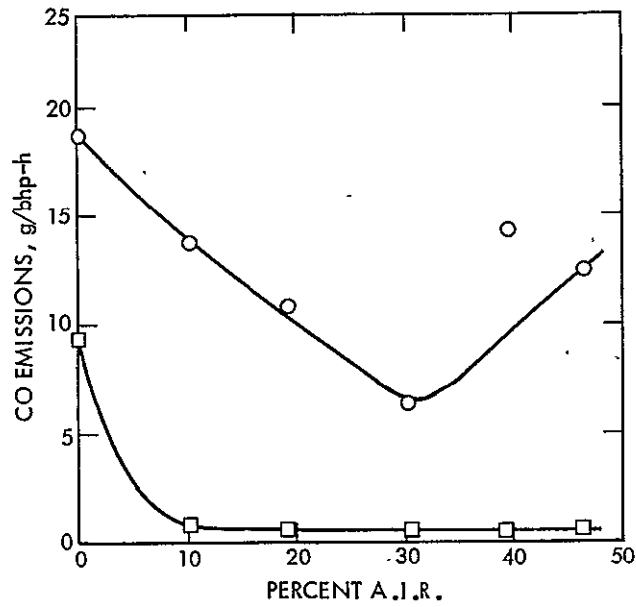
Figure 59.   CO Emissions for AIR Sensitivity Test
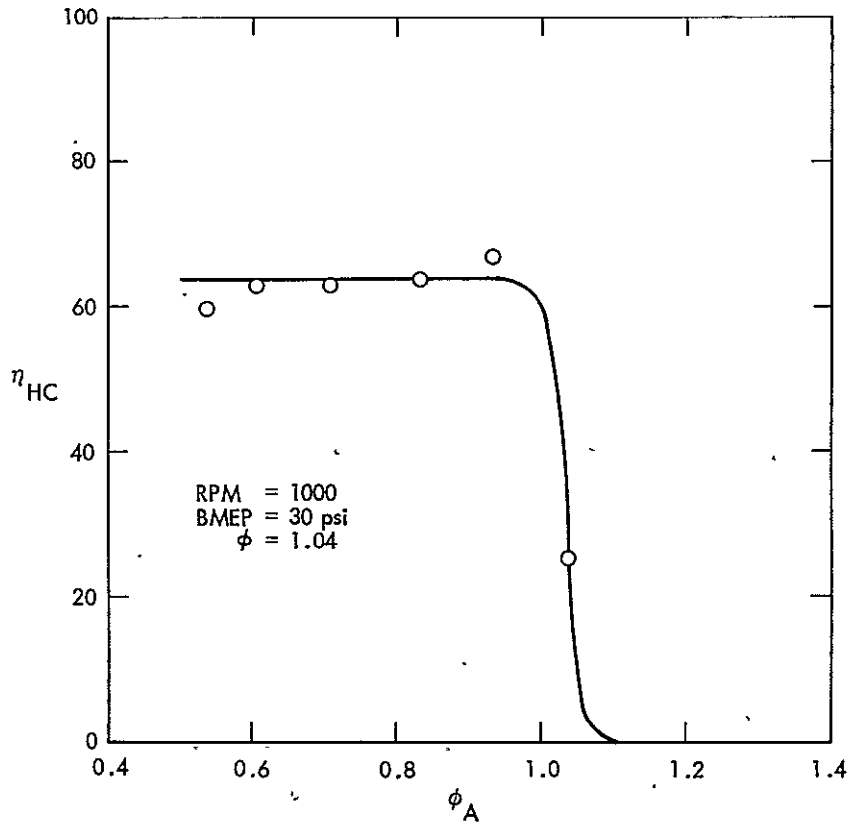
Figure 60.   HC Conversion Efficiency for
AIR Sensitivity Test

89
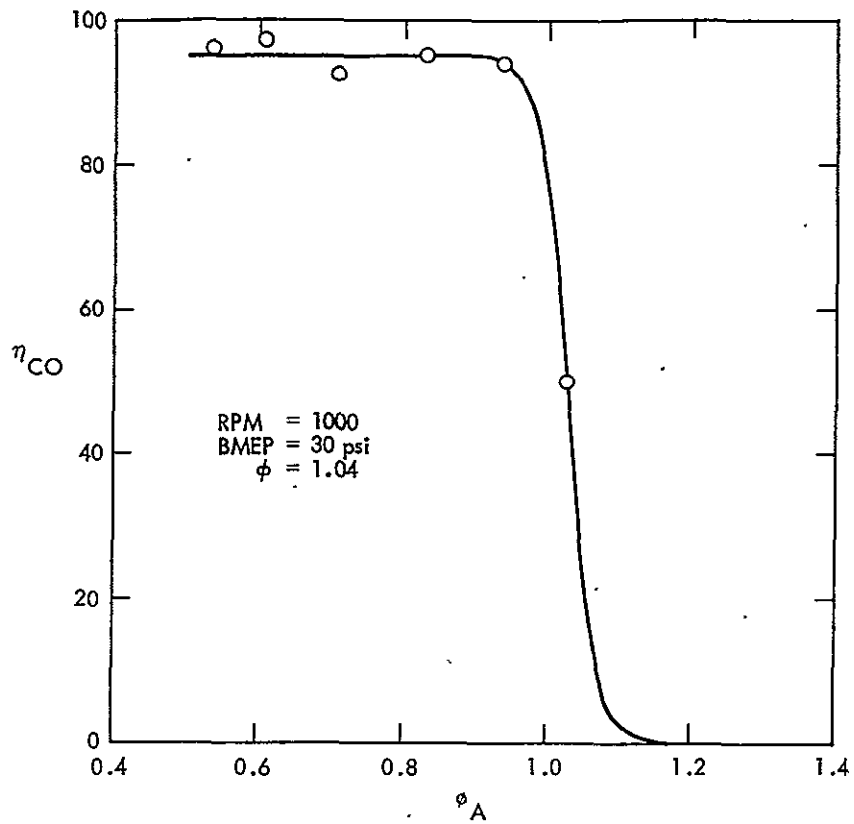
Figure 61. CO Conversion Efficiency for
AIR Sensitivity Test
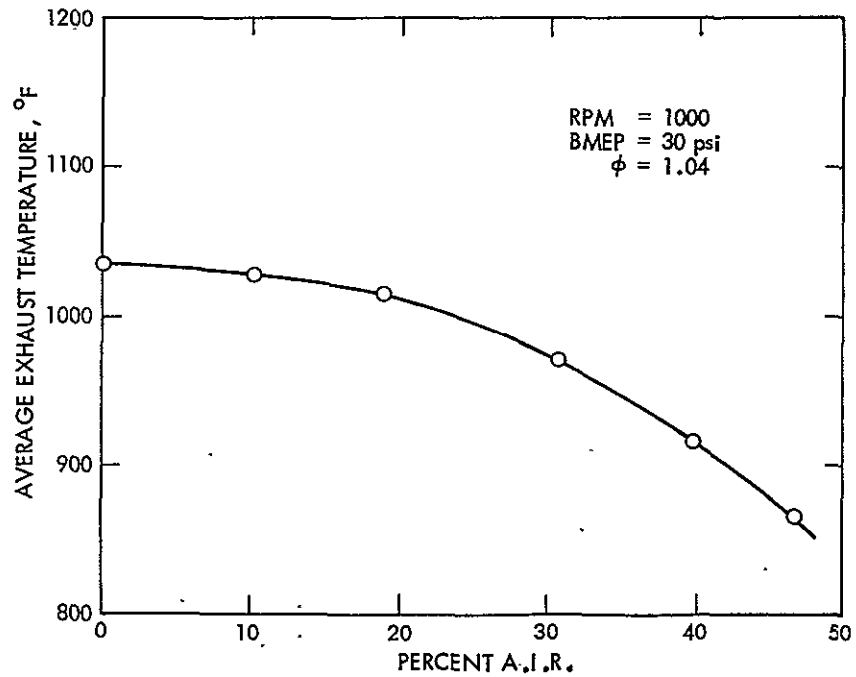
Figure 62. Average Exhaust Temperature for
AIR Sensitivity Test

90

equivalence ratio exceeds one, the conversion efficiencies drop rapidly. A plot of average exhaust temperature is given in Figure 62. The exhaust temperature drops continuously as more AIR flow is fed through the AIR distribution manifold.

SECTION VI

MODIFIED VEHICLE TESTS

SYSTEM DESCRIPTION

Based on the results of the engine dynamometer evaluations of EGR, AIR, and cold-start emissions systems, a modified emissions control system was selected for evaluation at the vehicle level. Interactions among the various system modifications were not considered in the selection process. Although it is recognized that such interactions probably exist, it was beyond the scope of the present work to examine thoroughly all combinations of the modifications studied.

Based on the driving cycle results from the EC dynamometer, EGR/Spark Advance Control Strategy No. 6 was chosen for implementation on the vehicle. This strategy gave the best fuel economy at the same emissions levels in these tests. The stock AIR strategy was maintained since test results indicated that adequate air was being supplied for the catalytic conversion of HC and CO under most operating conditions. The stock EGR delay time was used since no improvement was observed for other delay times.

The electrically-heated hot spot demonstrated some improvement in cold-start emissions; therefore, it was used in the vehicle tests. The exhaust system was the parallel path configuration, shown in Figure 37, with the cold-start catalyst unit and standard catalyst unit modified with the electrically-heated catalyst element, shown in Figure 39.

TEST RESULTS

Testing of the modified vehicle was done on the JPL chassis dynamometer facility. To provide a better baseline for the modified tests, the stock vehicle tests were made using the modified exhaust hardware with all exhaust gas being directed through the standard catalyst unit. The test results for these vehicle tests are given in Table 19. All tests were complete cold-start urban driving cycles. Emissions results are shown in both grams per bag and weighted g/mi over the driving cycle. Plots of the fuel economy and emissions are given in Figures 63, 64, and 65.

Results of the modified vehicle tests can be summarized by looking at three of the modified tests. In modified test No. 1, the vehicle matched the fuel economy and NO_x emissions of the baseline and reduced HC emissions from 0.5 to 0.4 g/mi and reduced CO emissions from 3.8 to 2.7 g/mi. For modified test No. 6, fuel economy increased from 15.0 to 15.9 MPG, HC emissions decreased from 0.5 to 0.4 g/mi and CO emissions decreased from 3.8 to 3.2 g/mi when NO_x emissions were allowed to increase from 1.1 to 1.6 g/mi. By making the NO_x emissions requirement less stringent, further increases in fuel economy and reductions of HC and CO emissions were possible. By letting NO_x emissions increase from 1.1 to 2.7 g/mi in test No. 3, fuel economy increased from 15.0 to 16.9 MPH, HC emissions were reduced from 0.5 to 0.21 g/mi and CO emissions decreased from 3.8 to 2.4 g/mi.. The fuel economy values discussed here are based on carbon balance calculations from the CVS emissions

Table 19. Chassis Dynamometer Results for Vehicle
with Modified Emissions Control System

Test	Day	Tape	Fuel Economy		HC (g)			CO (g)			NO$_x$ (g)			HC (g/mi)	CO (g/mi)	NO$_x$ (g/mi)	Notes
			MPG$_{wt}$	MPG$_{cvs}$	Bag 1	Bag 2	Bag 3	Bag 1	Bag 2	Bag 3	Bag 1	Bag 2	Bag 3				
Baseline	6279	I106	13.60	14.78	4.58	0.62	1.82	64.25	0.96	3.12	5.56	3.79	4.65	0.48	4.05	1.18	Mod config.
Baseline	6280	I231	13.74	14.86	3.98	0.60	1.02	58.85	1.46	2.94	4.84	3.69	4.42	0.39	3.79	1.10	
Baseline	6281	I232	14.16	15.10	4.17	0.85	3.52	60.28	1.03	2.06	4.41	3.67	4.50	0.62	3.75	1.09	
Average Baseline			13.83	14.91	4.24	0.69	2.12	61.13	1.15	2.71	4.94	3.72	4.52	0.50	3.86	1.12	
1	6292	I553	13.38	14.84	3.62	0.94	0.83	29.57	0.89	11.62	3.98	4.31	3.15	0.40	2.70	1.04	Choke open
2	6293	I554	14.26	15.99	2.67	0.32	0.58	63.97	0.29	9.29	4.80	14.06	5.26	0.24	4.41	2.55	Stock choke
3	6294	x616	15.06	16.95	2.30	0.32	0.45	37.92	0.12	3.20	6.22	14.64	5.83	0.21	2.43	2.75	
4	6295	x618	13.58	15.14	3.67	0.72	0.85	85.16	2.15	14.23	3.04	5.59	2.16	0.37	6.25	1.08	
5	6296	x619	14.08	16.90	3.45	0.53	0.63	72.85	1.73	10.22	3.84	8.49	3.01	0.32	5.18	1.58	
6	6301	x620	13.94	15.90	3.53	0.89	1.28	49.28	1.18	4.15	4.92	7.52	3.81	0.42	3.30	1.57	No CSC
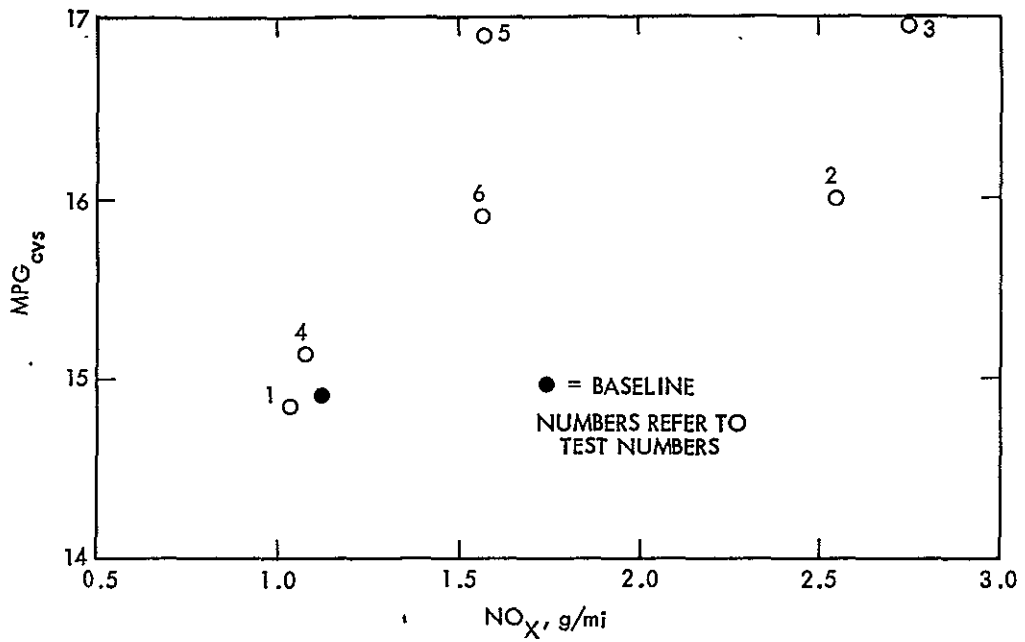
Figure 63. Fuel Economy Versus NO_x Emissions for Modified Vehicle Tests
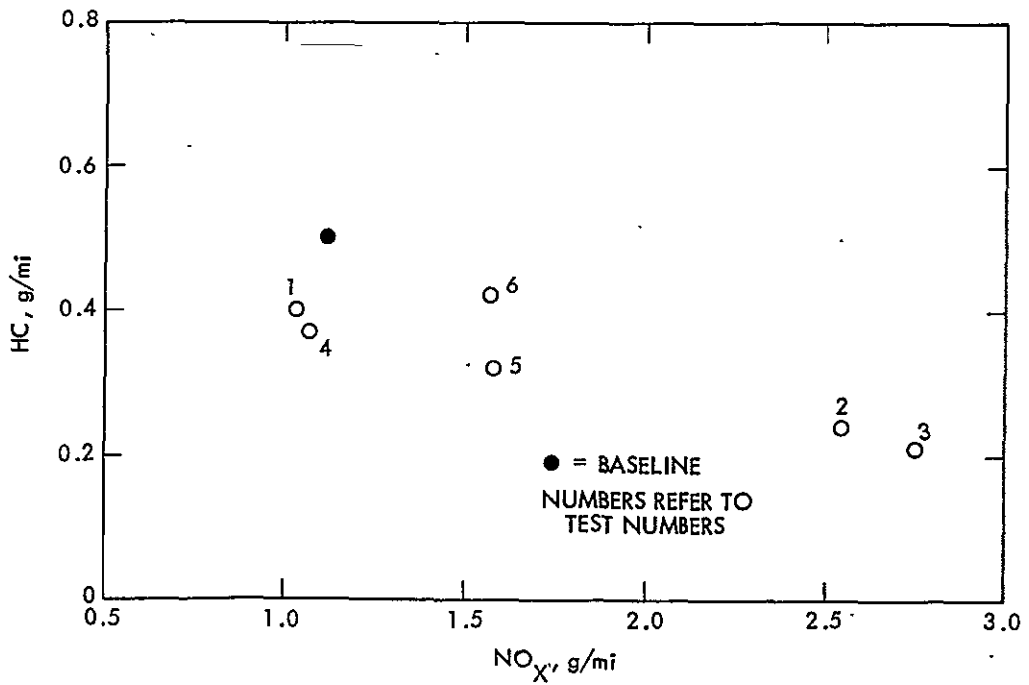
Figure 64. HC Emissions Versus NO_x Emissions for Modified Vehicle Tests

94
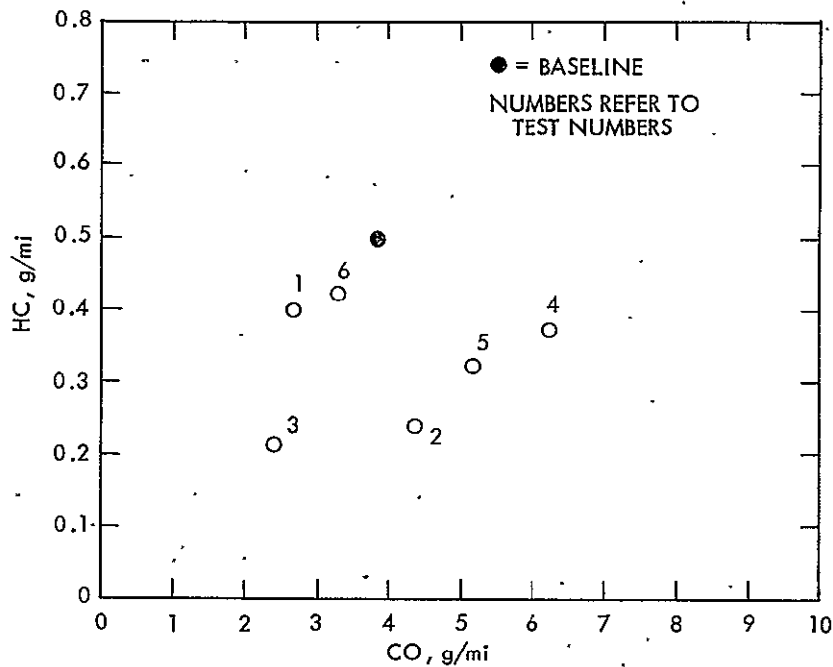
Figure 65. HC Emissions Versus CO Emissions
for Modified Vehicle Tests

results. This is the method used in the mileage numbers published from EPA
tests. These vehicle results are summarized in Table 20.

The results from the vehicle tests were not as good as expected.
Apparently., interactions among the various modifications tended to cancel
some of the individual benefits. The results again emphasize the difficulty
of demonstrating with hardware the potential of concepts which look technically
sound. With a more thorough evaluation of some of these concepts, it is likely
that more of their apparent potential could be achieved. It seems clear that
the selection and implementation of modified control strategies or new emis-
sions control devices is a complex process which must be treated from a systems
standpoint with all important interactions considered. The effect of engine
equivalence ratio variations should also be included in any future fuel
economy/emissions trade-off study.

Table 20. Modified Vehicle Test Results for
Urban Driving Cycle

Test	NO$_x$ Level (g/mi)	Results*
Baseline	1.1	MPG = 14.91 HC = 0.50 g/mi CO = 3.86 g/mi
1	1.1	Same MPG Reduce HC from 0.5 to 0.4 g/mi Reduce CO from 3.9 to 2.7 g/mi
6	1.6	Increase MPG from 15.0 to 15.9 Reduce HC from 0.5 to 0.4 g/mi Reduce CO from 3.9 to 3.3 g/mi
3	2.7	Increase MPG from 15.0 to 16.9 Reduce HC from 0.5 to 0.2 g/mi Reduce CO from 3.9 to 2.4 g/mi
*Fuel economy based on carbon balance technique.		

REFERENCES

1. EPA/FEA 1975 Gas Mileage Guide for New Car Buyers.

2. Chrysler Corporation Chassis Service Manual for the 1975 Passenger Car.

3. Austin, T. C. and Hellman, K. H., "Passenger Car Fuel Economy – Trends and Influencing Factors," SAE 730790, 1973.

4. Federal Register, Volume 42, No. 124, pg. 32988, June 28, 1977.

5. Austin, T. C., Michael, R. B., and Service, G. R., "Passenger Car Fuel Economy Trends Through 1976," SAE 750957, 1975.

6. Trayser, D. A., et al., A Study of the Influences of Fuel Atomization, and Mixing Processes on Pollutant Emissions from Motor-Vehicle Power-plants, Battelle Memorial Institute Report to the National Air Pollution Control Administration, Contract No. CPA 22-69-9, 30 April 1969.

7. Bartholomew, E., "Potentialities of Emission Reduction by Design of Induction Systems," SAE PT-2, 192 (1963-66).

8. Eltinge, L., Morsee, F. J. and Warren, A. J., "Potentialities of Further Emissions Reduction by Engine Modifications," SAE Paper 680123, 1968.

9. Evaluation of the Dresserator Emission Control System, Technology Assessment and Evaluation Branch, Environmental Protection Agency, August 1974.

10. John, J. E. A., "Lean Burn Engine Concepts – Emissions and Economy," SAE Paper 750930, 1975.

11. Hurter, D. A., et al., A Study of Technological Improvements in Automobile Fuel Consumption, Department of Transportation Report No. DOT-TSC-OST-74-40. I, II, III, December 1974.

12. Collins, M. H., "A Technique to Characterize Quantitatively the Air/Fuel Mixture in the Inlet Manifold of a Gasoline Engine," SAE Paper 690515, 1969.

13. Donahue, R. W., and Kent, R. H., Jr., "A Study of Mixture Distribution," SAE Quarterly Transaction, 4 (4), 546-558, 1950.

14. Robison, J. A., and Brehob, W. M., "The Influence of Improved Mixture Quality on Engine Exhaust Emissions and Performance," presented at Western States Combustion Institute Meeting, 25-26 October 1965.

15. Jones, J. H., and Gagliardi, J. C., "Vehicle Exhaust Emission Experiments Using a Pre-Mixed and Pre-Heated Air Fuel Charge," SAE paper 670485, 1967.

16. Yu, T. C., "Fuel Distribution Studies......A New Look at an Old Problem," SAE Transactions, 71, 596-613, 1963.

17. Lindsay, R., and Wilson, J., "Heat Pipe Vaporization of Gasoline-Vapipe," presented at First Symposium on Low Pollution Power and Alternative Automotive Power Systems Coordination Meeting, 14-19 October 1973.

18. Bond, W. D., "Quick-Heat Intake Manifolds for Reducing Cold Engine Emissions," SAE Paper 720935, 1972.

19. Request for Suspension of the 1977 Federal HC and CO Emissions Standards, submitted by Chrysler Corporation to the Environmental Protection Agency, January 1975.

20. "Chrysler's 'Electronic' Lean-Burn Engine," Machine Design, 10 July 1975.

21. Schweitzer, P. H., "Control of Exhaust Pollution Through a Mixture-Optimizer," SAE Paper 720254, 1972.

22. Pozniak, D. J., and Siewert, R. M., "Continuous Secondary Air Modulation - Its Effect on Thermal Manifold Reactor Performance," SAE Paper 730493, 1973.

23. Zechnall, R., Baumann, G., and Eisele, H., "Closed-Loop Exhaust Emission Control System with Electronic Fuel Injection," SAE Paper 730566, 1973.

24. Patterson, D. J., and Henein, N. A., Emissions from Combustion Engines and Their Control, Ann Arbor Sciences Publishers, Ann Arbor, Michigan 1972.

25. Mayo, J., "The Effect of Engine Design Parameters on Combustion Rate in Spark-Ignited Engines," SAE Paper 750355, 1975.

26. Brownson, D. A., and Stebar, R. F., "Factors Influencing the Effectiveness of Air Injection in Reducing Exhaust Emissions," SAE Paper 650526, 1965.

27. Herrin, R. J., "The Importance of Secondary Air Mixing in Exhaust Thermal Reactor Systems," SAE Paper 750174, 1975.

28. Lahiff, J. E., and Albertson, W. D., "Volume and Temperature Influences on the Effectiveness of Lean Thermal Reactors," SAE Paper 741168, 1974.

29. Ohigashi, S., et al., "Heat Capacity Changes Predict Nitrogen Oxides Reduction by Exhaust Gas Recirculation," SAE 710010.

30. Komiyama, K., and Heywood, J. B., "Predicting NO_x Emissions and Effects of Exhaust Gas Recirculation in Spark-Ignition Engines," SAE 730475.

31. Blumberg, P., and Kummer, J. T., "Prediction of NO Formation in Spark-Ignited Engines - An Analysis of Methods of Control," Combustion Science and Technology, 1971, vol. 4, pp. 73-95,

32. Engh, G. T., and Wallman, S., "Development of the Volvo Lambda-Sand System," SAE 770295, Feb. 1977.

33. Ghandi, H. S. et al., "Evaluation of Three-Way Catalysts - Part II," SAE Sp-414, Feb. 1977.

34. Mooney, J. J., et al., "Three-Way Conversion Catalysts - Part of the New Emission Control System," SAE 770365, Feb. 1977.

35. Quader, A. A., "Why Intake Charge Dilution Decreases Nitric Oxide Emission from Spark Ignition Engines," SAE 710009.

36. Dowdy, M. W., Hoehn, F. W., and Griffin, D. C., "Lean Mixture Engine Testing and Evaluation Program," paper presented at the 10th Intersociety Energy Conversion Engineering Conference, Aug. 17-22, 1975.

37. Hodges, J. L., "The Effect of Exhaust Recycle of Knock-Limited SI Engine Performance," SAE 750025.

38. Gumbleton, J. J., et al., "Optimizing Engine Parameters with Exhaust Gas Recirculation," SAE 740104.

39. Freeman, M. A., and Nicholson, R. C., "Valve Timing for Control of Oxides of Nitrogen (NO_x)," SAE 720121.

40. Thompson, A. L., "Buick's 1972 Exhaust Gas Recirculation System," SAE 750519.

41. Auiler, J. E., Zbrozek, J. D., and Blumberg, P. N., "Optimization of Automatic Engine Calibration for Better Fuel Economy - Methods and Applications," SAE 770076.

42. Juneja, Wiplove K., Kelley, William J., and Valentine, Richard W., "Computer Simulations of Emissions and Fuel Economy," SAE 780287.

43. Brownson, D. A., and Stebar, R. F., "Factors Influencing the Effectiveness of Air Injection in Reducing Exhaust Emissions," SAE 650526, Volume 74, 1966.

44. Steinhagen, W. K., "Design and Development of the GM Air Injection Reactor System," SAE 660106.

45. Thompson, W. B., "Air Pump for the GM Air Injection Reactor," SAE 660108.

46. Gast, R. A., "Pulsair - A Method for Exhaust System Induction of Secondary Air for Emissions Control," SAE 750172.

47. Pozniak, D. J., and Siewert, R. M., "Continuous Secondary Air Modulation - Its Effect on Thermal Manifold Reactor Performance," SAE 730493.

APPENDIX A

BASELINE VEHICLE DATA

Table A-1. Baseline Vehicle Test Results (Subaru Facility)

	1975 California Standard	Test No. 1	Test No. 2	Test No. 3	Average	EPA Certified Values
Urban Driving Cycle						
HC, g/mi	0.9	0.60	0.45	0.64	0.56	
CO, g/mi	9.0	3.47	3.70	4.02	3.73	
NO_x, g/mi	2.0	0.92	0.98	1.07	0.99	
Fuel Economy, mpg		14.90	14.57	14.79	14.75	15
Highway Driving Cycle						
Fuel Economy, mpg		20.11	19.92	19.92	19.98	20
Composite Cycle						
Fuel Economy, mpg		16.87	16.57	16.75	16.73	17

Olson Engineering Inc.

Vehicle Test Facility
15512 Commerce Lane
Huntington Beach, California 92649 (714) 894-9875

UNIT # 1
DATE: 10/08/75   TIME: 06:04:02
TEST # 4912
CHASSIS # PLY VALIANT
ENGINE # /
CLASS 4
DISP 225
WEIGHT 3500
TRAN AUTØ
AXEL /
CARB 2 BBL
ØDØM 3879
TEMP. 76
BAR 29.96
HUMID 38
J.P.L. COLD START / BASELINE

MØDE	------CONCENTRATION-----				-----MASS-----			--ACCUM MASS--		
	HC	CØ	NØ	CØ2	HC	CØ	NØ	HC	CØ	NØ
1-I	103.7	842.0	3.2	0.3	0.1	1.7	0.0	0.1	1.7	0.0
2-A	178.8	1647.0	3.9	0.5	0.1	1.5	0.0	0.2	3.2	0.0
31C	495.8	2643.0	59.6	1.5	0.8	9.1	0.3	1.0	12.3	0.3
4-C	292.2	1026.0	22.4	2.1	0.7	5.2	0.2	1.8	17.5	0.5
5-D	209.4	305.0	9.2	1.2	0.1	0.4	0.0	1.9	17.9	0.5
6-I	125.7	1469.0	1.9	0.5	0.2	5.7	0.0	2.1	23.6	0.5
7-A	105.8	670.0	41.8	2.6	0.2	2.9	0.3	2.4	26.4	0.8
8-C	83.6	80.0	76.0	3.6	0.2	0.4	0.5	2.5	26.8	1.3
9-C	77.7	25.0	52.7	3.0	0.2	0.1	0.4	2.7	26.9	1.7
10-D	28.0	16.0	8.7	1.0	0.0	0.1	0.0	2.8	27.0	1.8
11-I	19.1	14.0	4.5	0.6	0.0	0.0	0.0	2.8	27.0	1.8
12-A	31.6	29.0	51.8	2.2	0.0	0.1	0.2	2.8	27.0	1.9
13-C	25.6	17.0	28.3	1.9	0.0	0.0	0.1	2.9	27.1	2.0
14-D	13.5	14.0	25.5	0.6	0.0	0.0	0.1	2.9	27.1	2.1
15-I	16.8	14.0	4.7	0.6	0.0	0.0	0.0	2.9	27.1	2.1
16-A	23.5	29.0	53.0	2.1	0.0	0.0	0.1	2.9	27.1	2.2
17-D	19.0	25.0	14.4	1.2	0.0	0.0	0.0	2.9	27.2	2.2
18-I	16.1	17.0	5.1	0.6	0.0	0.0	0.0	2.9	27.2	2.2
●19-A	32.4	107.0	62.3	2.5	0.0	0.2	0.2	2.9	27.4	2.4
20-CØ	16.7	21.0	27.1	1.5	0.0	0.1	0.1	3.0	27.5	2.5
21-D	12.0●	12.0	27.1	0.6	0.0	0.0	0.0	3.0	27.5	2.5
22-I	14.9	12.0 ●	5.6	0.6	0.0	0.0	0.0	3.0	27.5	2.6
23-A	19.4	15.0	29.6	1.5	0.0	0.0	0.1	3.0	27.5	2.6
24-C	16.1	Y4.0	23.5	1>3●	0.0	0.0	0.1	3.0	27.5	2.7
25-D	12.1	12.0	11.2	0.7	0.0	0.0	0.0	3.0	27.5	2.7

A-3

X6-I	14.8	13.0	5.5	0.6	0.0	0.0	0.0	3.0	27.6	2.7
27-A	22.5	50.0	26.0	1.5	0.0	0.0	0.0	P3.0	27.6	2.7
28-C	14.3	22.0	24.3	1.1	0.0	0.1	0.1	3.1	27.7	2.9
29-D	15.2	14.0	15.4	1.1	P.0	0.0	0.0	3.1	27.7	2.9
30-I	14.4	10.0	5.7	0.6	0.0	0.0	0.0	3.1	27.7	2.9
31-A	21.9	13.0	31.9	1.6	0.0	0.0	0.1	3.1	27.7	3.0
32]D	14.3	10.0	16.4	1.0	0.0	0.0	0.1	3.1	27.7	3.0
33-I	14.1	11.0	5.7	0.6	0.0	0.0	0.0	3.1	27.8	3.1
34-A	19.9	56.0	22.5	1.4	0.0	0.1	0.1	3.1	27.9	3.1
35-D	13.0	16.0	9.6	0.8	0.0	0.0	0.0	3.2	27.9	3.1
36-A	24.4	16.0	36.2	1.8	0.0	0.0	0.1	3.2	27.9	3.2
37-D	12.5	12.0	10.2	0.8	0.0	0.0	0.0	3.2	28.0	3.3
38-A	23.3	43.0	38.1	1.9	0.0	0.1	0.1	3.2	28.0	3.4
39-C	12.4	7.0	24.2	1.2	0.0	0.0	0.2	3.3	28.1	3.5
40-C	10.8	5.0	23.9	1.2	0.0	0.0	0.2	3.3	28.1	3.6
41-C	8.2	1.0	22.6	1.0	0.00	0.0	0.1	3.3	28.1	4.0
42-D	9.3	1.0	10.5	0.8	0.0	0.0	0.0	3.3	28.1	4.0
43-A	18.5	10.0	35.3	1.6	0.0	0.0	0.1	3.3	28.1	4.1
44-C	10.0	7.0	20.1	1.0	0.0	0.0	0.1	3.3	28.2	4.2
45-D	7.5	3.0	9.8	0.7	0.0	0.0	0.0	3.3	28.2	4.2
46-I	9.8	4.0	5.9	0.5	0.0	0.0	0.0	3.4	28.2	4.2
47-A	24.8	85.0	34.4	1.7	0.0	0.2	0.1	3.4	28.3	4.3
48-D	8.7	2.0	8.4	0.7	0.0	0.0	0.0	3.4	28.3	4.4
49-A	13.7	5.0	29.6	1.3	0.0	0.0	0.1	3.4	28.3	4.5
50-C	9.0	3.0	27.4	1.1	0.0	0.0	0.1	3.4	28.4	4.5
51-D	6.7	1.0	7.1	0.6	0.0	0.0	0.0	3.4	28.4	4.6
52-I	9.3	1.0	5.3	0.5	0.0	0.0	0.0	3.4	28.4	4.6
53-A	21.1	23.0	43.3	1.6	0.0	0.0	0.1	3.4	28.4	4.6
54-D	14.6	25.0	17.0	1.1	0.0	0.0	0.0	3.4	28.4	4.7
55-I	9.5	9.0	6.0	0.5	0.0	0.0	0.0	3.5	28.4	4.7
56-A	12.3	27.0	24.3	1.2	0.0	0.1	0.1	3.5	28.5	4.7
57-C	8.1	12.0	15.3	0.9	0.0	0.0	0.0	3.5	28.5	4.8
58-D	7.3	0.0	10.9	0.6	0.0	0.0	0.0	3.5	28.5	4.8
59-I	9.0	0.0	5.3	0.5	0.0	0.0	0.0	3.5	28.5	4.8
60-A	12.6	2.0	23.0	1.1	0.0	0.0	0.1	3.5	28.5	4.9
61-C	8.5	2.0	26.3	1.2	30.0	0.0	0.1	3.5	28.5	5.0
62-D	7.3	2.0	12.4	0.8	0.0	0.0	0.0	3.5	28.5	5.0
63-I	8.6	2.0	5.3	0.5	0.0	0.0	0.0	3.5	28.5	5.0
64-A	16.2	7.0	27.9	1.5	0.0	0.0	0.1	3.5	28.5	5.1
65-D	7.4	5.0	9.6	0.7	0.0	0.0	0.0	3.5	28.5	5.1
66-I	7.9	5.0	5.6	0.5	0.0	0.0	0.0	3.5	28.5	5.1

TYPE	HC	CO	NO
IDLE	0.5	7.5	0.2
ACEL	0.6	5.2	1.7
CRSE	2.2	15.1	2.7
DCEL	0.3	0.6	0.5

MODE	HC	COP	NO	CO2	HC	CO	NO	HC	CO	NO
1-I	294.5	598.0	1.3	0.4	0.3	1.2	0.0	0.3	1.2	0.0
2-A	74.3	60.0	19.3	1.3	0.0	0.1	0.0	0.3	1.3	0.0
3-C	41.7	37.0	20.4	1.2	0.1	0.1	0.1	0.4	1.4	0.1
4-C	20.3	14.0	20.5	1.3	0.1	0.1	0.2	0.5	1.5	0.3
5-D	14.?	5.0	9.2	0.9	0.0	0.0	0.0	0.5	1.5	0.3
6-I	12.0	3.0	4.9	0.5	0.0	0.0	0.0	0.5	1.5	0.3
7-A	35.5	58.0	58.1	2.1	0.1	0.2	0.4	0.6	1.7	0.7
8-C	50.1	24.0	79.2	3.0	0.1	0.1	0.5	0.7	1.8	1.2
9-C	42.3	9.0	46.7	2.5	0.1	0.0	0.4	0.8	1.9	1.6
10-D	12.0	5.0	8.2	0.8	0.0	0.0	0.0	0.8	1.9	1.6
11-I	11.6	5.0	4.4	0.5	0.0	0.0	0.0	0.8	1.9	1.7
12-A	23.1	75.0	47.7	1.9	0.0	0.1	0.1	0.8	2.1	1.8
13-C	15.5	13.0	32.7	1.5	0.0	0.0	0.1	0.8	2.1	1.9
14-D	Y.1	6.0	32.7	0.5	0.0	0.0	0.1	0.8	2.1	2.0
15-I	10.8	5.0	4.6	0.5	0.0	0.0	0.0	0.8	2.1	2.0
16-A	22.7	25.0	52.6	2.0	0.0	0.0	0.1	0.9	2.1	2.1
17-D	13.0	39.0	15.9	1.0	0.0	0.1	0.0	0.9	2.2	2.1
18-I	11.1	3.0	4.5	0.5	0.0	0.0	0.0	0.9	2.2	2.1
19-A	27.8	84.0	59.3	2.3	0.0	0.1	0.2	0.9	2.3	2.3
20-C	10.9	18.0	40.1	1.3	0.0	0.1	0.2	0.9	2.4	2.4
21-D	8.2	4.0	9.6	0.5	0.0	0.0	0.0	0.9	2.4	2.5

TYPE	HC	CO	NO
IDLE	0.3	1.2	0.1
ACEL	0.2	0.6	0.8
CRSE	0.4	0.4	1.4
DCEL	0.1	0.1	0.2

UNIT # 1
DATE 10/08/75   TIME: 07:10:00
TEST # 4912
CHASSIS # PLY VALIANT
ENGINE # /
CLASS 4
DISP 225
WEIGHT 3500
TRAN AUTO
AXEL /
CARB 2 BBL
ODOM 3879
TEMP 76
BAR 29.96
HUMID 38

	CO2	NOx	CO	HC
Bag 1	2318.7	3.15	52.65	6.30
Bag 2	2305.3	3.60	1.20	0.45
Bag 3	1947.9	3.45	3.75	2.40

J.P.L. COLD START / BASELINE

BAG#	REV	HC	CO	NO	CO2	HC	CO	NO	CO2
AMB1		7.3	16.8	1.3	0.06				
EXH1	11481	149.1	602.6	25.2	1.70	0.84	7.02	0.42	309.17
AMB2		7.3	3.0	1.1	0.06				
EXH2	19706	12.7	10.7	16.8	1.01	0.06	0.16	0.48	307.37
AMB3		3.9	7.9	1.3	0.05				
EXH3	11473	57.2	49.0	27.3	1.43	0.32	0.50	0.46	259.72
WTD GRAMS/MILE						0.60	3.47	0.92	538.35

FUEL CONSUMPTION   1900.2 GM/TEST

14.90 MPG

```
INIT # 1
DATE: 10/08/75   TIME: 07:43:17
TEST # 4913
CHASSIS # PLY VALIANT
ENGINE # /
CLASS 4
DISP 225
WEIGHT 3500
TRAN AUTO
AXEL /
CARB 2 BBL
ODOM 3890
TEMP 76
BAR 29.96
HUMID 38
J.P.L. HIGHWAY CYCLE/ BASELINE
```

BAG#	REV	HC	CO	NO	CO2	HC	CO	NO	CO2
AMB1		6.3	5.9	0.7	0.05				
EXH1	17635	28.7	13.3	46.3	2.13	0.21	0.15	1.23	601.68
GRAMS/MILE						0.21	0.15	1.23	601.68

```
FUEL CONSUMPTION  149.73 GPM
```

UNIT # 1
DATE: 10/08/75   TIME: 19:57:11
TEST # 4919
CHASSIS # 75 PLY VALIA
ENGINE # /
CLASS 4
DISP 225
WEIGHT 3500
TRAN AUTO
AXEL /
CARB 2 BBL
ODOM 3903
TEMP 75
BAR 29.93
HUMID 51
J.P.L. COLD START BASELINE # 2

| | ------CONCENTRATION------ | | | | -----MASS----- | | | --ACCUM MASS-- | | |
MODE	HC	CO	NO	CO2	HC	CO	NO	HC	CO	NO
1-I	281.6	2627.0	4.0	1.0	0.3	5.3	0.0	0.3	5.3	0.0
2-A	371.0	2837.0	94.4	1.5	0.2	2.6	0.1	0.5	7.9	0.2
3-C	442.0	3000.0	24.9	1.4	0.3	10.4	0.1	1.2	18.3	0.3
4-C	196.0	886.0	12.5	2.1	0.5	4.5	0.1	1.7	22.8	0.4
5-D	87.8	457.0	7.3	1.1	0.1	0.6	0.0	1.8	23.3	0.4
6-I	36.4	59.0	2.6	0.6	0.1	0.2	0.0	1.8	23.6	0.4
7-A	88.2	535.0	40.8	2.7	0.2	2.3	0.3	2.0	25.9	0.7
8-C	90.1	86.0	70.8	3.6	0.2	0.4	0.5	2.2	26.2	1.2
9-C	95.3	25.0	47.9	3.0	0.2	0.1	0.4	2.4	26.4	1.6
10-D	28.5	12.0	7.7	0.9	0.0	0.0	0.0	2.5	26.4	1.6
11-I	18.2	10.0	3.5	0.6	0.0	0.0	0.0	2.5	26.4	1.6
12-A	34.4	58.0	49.8	2.3	0.0	0.1	0.2	2.5	26.5	1.8
13-C	31.5	11.0	26.4	1.9	0.0	0.0	0.1	2.6	26.6	1.9
14-D	18.0	5.0	26.4	0.6	0.0	0.0	0.0	2.6	26.6	1.9
15-I	16.4	5.0	3.9	0.6	0.0	0.0	0.0	2.6	26.6	2.0
16-A	33.4	76.0	51.0	2.3	0.0	0.1	0.1	2.6	26.7	2.0
17-D	17.7	23.0	12.8	1.0	0.0	0.0	0.0	2.6	26.7	2.1
18-I	15.1	8.0	4.0	0.6	0.0	0.0	0.0	2.6	26.7	2.1
19-A	33.6	68.0	65.8	2.6	0.0	0.1	0.2	2.7	26.8	2.2
20-C	17.4	13.0	29.3	1.4	0.0	0.0	0.1	2.7	26.9	2.4
21-D	11.9	4.0	29.8	0.6	0.0	0.0	0.0	2.7	26.9	2.4
22-I	14.2	5.0	4.2	0.6	0.0	0.0	0.0	2.7	26.9	2.4
23-A	21.7	6.0	28.6	1.5	0.0	0.0	0.1	2.7	26.9	2.5
24-C	16.4	4.0	19.7	1.2	0.0	0.0	0.0	2.7	26.9	2.6
25-D	11.7	3.0	8.1	0.6	0.0	0.0	0.0	2.7	26.9	2.6
26-I	14.0	4.0	4.1	0.6	0.0	0.0	0.0	2.7	26.9	2.6
27-A	20.5	9.0	30.4	1.6	0.0	0.0	0.0	2.8	26.9	2.6
28-C	13.2	8.0	23.3	1.1	0.0	0.0	0.1	2.8	26.9	2.8
29-D	15.0	7.0	12.7	1.0	0.0	0.0	0.0	2.8	26.9	2.8
30-I	13.4	3.0	4.3	0.5	0.0	0.0	0.0	2.8	26.9	2.8
31-A	24.6	6.0	33.2	1.7	0.0	0.0	0.1	2.8	27.0	2.9
32-D	15.3	3.0	14.2	0.9	0.0	0.0	0.0	2.8	27.0	2.9
33-I	13.3	4.0	4.3	0.5	0.0	0.0	0.0	2.8	27.0	2.9
34-A	17.8	7.0	23.9	1.4	0.0	0.0	0.1	2.9	27.0	3.0
35-D	12.5	7.0	9.7	0.7	0.0	0.0	0.0	2.9	27.0	3.0
36-A	26.9	9.0	34.4	1.8	0.0	0.0	0.1	2.9	27.0	3.1
37-D	12.6	2.0	7.9	0.7	0.0	0.0	0.0	2.9	27.0	3.2
38-A	28.8	67.0	37.1	1.9	0.0	0.1	0.1	2.9	27.1	3.3
39-C	13.8	6.0	21.8	1.1	0.0	0.0	0.2	3.0	27.2	3.5
40-C	13.9	4.0	30.6	1.3	0.0	0.0	0.2	3.0	27.2	3.7

A-7

41-C	11.2	5.0	19.3	1.0	0.0	0.0	0.1	3.0	27.2	3.8
42-D	11.9	6.0	6.9	0.7	0.0	0.0	0.0	3.0	27.2	3.8
43-A	24.9	11.0	33.9	1.8	0.0	0.0	0.1	3.1	27.2	3.9
44-C	12.8	4.0	17.4	1.0	0.0	0.0	0.1	3.1	27.3	4.0
45-D	10.3	1.0	6.5	0.6	0.0	0.0	0.0	3.1	27.3	●4.0
46-I	12.6	3.0	4.3	0.5	0.0	0.0	0.0	3.1	27.3	4.0
47-A	29.3	11.0	[3.5	1.8	0.0	0.0	0.1	3.1	27.3	4.1
48-D	11.7	6.0	6.7	0.6	0.0	0.0	0.0	3.2	27.3	4.2
49-A	21.4	67.0	24.7	1.4	0.0	0.1	0.1	3.2	27.5	4.3
50-C	12.9	4.0	28.5	1.0	0.0	0.0	0.1	3.2	27.5	4.4
51-D	9.6	1.0	5.4	0.5	0.0	0.0	0.0	3.2	27.5	4.4
52-I	12.2	2.0	4.6	0.5	0.0	0.0	0.0	3.2	27.5	4.4
53-A	28.9	16.0	43.3	1.9	0.0	0.0	0.1	3.2	27.5	4.4
54-D	19.6	33.0	13.5	0.8	0.0	0.0	0.0	3.2	27.5	4.5
55-I	12.5	11.0	4.7	0.5	0.0	0.0	0.0	3.2	27.5	4.5
56-A	18.3	11.0	21.2	1.3	0.0	0.0	0.1	3.3	27.6	4.5
57-C	11.5	6.0	15.1	0.8	0.0	0.0	0.0	3.3	27.6	4.6
58-D	10.2	4.0	10.7	0.6	0.0	0.0	0.0	3.3	27.6	4.6
59-I	11.9	2.0	4.6	0.5	0.0	0.0	0.0	3.3	27.6	4.6
60-A	18.2	6.0	21.3	1.1	0.0	0.0	0.1	3.3	27.6	4.7
61-C	13.5	3.0	23.6	1.3	0.0	0.0	0.1	3.3	27.6	4.8
62-D	11.6	3.0	8.4	0.7	0.0	0.0	0.0	3.3	27.6	4.8
63-I	11.9	3.0	4.4	0.5	0.0	0.0	0.0	3.3	27.6	4.8
64-A	28.1	10.0	27.3	1.5	0.0	0.0	0.1	3.4	27.6	4.9
65-D	10.8	5.0	12.2	0.6	0.0	0.0	0.0	3.4	27.6	4.9
66-I	11.3	4.0	4.2	0.5	0.0	0.0	0.0	3.4	27.6	4.9

TYPE	HC	CO	NO
IDLE	0.5	5.7	0.2
ACEL	0.7	5.6	1.9
CRSE	1.9	15.6	2.4
DCEL	0.3	0.8	0.5

	------CONCENTRATION------				-----MASS-----			--ACCUM MASS--		
MODE	HC	CO	NO	CO2	HC	CO	NO	HC	CO	NO
1-I	212.4	197.0	2.1	0.4	0.2	0.4	0.0	0.2	0.4	0.0
2-A	60.6	25.0	26.0	1.5	0.0	0.0	0.0	0.2	0.4	0.0
3-C	39.2	34.0 ●	21.0	1.3	0.1	0.1	0.1	0.3	0.5	0.2
4-C	24.6	10.0	21.9	1.3	0.1	0.1	0.2	0.4	0.6	0.3
5-D	14.9	1.0	3.5	0.8	0.0	0.0	0.0	0.4	0.6	0.4
6-I	12.6	0.0	4.1	0.5	0.0	0.0	0.0	0.4	0.6	0.4
7-A	48.5	233.0	55.0	2.2	0.1	1.0	0.4	0.5	1.6	0.8
8-C	74.5	50.0	70.7	3.0	0.2	0.2	0.5	0.7	1.8	1.3
9-C	55.8	12.0	43.2	2.5	0.1	0.1	0.3	0.8	1.9	1.6
10-D	13.7	2.0	7.4	0.8	0.0	0.0	0.0	0.8	1.9	1.6
11-I	11.3	4.0	3.6	0.5	0.0	0.0	0.0	0.8	1.9	1.6
12-A	27.8	21.0	50.8	2.1	0.0	0.0	0.2	0.9	1.9	1.8
13-C	16.6	7.0	33.0	1.5	0.0	0.0	0.1	0.9	1.9	1.9
14-D	8.6	1.0	33.0	0.5	0.0	0.0	0.1	0.9	1.9	2.0
15-I	10.2	2.0	4.0	0.5	0.0	0.0	0.0	0.9	1.9	2.0
16-A	33.4	53.0	56.9	2.2	0.0	0.1	0.1	0.9	2.0	2.1
17-D	16.2	23.0	12.2	0.9	0.0	0.0	0.0	0.9	2.0	2.1
18-I	10.5	4.0	3.9	0.5	0.0	0.0	0.0	0.9	2.0	2.1
19-A	37.2	79.0	61.8	2.4	0.0	0.1	0.2	1.0	2.2	2.3
20-C	12.8	11.0	42.6	1.2	0.0	0.0	0.2	1.0	2.2	2.5
21-D	7.5	3.0	12.9	0.5	0.0	0.0	0.0	1.0	2.2	2.5

TYPE	HC	CO	NO
IDLE	0.3	0.4	0.1
ACEL	0.2	1.3	0.8
CRSE	0.5	0.5	1.4
DCEL	0.1	0.0	0.2

A-8

UNIT # 1
DATE: 10/08/75   TIME: 20:43:20
TEST # 4919
CHASSIS # 75 PLY VALIA.
ENGINE # /
CLASS 4
DISP 225
WEIGHT 3500
TRAN AUTO
AXEL /
CARB 2 BBL
ODOM 3903
TEMP 75
BAR 29.93
HUMID 51

	CO_2	NO_x	CO	HC
Bag 1	2425.6	3.38	56.93	4.20
Bag 2	2346.8	3.75	1.35	0.53
Bag 3	1972.7	3.83	3.45	1.80

J.P.L. COLD START BASELINE # 2

BAG#	REV	HC	CO	NO	CO2	HC	CO	NO	CO2
AMB1		6.8	9.8	0.9	0.05				
EXH1	11450	100.4	645.6	24.6	1.77	0.56	7.59	0.45	323.41
AMB2		5.1	0.0	0.8	0.04				
EXH2	19661	12.5	3.7	16.1	1.01	0.07	0.13	0.50	312.90
AMB3		5.6	0.0	0.8	0.04				
EXH3	11451	46.1	33.2	27.3	1.44	0.24	0.46	0.51	263.02
WTD GRAMS/MILE						0.45	3.70	0.98	601.89

FUEL CONSUMPTION 1943.0 GM/TEST

14.57 MPG

UNIT # 1
DATE: 10/08/75   TIME: 21:16:34
TEST # 4920
CHASSIS # 75 PLY VALIA
ENGINE # /
CLASS 4
DISP 225
WEIGHT 3500
TRAN AUTO
AXEL /
CARB 2 BBL
ODOM 3914
TEMP 75
BAR 29.93
HUMID 51

J.P.L. HIGHWAY CYCLE /BASELINE # 2

BAG#	REV	HC	CO	NO	CO2	HC	CO	NO	CO2
AMB1		5.4	0.0	0.7	0.05				
EXH1	17613	29.4	10.4	46.1	2.15	0.23	0.19	1.31	607.29
GRAMS/MILE						0.23	0.19	1.31	607.29

FUEL CONSUMPTION 148.32 GPM

19.92 MPG

UNIT # 1
DATE: 10/09/75   TIME: 10:25:13
TEST # 4923
CHASSIS # PLY VALIANT
ENGINE # /
CLASS   4
DISP 225
WEIGHT 3500'
TRAN AUTØ
AXEL /
CARB 1 BBL.
ØDØM 3927
TEMP   78
BAR 29.98
HUMID 43
JPL CØLD START BASELINE #3

	-----CØNCENTRATIØN-----				-----MASS-----			---ACCUM MASS---		
MØDE	HC	CØ	NØ	CØ2	ØHC	CØ	NØ	HC	CO	NO
1-I	262.1	1175.0	0.3	0.4	0.3	2.4	0.0	0.3	2.4	0.0
2-A	500.0	3000.0	77.7	1.7	0.2	2.7	0.1	0.5	5.1	0.1
3-C	499.7	3000.0	26.8	1.4	0.9	10.4	0.1	1.3	15.5	0.3
4-C	227.0	804.0	12.0	2.1	0.6	4.1	0.1	1.9	19.6	0.4
5-D	198.6	419.0	11.4	1.1	0.1	0.5	0.0	2.0	20.1	0.4
6-I	63.2	526.0	1.6	0.6	0.1	2.0	0.0	2.2	22.1	0.4
7-A	83.4	266.0	41.2	2.5	0.2	1.1	0.3	2.3	23.3	0.7
8-C	79.2	60.0	82.5	3.6	0.2	0.3	0.6	2.5	23.5	1.2
9-C	80.7	24.0	53.8	2.9	0.2	0.1	0.4	2.7	23.7	1.7
10-D	25.0	14.0	9.1	1.0	0.0	0.0	0.0	2.8	23.7	1.7
11-I	14.7	14.0	3.5	0.5	0.0	0.0	0.0	2.8	23.	1.7
12-A	30.2	86.0	52.6	2.3	0.0	0.2	0.2	2.8	23.9	1.9
13-CØ	26.3	13.0	27.1	1.8	0.0	0.0	0.1	2.8	23.9	2.0
14-D	12.6	7.0	27.1	0.5	0.0	0.0	0.1	2.8	23.9	2.0
15-I	12.6	7.0	3.7	0.5	0.0	0.0	0.0	2.8	23.9	2.0
16-A	26.2	41.0	48.6	2.2	0.0	0.1	0.1	2.8	24.0	2.1
17-D	14.5	13.0	20.8	1.00	0.0	0.0	0.0	2.9	24.0	2.2
18-I	11.7	9.0	4.0	0.5	0.0	0.0	0.0	2.9	24.0	2.2
19-A	26.5	58.0	64.1	2.5	0.0	0.1	0.2	2.9	24.1	2.3
20-C	13.8	11.0 P	28.0	1.4	0.0	0.0	0.1	2.9	24.2	2.5
21-D	8.0	8.0	28.0	0.5	0.0	P.0	0.1	2.9	24.2	2.5

A-10

22-I	10.2	9.0	4.2	0.5 @	0.0	0.0	0.0	2.9	24.2	2.5
23-A	14.9	11.0	28.2	1.4	0.0	0.0	0.1	2.9	24.2	2.6
24-C	13.1	7.0	26.9	1.2	0.0	0.0	0.1	2.9	24.2	2.7
25-D	7.9	4.0	10.7	0.6	0.0	0.0	0.0	2.9	24.2	2.7
26-I	9>9	4.0	4.3	0.5	0.0	0.0	0.0	3.0	24.2	2.7
27-A	16.3	38.0	25.3	1.5	0.0	0.0.	0.0	3.0	24.2	2.7.
28-C	9.2	11.0	24.4	1.1	0.0	@0.0	0.1	3.0	24.3	2.9
29-D	11.4	6.0	19.3	1.0	0.0	0.0	0.0	3.0	24.3	2.9
30-I	9.6	5.0	4.7	0.5	0.0	0.0	0.0	3.0	24.3	2V9
31-A	18.5	9.0	29.4P	1.7	0.0	0.0	0.1	3.0	24.3	3.0
32-D	12.6	7.0	13.1	0.9	0.0	0.0	0.1	3.0	24.3	3.0
33-I	9.5	7.0	4.5	0.5	0.0	0.0	0.0	3.0	24.3	3.0
34-A	13.4	10.0	24.5	1.4	0.0	0.0	0.1	3.0	24>3	3.1
35-D	7.7	7.0	12.9	0.7	0.0	0.0	0.0	3.0	24.4	3.2
36-A	20.6	15.0	36.2	1.3	0.0	0.0	0.1	3.1	24.4	3.3
37-D	3.7	4.0	10.4	0.7	0.0	0.0	0.0	3.1	24.4	3.3
38-A	18.3	14.0	36.7	1.9	0.0	0.0	0.1	3.1	24.4	3.4
39-C	10.0	7.0	25.2	1.1	0.0	0.0	0.2	3.1	24.5	3.6
40-C	8.8	11.0	22.9	1.2	0.0''	0.1	0.2	3.1	24.5	3.9
41-C	6.8	8.0	23.3	1.0	0.0	0.0	0.2	3.2	24.6	4.0
42-D	8.4	9.0	11.0	0.7	0.0	0.0	0.0	3.2	24.6	4.0
43-A	18.0	16.0	32.4	1.7	0.0	0.0	0.1	3.2	24.6	4.1
44-C	7.9	8.0	20.6	1.0	0.0	0.0	0.1	3.2	24.6	4>2
45-D	6.3	7.0	11.6	0.6	0.0	0.0	0.0	3.2	24.6	4.3
46-I	8.1	9.0	4.9	0.5	0.0	0.0	0.0	3.2	24.7	4.3
47-A	16.9	12.0	34.7	1.8	0.0	0.0 P	0.1	3.2	24.7.	4.4
48-D	6.3	4.0	9.3	0.6	0.0	0.0	0.0	3.2	24.7	4.4
49-A	10.9	7.0	26.3	1.3	0.0	0.0	0.1	3.2	24.7	4.5
50-C	.8.2	6.0	27.2	1.0	0.0	0.0	0.1	3.3	24.7	4.6
51-D	5.5	5.0	7.9	0.5	0.0	0.0	0.0	3.3	24.7	4.6
52-I	7.5	5.0	4.9	0.5	0.0	0.0	0.0	3.3	24.7	4.6
53-A	16.2	10.0	32.9	1.7	0.0	0.0	0.0	3.3	24.8	4.7
54-D	15.8	74.0	25.2	0.9	0.0	0.1	0.0	3.3	24.8	4.7
55-I	8N2	27.0	5.0	0.5	0.0	0.0	0.0	3.3	24.9	4.7
56-A	10.1	12.0@	24.3	1.2	0.0	0.0	0.1	3.3	24.9	4.8
57-C	6.6	5.0P	15.7	0.3	0.0	0.0	0.0	3.3	24.9	P4.8
58-D	5.8	3.0	9.1	0.5	0.0	0.0	0.0	3.3	24.9	4.9
59-I	7.3	3.0	5.0	0.5	0.0	0.0	0.0	3.3	24.9	4.9
60-A	12.1	6.0	20.3	1.1	0.0	0.0	0.1	3.3	24.9	5.0
61-C	7.3	4.0	25.7	1.2	0.0	0.0	0.1	3.3	24.9	5.0
62-D	6.7	4.0	12.1	0.6	0.0	0.0	0.0	3.3	24.9	5.1
63-I	7.4	5.0	4.8	0.5	0.0	0.0	0.0	3.3	24.9	5.1
64-A	14.0	8.0	26.3	1.4	0.0	0.0	0.1	3.4	25.0	5.1
65-D	6.4	6.0	13.9	0.6	0.0	0.0	0.0	3.4	25.0	5.2
66-I	6.6	6.0	4.5	0.5	0.0	0.0	0.0	3.4	25.0	5.2

TYPE	HC	CØ	NØ
IDLE	0.5	4.6	0.1
ACEL	0.6	4.5	1.8
CRSE	2.0	15.2	2.6
DCEL	0.3	0.8	0.6

ZERØ CALIBRATIØN

INSTR	RANGE	VALUE	CMVTS	MVTS	ERR
CØ2	2	0	0	5	
CØ	2	0	-13	-15	
HC	1	4	5	-33	
NØX	1	0	0	12	

SPAN CALIBRATIØN

INSTR	RANGE	VALUE	CMVTS	GAIN	ERR
CØ2	2	416	4597	1.002	
CØ	2	2441	4517	1.004	
HC	1	4862	4947	0.986	
NØX	1	1872	3745	0.998	

ZERØ CALIBRATIØN

INSTR	RANGE	VALUE	CMVTS	MVTS	ERR
CØ2	2	0	2	7	
CØ	2	0	-10	-10	
HC	1	0	-5	-28	
NØX	1	0	0	10	

	-----CØNCENTRATIØN-----				-----MASS-----			--ACCUM MASS--		
MØDE	HC	CØ	NØ	CØ2	HC	CØ	NØ	HC	CØ	NØ
1-I	221.4	336.0	1.3	0.3	0.2	0.7	0.0	0.2	0.7	0.0
2-A	73.7 @	46.0	18.2	1.5	0.0	0.0	0.0	0.3	0.7	0.0
3-C	36.8	28.0	20.5	1.2	0.1	0.1	0.1	0.3	0.8	0.1
4-C	18.6	11.0	22.0	1.3	0.0	0.1	0.2	0.4	0.9	0.3
5-D	14.2	6.0	11.8	0.8	0.0	0.0	0.0	0.4	0.9	0.3
6-I	9.6	4.0	4.7	0.5	0.0	0.0	0.0	0.4	0.9	0.4
7-A	33.2	86.0	55.1	2.1	0.1	0.4	0.4	0.5	1.3	0.7
8-C	41.4	30.0	90.2	2.9	0.1	0.1	0.6	0.6	1.4	1.4
9-C	43.5	17.0	51.1	2.5	0.1	0.1	0.4	0.7	1.5	1.8
10-D	10.1	5.0	9.5	0.7	0.0	0.0	0.1	0.7	1.5	1.8
11-I	9.7	5.0	X.7	0.5	0.0	0.0	0.0	0.7	1.5	1.8
12-A	22.1	12.0	51.8	2.0	0.0	0.0	0.2	0.7	1.5	2.0
13-C	13.0	7.0	34.9	1.5	0.0	0.0	0.1	0.7	1.5	2.1
14-D	7.0	5.0	34.9	0.5	@0.0	0.0	0.1	0.7	1.6	2.2
15-I	8.5	6.0	4.8	0.5	0.0	0.0	0.0	0.7	1.6	2.2
16-A	19.5	16.0	52.6	2.0	0.0	0.0	0.1	0.7	1.6	2.3
17=D	12.6	74.0	21.3	0.9	0.0	0.1	0.1	0.7	1.7	2.3
18-I	8.7	13.0	5.0	0.5	0.0	0.0	0.0	0.8	1.7	2.3
19-A	23.8	27.0	69.0	2.3	0.0	0.0	0.2	0.8	1.8	2.5
20-C	8.6	11.0	50.3	1.1	0.0	0.0	0.2	0.8	1.8	2.6
21-D	6.0	8.0	13.1	0.5	0.0	0.0	0.0	0.8	1.8	2.6

TYPE	HC	CØ	NØ
IDLE	0.3	0.7	0.1
ACEL	0.2	0.5	0.8
CRSE	0.3	0.4	1.6
DCEL	0.0	0.2	0.2

```
UNIT # 1
DATE: 10/09/75   TIME: 11:21:12
TEST # 4923
CHASSIS # PLY VALIANT
ENGINE # /
CLASS   4
DISP 225
WEIGHT 3500
TRAN AUTØ
AXEL /
CARB 1 BBL
ØDØM 3927
TEMP 78
BAR 29.98
HUMID 43
```

	CO$_2$	NO$_x$	CO	HC
Bag 1	2386.9	3.45	64.95	7.88
Bag 2	2278.1	4.20	0.60	0.38
Bag 3	1989.2	4.13	2.85	1.80

JPL CØLD START BASELINE #3

BAG#	REV	HC	CØ	NØ	CØ2	HC	CØ	NØ	CØ2
AMB1		5.4	9.9	0.1	0.04				
EXH1	11466	181.5	733.7	24.8	1.73	1.05	8.66	0.46	318.25
AMB2		5.8	2.0	1.1	0.04				
EXH2	19677	10.5	5.8	18.7	0.98	0.05	0.08	0.56	303.75
AMB3		3.1	0.0	0.5	0.04				
EXH3	11455	43.2	31.6	30.2	1.45	0.24	0.38	0.55	265.23
WTD GRAMS/MILE						0.64	4.02	1.07	591.78

```
FUEL CØNSUMPTIØN   1914.3 GM/TEST

        14.79 MPG
```

```
UNIT # 1
DATE: 10/09/75   TIME: 11:53:01
TEST # 4924
CHASSIS # PLY VALIANT
ENGINE # /
CLASS   4
DISP 225
WEIGHT 3500
TRAN AUTØ
AXEL /
CARB 1 BBL
ØDØM 3927
TEMP 78
BAR 29.98
HUMID 43
```

JPL HIGHWAY CYCLE #3

BAG#	REV	HC	CØ	NØ	CØ2	HC	CØ	NØ	CØ2
AMB1		3.6	0.0	0.7	0.05				
EXH1	17611	22.8	6.6	52.3	2.15	0.18	0.12	1.46	607.77
GRAMS/MILE						0.18	0.12	1.46	607.77

```
FUEL CØNSUMPTIØN   148.27 GPM
```

APPENDIX B

CALIBRATIONS FOR EGR
VALVE AND AIR PUMP

CALIBRATION OF EGR VALVE

The EGR valve was calibrated using room temperature nitrogen gas to determine the flow rate characteristics of the valve. These results were needed to provide an indication of the EGR flow rate through the valve during engine operation. A schematic of the test setup is shown in Figure B-1. The nitrogen gas was supplied to the valve from a plenum chamber. Flow rate was measured using a Meriam laminar flow element. Pressures and temperatures measured during these calibration tests are identified in the figure. Photographs of the test setup are given in Figures B-2 and B-3.

Calibration curves based on these tests are given in Figures B-4 and B-5. These curves have been used to estimate EGR flow rate from measurements of valve pressure drop, valve control pressure (P_{vac}), exhaust gas temperature, ambient pressure, and ambient temperature.
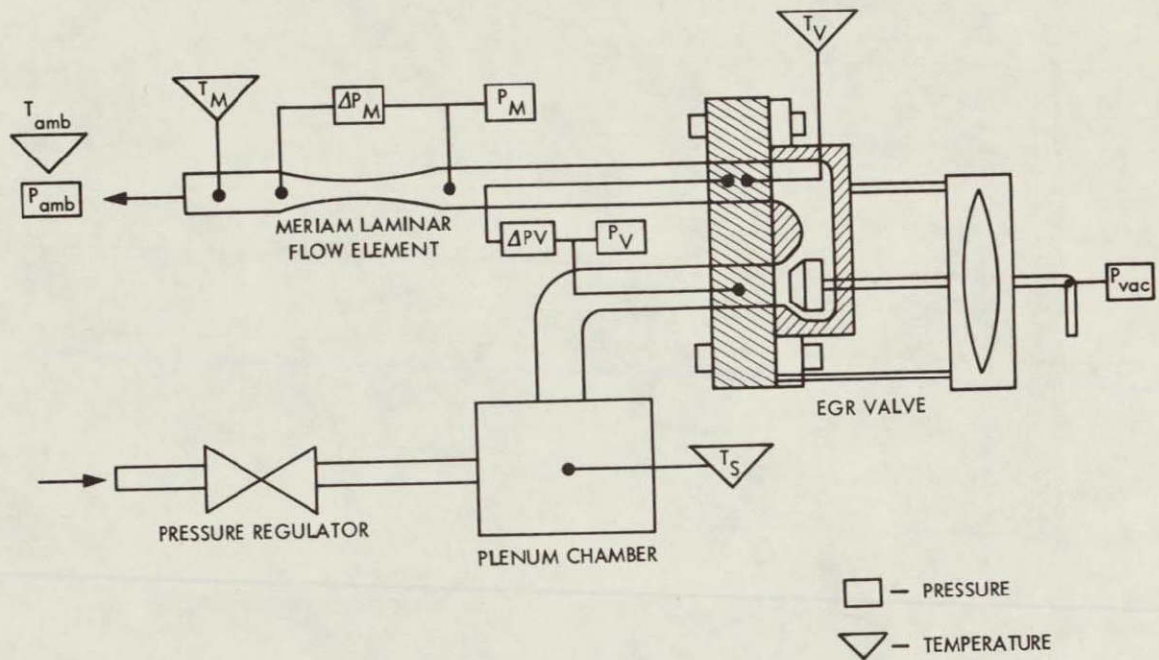
Figure B-1. Flow Rate Calibration Schematic
             for EGR Valve
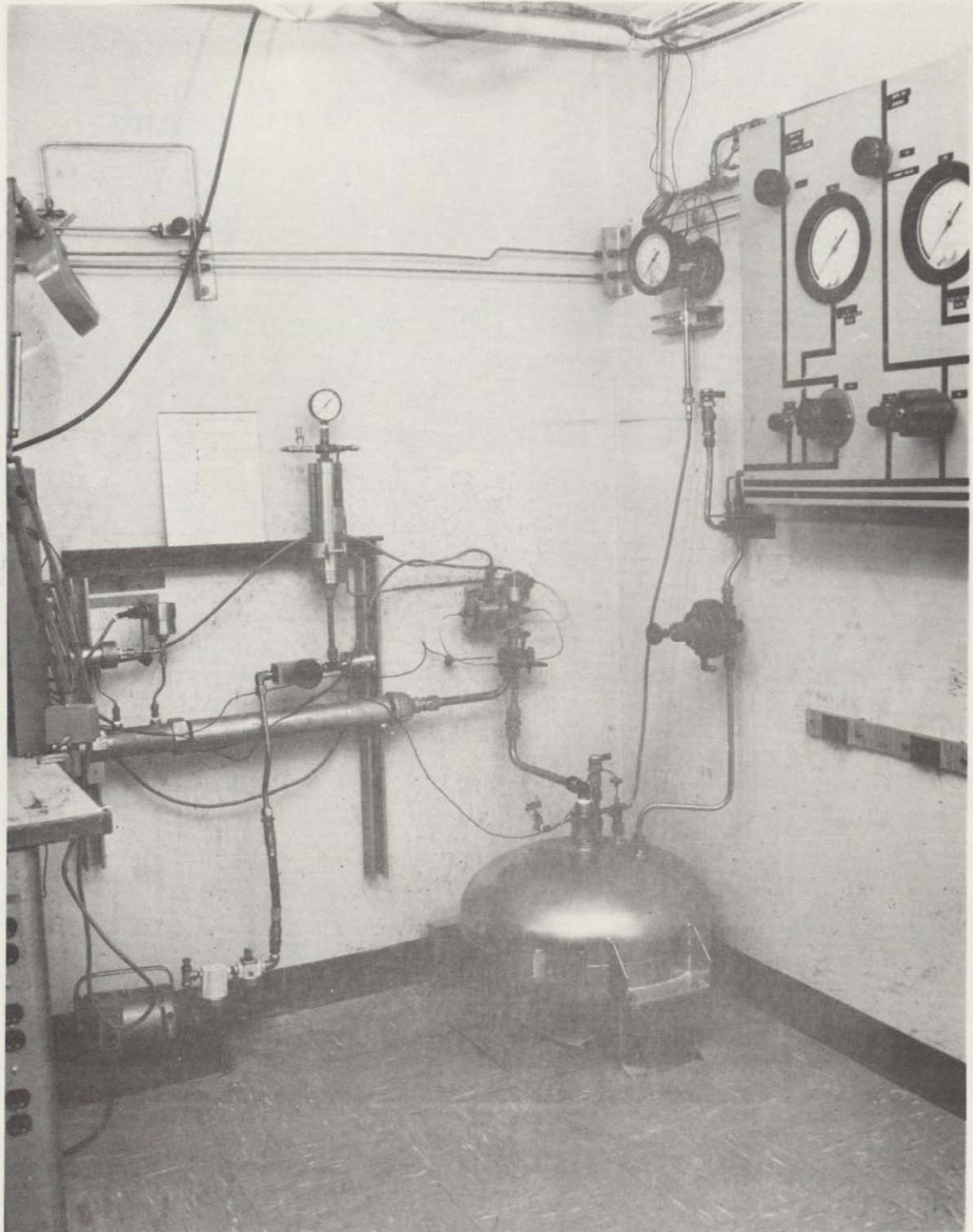
Figure B-2. Test Setup for EGR Valve Calibration
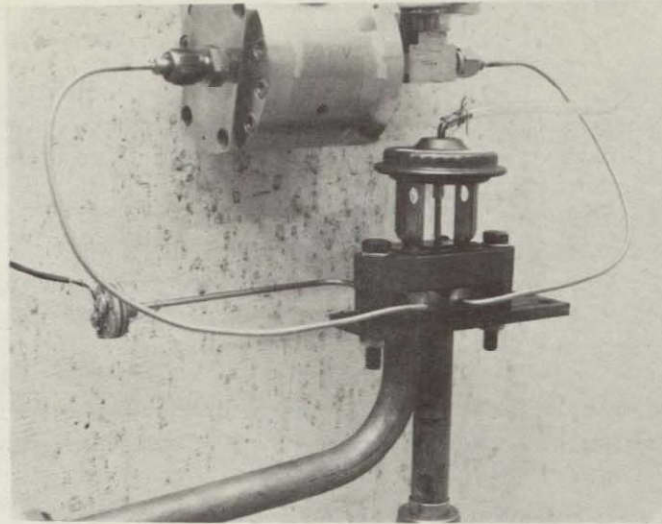
Figure B-3. EGR Valve Calibration
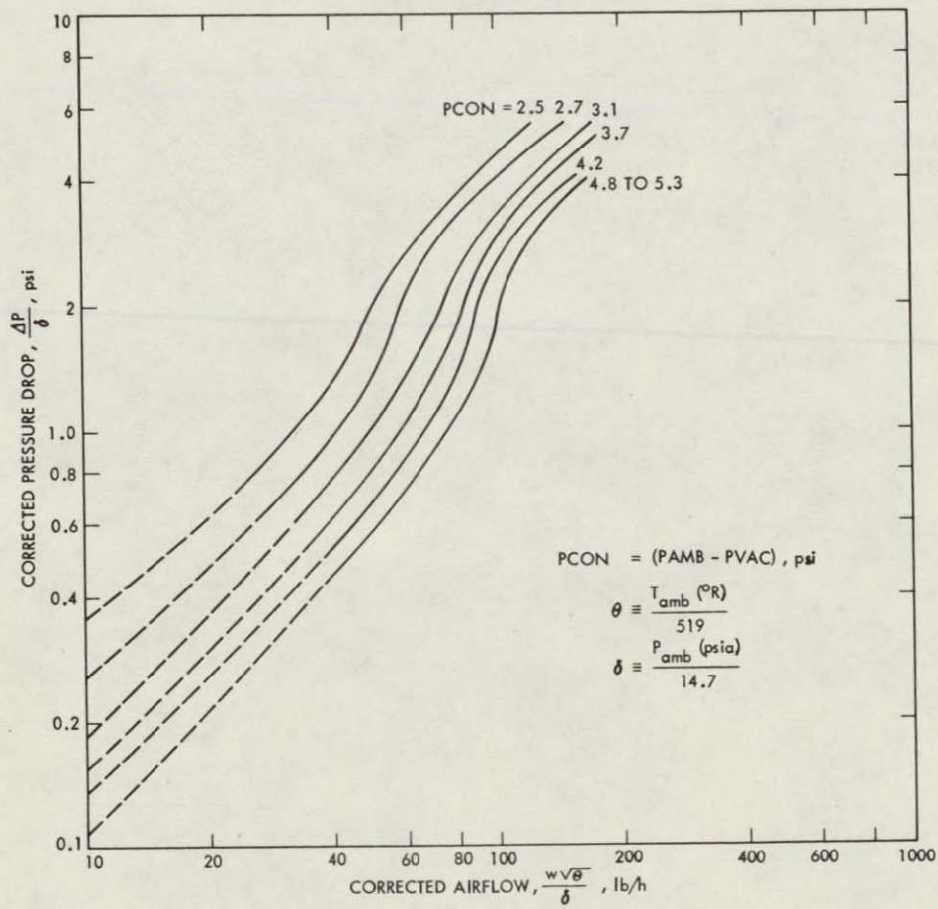
Figure B-4. Flow Rate Calibration Curve for
EGR Valve No. 1

CALIBRATION OF AIR PUMP

The AIR pump was calibrated using room temperature air to determine the flow rate characteristics of the pump. These results were needed to provide a measure of the air flow rate provided by the pump during engine operation. A schematic of the test setup is shown in Figure B-6. The pump was driven by an electric motor and variable pulley belt drive. Flow rate was measured using a Meriam laminar flow element. Pressures and temperatures measured during these calibration tests are identified in the figure. Photographs of the test setup are given in Figures B-7 and B-8.

Calibration curves based on these tests are given in Figure B-9. These curves have been used to estimate AIR flow rate from measurements of pump RPM, pump pressure ratio, ambient pressure, and ambient temperature.
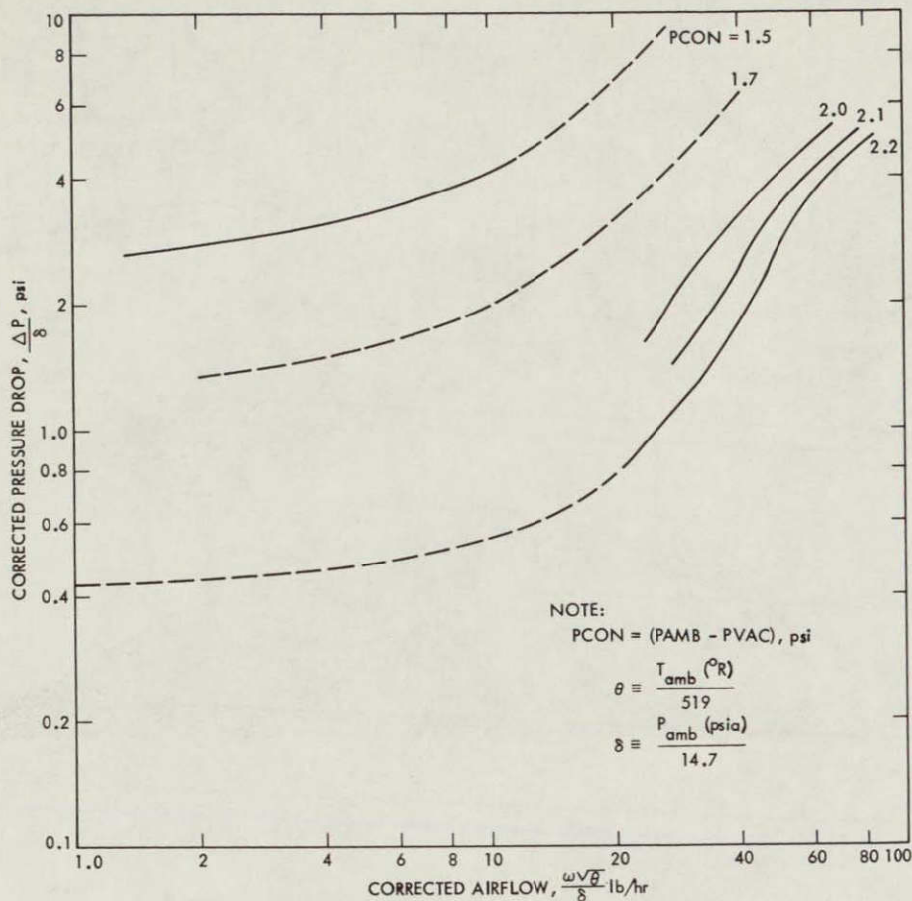
Figure B-5. Flow Rate Calibration Curve for
EGR Valve No. 1
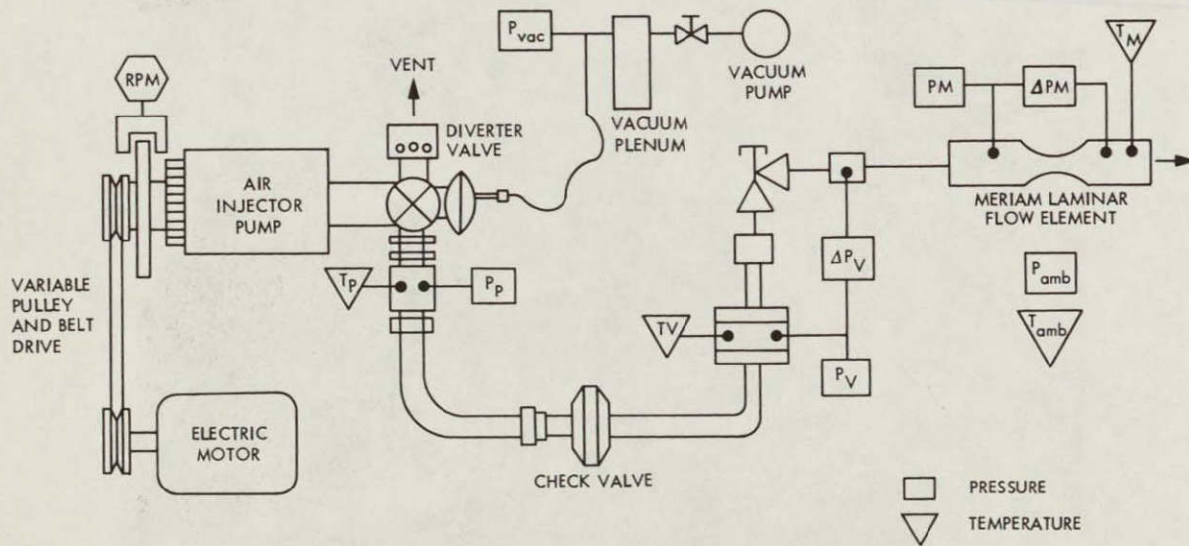
Figure B-6. Flow Rate Calibration Schematic
for AIR Injector Pump
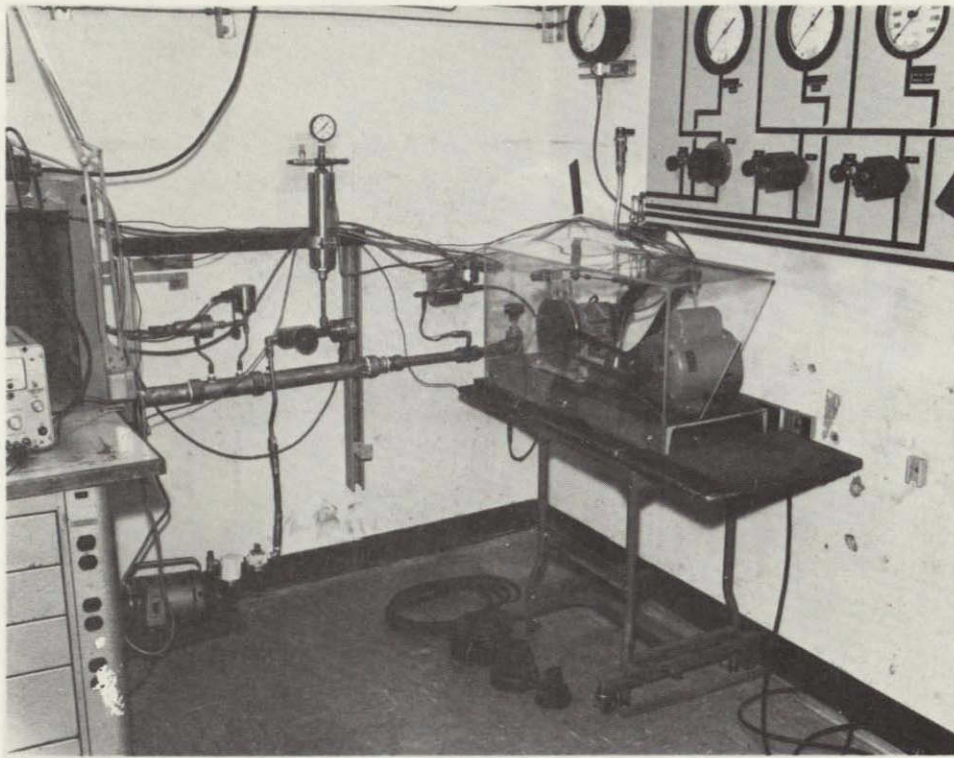
Figure B-7.   Test Setup for AIR Pump Calibration
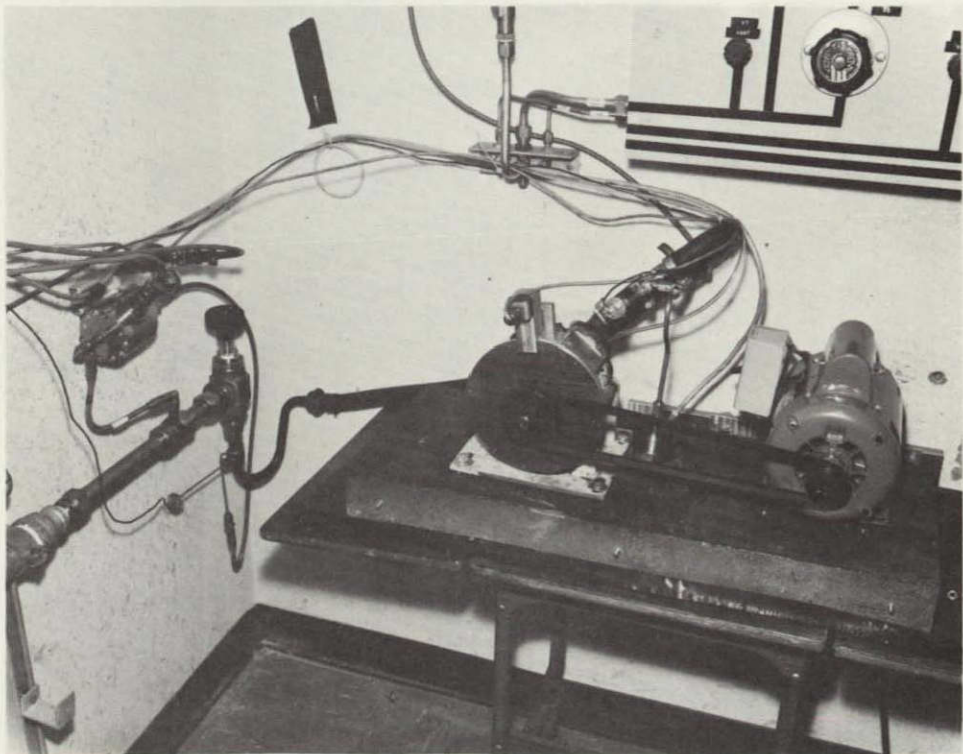
Figure B-8.   AIR Pump Calibration
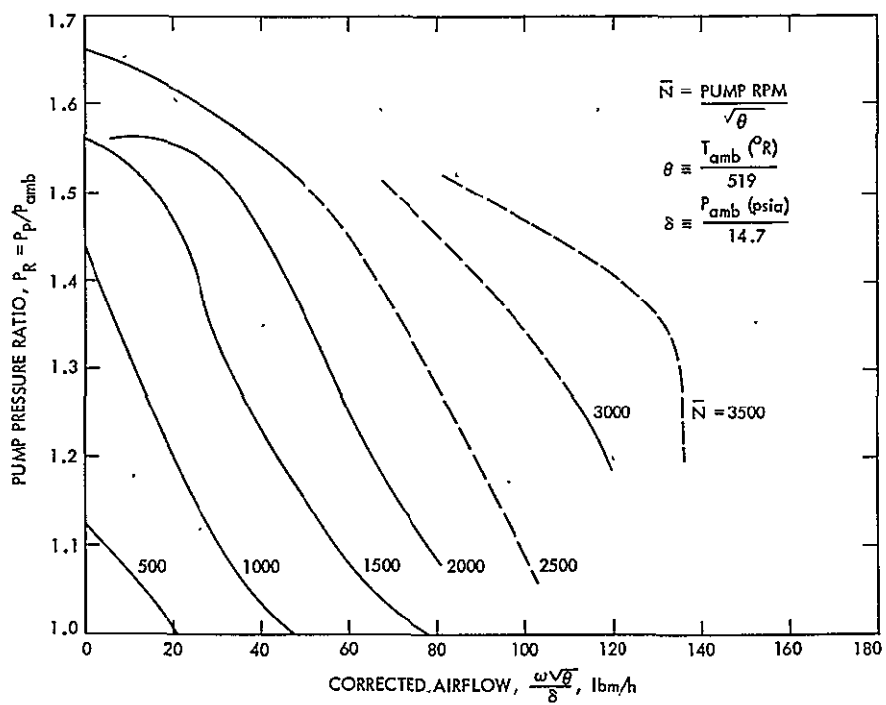
Figure B-9.   Calibration Curve for AIR Pump

APPENDIX C

BASELINE ENGINE DATA

Table C-1. Stock Baseline Engine Data

Sequence No.	RPM	BMEP (psi)	$\dot{m}_{gaso}$ (lbm/h)	$\dot{m}_{air}$ (lbm/h)	% A.I.R.	% EGR	P_man ("Hg vac)	Spark Advance (°BTDC)	Average T_{exh} (°F)	φ	φA	φE	BSFC (lbm/bhp-h)	Emissions Data*	BSNOx (g/bhp-h)	BSHC (g/bhp-h)	BSCO (g/bhp-h)	η_{HC}	η_{CO}
144.06	1035	0.0	5.70	62.2	40	16	17.88	4.2	1249	1.324	0.772	1.088		U					
145.06	1031	0.0	5.68	62.2										D					
144.09	993	20.1	5.07	74.4	35	15	15.90	17.3	977	0.986	0.626	0.834	0.895	U	3.14	3.64	29.26		
145.09	993	20.1	5.08	74.4										D	3.51	1.72	-0.90	52.8	96.9
146.39	1070	88.8	16.78	221.2	5	0	0.47	4.1		1.096	1.039	1.096	0.622	U	4.56	1.26	130.03		
147.39	1070	88.8	16.78	221.2										D	2.83	0.14	41.22	88.9	68.3
146.42	1037	83.3	15.03	197.1	7	1	1.84	1.9		1.102	1.019	1.092	0.613	U	4.11	1.19	100.55		
147.42	1037	83.3	15.03	197.1										D	2.74	0.16	17.36	86.6	82.7
142.03	1476	2.0	6.20	63.6	42	18	20.12	24.2	1217	1.408	0.780	1.135		U					
143.03	1476	2.0	6.20	63.6										D				75.5	
142.06	1501	19.7	7.86	108.8	31	24	14.29	35.5	1067	1.044	0.703	0.781	0.933	U	2.75	6.09	16.22		
143.06	1501	19.7	7.86	108.8										D	3.30	0.91	0.21	85.1	98.7
142.09	1502	40.1	10.85	164.0	24	24	7.76	29.0	1106	0.956	0.721	0.712	0.634	U	2.25	6.14	9.36		
143.09	1502	40.1	10.85	164.0										D	2.63	0.78	0.35	87.3	96.3
142.12	1450	60.0	14.29	212.6	18	17	3.02	18.5	1181	0.971	0.789	0.796	0.578	U	3.24	2.25	5.03		
143.12	1450	60.0	14.29	212.6										D	3.86	0.29	0.27	87.1	94.6
142.15	1542	79.9	18.93	240.2	16	17	1.87	20.6	1168	1.139	0.941	0.932	0.540	U	1.97	2.25	95.25		
143.15	1542	79.9	18.93	240.2										D	1.94	0.22	1.74	90.2	98.2
142.18	1564	100.8	19.66	295.4	13	0	2.53	21.2	1206	0.962	0.826	0.962	0.439	U	18.49	1.24	6.46		
143.18	1546	100.8	19.66	295.4										D	20.19	0.21		83.1	
142.21	1513	111.9	24.20	307.1	11	0	0.82	19.9	1178	1.139	1.008	1.139	0.503	U	7.34	1.82	113.00		
143.21	1513	111.9	24.20	307.1										D	5.16	0.30	43.34	83.5	61.7
146.18	1995	2.0	7.73	86.6	41	15	19.95	37.4	1214	1.290	0.735	1.088		U					
147.18	1995	2.0	7.73	86.6										D					
146.21	2036	20.3	11.31	174.6	26	31	11.43	37.8	1117	0.937	0.681	0.638	0.964	U	2.62	23.38	21.71		
147.21	2036	20.3	11.31	174.6										D	3.27	3.77	0.69	83.9	96.8
146.24	2041	40.2	16.11	258.0	19	19	5.79	23.2	1254	0.902	0.719	0.720	0.691	U	3.11	4.42	10.48		
147.24	2041	40.2	16.11	258.0										D	3.66	0.62	0.32	86.0	97.0
146.27	2036	59.8	19.59	298.8	17	16	3.42	21.4	1278	0.947	0.778	0.789	0.566	U	4.83	0.95	7.65		
147.27	2036	59.8	19.59	298.8										D	5.48	0.12	0.20	87.4	97.4
146.30	2060	79.6	22.71	348.0	15	3	4.21	21.9	1290	0.943	0.795	0.912	0.487	U	15.53	0.61	5.48		
147.30	2060	79.6	22.71	348.0										D	16.96	0.09	0.17	85.3	96.9
146.33	1981	99.7	26.23	375.6	14	0	2.45	21.7	1304	1.010	0.864	1.007	0.468	U	17.03	0.47	18.61		
147.33	1981	99.7	26.23	375.6										D	18.28	0.08	0.50`	83.0	97.3
146.36	2019	107.0	31.54	399.1	12	0	1.31	22.1	1292	1.142	0.992	1.140	0.514	U	7.40	0.78	96.06		
147.36	2019	107.0	31.54	399.1										D	6.05	0.20	47.06	74.4	51.0
144.12	2516	0.0	9.49	147.6	34	34	16.63	40.8	1152	0.930	0.604	0.601		U					
145.12	2516	0.0	9.49	147.6										D					
144.16	2512	20.5	13.78	211.0	26	29	12.20	40.5	1195	0.944	0.691	0.654	0.942	U	3.58	9.52	19.63		
145.16	2512	20.5	13.78	211.0										D	4.19	1.59	0.59	83.3	97.0
144.18	2490	39.8	17.94	271.0	21	23	8.64	35.8	1237	0.957	0.748	0.728	0.638	U	5.32	2.09	10.61		
145.18	2490	39.8	17.94	271.0										D	5.90	0.29	0.28	86.1	97.4
144.21	2485	59.8	23.56	363.5	16	14	3.80	24.7	1345	0.937	0.781	0.795	0.558	U	6.61	0.43	6.33		

Table C-1. Stock Baseline Engine Data (Contd)

Sequence No.	RPM	BMEP (psi)	$\dot{m}_{gaso}$ (lbm/h)	$\dot{m}_{air}$ (lbm/h)	% A.I.R.	% EGR	P_{man} ("Hg vac)	Spark Advance (°BTDC)	Average T_{exh} (°F)	ϕ	ϕ_A	ϕ_E	BSFC (lbm/bhp-h)	Emissions Data*	$BSNO_x$ (g/bhp-h)	BSHC (g/bhp-h)	BSCO (g/bhp-h)	η_{HC}	η_{CO}
145.21	2485	59.8	23.56	363.5										D	7.21	0.05	0.17	88.4	97.3
144.24	2548	79.6	28.26	436.3	13	3	4.08	25.6	1370	0.936	0.808	0.905	0.490	U	17.61	0.28	4.69		
145.24	2548	79.6	28.26	436.3										D	18.63	0.04	0.15	85.7	96.8
144.27	2525	99.7	35.58	481.1	11	1	2.37	25.7	1414	1.069	0.947	1.060	0.497	U	13.58	0.18	33.07		
145.27	2525	99.7	35.58	481.1										D	12.37	0.03	4.00	83.3	87.9
144.30	2503	103.4	38.13	483.2	11	1	1.86	25.3	1390	1.141	1.013	1.134	0.519	U	7.39	0.51	92.33		
145.30	2503	103.4	38.13	483.2										D	7.12	0.31	71.54	39.2	22.6
144.33	2958	0.7	11.67	180.4	32	35	16.01	42.3	1219	0.935	0.624	0.596		U					
145.33	2958	0.7	11.67	180.4										D					
146.03	3033	20.4	16.90	263.9	24	27	12.03	42.5	1272	0.925	0.692	0.659	0.961	U	5.75	7.73	19.27		
147.03	3033	20.4	16.90	263.9										D	6.62	1.17	0.57	84.9	97.0
146.06	3044	39.3	22.03	344.0	19	20	8.66	37.6	1328	0.926	0.741	0.728	0.641	U	7.46	1.12	7.81		
147.06	3044	39.3	22.03	344.0										D	8.30	0.14	0.22	87.5	97.2
146.09	3021	59.8	29.87	468.5	13	8	4.90	24.4	1460	0.922	0.792	0.846	0.582	U	10.23	0.19	4.53		
147.09	3021	59.8	29.87	468.5										D	11.04	0.02	0.13	89.5	97.1
146.12	3059	79.6	35.15	535.2	11	2	3.76	28.3	1482	0.949	0.839	0.930	0.508	U	18.78	0.16	5.11		
147.12	3059	79.6	35.15	535.2										D	19.66	0.02	0.14	87.5	97.3
146.15	2985	96.6	45.27	564.2	9	1	2.56	28.7	1465	1.160	1.050	1.147	0.553	U	7.78	0.57	105.02		
147.15	2985	96.6	45.27	564.2										D	7.72	0.44	93.06	22.8	11.4
148.06	3503	0.6	14.19	214.8	32	30	15.48	41.9	1304	0.955	0.657	0.640		U					
149.06	3503	0.6	14.19	214.8										D					
148.09	3567	39.7	26.61	411.1	18	18	8.24	34.9	1391	0.936	0.761	0.756	0.662	U	11.07	0.56	7.23		
149.09	3567	39.7	26.61	411.1										D	11.06	0.07	0.19	87.5	97.4
148.12	3541	59.9	35.27	541.7	7	13	4.83	25.3	1511	0.941	0.814	0.874	0.586	U	15.47	0.17	4.66		
149.12	3541	59.9	35.27	541.7										D	15.69	0.02	0.14	88.2	97.0
148.15	3500	79.6	41.58	606.3	1	11	3.42	25.5	1551	0.991	0.878	0.976	0.525	U	22.67	0.10			
149.15	3500	79.6	41.58	606.3										D	22.83	0.02	0.26	80.0	
148.18	3554	85.9	50.34	621.5	2	10	3.18	25.5	1518	1.171	1.041	1.152	0.581	U	8.83				
149.18	3554	85.9	50.34	621.5										D	8.45				
150.06	4086	1.7	18.39	254.3	28	20	15.01	43.4	1425	1.045	0.733	0.825	9.203	U					
151.06	4086	1.7	18.39	254.3										D					
150.09	4037	40.3	34.16	532.9	15	15	5.20	26.0	1543	0.927	0.783	0.783	0.739	U	8.92	0.19	6.62		
151.09	4037	40.3	34.16	532.9										D	9.16	0.02	0.22	89.5	96.7
150.12	4045	60.1	41.23	617.4	12	5	4.14	26.3	1584	0.965	0.839	0.918	0.597	U	18.53	0.07	5.31		
151.12	4045	60.1	41.23	617.4										D	18.93	0.01	0.20	85.7	96.2
150.16	4071	72.9	52.17	647.2	12	2	3.47	26.7	1571	1.165	1.022	1.141	0.619	U	9.65	0.50	118.02		
151.16	4071	72.9	52.17	647.2										D	8.29	0.50	128.54	0.0	0.0

*U = Upstream of catalytic converter; D = downstream of catalytic converter.

Figure C-1.   Fuel Consumption Versus BMEP for
              Stock Engine — 1000 RPM
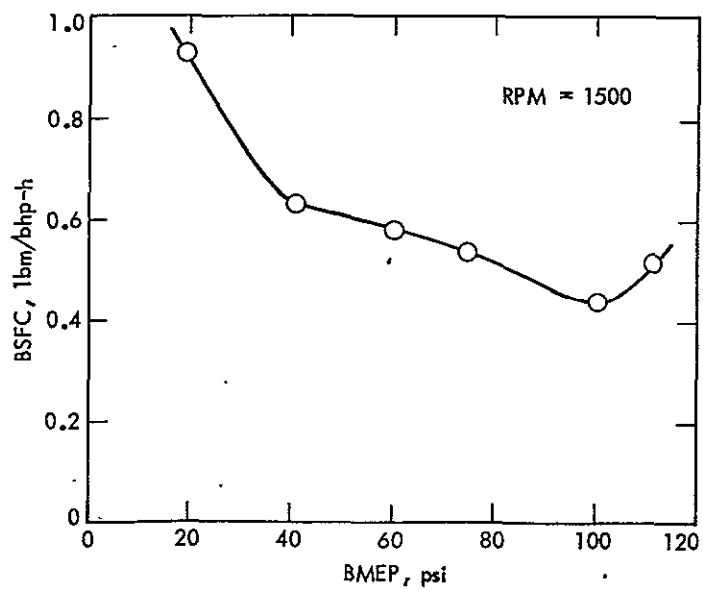
Figure C-2.   Fuel Consumption Versus BMEP for
              Stock Engine — 1500 RPM
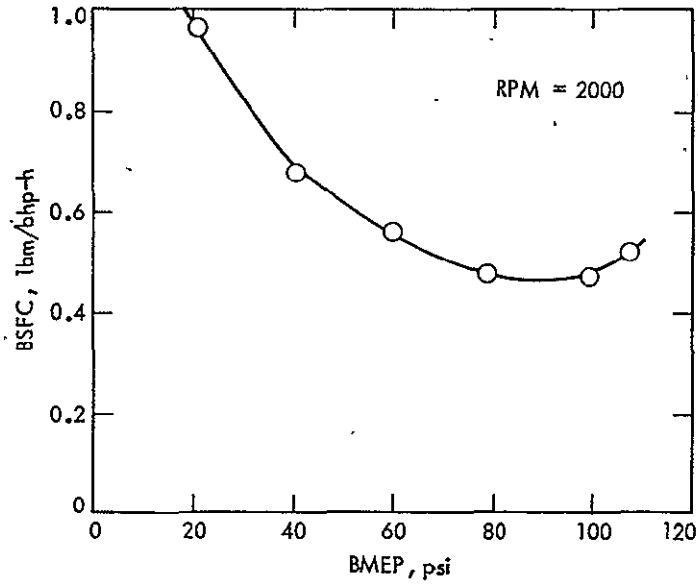
Figure C-3.   Fuel Consumption Versus BMEP
              for Stock Engine - 2000 RPM
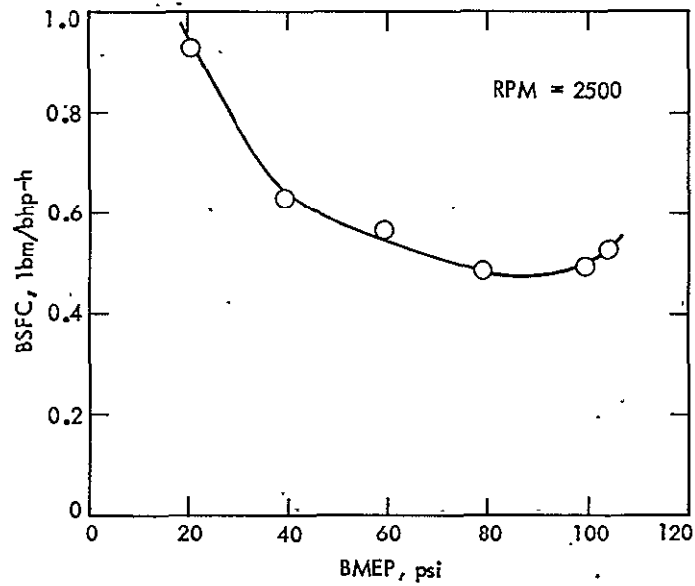
Figure C-4.   Fuel Consumption Versus BMEP
              for Stock Engine - 2500 RPM
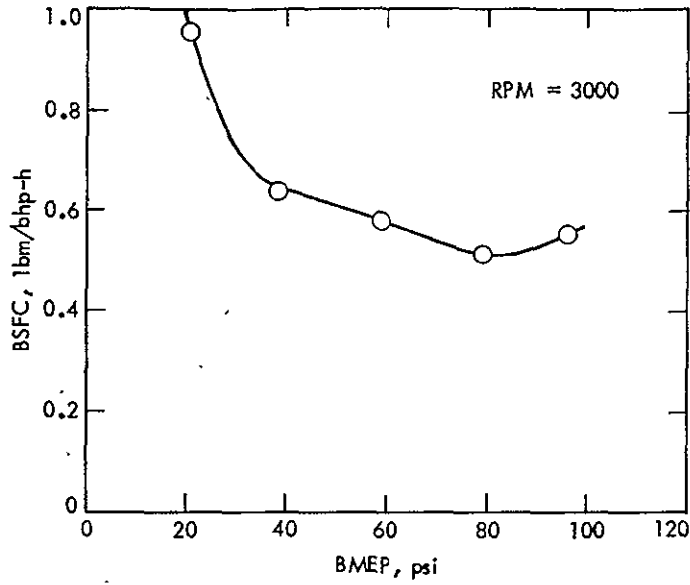
Figure C-5. Fuel Consumption Versus BMEP
for Stock Engine - 3000 RPM
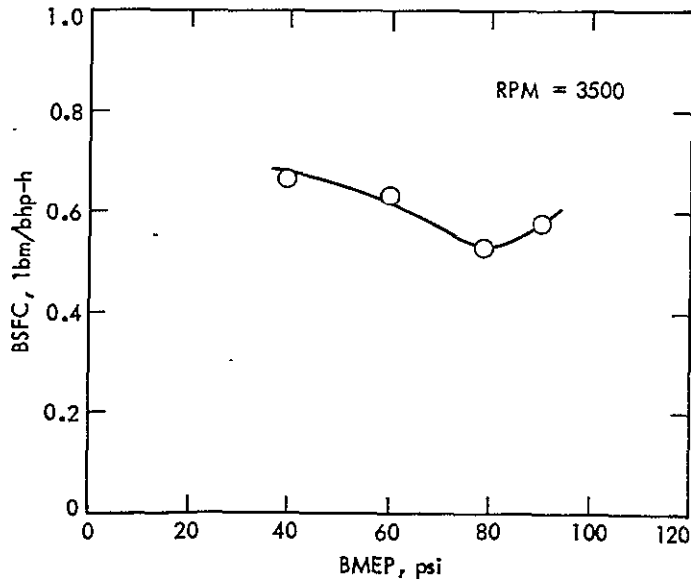
Figure C-6. Fuel Consumption Versus BMEP
for Stock Engine - 3500 RPM
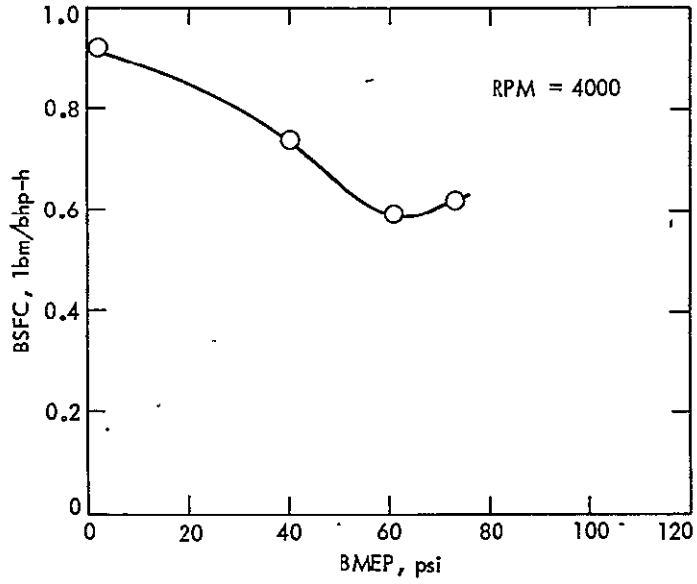
Figure C-7. Fuel Consumption Versus BMEP
for Stock Engine - 4000 RPM
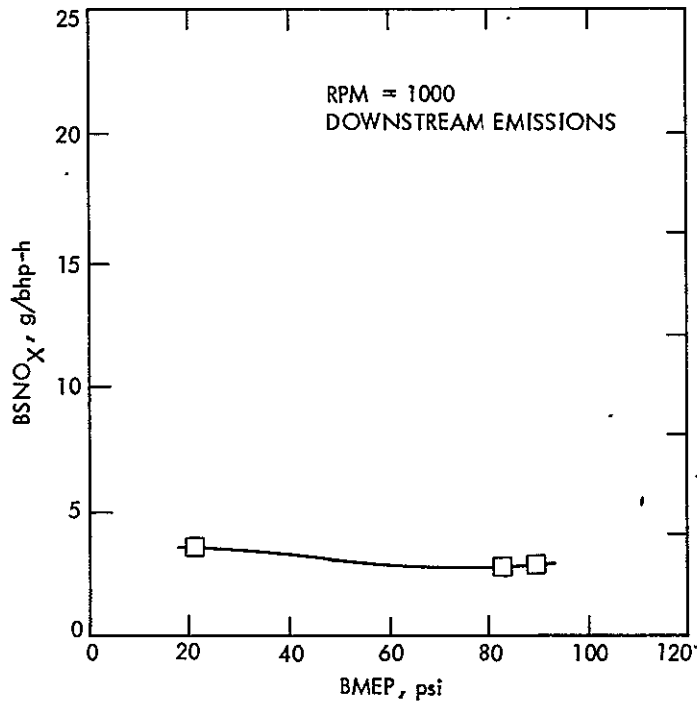
Figure C-8. Downstream NO_x Emissions Versus
BMEP for Stock Engine - 1000 RPM
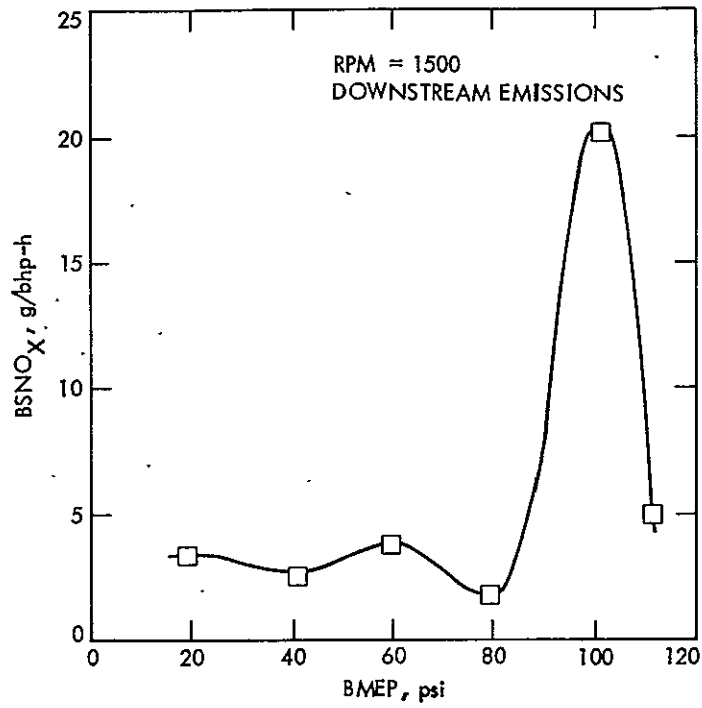
Figure C-9.   Downstream NO_x Emissions Versus
            BMEP for Stock Engine - 1500 RPM
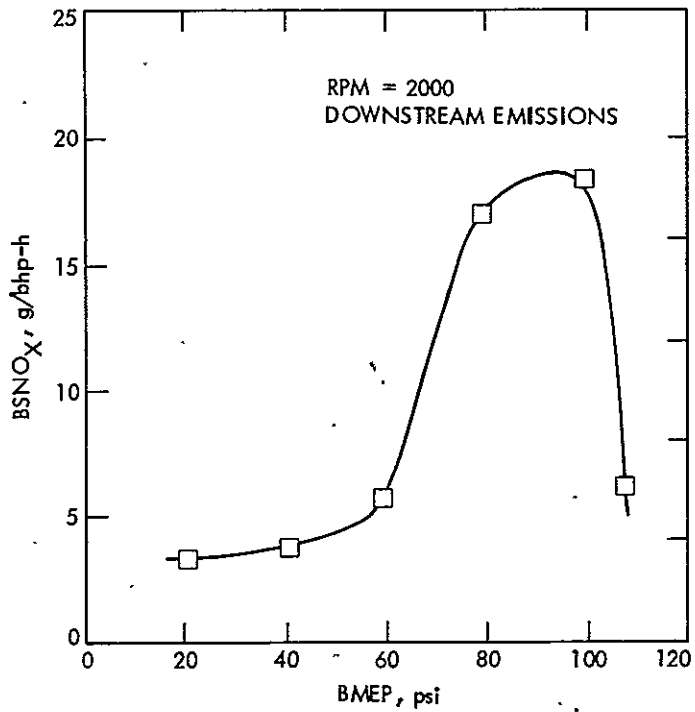
Figure C-10.   Downstream NO_x Emissions Versus
            BMEP for Stock Engine - 2000 RPM
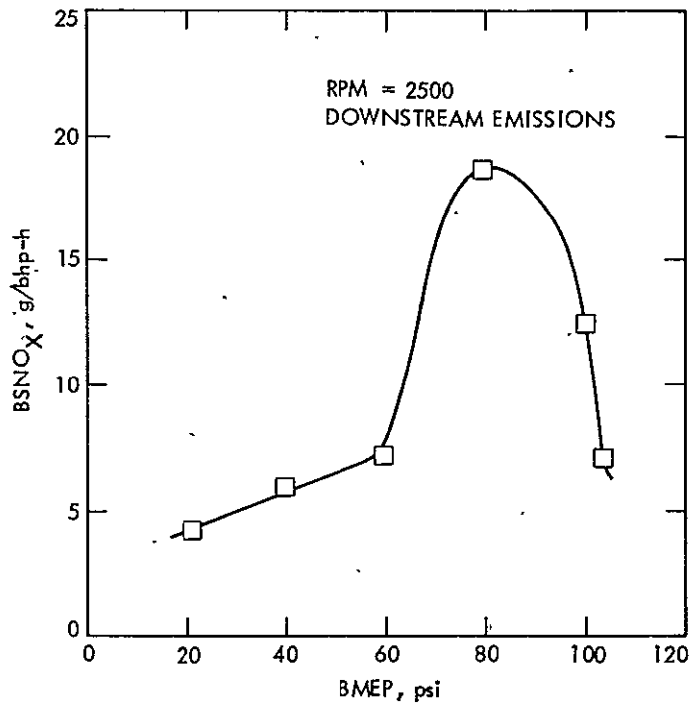
Figure C-11. Downstream NO_x Emissions Versus
BMEP for Stock Engine – 2500 RPM
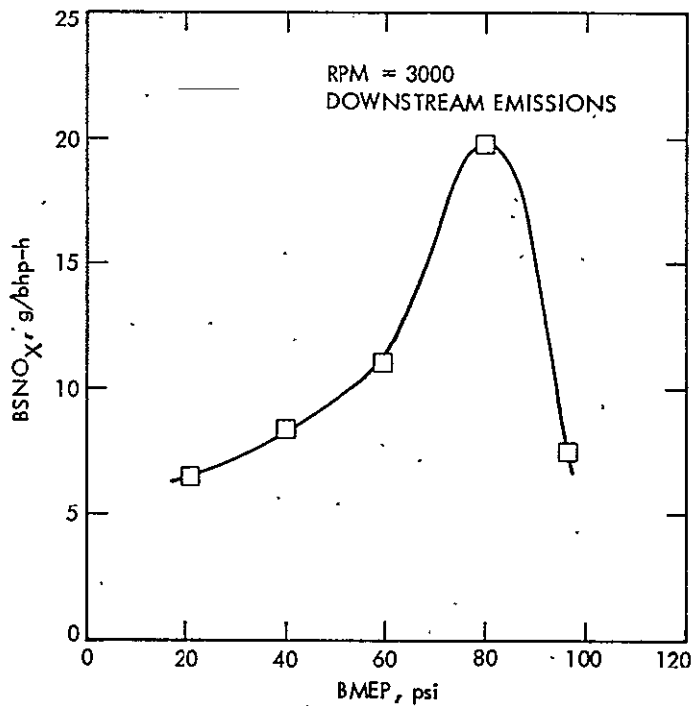
Figure C-12. Downstream NO_x Emissions Versus
BMEP for Stock Engine – 3000 RPM
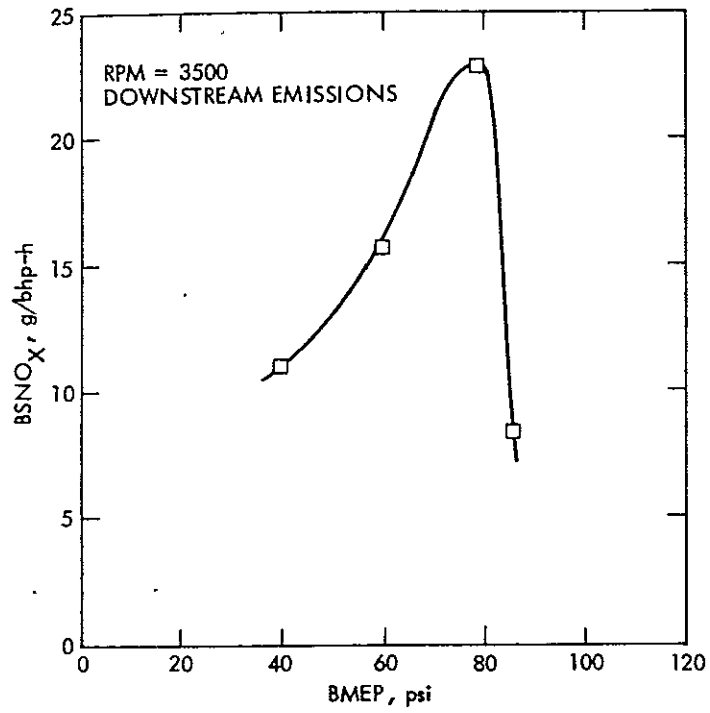
Figure C-13. Downstream NO$_X$ Emissions Versus
BMEP for Stock Engine - 3500 RPM
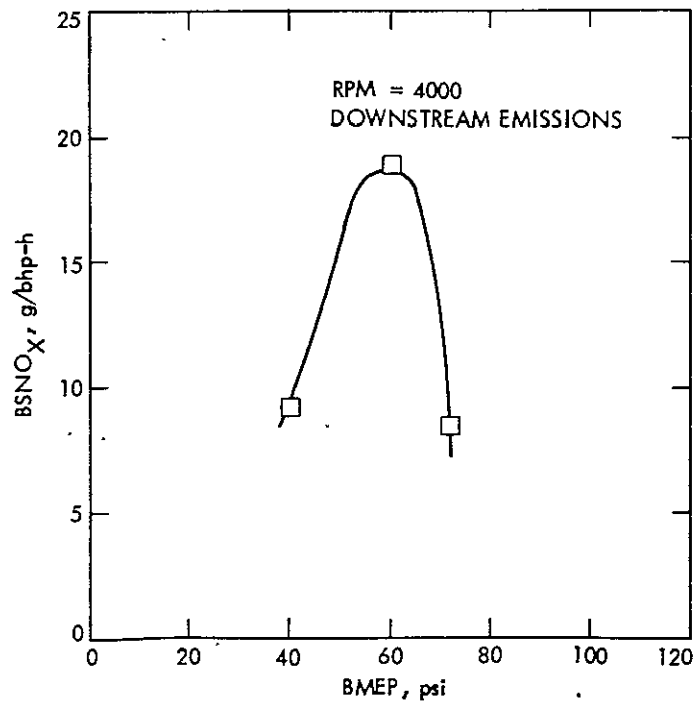
Figure C-14. Downstream NO$_X$ Emissions Versus
BMEP for Stock Engine - 4000 RPM
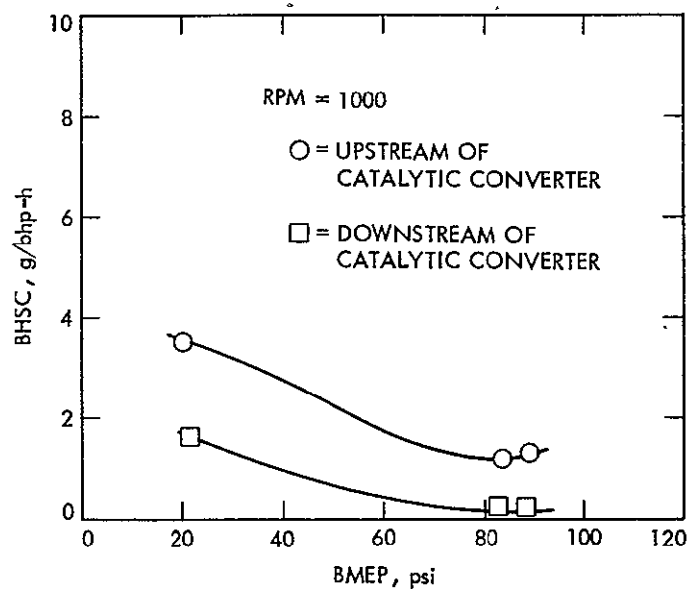
Figure C-15. HC Emissions Versus BMEP
for Stock Engine - 1000 RPM
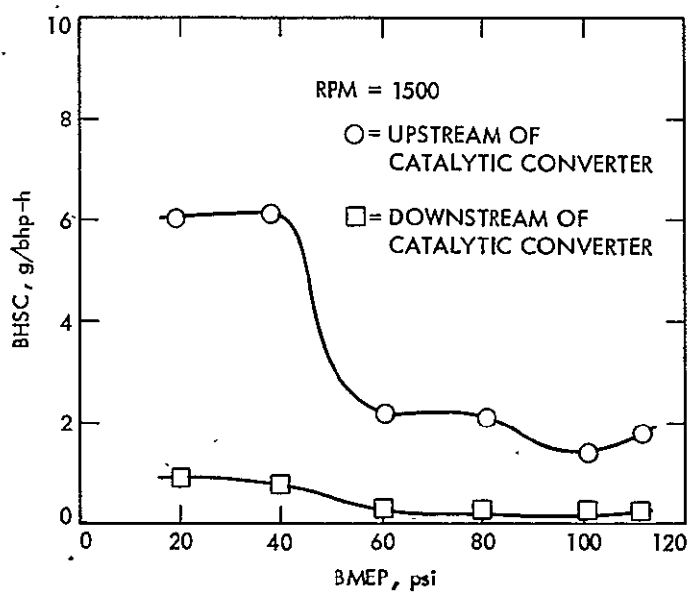
Figure C-16. HC Emissions Versus BMEP
for Stock Engine - 1500 RPM
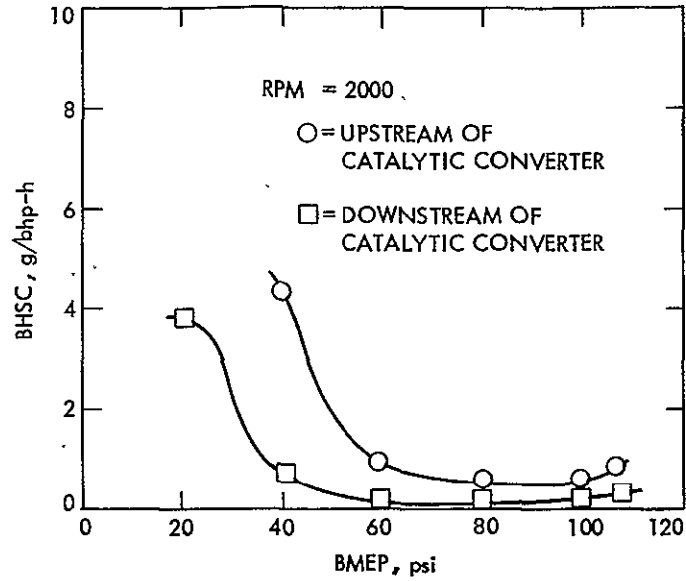
Figure C-17.   HC Emissions Versus BMEP
               for Stock Engine – 2000 RPM
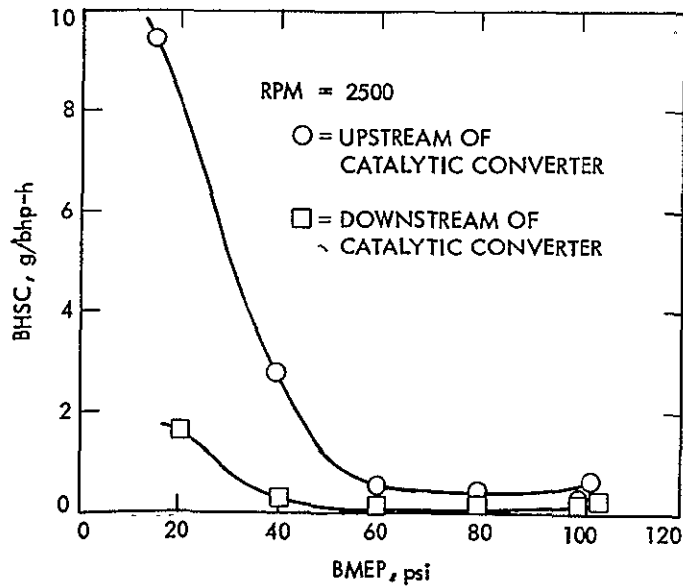
Figure C-18.   HC Emissions Versus BMEP
               for Stock Engine – 2500 RPM
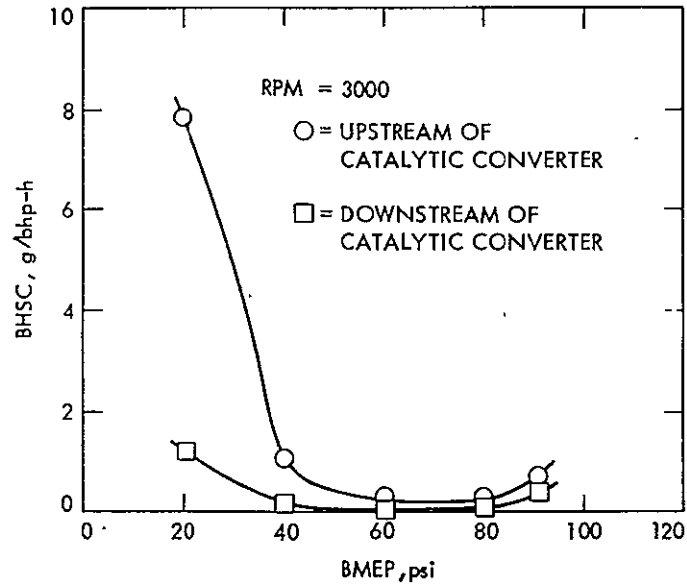
Figure C-19.   HC Emissions Versus BMEP
for Stock Engine - 3000 RPM
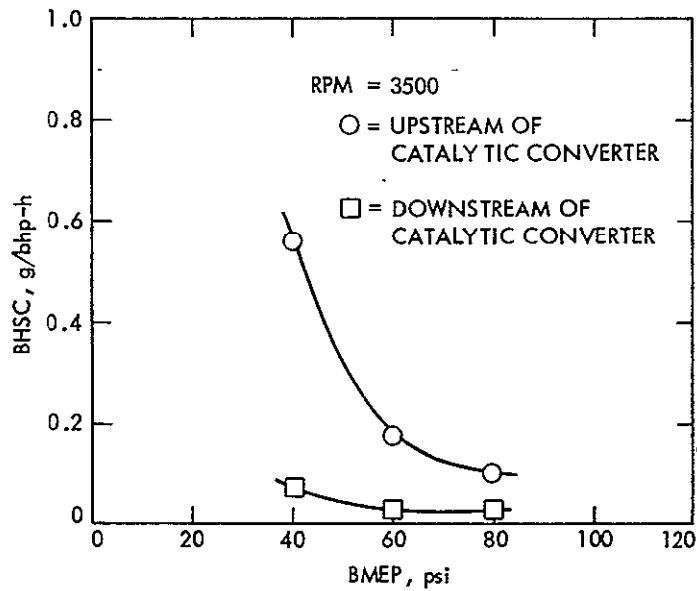
Figure C-19.   HC Emissions Versus BMEP
for Stock Engine - 3500 RPM
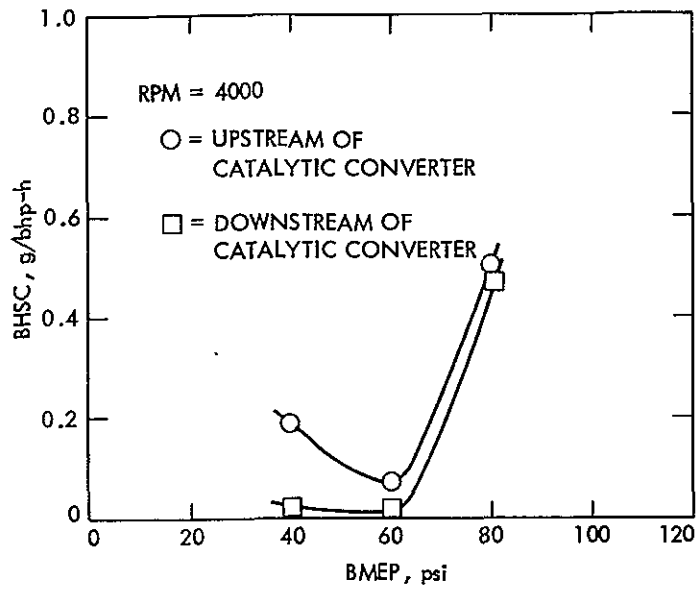
Figure C-21. HC Emissions Versus BMEP
for Stock Engine – 4000 RPM
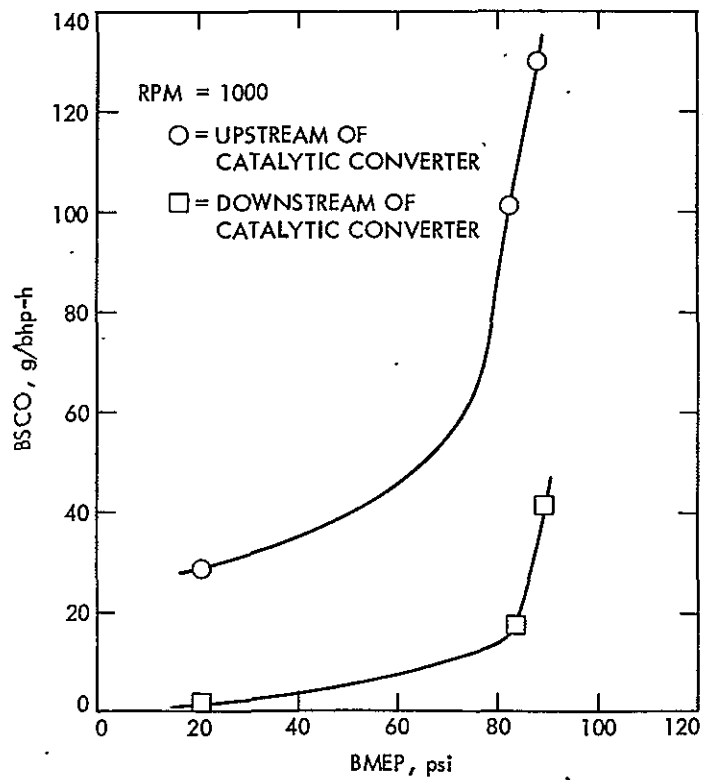
Figure C-22. CO Emissions Versus BMEP
for Stock Engine – 1000 RPM

C-14
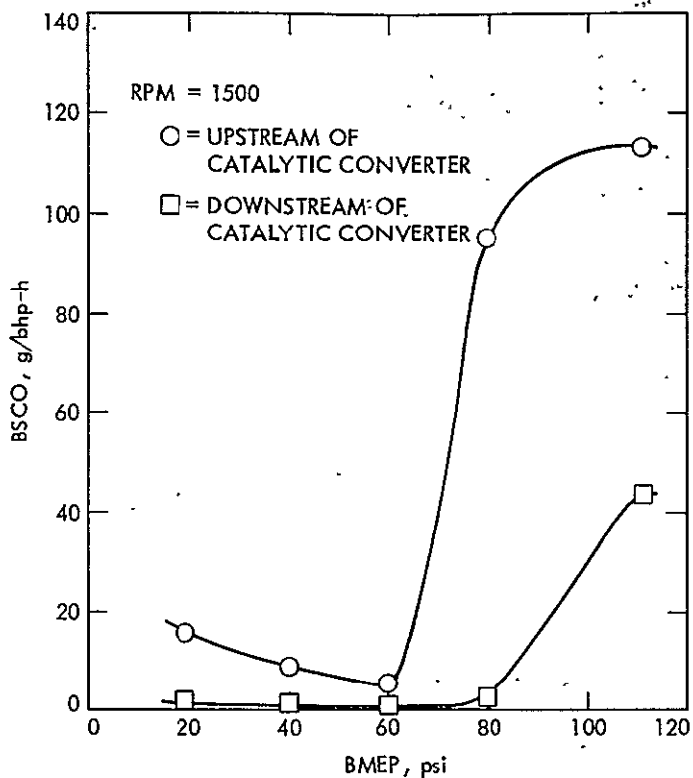
Figure C-23.   CO Emissions Versus BMEP
for Stock Engine – 1500 RPM
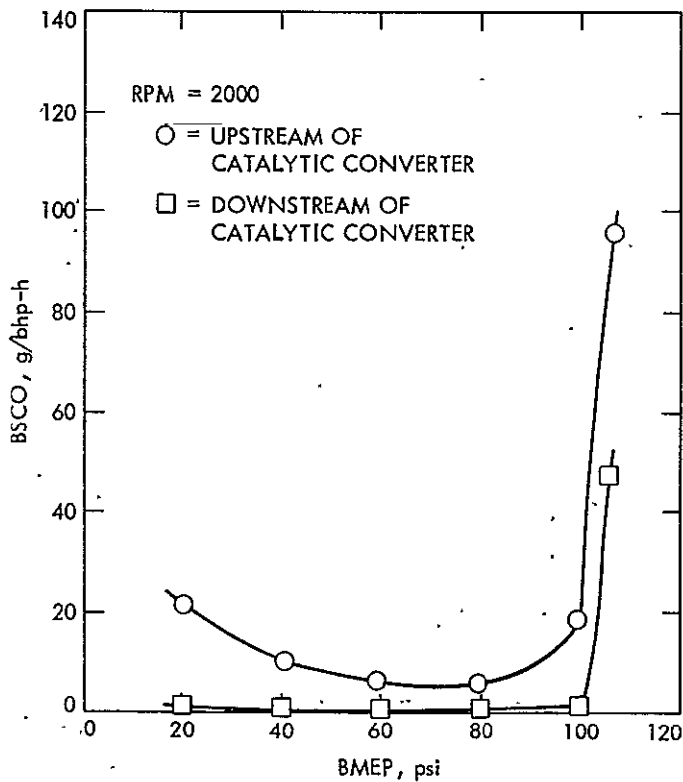
Figure C-24.   CO Emissions Versus BMEP
for Stock Engine – 2000 RPM
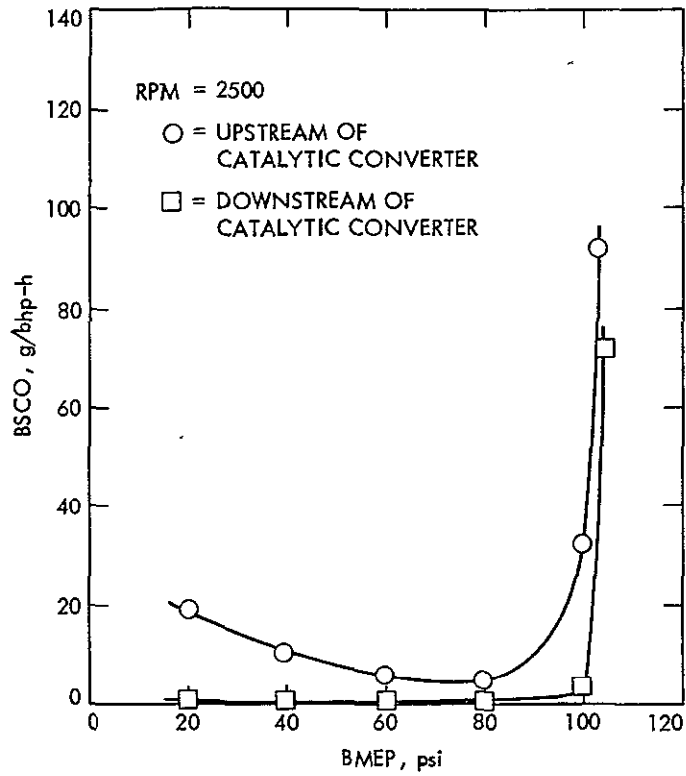
Figure C-25.　CO Emissions Versus BMEP
for Stock Engine - 2500 RPM
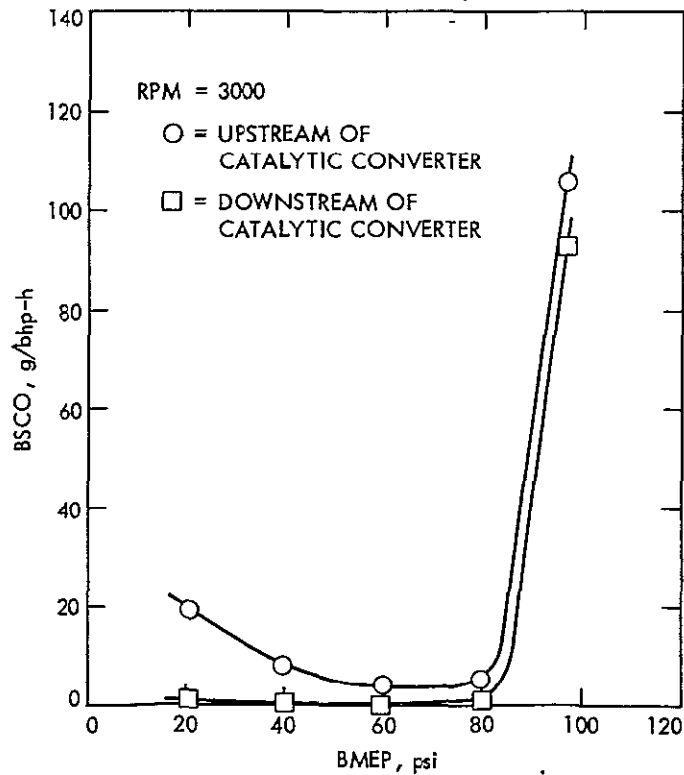
Figure C-26.　CO Emissions Versus BMEP
for Stock Engine - 3000 RPM
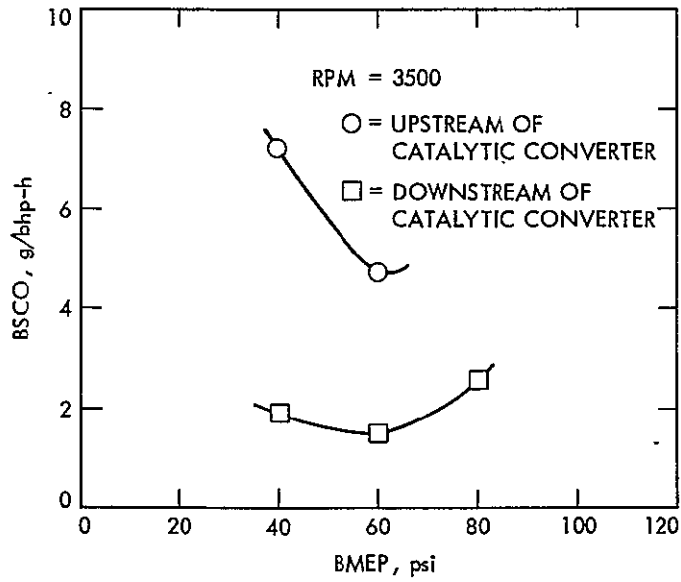
Figure C-27.   CO Emissions Versus BMEP
               for Stock Engine – 3500 RPM
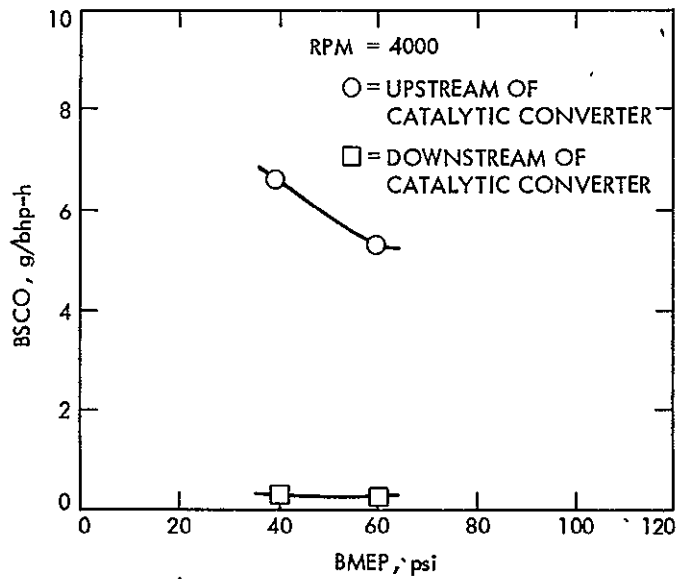
Figure C-28.   CO Emissions Versus BMEP
               for Stock Engine – 4000 RPM

APPENDIX D

EGR/SPARK ADVANCE SENSITIVITY DATA

Table D-1. EGR/Spark Advance Sensitivity Data for
RPM = 1000 and BMEP = 30.6 psi

Sequence No.	Spark Advance (°BTDC)	% EGR	BSFC (1bm/bhp-h)	Emissions Data*	BSNO$_x$ (g/bhp-h)	BSHC (g/bhp-h)	BSCO (g/bhp-h)	Average T$_{exh}$ (°F)
3115.10	30.6	5	0.674	D	13.54	0.71	0.58	934
3115.28	30.9	5	0.648	U	12.95	3.32	15.97	902
3115.13	20.6	4	0.686	D	8.79	0.59	0.54	974
3115.31	20.6	4	0.702	U	8.95	2.78		963
3115.16	10.8	2	0.765	D	6.46	0.38	0.42	1068
3115.34	9.5	2	0.758	U	6.56	2.04	11.51	1062
3161.27	35.5	12	1.047	D	17.58	1.04	0.62	894
3160.27	35.5	12	1.047	U	17.62	3.38	30.17	894
3161.24	26.2	12	1.062	D	12.80	0.90	0.53	926
3160.24	26.2	12	1.062	U	12.60	3.10	26.66	926
3161.21	15.2	10	1.117	D	8.77	0.60	0.32	1012
3160.21	15.2	10	1.117	U	8.57	2.36	18.03	1012
3115.37	39.8	28	0.684	D	2.22	1.72	0.38	930
3115.52	39.5	28	0.649	U	2.28	7.04	3.74	922
3115.40	29.5	26	0.708	D	1.74	1.47	0.32	963
3115.49	30.4	25	0.691	U	1.71	5.51	5.17	972
3115.43	20.0	22	0.762	D	1.52	0.82	0.30	1026
3115.46	21.0	22	0.774	U	1.50	4.71	6.32	1031

*D = downstream of catalytic converter; U = upstream of catalytic converter.
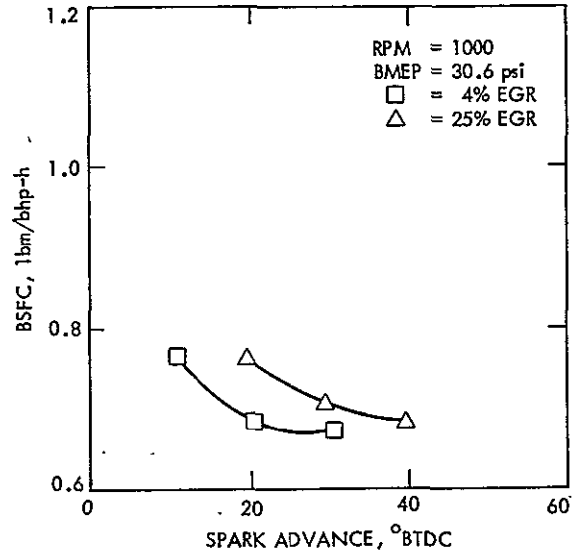
Figure D-1. Fuel Consumption Versus Spark Advance for EGR/Spark
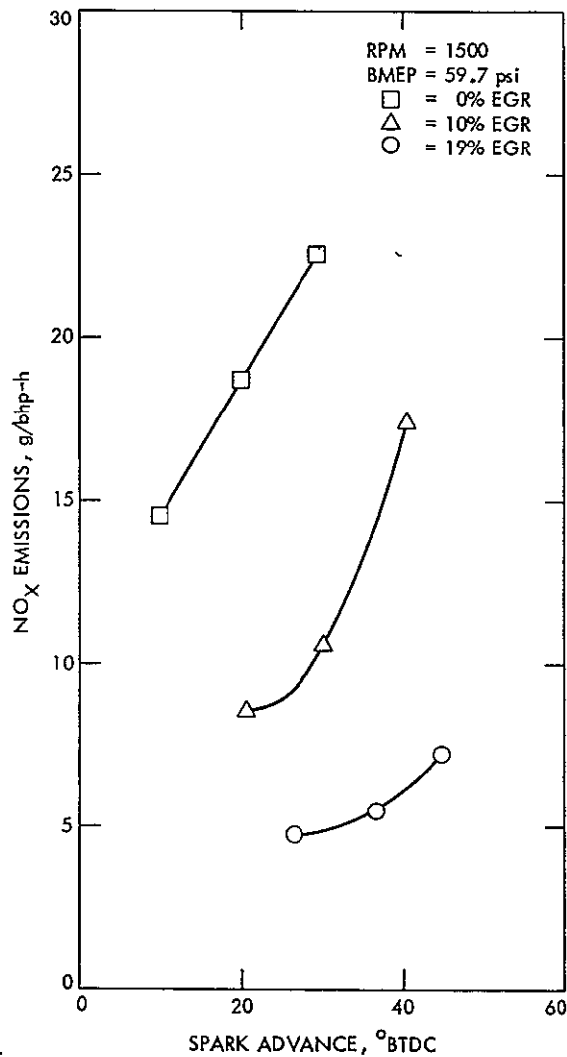Advance Tests - RPM = 1000, BMEP = 30.6 psi
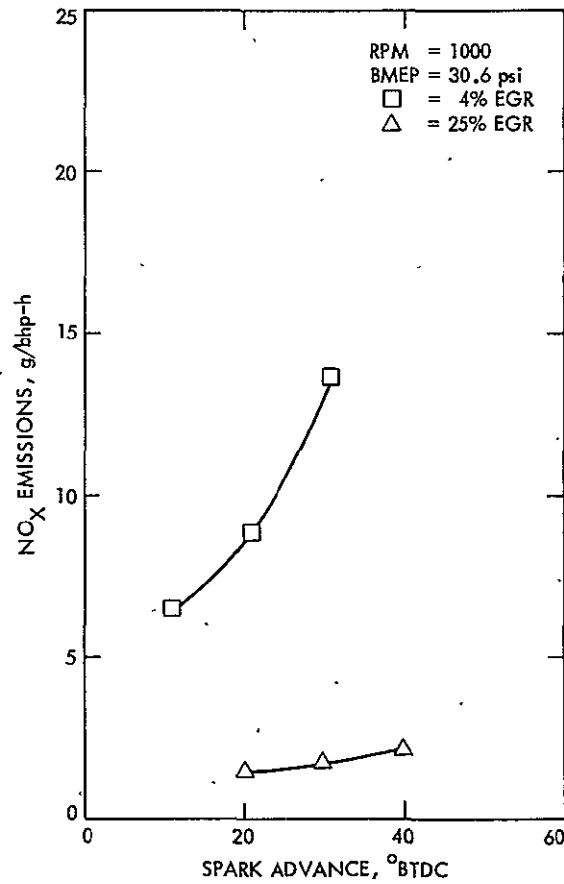
Figure D-2. NO$_x$ Emissions Versus Spark Advance for EGR/Spark
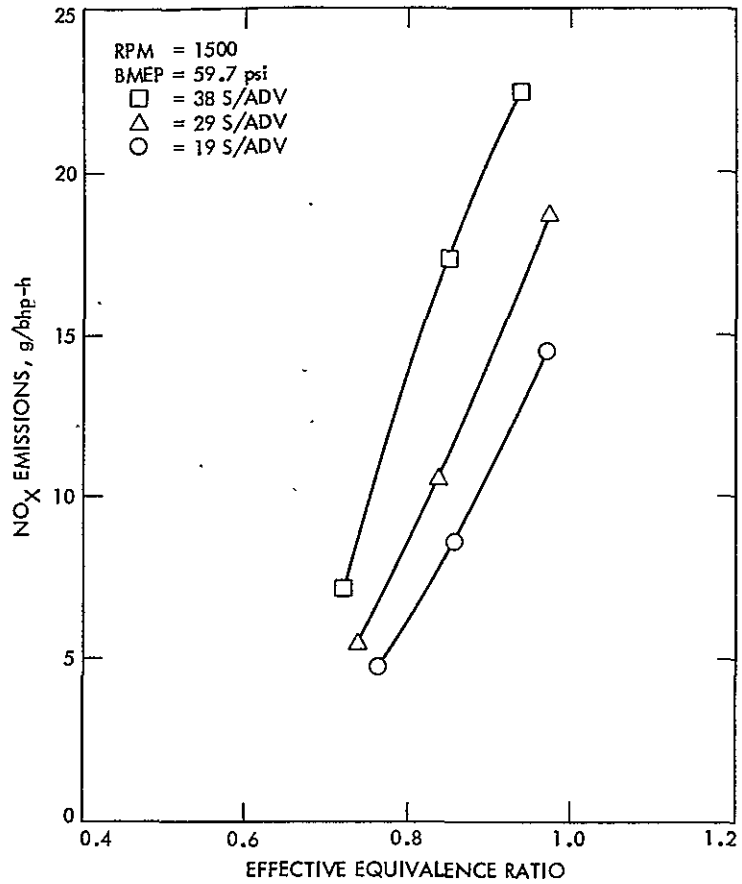Advance Sensitivity Tests - RPM = 1000, BMEP = 30.6 psi
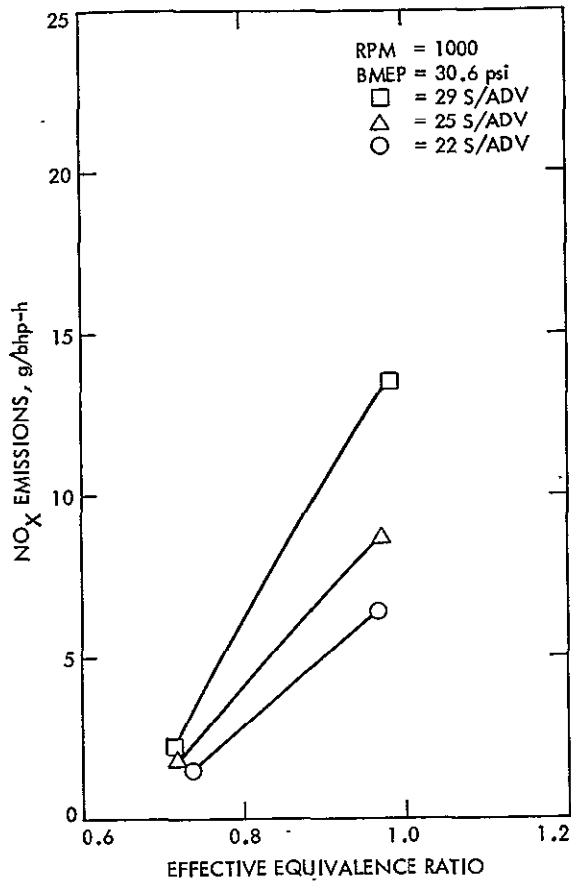
Figure D-3. NO$_x$ Emissions Versus Effective Equivalence Ratio for EGR/Spark Advance Sensitivity Tests - RPM = 1000, BMEP = 30.6 psi
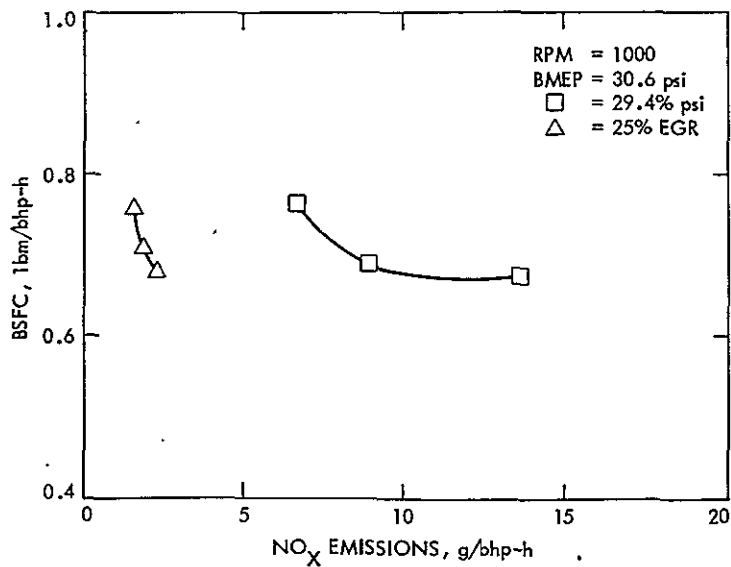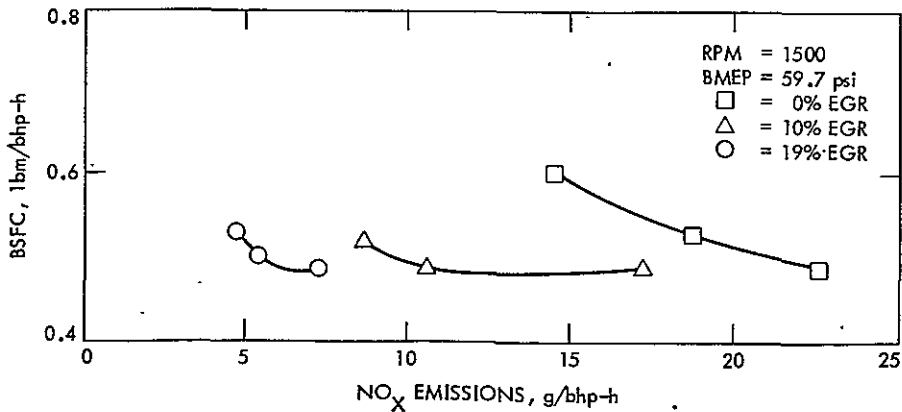

Figure D-4. Fuel Consumption Versus NO$_x$ Emissions for EGR/Spark Advance Sensitivity Tests - RPM = 1000, BMEP = 30.6 psi
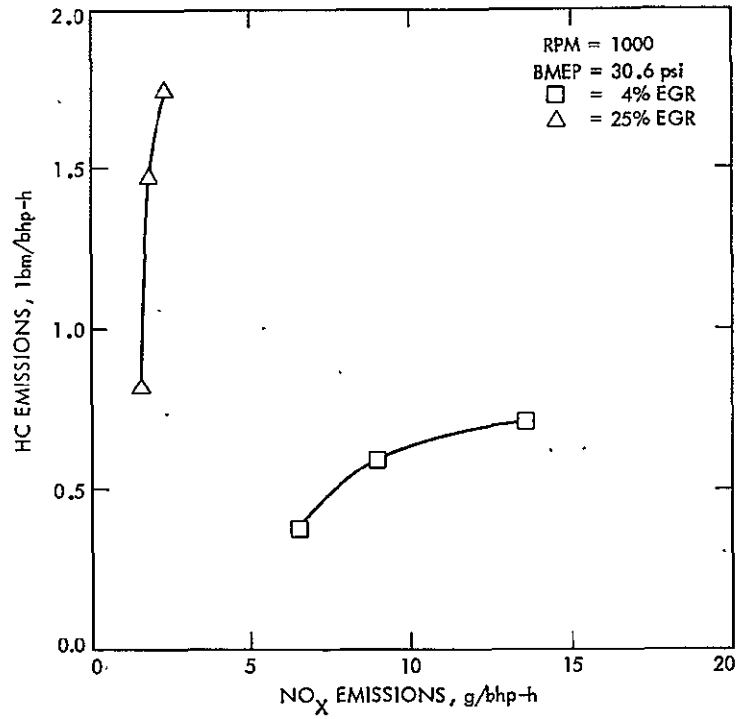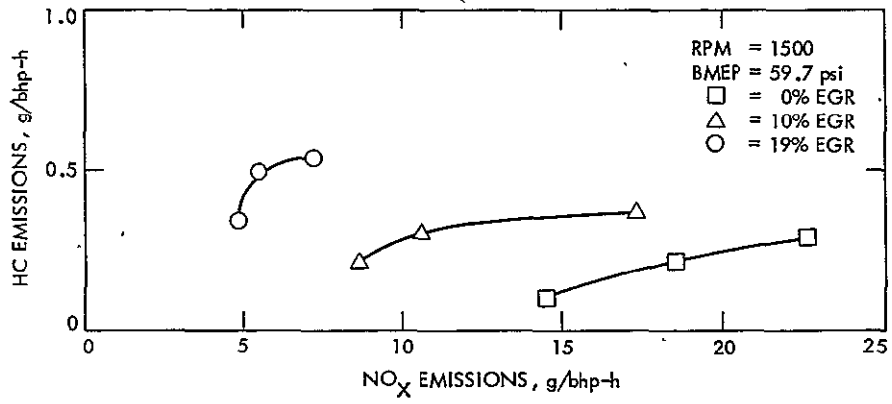
Figure D-5. Fuel Consumption Versus NO$_X$ Emissions for EGR/Spark
Advance Sensitivity Tests – RPM = 1000, BMEP = 30.6
psi

Table D-2. EGR/Spark Advance Sensitivity Data for
RPM = 1500 and BMEP = 19.8 psi

Sequence No.	Spark Advance (°BTDC)	% EGR	BSFC (1bm/bhp-h)	Emissions Data*	$BSNO_x$ (g/bhp-h)	BSHC (g/bhp-h)	BSCO (g/bhp-h)	Average T_{exh} (°F)
3105.05	41.2	5	0.878	D	17.33	0.42	0.42	1025
3105.08	40.7	5	0.849	U	18.30	2.55	6.61	1022
3105.11	30.1	5	0.870	D	10.94	0.37	0.40	1064
3105.14	29.6	5	0.895	U	10.65	2.10	7.09	1068
3105.17	21.8	4	0.995	D	7.81	0.32	0.36	1149
3105.20	21.3	4	0.972	U	7.45	1.54	5.36	1148
3159.48	40.7	19	0.904	D	13.88	0.82	0.24	
3158.48	40.7	19	0.904	U	13.52	1.89	9.97	
3159.45	31.4	17	0.874	D	9.21	0.63	0.20	
3158.45	31.4	17	0.874	U	9.27	1.61	9.13	
3159.42	21.2	16	0.918	D	6.06	0.48	0.22	
3158.42	21.2	16	0.918	U	5.98	1.38	9.69	
3106.10	46.0	28	0.931	D	4.03	4.90	0.40	1030
3106.13	46.1	28	0.914	U	3.92	18.88	6.98	1027
3106.16	35.3	26	0.942	D	2.50	2.42	0.41	1082
3106.19	35.4	26	0.961	U	2.50	10.22	7.80	1081
3106.22	25.4	21	0.976	D	2.24	1.00	0.47	1164
3106.25	25.7	21	0.983	U	2.21	6.39	10.75	1168
3106.28	50.9	38	0.947	D	3.64	5.76	0.68	918
3106.31	51.0	37	0.981	U	3.36	24.62	6.65	903
3106.34	40.7	36	1.005	D	2.08	5.79	0.68	966
3106.37	41.0	37	1.022	U	1.82	25.09	7.22	951
3106.40	28.9	47	1.096	D	1.39	5.16	0.92	
3106.42	28.9	46	1.070	U	1.29	26.53	13.37	

*D = downstream of catalytic converter; U = upstream of catalytic converter.
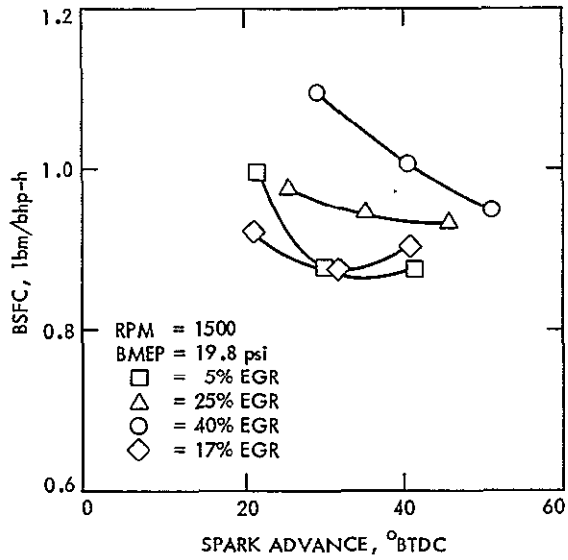
Figure D-6. Fuel Consumption Versus Spark Advance for EGR/Spark Advance Tests – RPM = 1500, BMEP = 19.8 psi
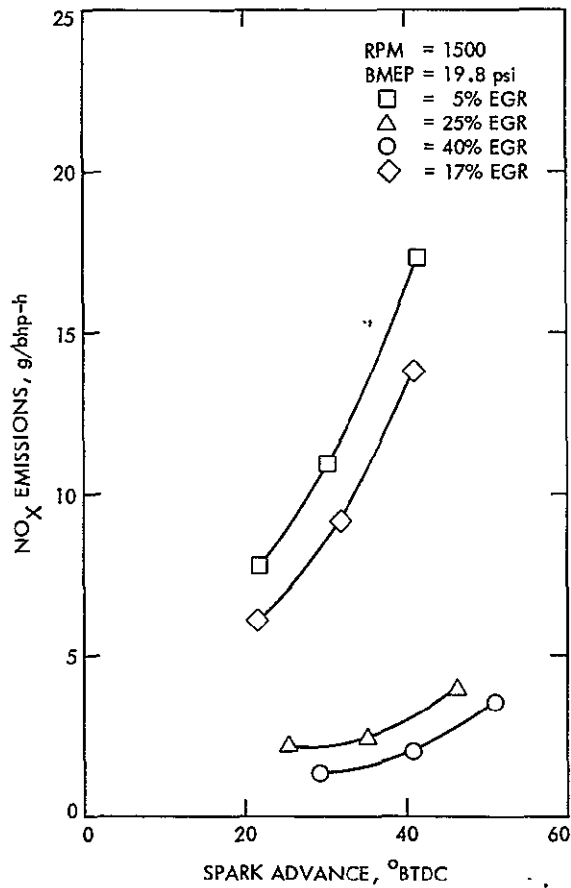
Figure D-7. NO_x Emissions Versus Spark Advance for EGR/Spark Advance Sensitivity Tests – RPM = 1500, BMEP = 19.8 psi
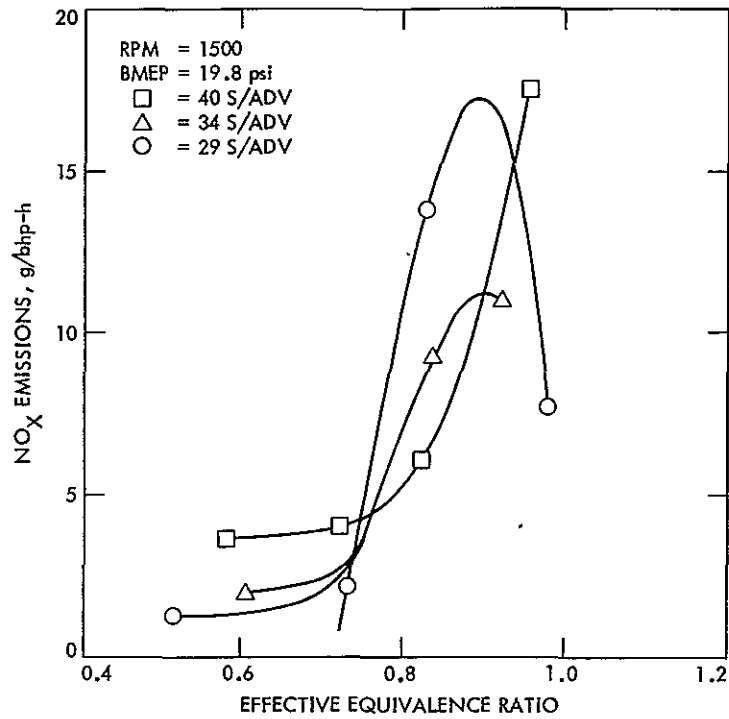
Figure D-8. NO$_x$ Emissions Versus Effective Equivalence Ratio for EGR/Spark Advance Sensitivity Tests – RPM = 1500, BMEP = 19.8 psi
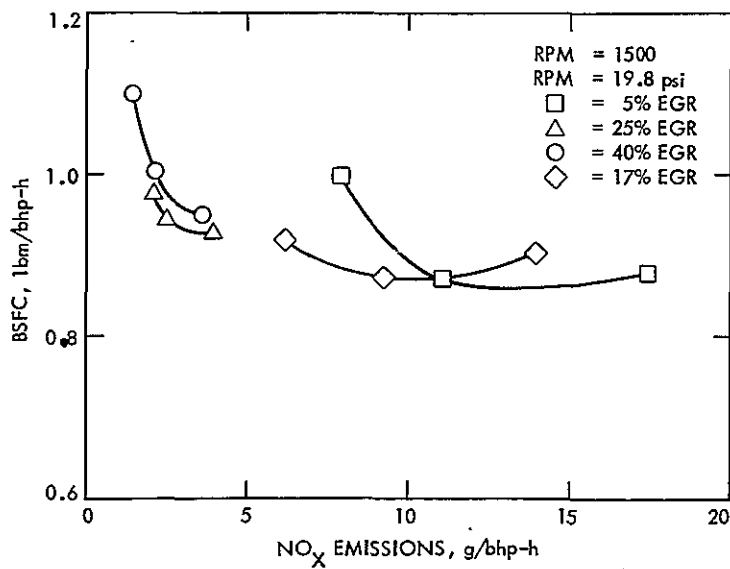
Figure D-9. Fuel Consumption Versus NO$_x$ Emissions for EGR/Spark Advance Sensitivity Tests – RPM = 1500, BMEP = 19.8 psi
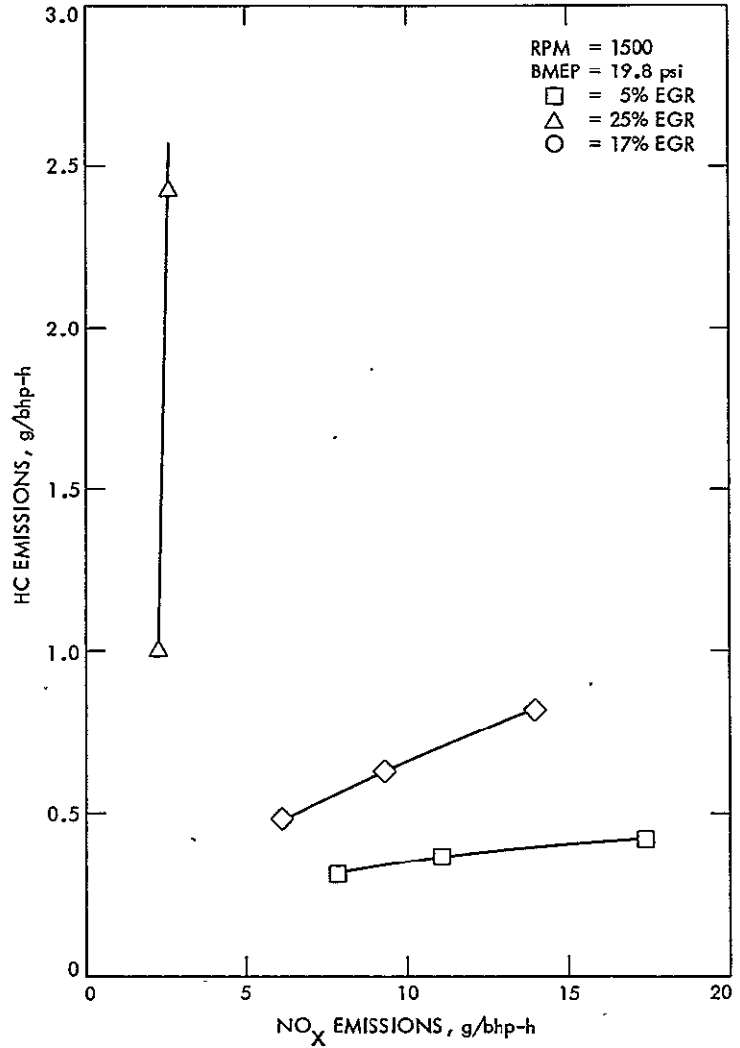
Figure D-10. Fuel Consumption Versus NO$_x$ Emissions for EGR/Spark Advance Sensitivity Tests - RPM = 1500, BMEP = 19.8 psi

Table D-3. EGR/Spark Advance Sensitivity Data for
RPM = 1500 and BMEP = 40.0 psi

Sequence No.	Spark Advance (°BTDC)	% EGR	BSFC (1bm/bhp-h)	Emissions Data*	$BSNO_x$ (g/bhp-h)	BSHC (g/bhp-h)	BSCO (g/bhp-h)	Average T_{exh} (°F)
3159.06	34.4	2	0.580	D	16.67	0.33	0.14	1083
3158.06	34.4	2	0.580	U	18.38	1.61	6.72	1083
3159.09	23.8	1	0.594	D	11.70	0.26	0.15	1128
3158.09	23.8	1	0.594	U	12.16	1.27	8.34	1128
3159.12	13.8	0	0.661	D	8.96	0.16	0.15	1208
3158.12	13.8	0	0.661	U	8.91	0.79	8.71	1208
3159.15	7.9	0	0.738	D	8.76	0.08	0.11	1288
3158.15	7.9	0	0.738	U	8.19	0.56	5.77	1288
3159.18	49.8	19	0.560	D	7.98	0.42	0.14	1022
3158.18	49.8	19	0.560	U	8.50	1.97	7.65	1022
3159.21	40.6	17	0.563	D	6.26	0.39	0.15	1062
3158.21	40.6	17	0.563	U	6.42	1.93	7.84	1062
3159.24	29.9	17	0.610	D	3.95	0.34	0.16	1114
3158.24	29.9	17	0.610	U	3.90	1.94	9.75	1114
3159.27	20.9	14	0.671	D	3.60	0.22	0.16	1181
3158.27	20.9	14	0.671	U	3.54	1.33	9.26	1181
3159.30	50.8	29	0.599	D	4.10	1.56	0.28	1005
3158.30	50.8	29	0.599	U	3.97	10.29	12.96	1005
3159.33	41.1	28	0.607	D	3.07	1.25	0.27	1027
3158.33	41.1	28	0.607	U	2.85	8.40	13.62	1027
3159.36	31.9	25	0.656	D	2.19	1.26	0.37	1075
3158.36	31.9	25	0.656	U	2.06	9.89	18.78	1075
3159.39	21.8	21	0.738	D	2.19	1.32	0.47	1137
3158.39	21.8	21	0.738	U	1.96	12.08	21.07	1137

*D = downstream of catalytic converter; U = upstream of catalytic converter.
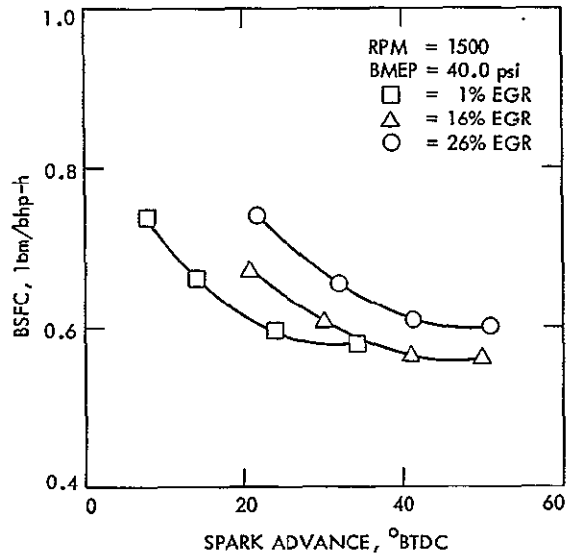
Figure D-11. Fuel Consumption Versus Spark Advance for EGR/Spark Advance Tests - RPM = 1500, BMEP = 40.0 psi
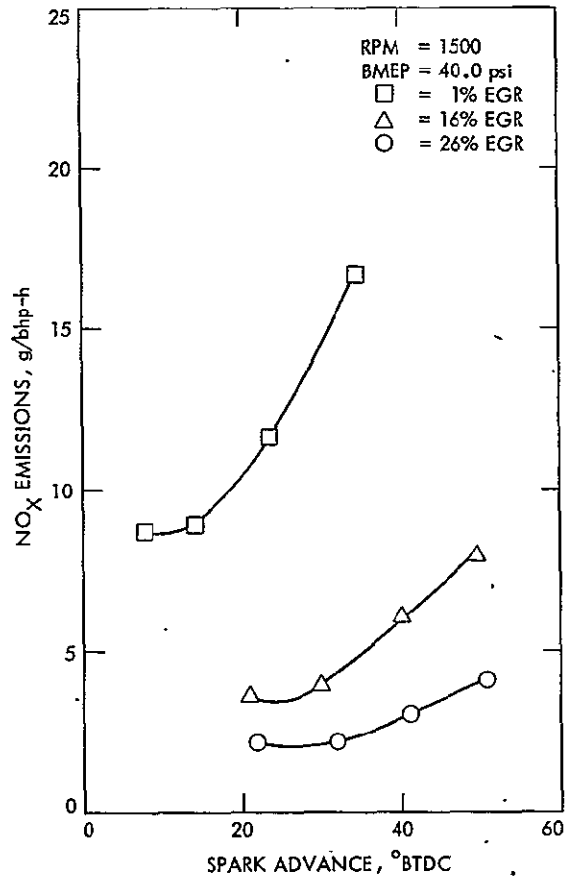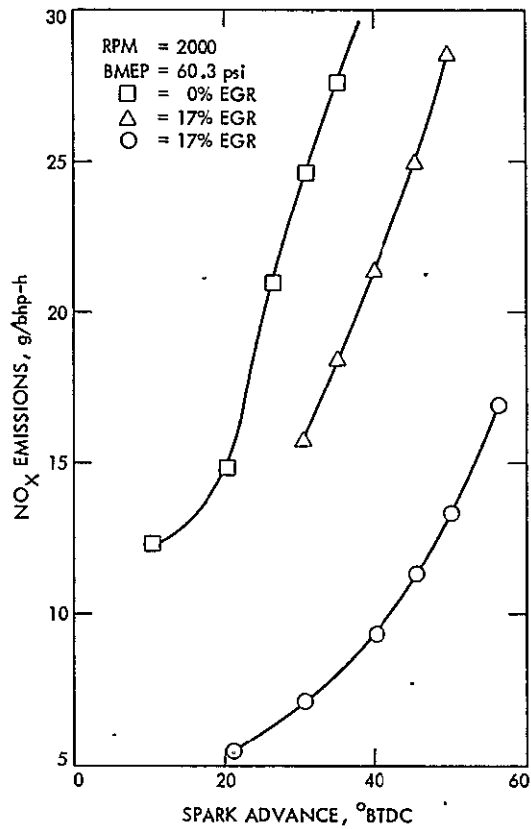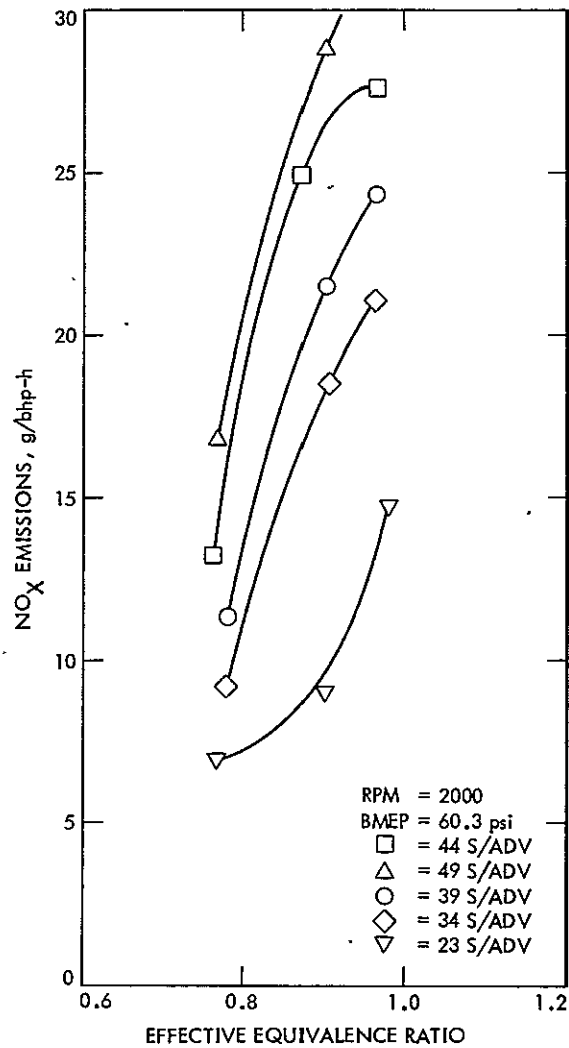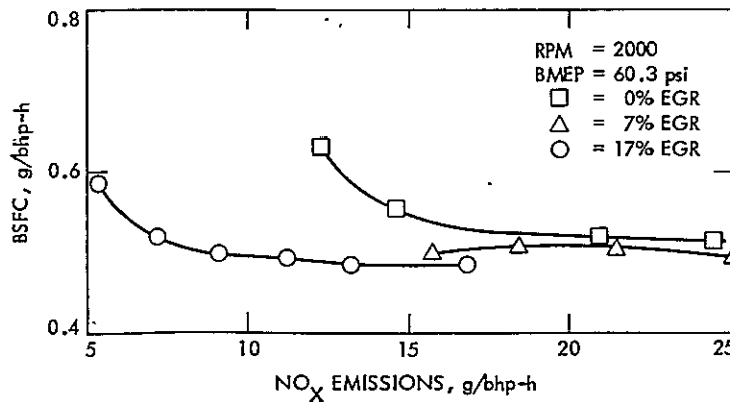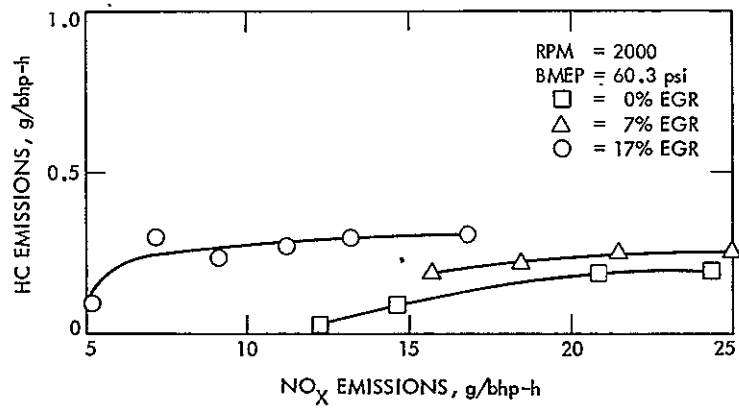

Figure D-12. NO$_x$ Emissions Versus Spark Advance for EGR/Spark Advance Sensitivity Tests - RPM = 1500, BMEP = 40.0 psi

D-11
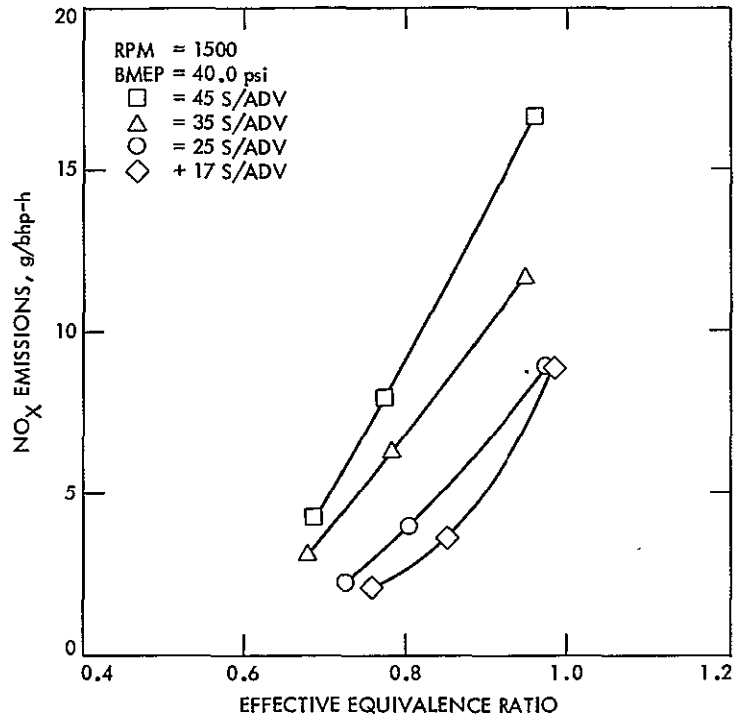
Figure D-13.   NO$_x$ Emissions Versus Effective Equivalence Ratio
for EGR/Spark Advance Sensitivity Tests -
RPM = 1500, BMEP = 40.0 psi
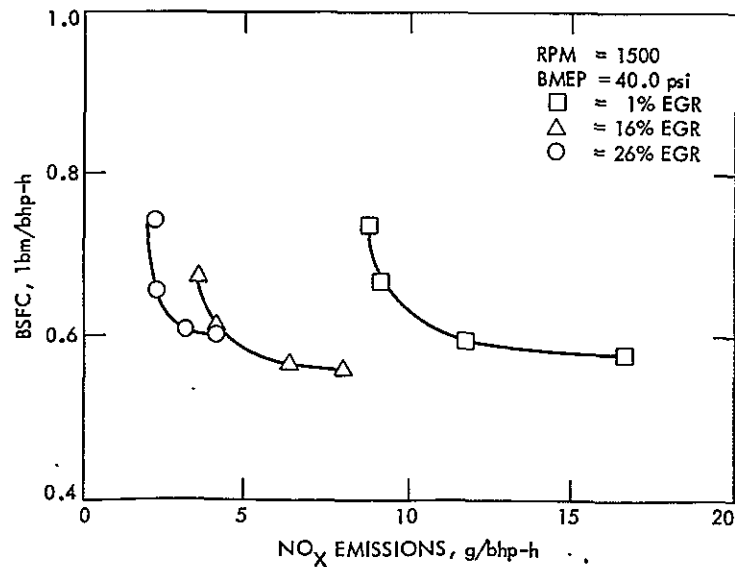
Figure D-14.   Fuel Consumption Versus NO$_x$ Emissions for EGR/Spark
Advance Sensitivity Tests - RPM = 1500, BMEP = 40.0 psi
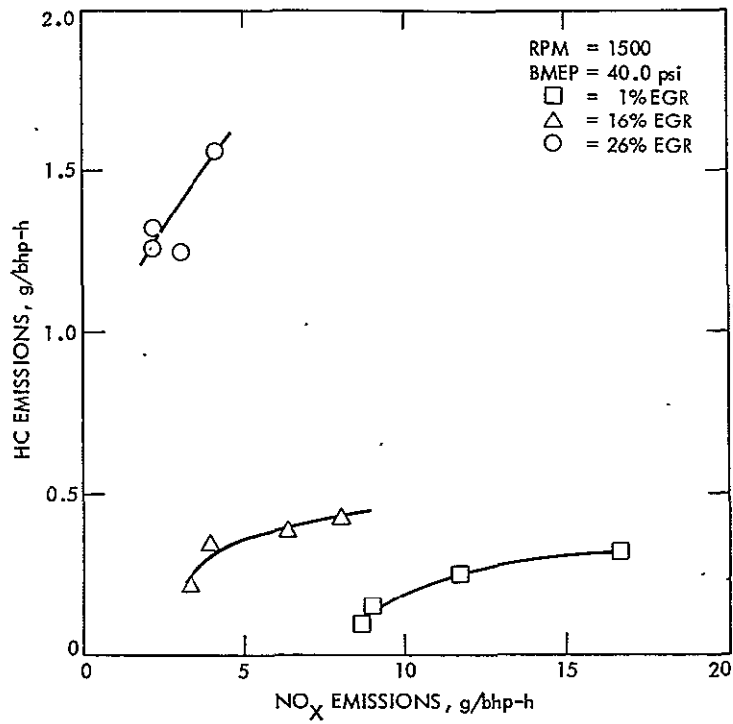
Figure D-15. Fuel Consumption Versus NO_x Emissions for EGR/Spark Advance Sensitivity Tests - RPM = 1500, BMEP = 40.0 psi

Table D-4. EGR/Spark Advance Sensitivity Data for
RPM = 1500 and BMEP = 59.9 psi

Sequence No.	Spark Advance (°BTDC)	% EGR	BSFC (1bm/bhp-h)	Emissions Data*	BSNO$_x$ (g/bhp-h)	BSHC (g/bhp-h)	BSCO (g/bhp-h)	Average T$_{exh}$ (°F)
3110.32	29.1	0	0.491	D	22.54	0.28	0.31	1136
3110.35	28.8	0	0.490	U	24.30	1.91	5.84	1133
3110.38	19.7	0	0.531	D	18.64	0.22	0.27	1189
3110.41	19.1	0	0.530	U	18.67	1.52	4.84	1190
3110.44	9.7	0	0.604	D	14.49	0.11	0.26	1284
3110.47	9.9	0	0.604	U	14.27	0.78	3.87	1283
3110.50	40.2	11	0.489	D	17.32	0.37	0.25	1076
3110.53	40.2	11	0.491	U	19.08	2.31	4.34	1077
3110.56	30.3	12	0.485	D	10.55	0.31	0.25	1108
3110.59	30.9	-11	0.506	U	11.73	2.11	4.91	1108
3111.01	20.2	9	0.523	D	8.60	0.21	0.25	1182
3111.03	21.2	8	0.542	U	8.80	1.72	5.51	1181
3112.08	44.8	20	0.485	D	7.18	0.54	0.73	1048
3112.11	45.0	20	0.489	U	7.18	3.92	8.85	1046
3112.14	36.4	19	0.502	D	5.42	0.51	0.35	1089
3112.17	36.7	19	0.507	U	5.62	3.47	6.73	1090
3112.20	26.4	18	0.532	D	4.75	0.33	0.28	1153
3112.23	26.3	18	0.534	U	4.44	2.47	5.06	1153

*D = downstream of catalytic converter; U = upstream of catalytic converter.
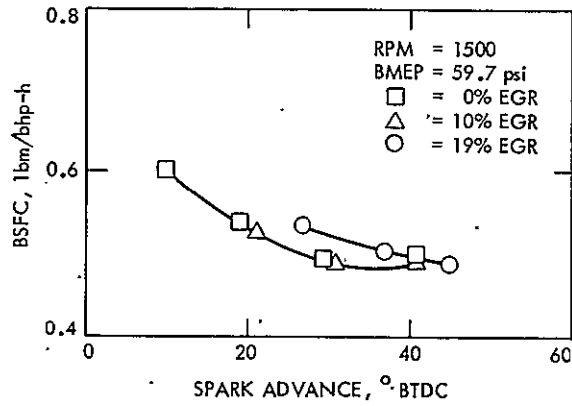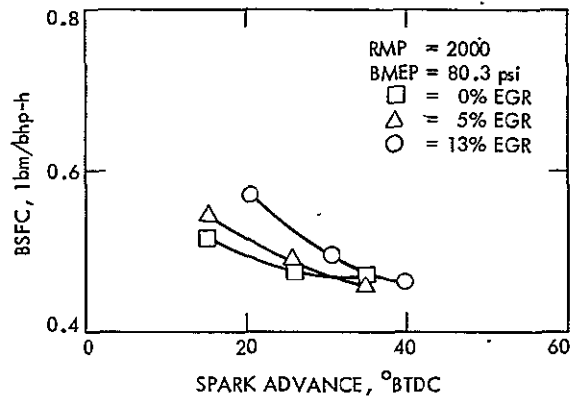
Figure D-16.   Fuel Consumption Versus Spark Advance for EGR/Spark
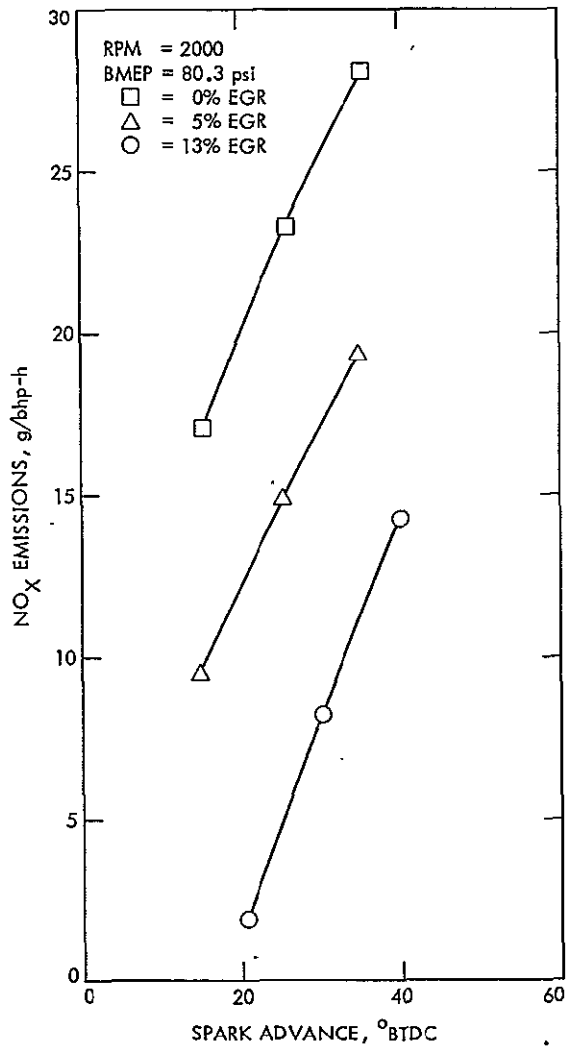Advance Tests - RPM = 1500, BMEP = 59.7 psi

Figure D-17. NO_x Emissions Versus Spark Advance for EGR/Spark
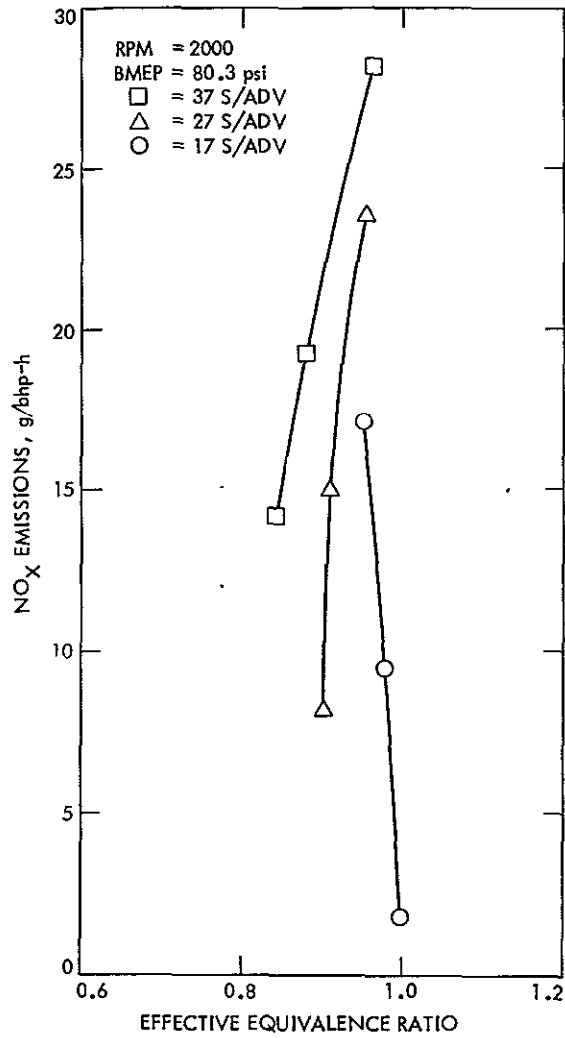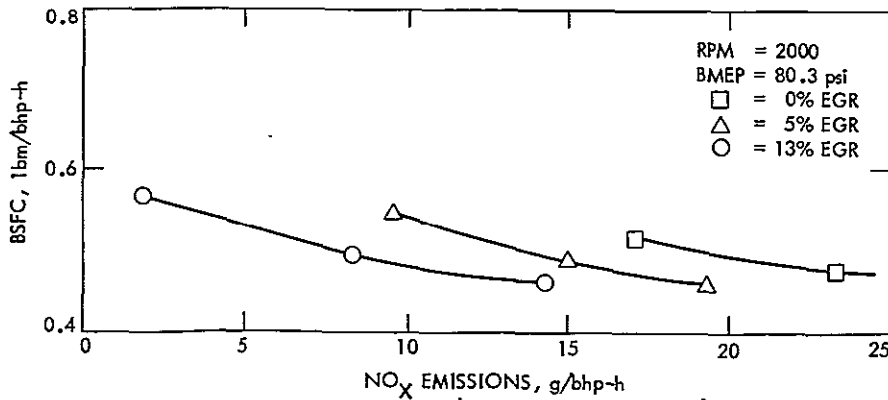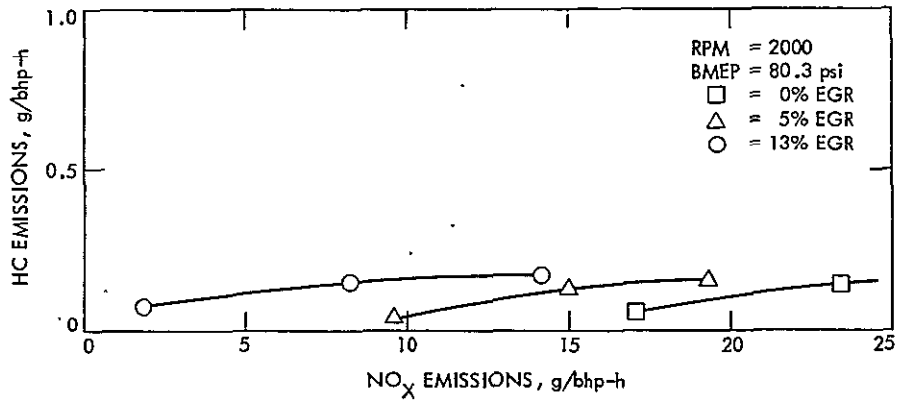Advance Sensitivity Tests - RPM = 1500, BMEP = 59.7 psi

Figure D-18. NO$_x$ Emissions Versus Effective Equivalence Ratio for EGR/Spark Advance Sensitivity Tests - RPM = 1500, BMEP = 59.7 psi

Figure D-19. Fuel Consumption Versus NO$_x$ Emissions for EGR/Spark Advance Sensitivity Tests - RPM = 1500, BMEP = 59.7 psi

Figure D-20. Fuel Consumption Versus NO_x Emissions for EGR/Spark
Advance Sensitivity Tests – RPM = 1500, BMEP = 59.7 psi

Table D-5. EGR/Spark Advance Sensitivity Data for
RPM = 2000 and BMEP = 60 psi

Sequence No.	Spark Advance (°BTDC)	% EGR	BSFC (lbm/bhp-h)	Emissions Data*	$BSNO_x$ (g/bhp-h)	BSHC (g/bhp-h)	BSCO (g/bhp-h)	Average T_{exh} (°F)
2093.04	40.4	0	0.506	D	30.93	0.24	0.24	1189
3093.01	35.0	0	0.511	D	27.54	0.22	0.22	1203
2093.06	30.7	0	0.513	D	24.34	0.20	0.22	1219
2093.08	25.7	0	0.519	D	20.90	0.18	0.23	1244
3159.54	20.5	0	0.552	D	14.62	0.08	0.11	
3158.54	20.5	0	0.552	U	14.52	0.58	5.13	
3159.51	10.2	0	0.634	D	12.15	0.03	0.10	
3158.51	10.2	0	0.634	U	12.18	0.20	3.96	
2093.12	50.1	7	0.515	D	28.73	0.26	0.26	1153
2093.10	45.6	7	0.494	D	24.89	0.25	0.26	1159
2093.14	40.3	7	0.505	D	21.41	0.24	0.24	1168
2093.16	35.3	7	0.509	D	18.44	0.22	0.25	1184
2093.18	30.5	6	0.499	D	15.69	0.18	0.26	1210
3161	27.5	7	0.531	D	12.86	0.18	0.17	1242
3160.09	27.5	7	0.531	U	11.76	1.09	6.85	1242
3161	16.8	6	0.600	D	8.99	0.05	0.14	1338
3160.06	16.8	6	0.600	U	8.09	0.31	5.70	1338
2094.24	50.7	10	0.492	D	24.09	0.27	0.24	1137
2094.22	45.6	11	0.489	D	20.81	0.24	0.23	1155
2094	40.7	10	0.499	D	17.50	0.23	0.23	1169
2094	35.2	10	0.492	D	14.37	0.21	0.23	1186
2093.20	50.5	17	0.485	D	13.18	0.30	0.24	1114
2093.26	40.6	16	0.497	D	9.09	0.24	0.23	1153
3161	31.0	17	0.520	D	7.14	0.29	0.17	1207
3160.15	31.0	17	0.520	U	6.38	1.80	6.54	1207
3161.15	20.9	16	0.567	D	5.31	0.10	0.19	1287
3160.12	20.9	16	0.587	U	4.79	0.72	7.94	1287
2094.08	55.1	19	0.485	D	14.11	0.32	0.22	1103
2094	55.5	19	0.478	D	15.70	0.32	0.19	1100
2094.06	50.8	19	0.483	D	12.20	0.32	0.23	1116
2094.14	50.8	19	0.486	D	12.92	0.30	0.20	1115
2094.10	45.6	19	0.490	D	10.28	0.28	0.22	1134
2094	45.7	19	0.488	D	10.43	0.28	0.20	1131
2094.12	40.8	19	0.491	D	8.81	0.25	0.23	1146
2094	40.7	19	0.497	D	9.02	0.25	0.20	1158

*D = downstream of catalytic converter; U = upstream of catalytic converter.
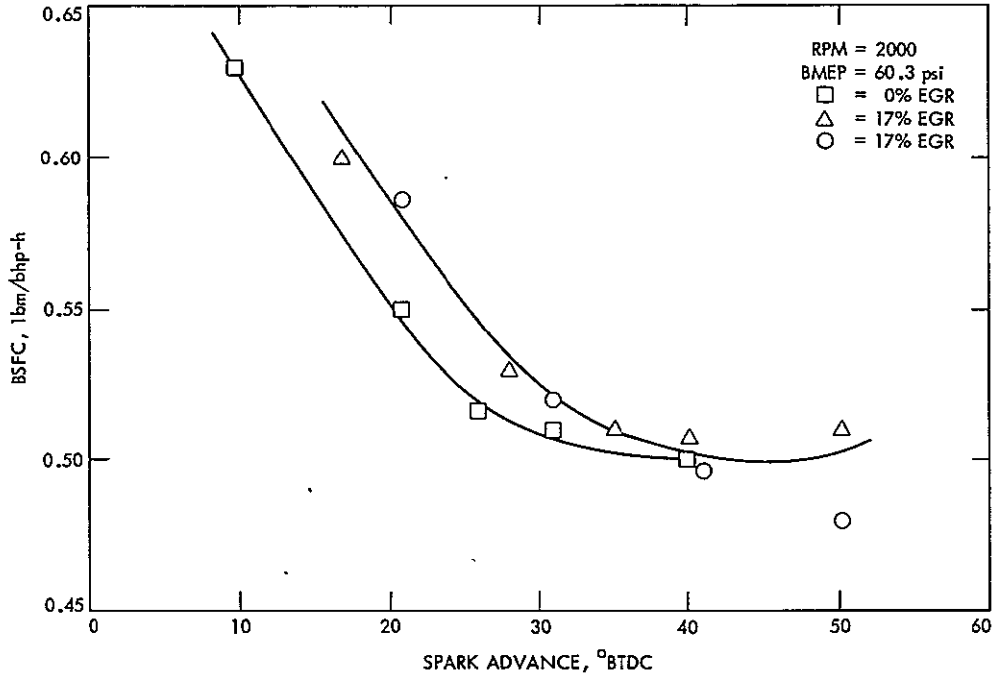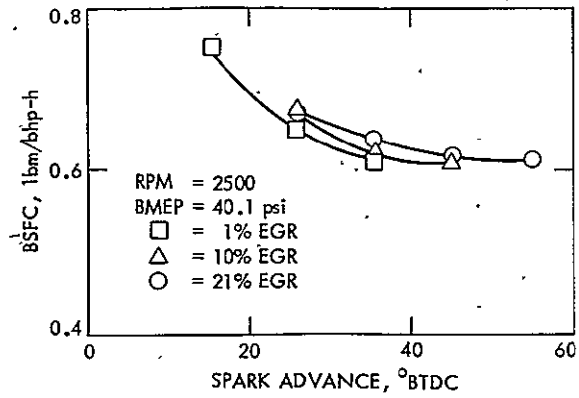
Figure D-21. Fuel Consumption Versus Spark Advance for EGR/Spark
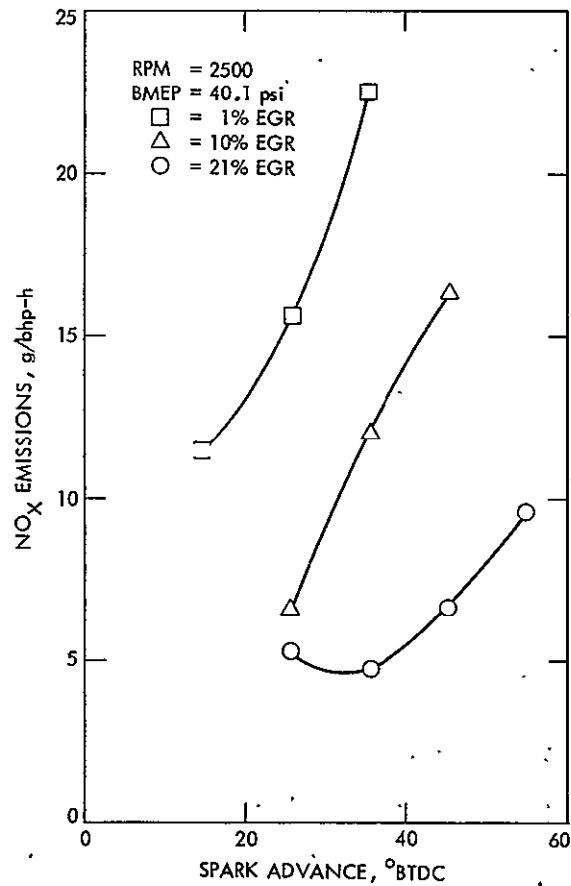Advance Tests - RPM = 2000, BMEP = 60.3 psi

Figure D-22. NO_x Emissions Versus Spark Advance for EGR/Spark
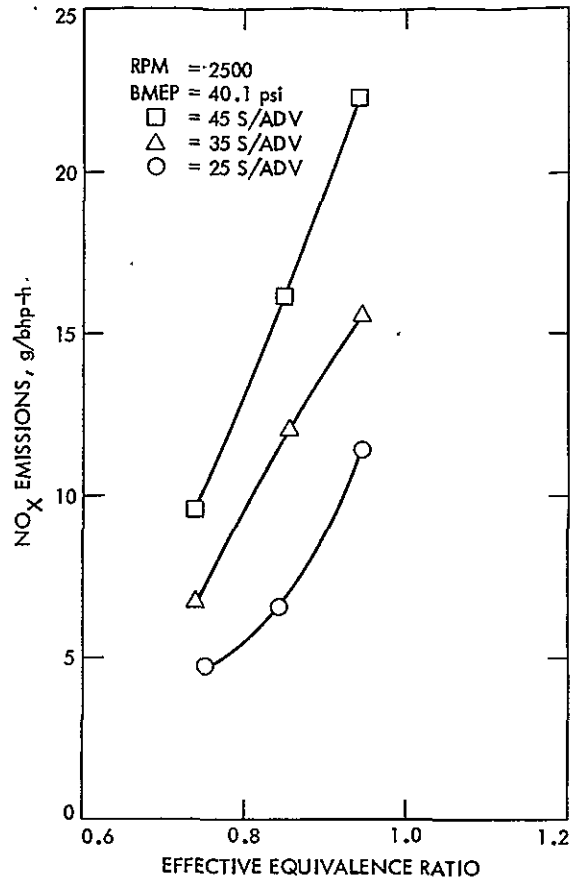Advance Sensitivity Tests - RPM = 2000, BMEP = 60.3 psi

Figure D-23. NOₓ Emissions Versus Effective Equivalence Ratio for EGR/Spark Advance Sensitivity Tests - RPM = 2000, BMEP = 60.3 psi
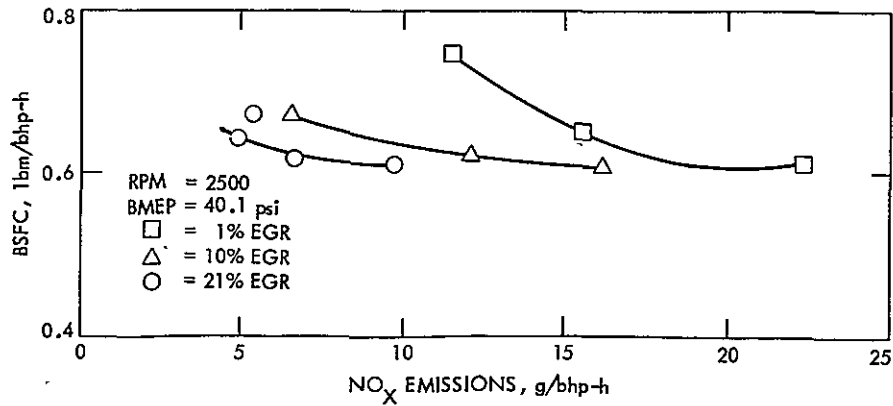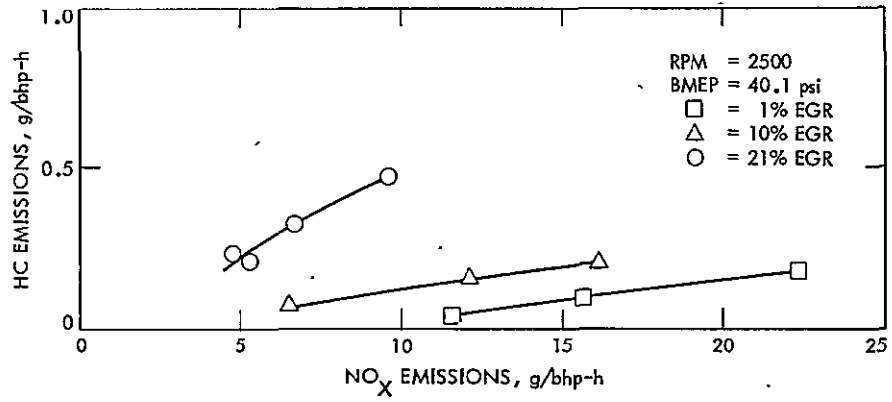

Figure D-24. Fuel Consumption Versus NOₓ Emissions for EGR/Spark Advance Sensitivity Tests - RPM = 2000, BMEP = 60.3 psi

Figure D-25. Fuel Consumption Versus NO_x Emissions for EGR/Spark
Advance Sensitivity Tests – RPM = 2000, BMEP = 60.3 psi

Table D-6. EGR/Spark Advance Sensitivity Data for
RPM = 2000 and BMEP = 80.3 psi

Sequence No.	Spark Advance (°BTDC)	% EGR	BSFC (lbm/bhp-h)	Emissions Data*	BSNO$_x$ (g/bhp-h)	BSHC (g/bhp-h)	BSCO (g/bhp-h)	Average T$_{exh}$ (°F)
3108.32	35.1	0	0.468	D	28.06	0.17	0.23	1221
4109.01	35.2	0	0.465	U	28.90	1.32	2.53	1223
3109.05	25.9	0	0.474	D	23.34	0.15	0.21	1262
3109.08	25.7	0	0.467	U	23.69	0.97	7.54	1261
3109.11	15.1	0	0.517	D	17.08	0.06	0.21	1347
3109.14	14.8	0	0.517	U	18.11	0.34	6.80	1348
3109.17	34.7	6	0.457	D	19.25	0.16	0.24	1214
3109.20	35.0	6	0.454	U	20.52	1.25	2.69	1212
4110.01	25.5	5	0.485	D	14.98	0.13	0.50	1268
3110.05	25.6	5	0.482	U	15.81	0.82	3.11	1272
3110.08	15.0	.5	0.547	D	9.53	0.03	0.38	1376
3110.11	15.1	4	0.538	U	10.12	0.16	5.95	1373
3110.14	39.8	13	0.460	D	14.21	0.18	0.44	1190
3110.17	39.7	13	0.466	U	13.96	1.44	10.45	1190
3110.20	30.3	13	0.494	D	8.21	0.15	0.95	1238
3110.23	30.1	13	0.483	U	8.41	1.04	25.10	1239
3110.26	20.7	12	0.570	D	1.81	0.08	12.40	1280
3110.29	21.0	12	0.571	U	3.19	0.64	74.25	1292

*D = downstream of catalytic converter; U = upstream of catalytic converter.
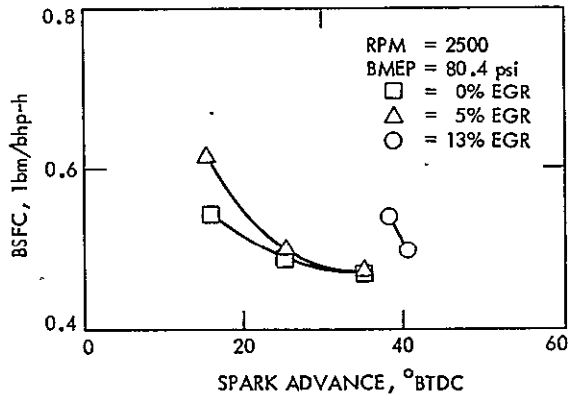
Figure D-26. Fuel Consumption Versus Spark Advance for EGR/Spark Advance Tests – RPM = 2000, BMEP = 80.3 psi
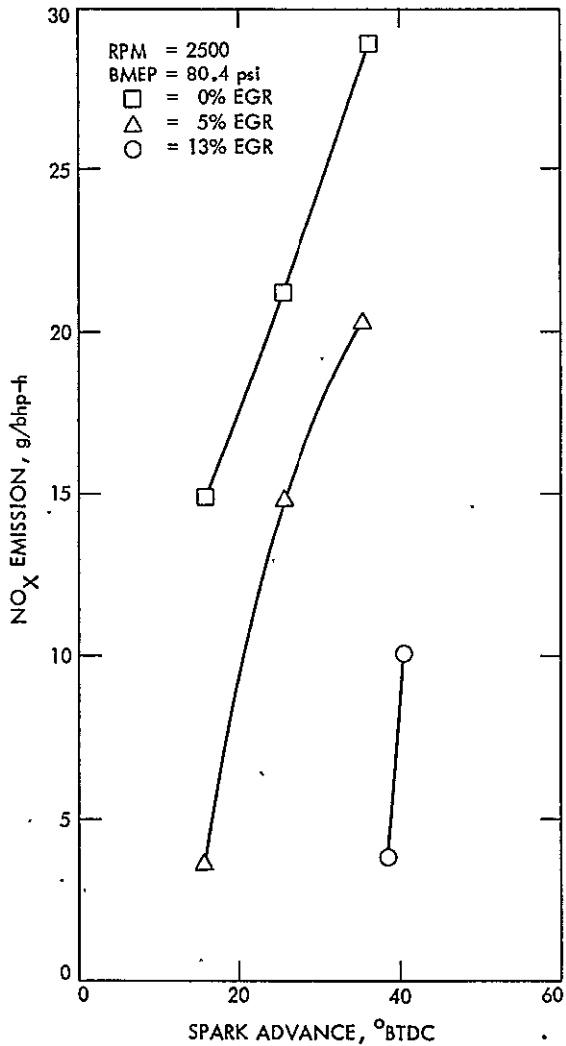

Figure D-27. NO_x Emissions Versus Spark Advance for EGR/Spark Advance Sensitivity Tests – RPM = 2000, BMEP = 80.3 psi
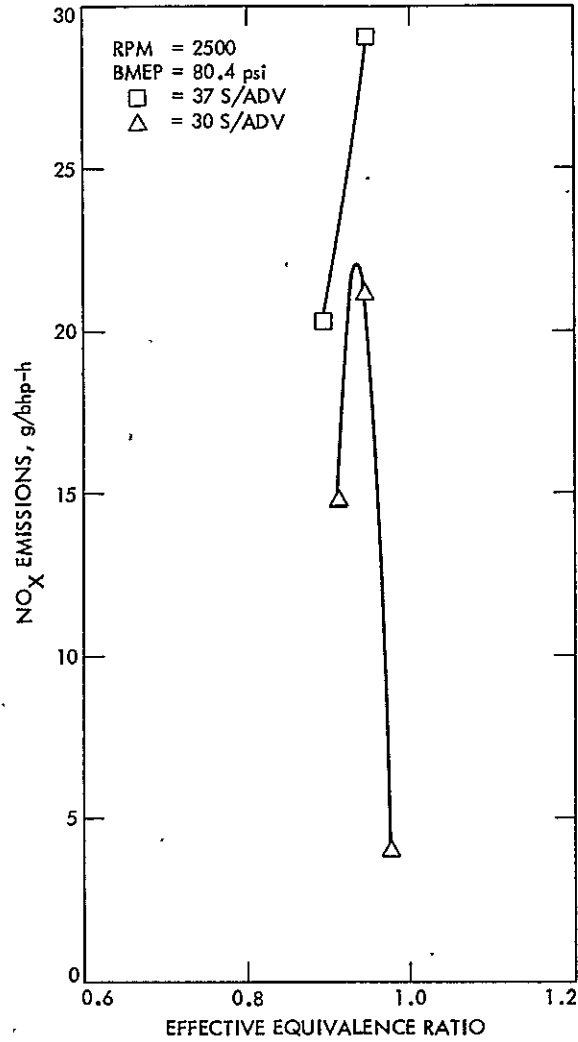
D-23

Figure D-28. NO_x Emissions Versus Effective Equivalence Ratio for EGR/ Spark Advance Sensitivity Tests - RPM = 2000, BMEP = 80.3 psi

Figure D-29. Fuel Consumption Versus NO_x Emissions for EGR/Spark Advance Sensitivity Tests - RPM = 2000, BMEP = 80.3 psi

Figure D-30. Fuel Consumption Versus NO_x Emissions for EGR/Spark
Advance Sensitivity Tests - RPM = 2000, BMEP = 80.3 psi

Table D-7. EGR/Spark Advance Sensitivity Data for
RPM = 2500 and BMEP = 40 psi

Sequence No.	Spark Advance (°BTDC)	% EGR	BSFC (lbm/bhp-h)	Emissions Data*	$BSNO_x$ (g/bhp-h)	BSHC (g/bhp-h)	BSCO (g/bhp-h)	Average T_{exh} (°F)
4107.01	35.4	1	0.612	D	22.34	0.17	0.29	1287
3107.05	35.5	1	0.612	U	22.59	0.84	4.10	1289
3107.08	25.9	1	0.647	D	15.59	0.09	0.24	1349
3107.11	25.9	1	0.653	U	15.58	0.52	9.02	1351
3107.14	14.9	0	0.748	D	11.47	0.04	0.21	1463
3107.17	15.0	0	0.749	U	11.26	0.23	5.90	1460
3107.20	45.2	12	0.608	D	16.15	0.20	0.28	1226
3107.23	45.4	11	0.606	U	17.48	1.24	3.87	1223
3107.26	35.5	10	0.619	D	12.06	0.15	0.28	1266
3107.29	35.4	10	0.624	U	12.33	0.93	3.77	1270
3108.08	25.5	10	0.670	D	6.50	0.06	0.02	1348
3108.11	25.6	9	0.689	U	6.70	0.61	0.01	1350
3108.14	55.0	23	0.609	D	9.59	0.46	0.37	1178
3108.17	55.1	23	0.609	U	10.10	3.40	5.53	1175
3108.20	45.2	22	0.613	D	6.61	0.32	0.36	1207
3108.23	45.1	22	0.615-	U	6.43	2.36	5.12	1207
3108.26	35.1	20	0.638	D	4.73	0.23	0.33	1269
3108.29	35.2	20	0.643	U	4.84	1.79	4.54	1271
3161.18	25.5	19	0.672	D	5.23	0.22	0.23	1301
3160.18	25.5	19	0.672	U	4.79	1.54	10.23	1301

*D = downstream of catalytic converter; U = upstream of catalytic converter.
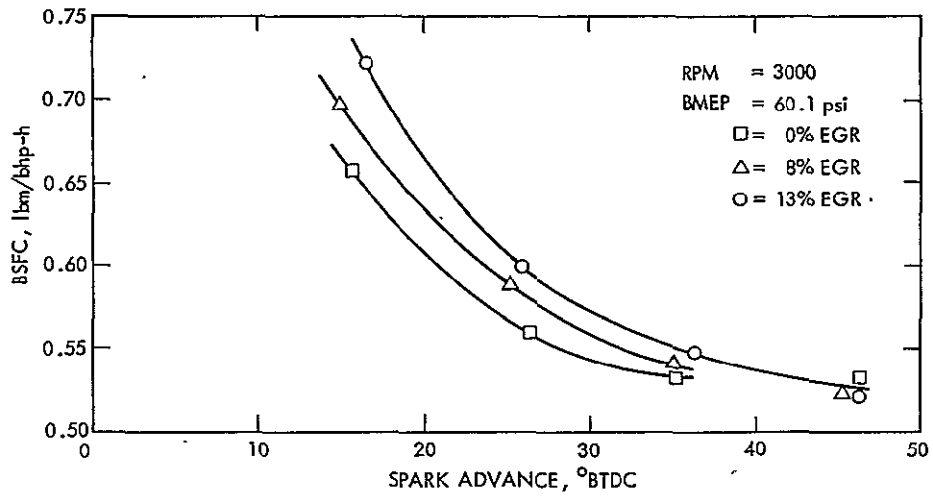
Figure D-31. Fuel Consumption Versus Spark Advance for EGR/Spark
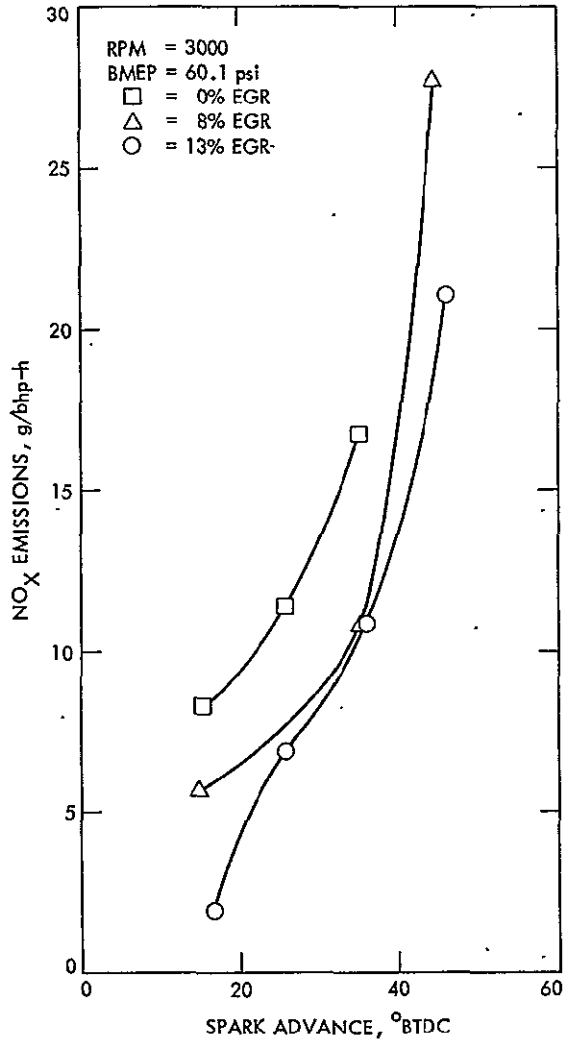Advance Tests - RPM = 2500, BMEP = 40.1 psi

Figure D-32. NO_x Emissions Versus Spark Advance for EGR/Spark Advance
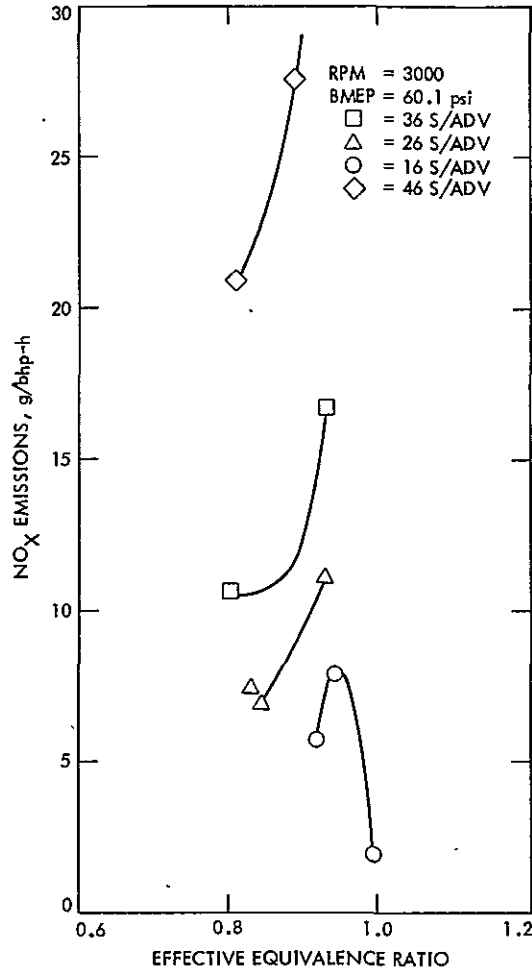Sensitivity Tests - RPM = 2500, BMEP = 40.1 psi

Figure D-33. NO$_x$ Emissions Versus Effective Equivalence Ratio for EGR/ Spark Advance Sensitivity Tests – RPM = 2500, BMEP = 40.1 psi
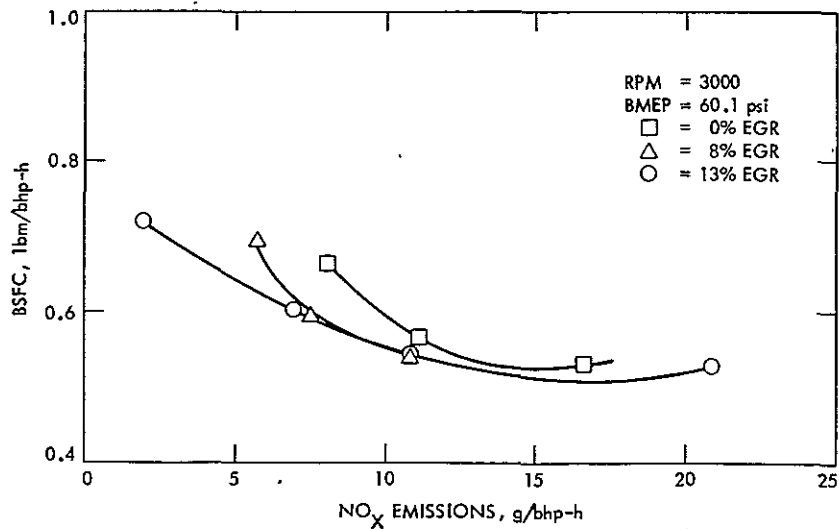

Figure D-34. Fuel Consumption Versus NO$_x$ Emissions for EGR/Spark Advance Sensitivity Tests – RPM = 2500, BMEP = 40.1 psi
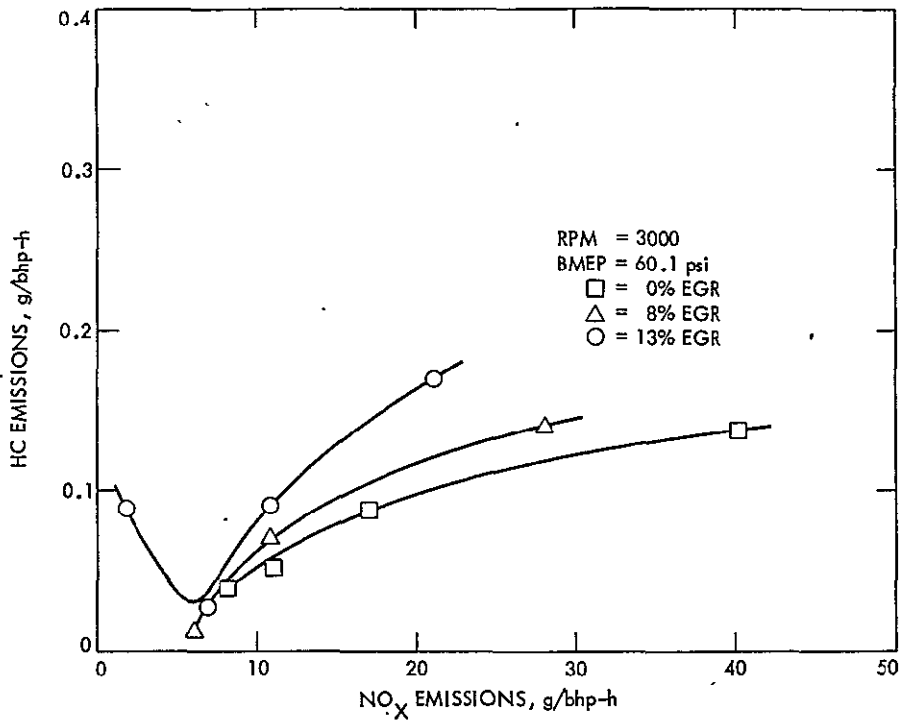
Figure D-35. Fuel Consumption Versus NO_x Emissions for EGR/Spark Advance Sensitivity Tests – RPM = 2500, BMEP = 40.1 psi

Table D-8. EGR/Spark Advance Sensitivity Data for
RPM = 2500 and BMEP = 80 psi

Sequence No.	Spark Advance (°BTDC)	% EGR	BSFC (1bm/bhp-h)	Emissions Data*	$BSNO_x$ (g/bhp-h)	BSHC (g/bhp-h)	BSCO (g/bhp-h)	Average T_{exh} (°F)
3119.10	35.7	0	0.473	D	28.97	0.12	0.20	1311
3119.13	35.7	0	0.472	U	28.95	0.69	5.68	1313
3119.16	25.4	0	0.488	D	21.27	0.06	0.20	1371
3119.19	25.5	0	0.487	U	21.55	0.37	5.66	1368
3104.10	16.0	0	0.547	D	15.01	0.02	0.21	1495
4120.01	15.9	0	0.544	U	15.71	0.09	5.37	1490
3120.05	35.4	6	0.472	D	20.37	0.12	0.28	1300
3120.08	35.5	5	0.475	U	21.02	0.69	3.10	1301
3120.11	25.8	5	0.495	D	14.88	0.05	0.27	1382
3120.14	25.4	4	0.500	U	15.66	0.29	2.49	1374
3120.17	15.3	4	0.615	D	3.42	0.12	33.61	1497
3120.20	40.4	12	0.497	D	10.07	0.12	1.65	1269
3120.23	40.3	12	0.502	U	9.84	0.72	39.69	1269
4105.01	38.6	14	0.533	U	6.27	0.94	95.36	1269

*D = downstream of catalytic converter; U = upstream of catalytic converter.

Figure D-36.   Fuel Consumption Versus Spark Advance for EGR/Spark
Advance Tests - RPM = 2500, BMEP = 80.4 psi

Figure D-37. NO_x Emissions Versus Spark Advance for EGR/Spark Advance
Sensitivity Tests - RPM = 2500, BMEP = 80.4 psi

D-31

Figure D-38. NO_x Emissions Versus Effective Equivalence Ratio for EGR/Spark Advance Sensitivity Tests - RPM = 2500, BMEP = 80.4 psi
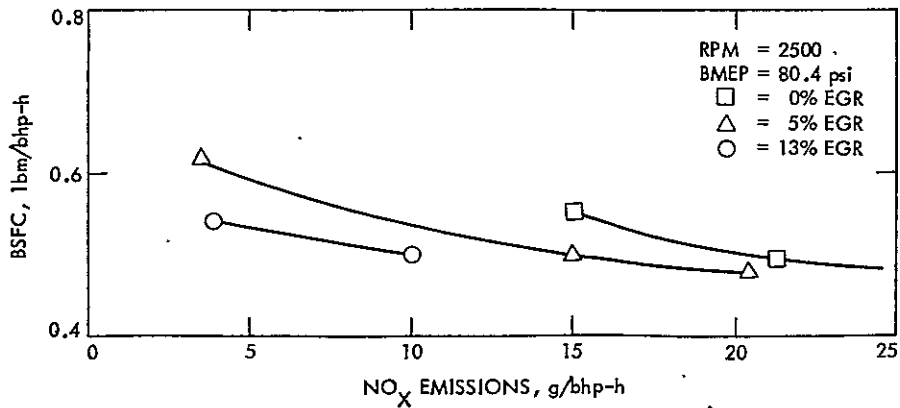
Figure D-39. Fuel Consumption Versus NO_x Emissions for EGR/Spark Advance Sensitivity Tests - RPM = 2500., BMEP = 80.4 psi

D-32
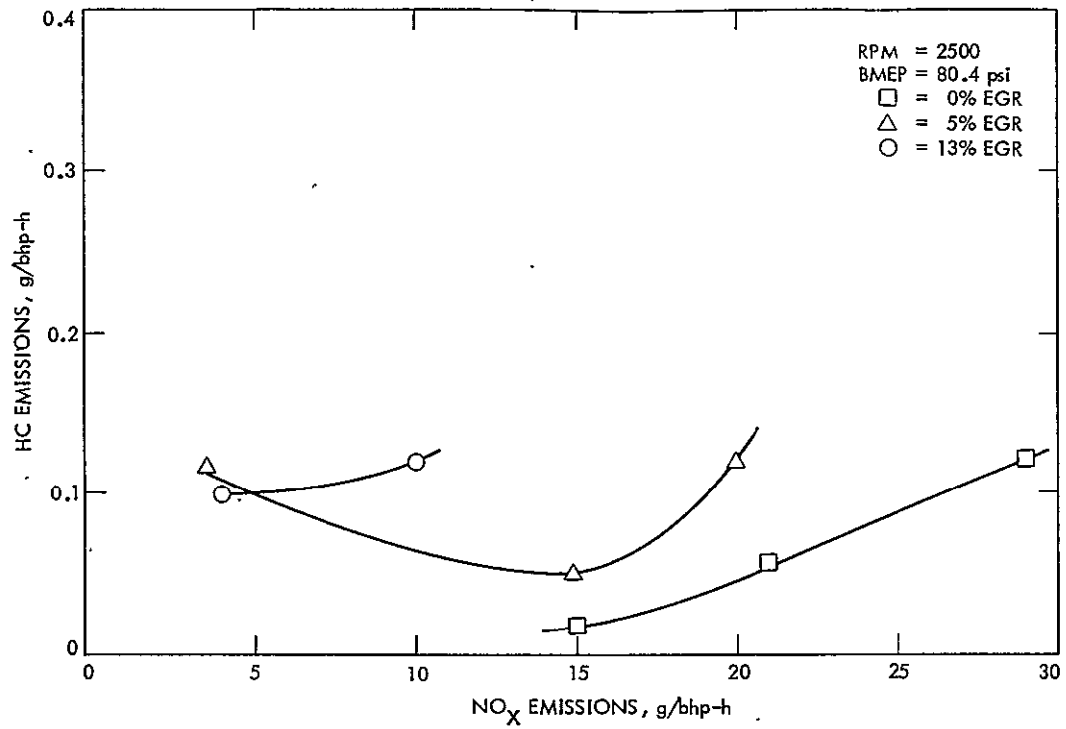
Figure D-40. Fuel Consumption Versus NO_x Emissions for EGR/Spark Advance Sensitivity Tests - RPM = 2500, BMEP = 80.4 psi

Table D-9. EGR/Spark Advance Sensitivity Data for
RPM = 3000 and BMEP = 60 psi

Sequence No.	Spark Advance (°BTDC)	% EGR	BSFC (1bm/bhp-h)	Emissions Data*	BSNO$_x$ (g/bhp-h)	BSHC (g/bhp-h)	BSCO (g/bhp-h)	Average T$_{exh}$ (°F)
3161.30	45.8	0	0.532	D	39.86	0.14	0.18	1329
3160.30	45.8	0	0.532	U	37.72	0.78	5.71	1329
3112.26	35.4	0	0.529	D	16.69	0.09	0.23	1370
3112.29	36.0	0	0.529	U	21.28	0.59	2.92	1370
3112.32	25.8	0	0.565	D	11.15	0.05	0.20	1449
3112.35	25.8	0	0.563	U	14.66	0.23	2.21	1446
3112.38	15.4	0	0.665	D	7.95	0.04	0.15	1498
3112.40	15.6	0	0.662	U	12.41	0.06	1.43	1498
3161.33	44.6	6	0.526	D	27.64	0.14	0.21	1306
3160.33	44.6	6	0.526	U	25.75	0.82	7.52	1306
3112.43	35.4	7	0.542	D	10.62	0.07	0.24	1498
3112.46	35.4	7.	0.544	U	13.75	0.48	3.22	1498
3112.49	25.2	11	0.590	D	7.35	0.03	0.18	
3112.52	25.2	13	0.584——	U	9.46	0.20	4.81	
3112.55	14.8	7	0.696	D	5.67	0.01	0.24	
3112.58	15.1	4	1.562	U	9.05	0.02	5.36	
3161.36	46.3	14	0.525	D	20.88	0.17	0.19	1262
3160.36	46.3	14	0.525	U	19.37	0.93	5.98	1262
3114.08	36.0	13	0.544	D	10.71	0.09	0.27	1351
3114.23	35.7	13	0.540	U	10.78	0.49	3.59	1351
3114.11	25.8	12	0.602	D	6.86	0.03	0.28	1454
3114.20	25.2	12	0.600	U	6.95	0.17	3.51	1452
3114.14	16.7	12	0.723	D	1.88	0.09	31.70	1533
3114.17	16.7	12	0.714	U	2.41	0.26	60.11	1521

*D = downstream of catalytic converter; U = upstream of catalytic converter.

Figure D-41. Fuel Consumption Versus Spark Advance for EGR/Spark
Advance Tests – RPM = 3000, BMEP = 60.1 psi

Figure D-42. NO$_x$ Emissions Versus Spark Advance for EGR/Spark Advance
Sensitivity Tests – RPM = 3000, BMEP = 60.1 psi

D-35

Figure D-43. NO_x Emissions Versus Effective Equivalence Ratio for EGR/Spark Advance Sensitivity Tests - RPM = 3000, BMEP = 60.1 psi

Figure D-44. Fuel Consumption Versus NO_x Emissions for EGR/Spark Advance Sensitivity Tests - RPM = 3000, BMEP = 60.1 psi

Figure D-45.   Fuel Consumption Versus NO$_x$ Emissions for EGR/Spark
Advance Sensitivity Tests - RPM = 3000, BMEP =
60.1 psi

APPENDIX E

EGR/SPARK ADVANCE STRATEGIES

Table E-1. Engine Dynamometer Data Used for EGR/SA Strategy No. 1

Sequence No.	RPM	BMEP (psi)	Spark Advance (°BTDC)	P_{man} ("Hg vac.)
115.10	1000	30	30	15.9
105.11	1500	20	30	17.4
159.088	1500	40	35	13.8
110.32	1500	60	30	10.0
103.14	2000	40	25	13.2
93.04	2000	60	40	9.7
109.1	2000	80	35	6.5
107.01	2500	40	35	13.8
119.10	2500	80	35	6.0
112.26	3000	60	35	9.4
114.26	750	0	35	21.3

This strategy is for zero EGR.

Table E-2. Engine Dynamometer Data Used for EGR/SA Strategy No. 2

Sequence No.	RPM	BMEP (psi)	Spark Advance (°BTDC)	Percent EGR	Percent Poppet Position*	P_{man} ("Hg vac.)	P_{exh} (psia)
115.37	1000	30	40	28	12	11.2	14.24
159.456	1500	20	30	17	3	17.3	14.42
159.308	1500	40	50	29	71	7.7	14.30
112.8	1500	60	45	20	78	4.6	14.64
103.34	2000	40	50	25	69	8.3	14.53
94.12	2000	60	40	19	93	5.0	14.86
110.20	2000	80	30	13	77	2.5	14.40
108.20	2500	40	45	22	74	9.2	14.86
120.11	2500	80	35	5	10	3.3	16.99
112.43	3000	60	35	7	14	7.0	16.70
114.26	750	0	25	23	2	21.3	14.18

*Refers to percent of full poppet travel in EGR valve.

Table E-3. Engine Dynamometer Data Used for EGR/SA Strategy No. 3

Sequence No.	RPM	BMEP (psi)	Spark Advance (°BTDC)	Percent EGR	Percent Poppet Position*	P_{man} ("Hg vac.)	P_{exh} (psia)
115.37	1000	30	40	28	12	11.2	14.24
116.16	1500	20		26	2	16.9	14.56
159.338	1500	40		28	69	7.2	14.34
112.14	1500	60		19	78	4.4	14.73
119.01	2000	40		23	65	8.1	14.64
161.15	2000	60		17	97	4.6	14.93
110.26	2000	80		12	75	1.2	16.02
108.26	2500	40		20	75	8.5	15.03
120.11	2500	80		5	10	3.3	16.98
112.49	3000	60		11	12	5.5	17.35
114.26	750	0	25	23	2	21.3	14.18

*Refers to percent of full poppet travel in EGR valve.

Table E-4. Engine Dynamometer Data Used for EGR/SA Strategy No. 4

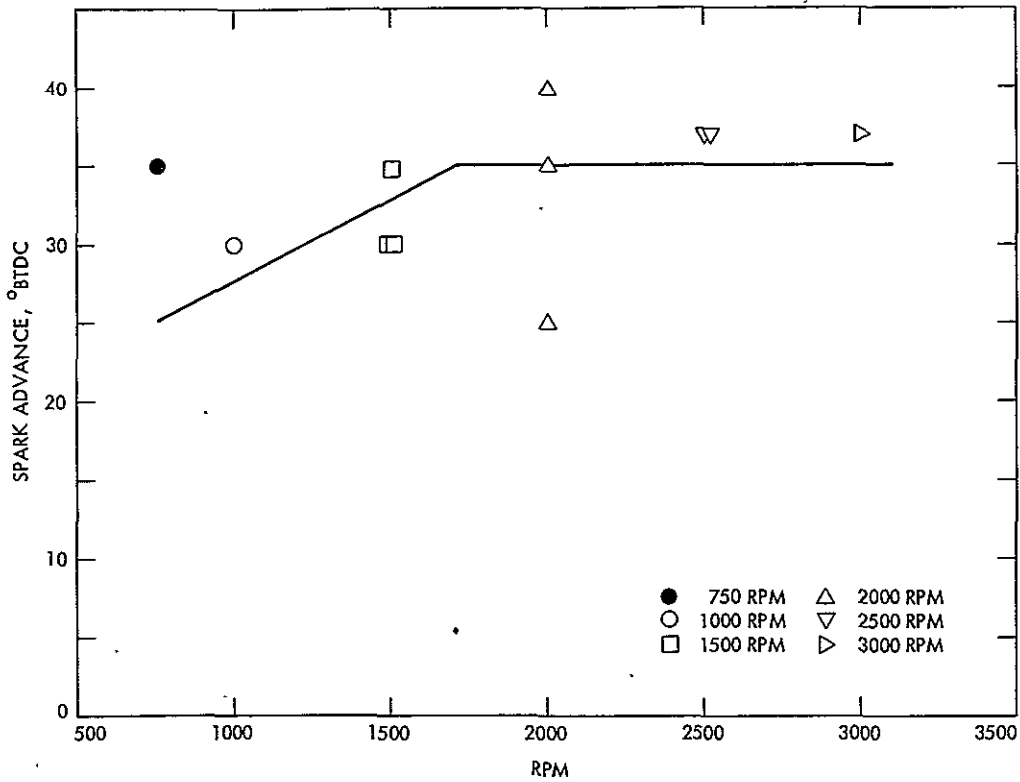| Sequence No.	RPM	BMEP (psi)	Spark Advance (°BTDC)	Percent EGR	Percent Poppet Postion*	P_{man} ("Hg vac.)	P_{exh} (psia)
115.43	1000	30	20	22	11	9.8	14.28
116.40	1500	20	30	46	15	13.3	14.48
159.368	1500	40	30	25	72	6.6	14.45
112.20	1500	60	25	18	76	4.0	14.85
119.06	2000	40	30	21	72	7.1	14.78
161.15	2000	60	20	16	98	3.3	15.19
110.26	2000	80	20	12	75	1.2	16.02
108.26	2500	40	35	20	75	8.5	15.03
120.17	2500	80	15	4	9	1.8	17.90
114.14	3000	60	15	12	69	2.1	17.50
115.02	750	0	25		14	13.5	14.05

*Refers to percent of full poppet travel in EGR valve.

Table E-5. Engine Dynamometer Data Used for EGR/SA Strategy No. 5

Sequence No.	RPM	BMEP (psi)	Spark Advance (°BTDC)	Percent EGR	Percent Poppet Position*	P_{man} ("Hg vac.)	P_{exh} (psia)
115.43	1000	30	20	22	11	9.8	14.28
116.40	1500	20	30	46	15	13.3	14.48
159.368	1500	40	30	25	72	6.6	14.45
112.20	1500	60	25	18	76	4.0	14.85
119.06	2000	40	30	21	72	7.1	14.78
161.15	2000	60	20	16	98	3.3	15.19
110.26	2000	80	20	12	75 ·	1.2	16.02
108.26	2500	40	35	20	75	8.5	15.03
120.17	2500	80	15	4	9	1.8	17.90
114.14	3000	60	15	12	69	2.1	17.50
115.02	750	0	25		14	13.5	14.05

*Refers to percent of full poppet travel in EGR valve.

Table E-6. Engine Dynamometer Data Used for Implementation of EGR/SA Strategy No. 6

Sequence No.	RPM	BMEP (psi)	Spark Advance (°BTDC)	Percent EGR	Percent Poppet Position*	P_{man} ("Hg vac.)	P_{exh} (psia)
115.43	1000	30	20	22	11	9.8	14.28
106.40	1500	20	29	47	15	8.3	14.48
159.36	1500	40	32	25	72	6.6	14.45
112.30	1500	60	26	18	76	4.0	14.85
119.06	2000	40	30	21	72	7.1	14.78
161.15	2000	60	21	16	98	3.3	15.19
110.26	2000	80	21	12	75	1.2	16.03
108.26	2500	40	35	20	75	8.5	15.03
120.17	2500	80	15	4	9	1.8	17.90
114.14	3000	60	17	12	69	2.1	17.50
115.02	750	0	25		14	13.5	14.05

*Refers to percent of full poppet travel in EGR valve.

Table E-7. Engine Dynamometer Data Used for EGR/SA Strategy No. 7

Sequence No.	RPM	BMEP (psi)	Spark Advance (°BTDC)	Percent EGR	Percent Poppet Position*	P_{man} ("Hg vac.)	P_{exh} (psia)
115.43	1000	30	20	22	11	9.8	14.28
116.40	1500	20	30	46	15	13.3	14.48
159.368	1500	40	30	25	72	6.6	14.45
112.20	1500	60	25	18	76	4.0	14.85
119.06	2000	40	30	21	72	7.1	14.78
161.15	2000	60	20	16	98	3.3	15.19
110.26	2000	80	20	12	75	1.2	16.02
108.26	2500	40	35	20	75	8.5	15.03
120.17	2500	80	15	4	9	1.8	17.90
114.14	3000	60	15	12	69	2.1	17.50
115.02	750	0	25		14	·13.5	14.05

*Refers to percent of full poppet travel in EGR valve.

Table E-8. Engine Dynamometer Data Used for EGR/SA Strategy No. 8

Sequence No.	RPM	BMEP (PSI)	Spark Advance (°BTDC)	Percent EGR	Percent Poppet Position*	P_{man} ("Hg vac.)	P_{exh} (psia)
115.43	1000	30	20	22	11	9.8	14.28
116.40	1500	20	30	46	15	13.3	14.48
159.368	1500	40	30	25	72	6.6	14.45
112.20	1500	60	25	18	76	4.0	14.85
119.06	2000	40	30	21	72	7.1	14.78
161.15	2000	60	20	16	98	3.3	15.19
110.26	2000	80	20	12	75	1.2	16.02
108.26	2500	40	35	20	75	8.5	15.03
120.17	2500	80	15	4	9	1.8	17.90
114.14	3000	60	15	12	69	2.1	17.50
115.02	750	0	25		14	13.5	14.05

*Refers to percent of full poppet travel in EGR valve.

Figure E-1. EGR/Spark Advance Strategy No. 1
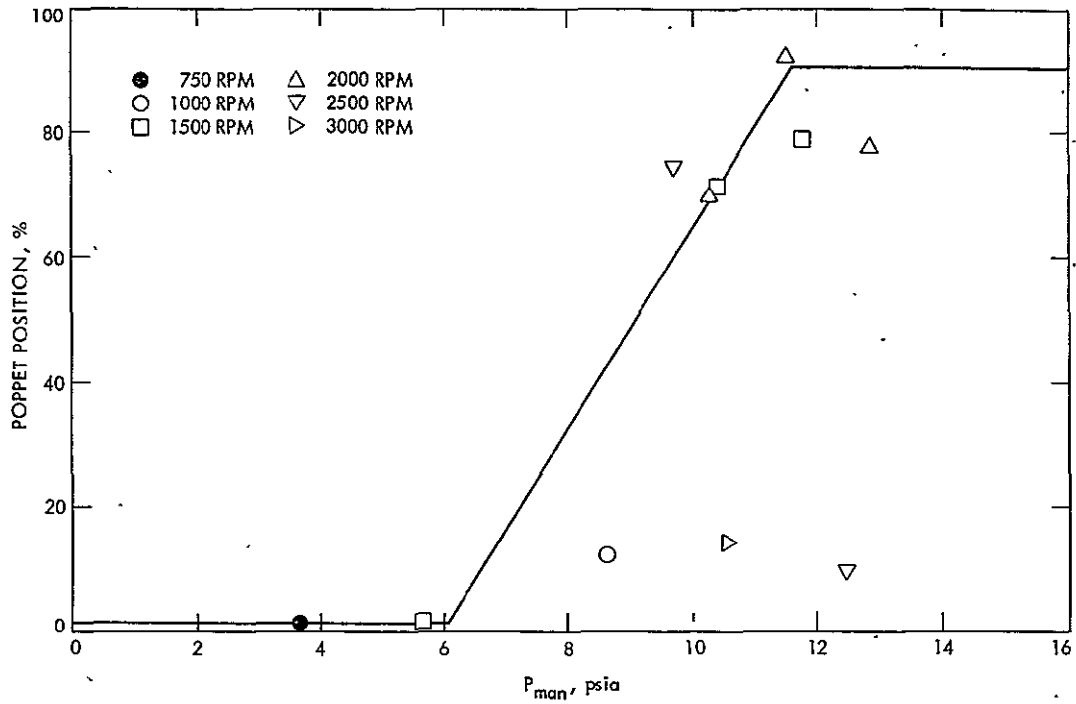
Figure E-2.   EGR Strategy No. 2
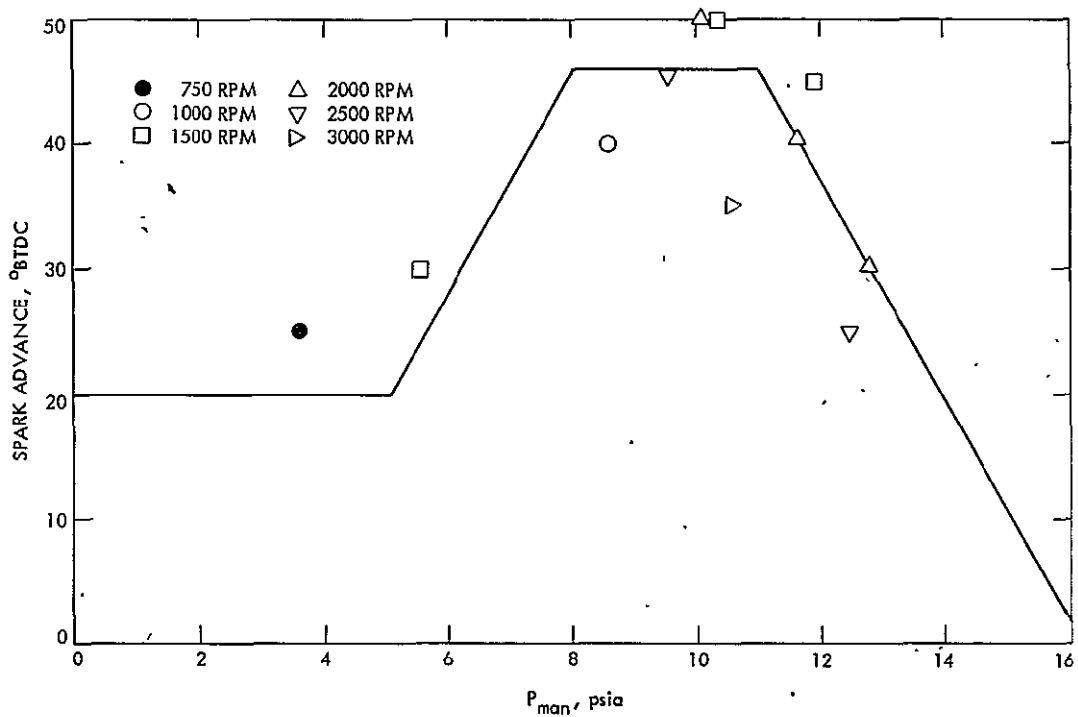
Figure E-3.   Spark Advance Strategy No. 2
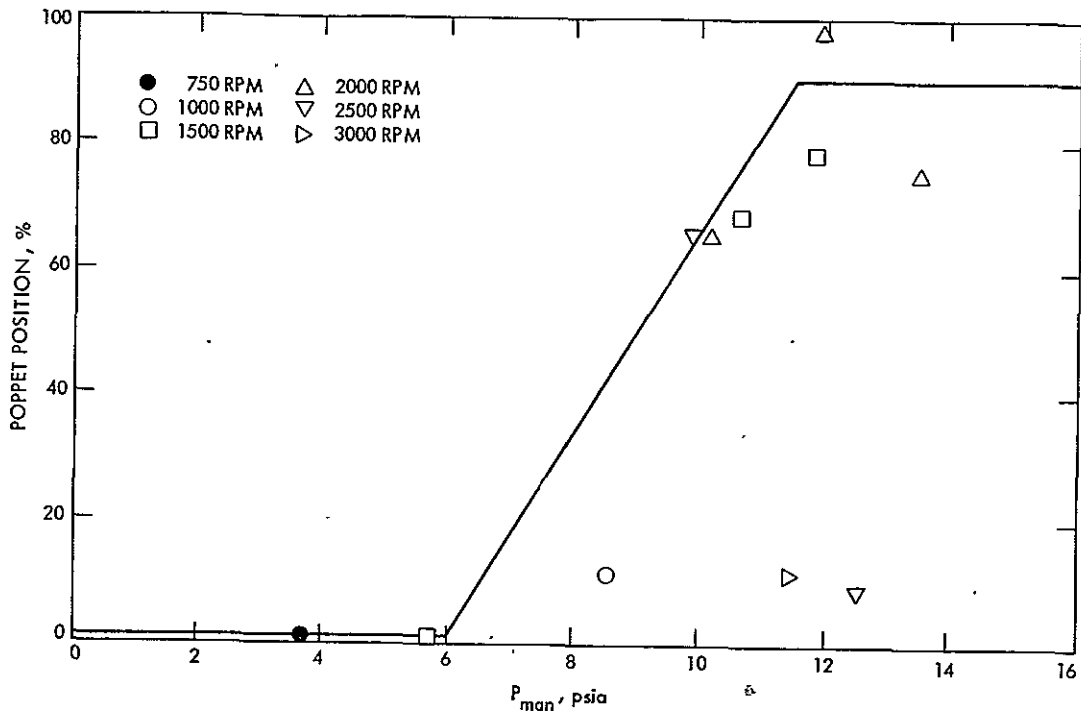
Figure E-4. EGR Strategy No. 3
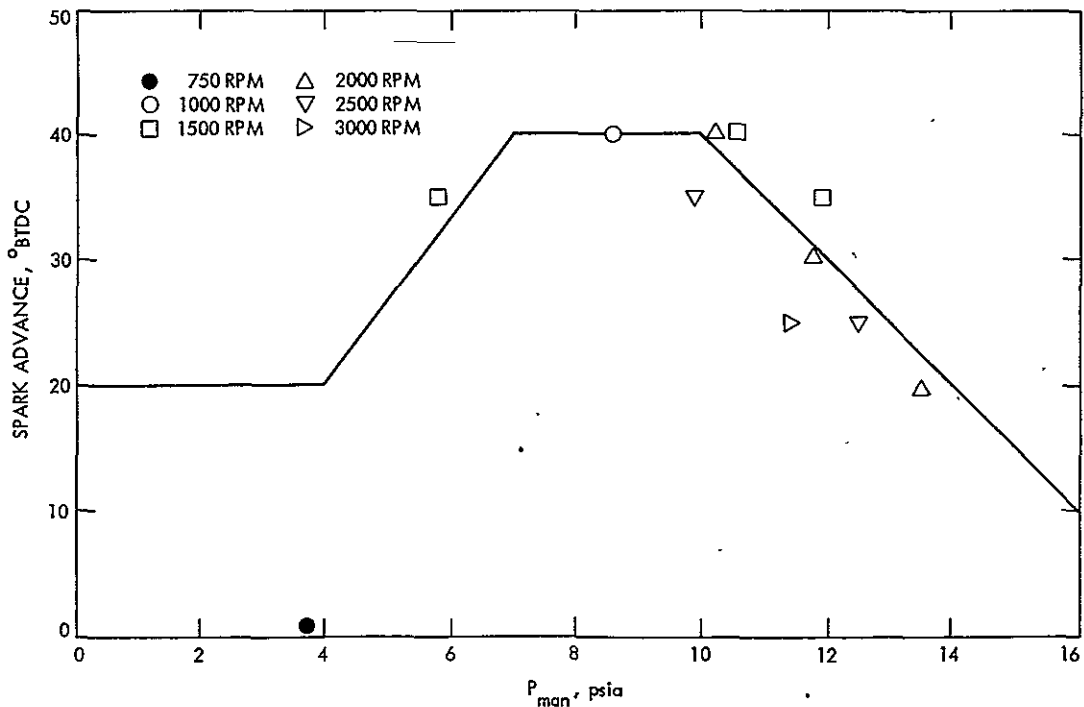
Figure E-5. Spark Advance Strategy No. 3
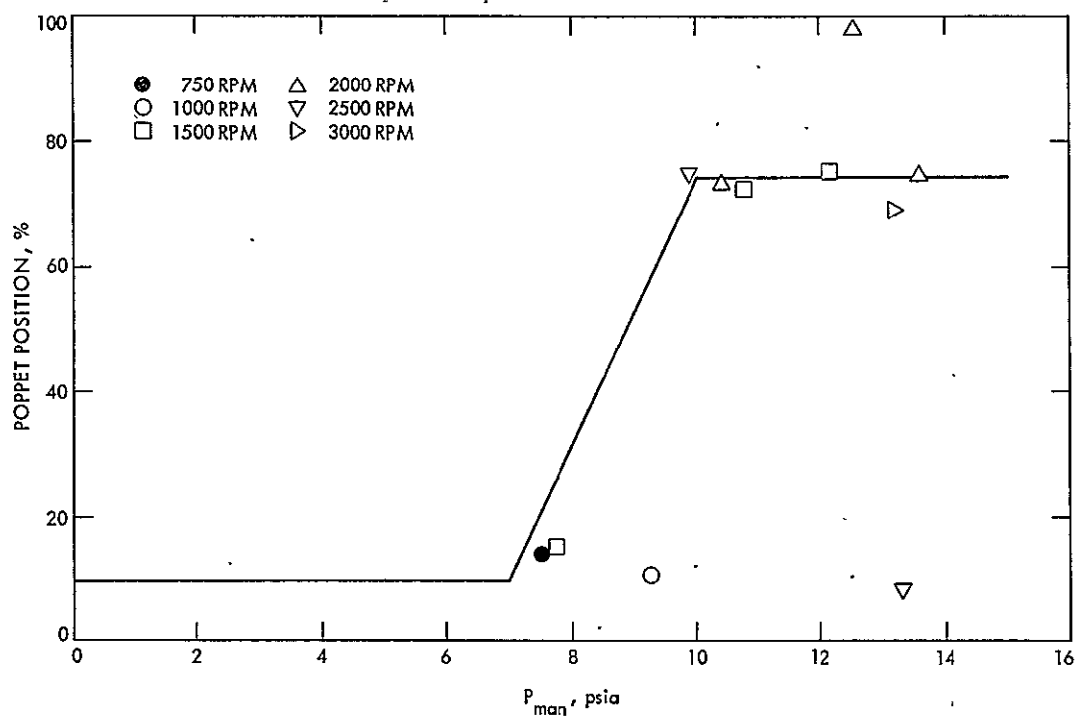
Figure E-6.   EGR Strategy No. 4
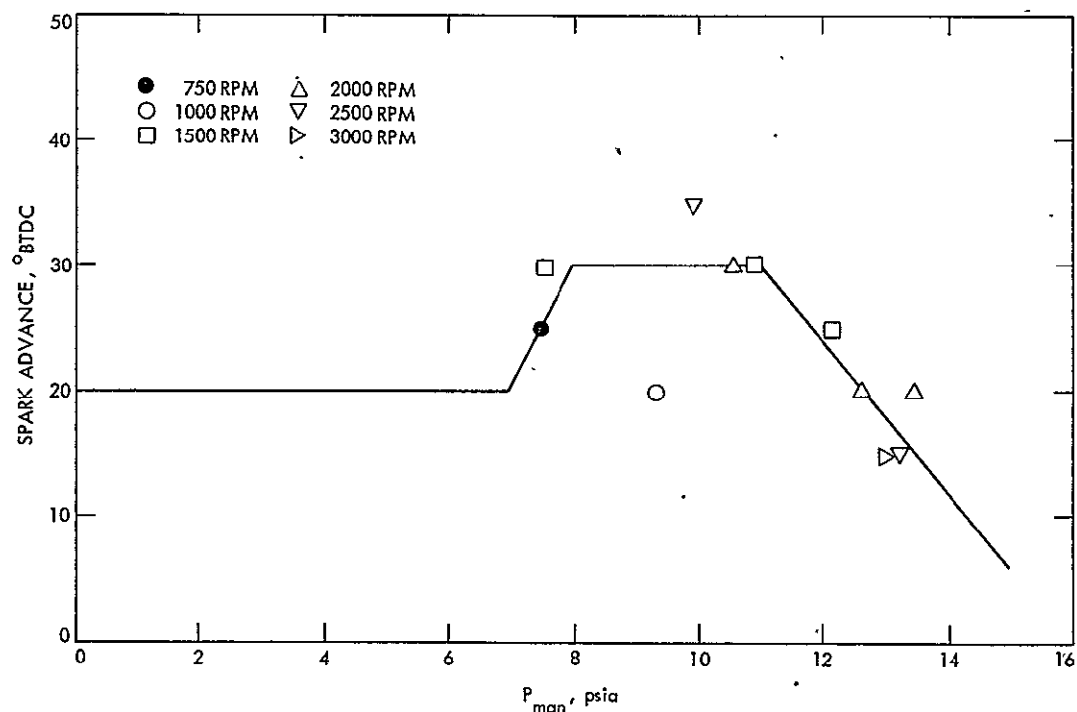
Figure E-7.   Spark Advance Strategy No. 4
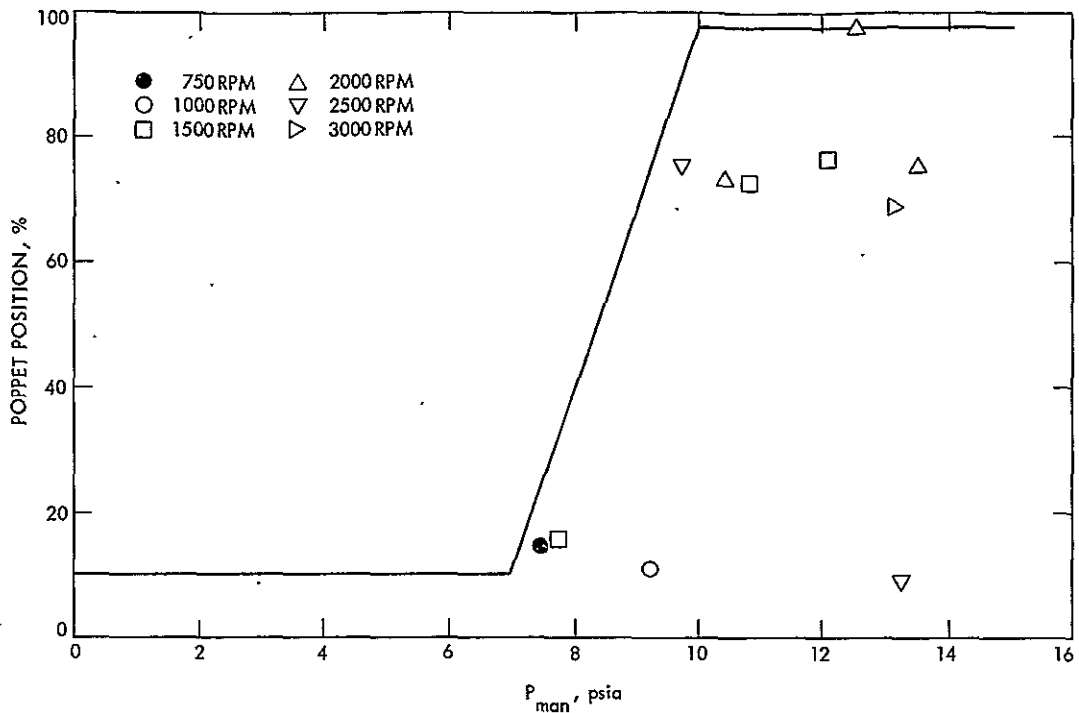
Figure E-8.   EGR Strategy No. 5
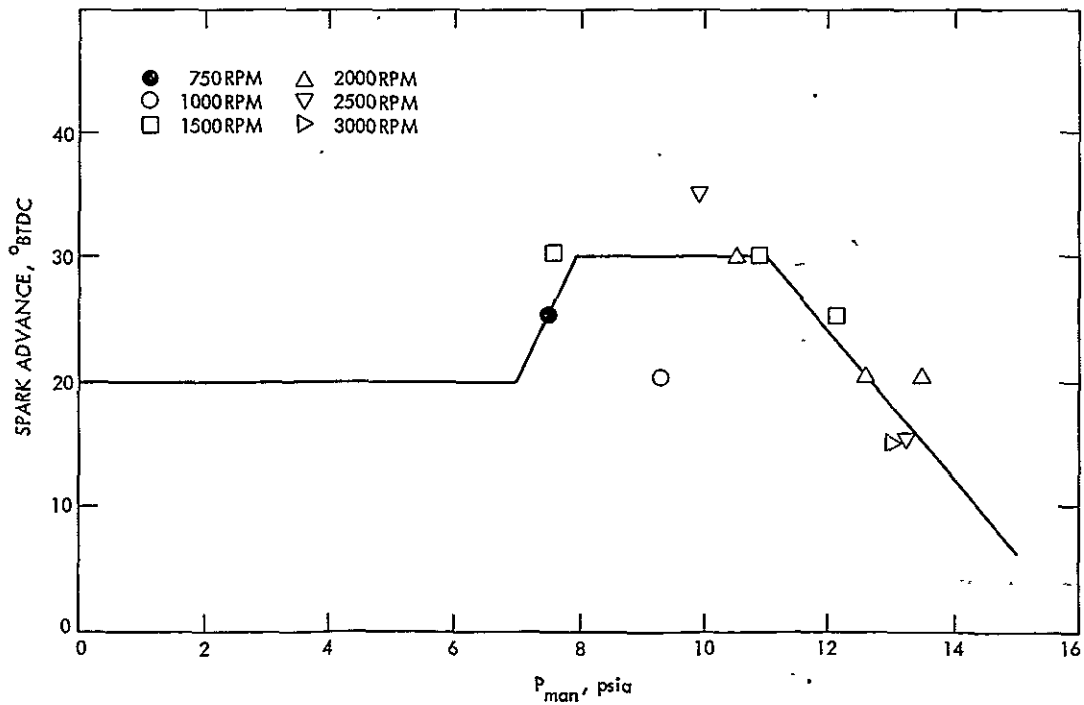
Figure E-9.   Spark Advance Strategy No. 5
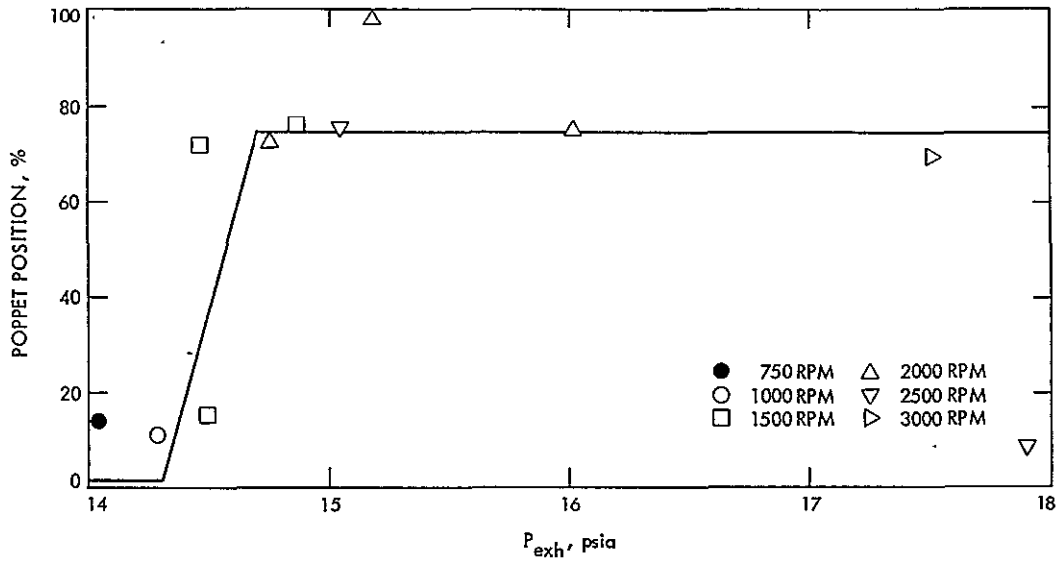
Figure E-10. EGR Strategy No. 6
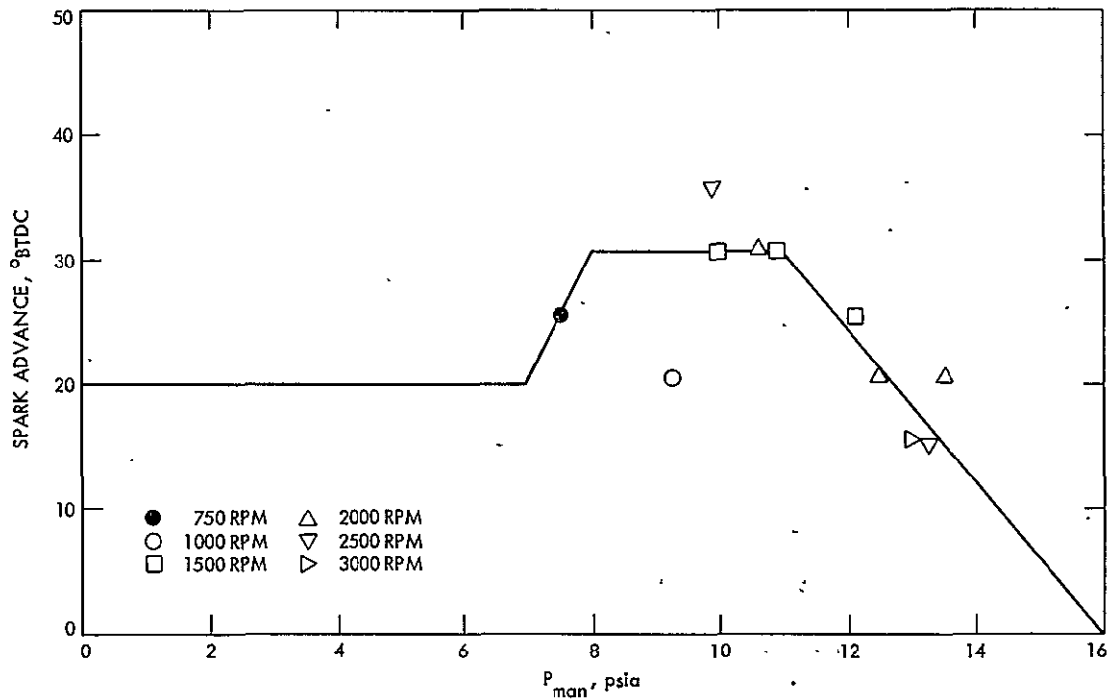
Figure E-11. Spark Advance Strategy No. 6
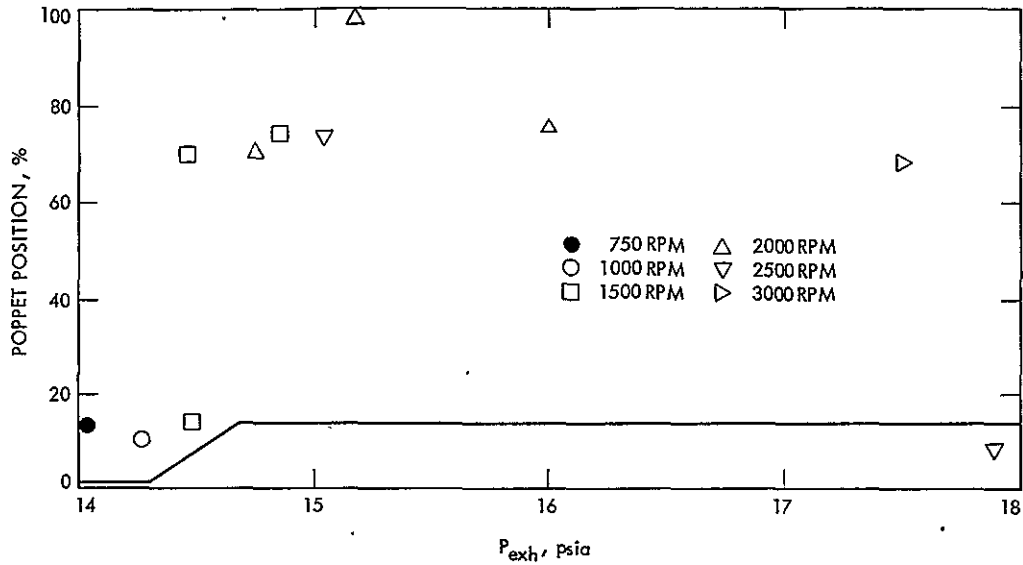
Figure E-12. EGR Strategy No. 7
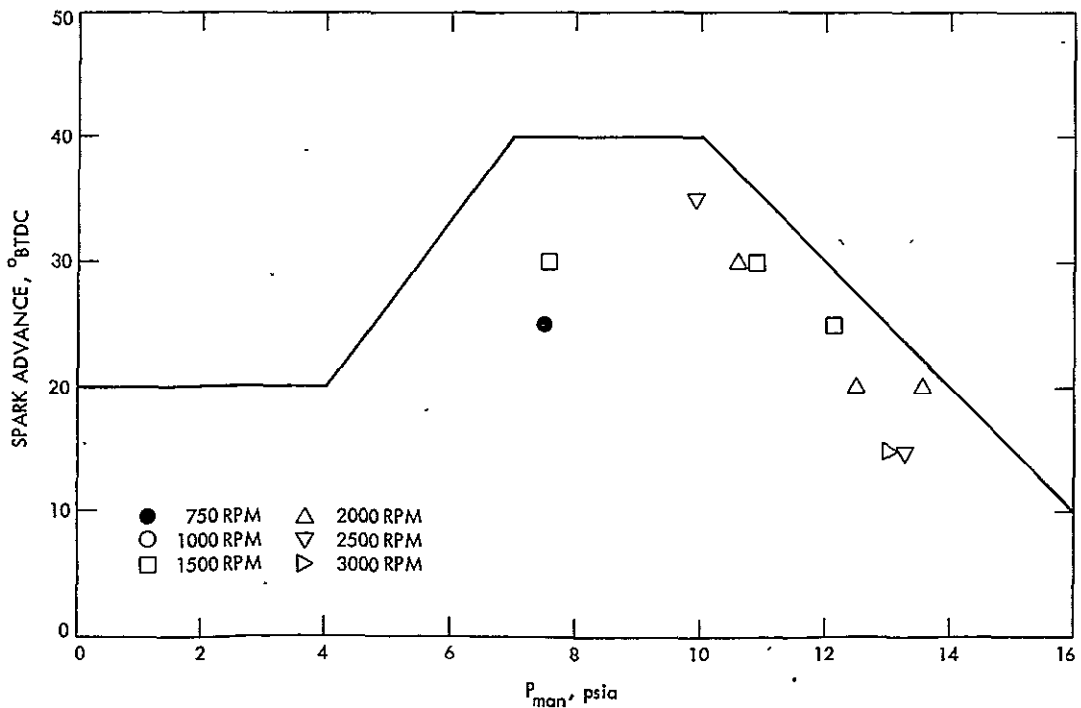
Figure E-13. Spark Advance Strategy No. 7
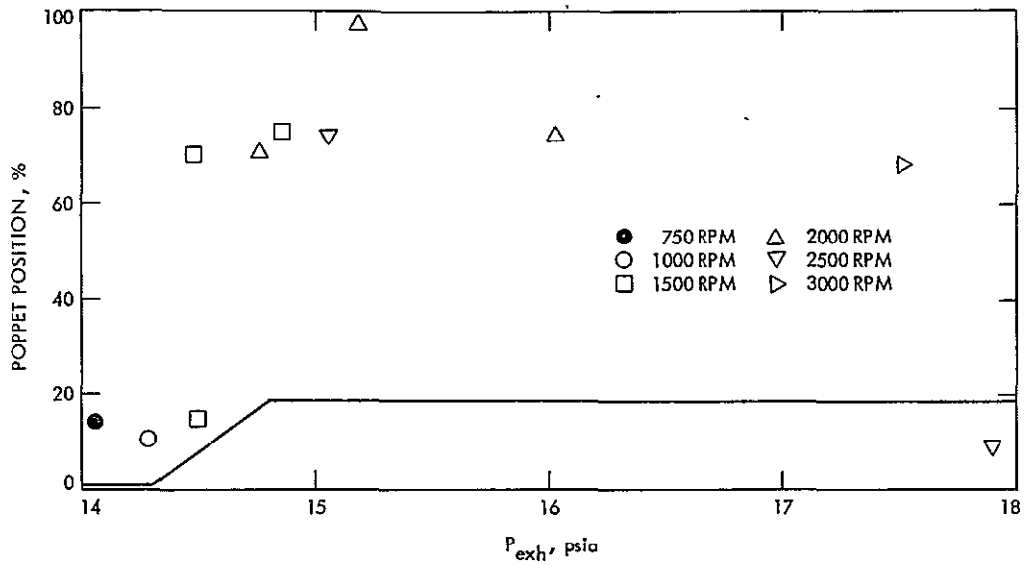
Figure E-14.   EGR Strategy No. 8
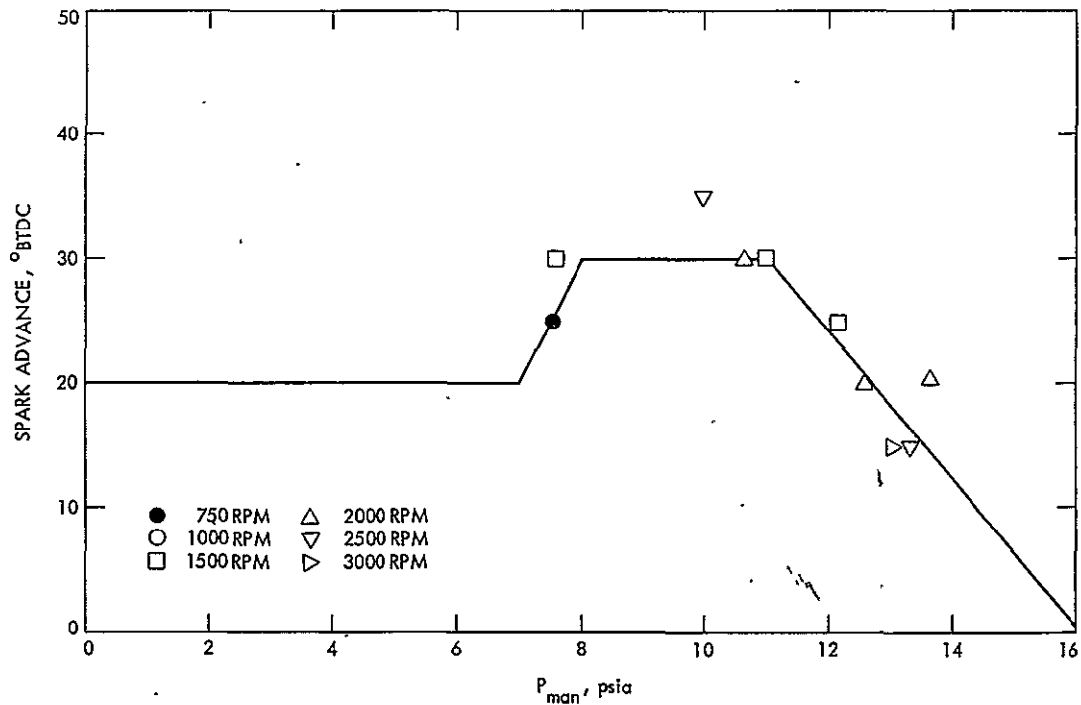
Figure E-15.   Spark Advance Strategy No. 8

APPENDIX F

A.I.R. SENSITIVITY DATA

C-3

Table F-1. A.I.R. Sensitivity Test Results for RPM = 1500 and BMEP = 20 psi

Sequence No.	RPM	BMEP (psi)	$\dot{m}_{gaso}$ (lbm/h)	$\dot{m}_{air}$ (lbm/h)	% A.I.R.	% EGR	Spark Advance (°BTDC)	Average T_{exh} (°F)	ϕ	ϕ_A	ϕ_E	BSFC (lbm/bhp-h)	Emissions Data*	$BSNO_x$ (g/bhp-h)	BSHC (g/bhp-h)	BSCO (g/bhp-h)	$\dot{m}_{A.I.R.}$ (lbm/h)	$\dot{m}_{EGR}$ (lbm/h)	η_{HC}	η_{CO}
3156.33	1476	20.2	7.68	114.8	0.07	23.74	35.78	1138	0.966	0.967	0.728	0.9046	U	1.392	8.60	35.7	0.09	38.12		
3157.33	1476	20.2	7.68	114.8	0.07	23.74	35.78	1138	0.966	0.967	0.728	0.9046	D	1.480	1.285	0.476	0.09	38.12	85.06	98.67
3156.30	1501	20.3	7.70	114.3	8.05	24.12	36.76	1129	0.974	0.892	0.728	0.8880	U	1.71	7.88	26.400	10.66	38.80		
3157.30	1501	20.3	7.70	114.3	8.05	24.12	36.76	1129	0.974	0.892	0.728	0.8880	D	1.79	1.28	0.40	10.66	38.80	83.76	98.48
3156.27	1510	20.1	7.64	114.4	14.69	24.39	37.20	1118	0.966	0.816	0.719	0.8891	U	.2.17	7.87	24.50	21.01	39.36		
3157.27	1510	20.1	7.64	114.4	14.69	24.39	37.20	1118	0.966	0.816	0.719	0.8891	D	2.25	1.38	0.36	21.01	39.36	82.46	98.53
3156.24	1519	20.2	7.65	114.6	20.01	24.50	37.08	1100	0.966	0.762	0.718	0.8780	U	2.53	7.52	18.88	30.58	39.66		
3157.24	1519	20.2	7.65	114.6	20.01	24.50	37.08	1100	0.966	0.762	0.718	0.8780	D	2.69	1.42	0.28	30.58	39.66	81.11	98.52
3156.21	1538	20.2	11.02	114.7	24.53	24.22	37.76	1085	1.389	1.026	1.029	1.2484	U	2.77	7.71	13.74	40.80	40.22		
3157.21	1538	20.2	11.02	114.7	24.53	24.22	37.76	1085	1.389	1.026	1.029	1.2484	D	2.91	1.51	0.23	40.80	40.22	80.41	98.33

*U = Upstream of catalytic converter; D = downstream of catalytic converter.
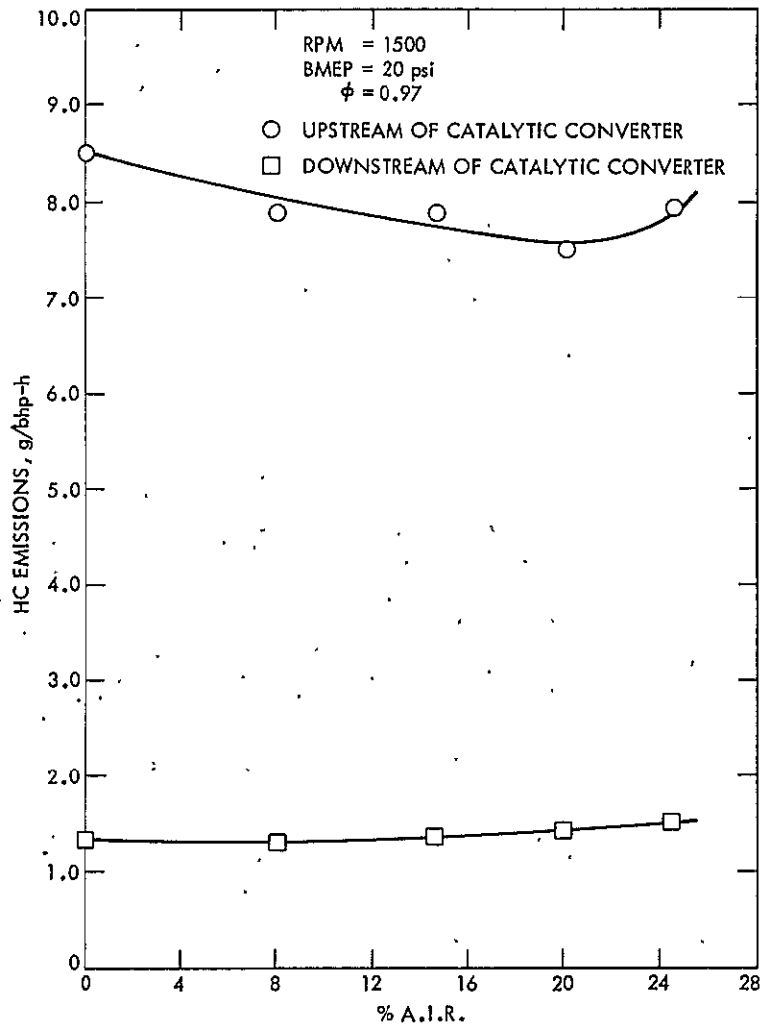
Figure F-1. HC Emissions for A.I.R. Sensitivity
Tests -   RPM = 1500
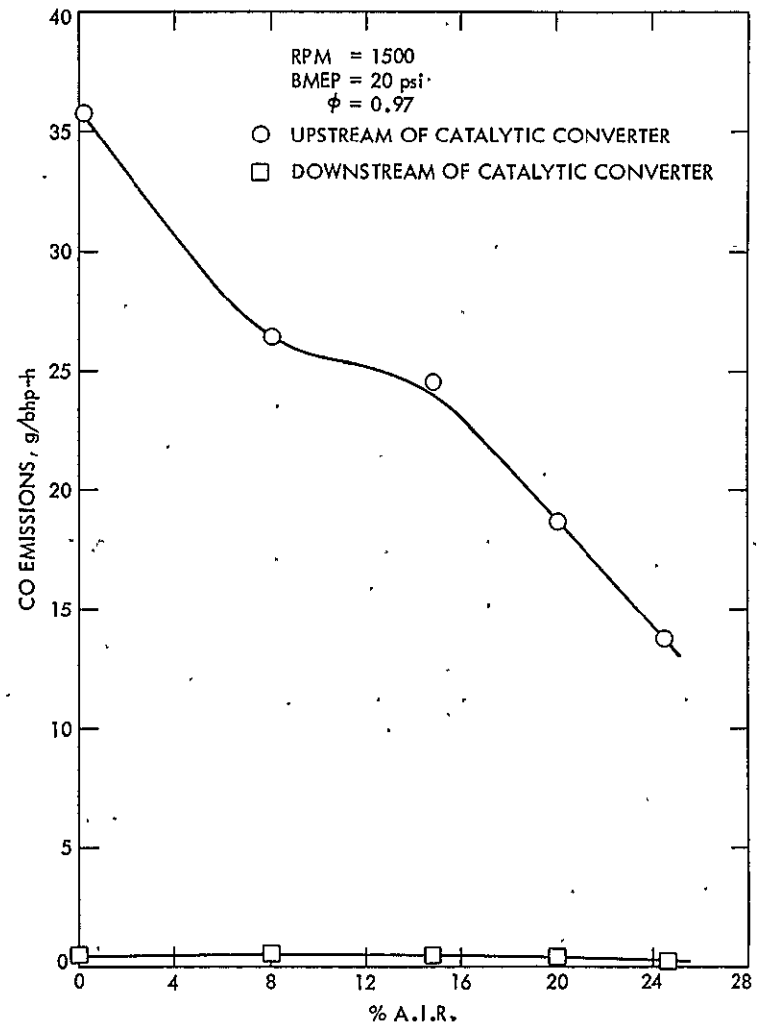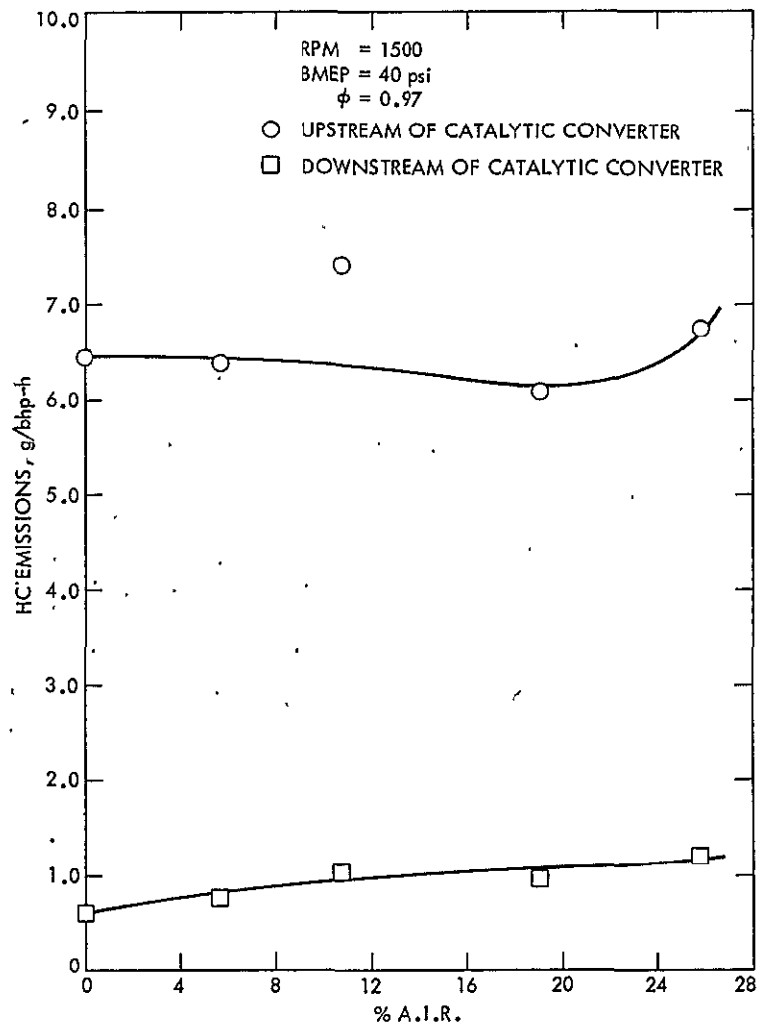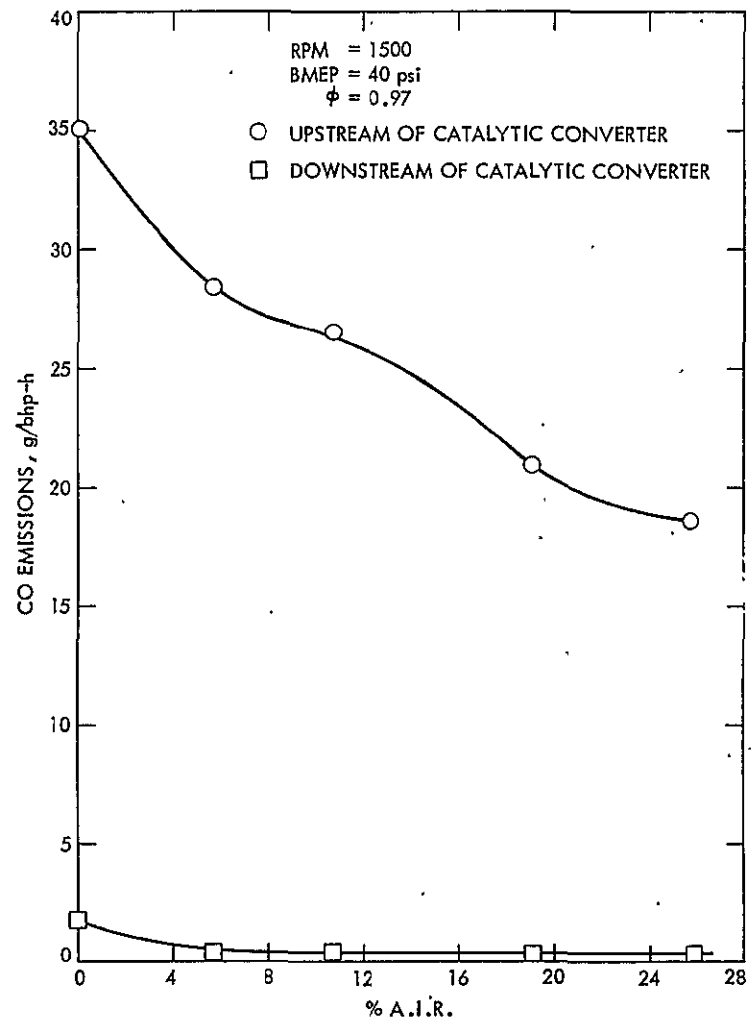BMEP = 20 psi
ϕ = 0.97

Figure F-2. CO Emissions for A.I.R. Sensitivity
Tests -   RPM = 1500
BMEP = 20 psi
ϕ = 0.97

Table F-2. A.I.R. Sensitivity Test Results for RPM = 1500 and BMEP = 40 psi

Sequence No.	RPM	BMEP (psi)	$\dot{m}_{gaso}$ (lbm/h)	$\dot{m}_{air}$ (lbm/h)	% A.I.R.	% EGR	Spark Advance (°BTDC)	Average T_{exh} (°F)	ϕ	ϕ_A	ϕ_E	BSFC (lbm/bhp-h)	Emissions Data*	BSNO$_x$ (g/bhp-h)	BSHC (g/bhp-h)	BSCO (g/bhp-h)	$\dot{m}_{A.I.R.}$ (lbm/h)	$\dot{m}_{EGR}$ (lbm/h)	η_{HC}	η_{CO}
3156.06	1529	40.1	11.17	166.9	0.07	23.12	29.49	1178	0.967	0.968	0.733	0.6337	U	1.42	6.42	35.039	0.12	53.58		
3157.06	1529	40.1	11.17	166.9	0.07	23.12	29.49	1178	0.967	0.968	0.733	0.6337	D	1.39	0.64	1.846	0.12	53.58	90.03	94.73
3156.09	1528	40.1	11.15	166.5	5.74	23.24	29.71	1165	0.968	0.910	0.732	0.6422	U	1.65	6.38	28.555	10.81	53.97		
3157.09	1528	40.1	11.15	166.5	5.74	23.24	29.71	1165	0.968	0.910	0.732	0.6422	D	1.72	0.77	0.441	10.81	53.97	87.93	98.46
3156.12	1527	39.9	11.19	166.9	10.69	23.56	29.74	1156	0.969	0.860	0.730	0.6462	U	1.95	7.44	26.574	21.29	54.89		
3157.12	1527	39.9	11.19	166.9	10.69	23.56	29.95	1156	0.969	0.860	0.730	0.6462	D	2.03	1.04	0.403	21.29	54.89	86.02	98.48
3156.15	1542	40.2	11.11	166.2	19.00	24.16	29.95	1126	0.967	0.774	0.722	0.6316	U	2.38	6.14	20.969	41.59	56.58		
3157.15	1542	40.2	11.11	166.2	19.00	24.16	29.95	1126	0.967	0.722	0.722	0.6316	D	2.43	0.99	0.330	41.59	56.58	83.88	98.43
3156.18	1545	39.8	11.15	165.1	25.86	24.77	30.00	1088	0.976	0.712	0.723	0.6381	U	2.94	6.76	18.658	61.48	58.03		
3157.18	1545	39.8	11.15	165.1	25.86	24.77	30.00	1088	0.976	0.712	0.723	0.6381	D	2.95	1.21	0.316	61.48	58.03	82.10	98.31

*U = Upstream of catalytic converter; D = downstream of catalytic converter.

Figure F-3. HC Emissions for A.I.R. Sensitivity
Tests – RPM = 1500
BMEP = 40 psi
ϕ = 0.97

Figure F-4. CO Emissions for A.I.R. Sensitivity
Tests – RPM = 1500
BMEP = 40 psi
ϕ = 0.97

Table F-3. A.I.R. Sensitivity Test Results for RPM = 1500 and BMEP = 60 psi

Sequence No.	RPM	BMEP (psi)	$\dot{m}_{gaso}$ (lbm/h)	$\dot{m}_{air}$ (lbm/h)	% A.I.R.	% EGR	Spark Advance (°BTDC)	Average T_{exh} (°F)	ϕ	ϕ_A	ϕ_E	BSFC (lbm/bhp-h)	Emissions Data*	BSNO$_x$ (g/bhp-h)	BSHC (g/bhp-h)	BSCO (g/bhp-h)	$\dot{m}_{A.I.R.}$ (lbm/h)	$\dot{m}_{EGR}$ (lbm/h)	η_{HC}	η_{CO}
3124.42	1483	59.5	13.80	218.2	0.09	9.17	20.39	1231	0.914	0.914	0.826	0.5504	U	5.44	2.19	4.90	0.22	23.42		
3124.06	1541	59.9	13.78	221.9	0.10	10.23	21.53	1235	0.900	0.898	0.802	0.5241	D	5.17	0.21	0.24	0.24	26.86	90.41	95.10
3124.39	1506	59.9	13.89	218.3	4.51	9.84	20.74	1218	0.915	0.873	0.821	0.5427	U	5.37	2.11	5.08	11.02	25.44		
3124.09	1495	59.9	13.14	214.9	4.48	10.00	21.44	1213	0.883	0.843	0.792	0.5156	D	5.52	0.22	0.23	10.69	25.34	89.57	95.47
3124.36	1503	60.0	13.90	218.9	8.21	9.82	20.62	1204	0.918	0.839	0.824	0.5448	U	5.43	2.02	5.03	20.83	25.35		
3124.12	1464	59.8	13.24	213.5	8.80	9.69	20.47	1196	0.813	0.814	0.806	0.5321	D	5.52	0.23	0.25	21.87	24.34	88.61	95.03
3124.33	1532	59.7	13.89	220.8	14.79	10.98	22.28	1168	0.909	0.769	0.805	0.5322	U	5.76	1.93	4.18	40.62	28.95		
3124.15	1514	59.6	13.91	219.5	15.18	10.47	21.54	1170	0.916	0.770	0.816	0.5429	D	5.84	0.23	0.22	41.79	27.29	88.08	94.74
3124.30	1536	59.8	13.91	220.5	20.60	11.22	22.10	1135	0.911	0.716	0.805	0.5330	U	5.91	1.81	3.59	60.83	29.63		
3124.21	1518	59.6	13.90	219.8	20.96	9.97	21.75	1133	0.913	0.715	0.819	0.5436	D	6.06	0.26	0.23	61.50	25.70	85.64	93.59
3124.27	1511	59.9	13.82	219.2	25.87	10.73	21.68	1096	0.914	0.665	0.809	0.5390	U	6.18	1.78	9.58	81.39	28.01		
3124.24	1527	59.9	13.89	220.3	25.97	11.30	21.74	1089	0.911	0.667	0.804	0.5333	D	6.27	0.28	0.24	81.21	29.85	84.27	97.49

*U = Upstream of catalytic converter; D = downstream of catalytic converter.
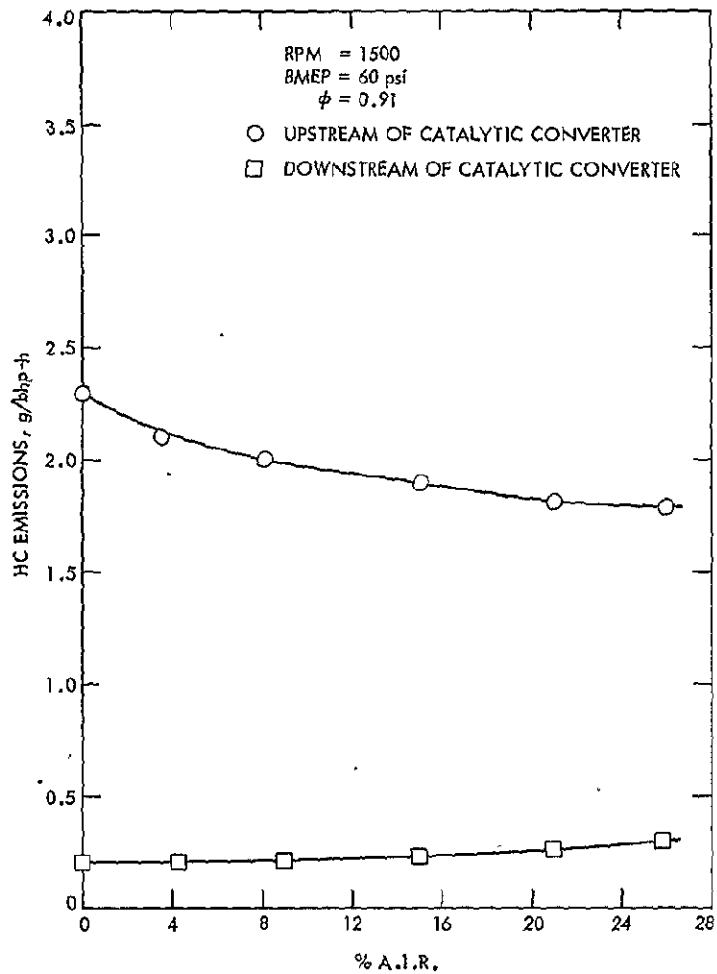
Figure F-5. HC Emissions for A.I.R. Sensitivity
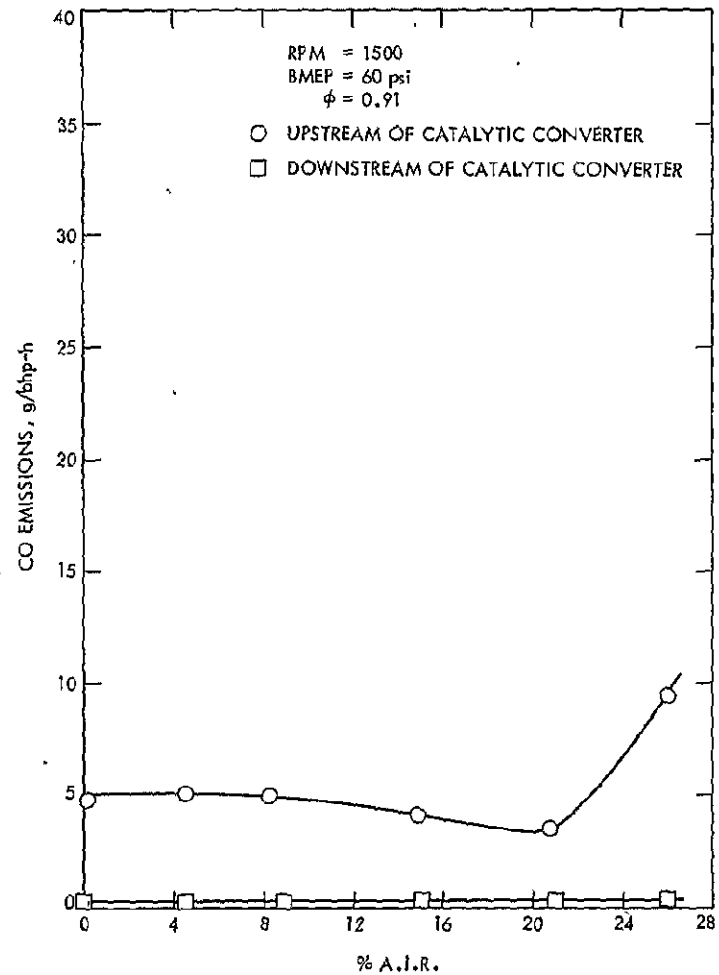Tests - RPM = 1500
BMEP = 60 psi
φ = 0.91

Figure F-6. CO Emissions for A.I.R. Sensitivity
Tests - RPM = 1500
BMEP = 60 psi
φ = 0.91

F-7

Table F-4. A.I.R. Sensitivity Test Results for RPM = 2000 and BMEP = 60 psi

Sequence No.	RPM	BMEP (psi)	$\dot{m}_{gaso}$ (lbm/h)	$\dot{m}_{air}$ (lbm/h)	% A.I.R.	% EGR	Spark Advance (°BTDC)	Average T_{exh} (°F)	ϕ	ϕ_A	ϕ_E	BSFC (lbm/bhp-h)	Emissions Data*	BSNO$_x$ (g/bhp-h)	BSHC (g/bhp-h)	BSCO (g/bhp-h)	$\dot{m}_{A.I.R.}$ (lbm/h)	$\dot{m}_{EGR}$ (lbm/h)	η_{HC}	η_{CO}
3152.03	2032	60.2	18.92	292.2	0.01	15.45	24.20	1333	0.936	0.937	0.784	0.5463	U	4.46	1.99	10.97	0.04	56.84		
3154.03	2032	60.2	18.92	292.2	0.01	15.45	24.20	1333	0.936	0.937	0.784	0.5463	D	4.35	0.20	0.92	0.04	56.84	89.95	91.61
3152.06	2027	59.9	18.94	288.8	6.43	15.79	24.47	1313	0.948	0.884	0.791	0.5498	U	4.90	1.55	9.28	21.15	57.72		
3154.06	2027	59.9	18.94	288.8	6.43	15.79	24.47	1313	0.948	0.884	0.791	0.5498	D	4.98	0.16	0.26	21.15	57.72	89.68	97.20
3152.09	2032	60.1	18.94	288.2	11.91	16.14	24.66	1285	0.950	0.831	0.789	0.5460	U	5.28	1.31	7.68	41.46	59.09		
3154.09	2032	60.1	18.94	288.2	11.91	16.14	24.66	1285	0.950	0.831	0.789	0.5460	D	5.44	0.15	0.22	41.46	59.09	88.55	97.14
3152.12	2032	60.0	19.04	287.9	16.69	16.46	24.47	1252	0.956	0.789	0.791	0.5504	U	5.52	1.26	6.25	61.50	60.39		
3154.12	2032	60.0	19.04	287.9	16.69	16.46	24.47	1252	0.956	0.789	0.791	0.5504	D	5.71	0.16	0.19	61.50	60.39	87.30	96.96
3152.15	2015	60.1	19.08	285.0	21.10	16.84	24.58	1223	0.967	0.754	0.797	0.5550	U	5.77	1.24	6.11	81.36	61.54		
3154.15	2015	60.1	19.08	285.0	21.10	16.84	24.58	1223	0.967	0.754	0.797	0.5550	D	5.91	0.18	0.18	81.36	61.54	85.48	92.05
3152.18	2007	60.0	18.41	283.2	25.15	17.21	24.45	1193	0.940	0.692	0.770	0.5381	U	5.95	1.24	5.02	101.58	62.67		
3154.18	2007	60.0	18.41	283.2	25.15	17.21	24.45	1193	0.940	0.692	0.770	0.5381	D	6.07	0.21	0.18	101.58	62.67	83.06	96.41

*U = Upstream of catalytic converter; D = downstream of catalytic converter.
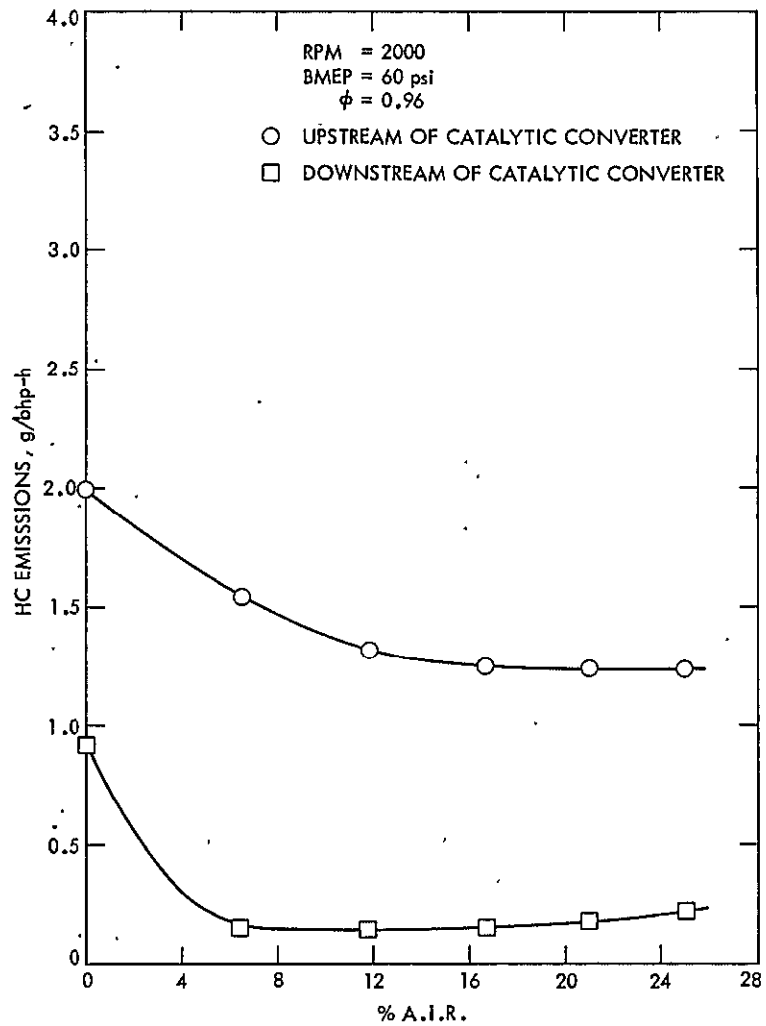
Figure F-7. HC Emissions for A.I.R. Sensitivity
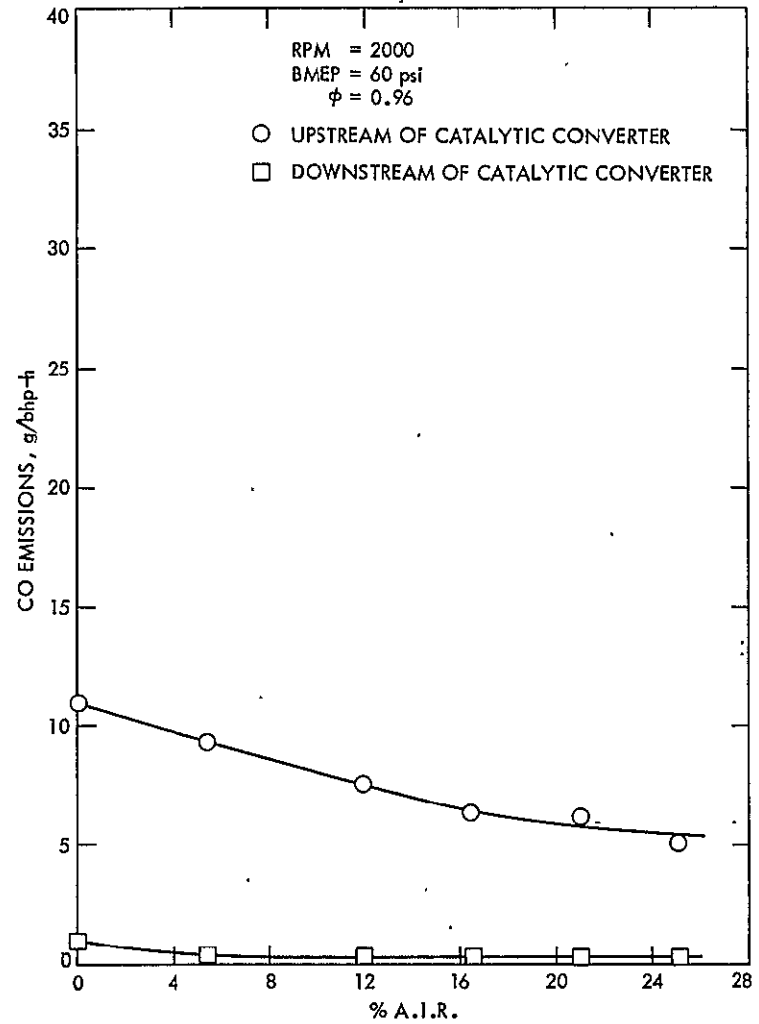Tests – RPM = 2000
BMEP = 60 psi
ϕ = 0.96

Figure F-8. CO Emissions for A.I.R. Sensitivity
Tests – RPM = 2000
BMEP = 60 psi
ϕ = 0.96

Table F-5. A.I.R. Sensitivity Test Results for RPM = 2000 and BMEP = 80 psi

Sequence No.	RPM	BMEP (psi)	$\dot{m}_{gaso}$ (lbm/h)	$\dot{m}_{air}$ (lbm/h)	% A.I.R.	% EGR	Spark Advanced (°BTDC)	Average T_{exh} (°F)	ϕ	ϕ_A	ϕ_E	BSFC (lbm/bhp-h)	Emissions Data*	$BSNO_x$ (g/bhp-h)	BSHC (g/bhp-h)	BSCO (g/bhp-h)	$\dot{m}_{A.I.R.}$ (lbm/h)	$\dot{m}_{EGR}$ (lbm/h)	η_{HC}	η_{CO}
3125.22	2029	80.6	22.24	342.7	0.05	2.93	23.21	1342	0.937	0.939	0.910	0.4786	U	15.45	1.34	3.09	0.19	11.03		
3124.45	2010	80.5	21.55	339.3	0.06	2.97	22.92	1338	0.918	0.918	0.890	0.4688	D	15.60	0.16	0.32	0.21	11.04	88.05	89.64
3125.19	2024	80.5	22.21	341.6	2.67	2.99	23.06	1333	0.942	0.914	0.911	0.4802	U	15.59	1.17	3.09	9.96	11.22		
3124.48	2009	80.3	21.55	338.5	2.87	2.96	22.84	1329	0.920	0.893	0.892	0.4704	D	15.97	0.14	0.21	10.67	10.97	80.03	93.20
3125.16	2020	80.5	22.18	340.8	5.41	3.00	22.89	1322	0.942	0.888	0.912	0.4806	U	15.70	1.00	3.27	20.73	11.24		
3124.51	2009	80.5	21.55	337.7	5.56	3.01	23.03	1316	0.923	0.869	0.894	0.4694	D	15.97	0.15	0.20	21.15	11.14	85.00	93.88
3125.13	2008	80.5	22.10	339.5	10.21	2.87	22.82	1293	0.941	0.840	0.913	0.4813	U	16.09	0.82	2.59	41.11	10.67		
3124.54	2006	80.4	21.55	337.3	10.33	3.05	22.91	1287	0.924	0.824	0.895	0.4712	D	16.45	0.14	0.18	41.28	11.28	82.92	93.05
3125.10	2011	80.6	21.53	339.4	14.63	2.96	23.07	1264	0.917	0.776	0.889	0.4683	U	16.28	0.73	2.27	61.86	11.01		
3124.57	1998	80.5	21.63	336.3	14.64	3.10	23.02	1256	0.930	0.787	0.900	0.4731	D	16.56	0.14	0.17	61.30	11.44	80.82	92.51
3125.07	2058	80.3	22.08	348.3	17.80	3.00	23.30	1245	0.916	0.746	0.888	0.4704	U	16.86	0.71	2.25	80.29	11.47		
3124.60	1974	80.5	21.67	333.8	18.55	2.78	22.94	1231	0.938	0.756	0.912	0.4805	D	16.61	0.15	0.17	80.97	10.15	78.87	92.44
3125.04	2042	80.4	22.09	346.0	21.58	2.86	23.13	1220	0.923	0.715	0.896	0.4733	U	16.87	0.72	2.31	101.30	10.83		
3125.01	2034	80.5	22.11	345.9	21.53	2.74	23.10	1219	0.924	0.716	0.898	0.4740	D	16.36	0.15	0.19	100.95	10.36	79.17	91.77

*U = Upstream of catalytic converter; D = downstream of catalytic converter.

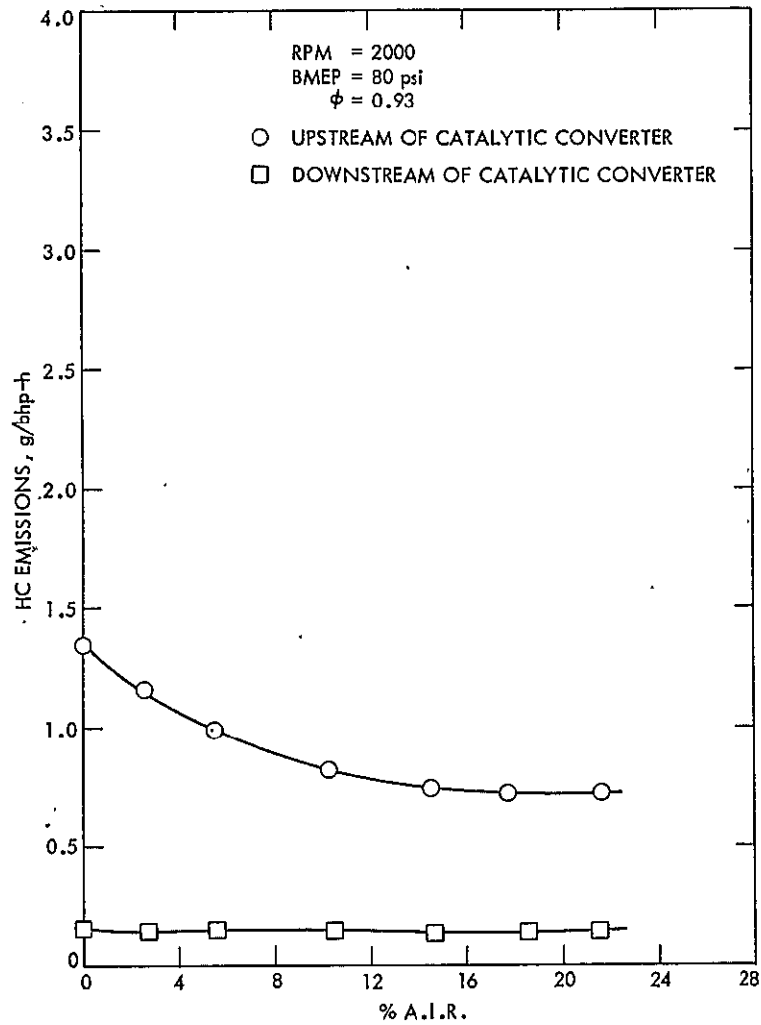Figure F-9.   HC Emissions for A.I.R. Sensitivity
              Tests –   RPM = 2000
                        BMEP = 80 psi
                           ϕ = 0.93

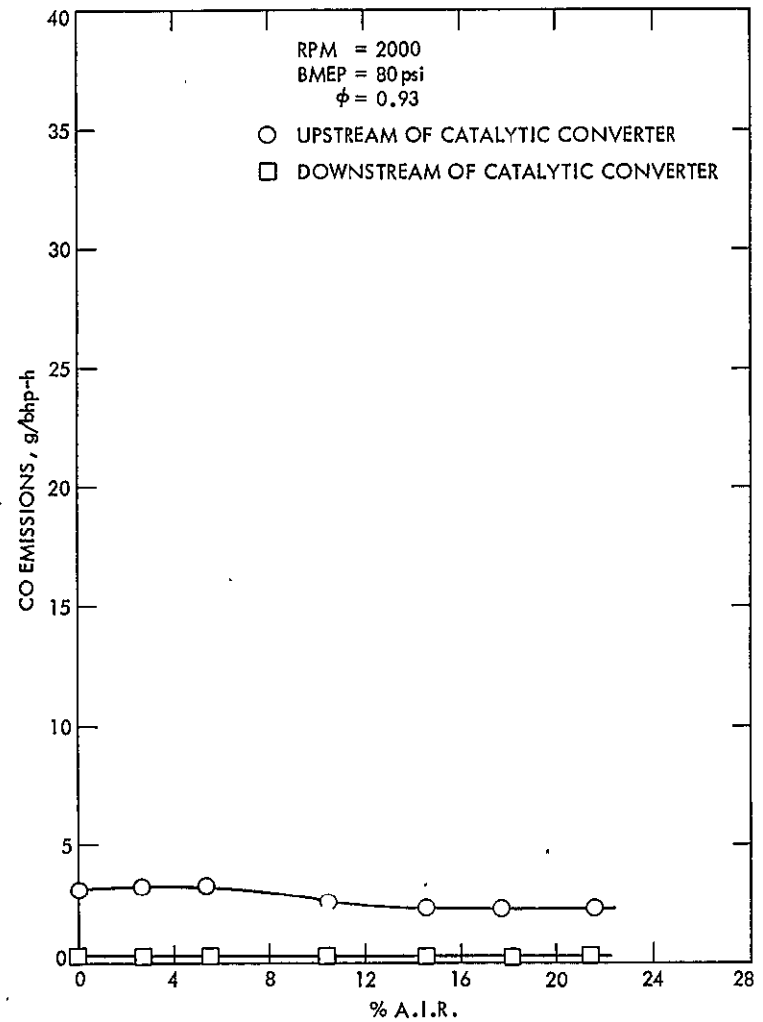Figure F-10.   CO Emissions for A.I.R. Sensitivity
               Tests –   RPM = 2000
                         BMEP = 80 psi
                            ϕ = 0.93

Table F-6. A.I.R. Sensitivity Test Results for RPM = 2500 and BMEP = 40 psi

Sequence No.	RPM	BMEP (psi)	$\dot{m}_{gaso}$ (lbm/h)	$\dot{m}_{air}$ (lbm/h)	% A.I.R.	% EGR	Spark Advance (°BTDC)	Average T_{exh} (°F)	ϕ	ϕ_A	ϕ_E	BSFC (lbm/bhp-h)	Emissions Data*	$BSNO_x$ (g/bhp-h)	BSHC (g/bhp-h)	BSCO (g/bhp-h)	$\dot{m}_{A.I.R.}$ (lbm/h)	$\dot{m}_{EGR}$ (lbm/h)	η_{HC}	η_{CO}
3129.44	2499	40.2	17.98	277.6	0.04		34.28		0.937	0.937		0.6313	U	4.21	2.29	8.61	0.12			
3129.08	2555	40.2	18.59	283.2	0.00	18.44	34.58	1341	0.949	0.950	0.765	0.6372	D	4.10	0.19	1.93	0.01	68.26	91.70	77.58
3129.38	2490	40.2	18.00	276.0	6.59	18.74	34.10	1310	0.943	0.878	0.758	0.6274	U	4.61	1.78	4.54	20.73	67.81		
3129.11	2513	40.3	18.02	278.9	6.67	18.74	34.30	1319	0.935	0.869	0.750	0.6304	D	4.63	0.18	0.36	21.30	68.58	89.89	92.07
3129.35	2514	40.2	17.98	277.1	12.27	19.34	34.36	1291	0.938	0.817	0.744	0.6256	U	5.12	1.58	0.61	41.25	70.78		
3129.14	2524	40.3	18.05	278.9	12.18	19.28	34.27	1294	0.933	0.816	0.747	0.6242	D	5.14	0.21	0.32	41.20	70.90	86.71	47.54
3129.32	2516	40.1	17.98	277.3	17.07	19.77	34.26	1267	0.937	0.770	0.743	0.6271	U	5.52	1.78	4.04	60.76	72.77		
3129.17	2523	40.2	18.56	278.3	17.07	19.64	34.42	1269	0.964	0.791	0.766	0.6434	D	5.55	0.20	0.29	61.13	72.57	88.76	92.82
3129.29	2468	40.5	18.04	274.5	21.63	19.84	33.92	1232	0.949	0.735	0.752	0.6364	U	5.67	1.92	3.05	80.85	72.42		
3129.20	2514	40.2	17.96	277.6	21.50	20.05	34.41	1240	0.936	0.725	0.739	0.6260	D	5.88	0.21	0.29	80.92	74.09	89.06	90.49
3129.26	2508	40.2	18.00	276.9	25.56	20.48	34.37	1211	0.940	0.689	0.738	0.6274	U	6.18	1.95	9.87	101.37	75.94		
3129.23	2514	40.4	18.03	277.2	25.46	20.49	34.34	1212	0.941	0.690	0.738	0.6252	D	5.98	0.25	0.29	101.01	76.08	87.18	97.06

*U = Upstream of catalytic converter; D = downstream of catalytic converter.
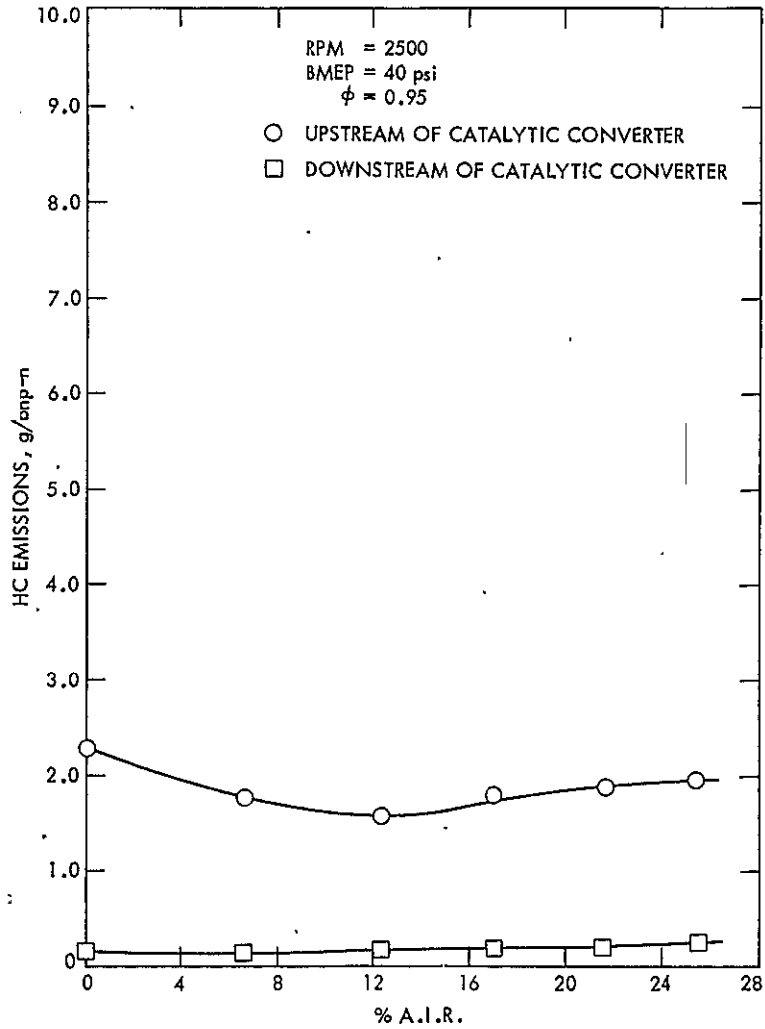
Figure F-11. HC Emissions for A.I.R. Sensitivity
Tests – RPM = 2500
BMEP = 40 psi
ϕ = 0.95

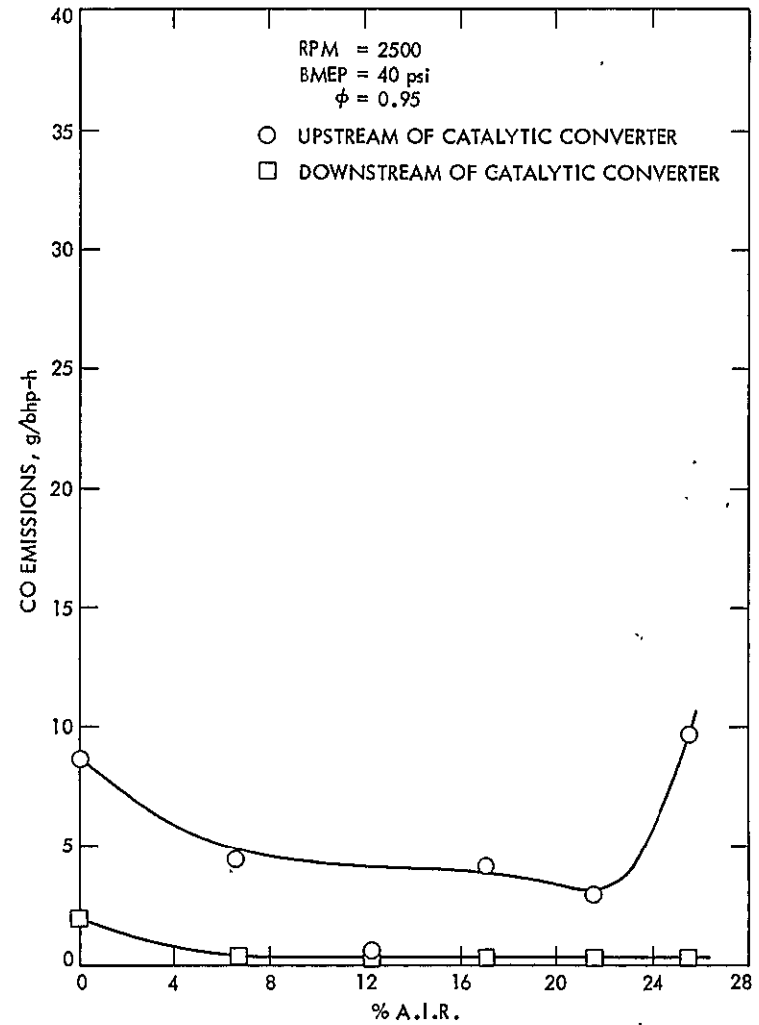
Figure F-12. CO Emissions for A.I.R. Sensitivity
Tests – RPM = 2500
BMEP = 40 psi
ϕ = 0.95

Table F-7. A.I.R. Sensivitity Test Results for RPM = 2500 and BMEP = 80 psi

Sequence No.	RPM	BMEP (psi)	$\dot{m}_{gaso}$ (lbm/h)	$\dot{m}_{air}$ (lbm/h)	% A.I.R.	% EGR	Spark Advance (°BTDC)	Average T_{exh} (°F)	ϕ	ϕ_A	ϕ_E	BSFC (lbm/bhp-h)	Emissions Data*	$BSNO_x$ (g/bhp-h)	BSHC (g/bhp-h)	BSCO (g/bhp-h)	$\dot{m}_{A.I.R.}$ (lbm/h)	$\dot{m}_{EGR}$ (lbm/h)	η_{HC}	η_{CO}
3124.03	2515	80.3	28.13	432.9	0.05	2.11	25.48	1423	0.939	0.940	0.919	0.4897	U	16.59	0.720	3.40	0.24	9.94		
3123.32	2501	80.4	27.50	433.9	0.02	2.25	25.28	1424	0.918	0.917	0.895	0.4815	D	15.55	0.11	0.29	0.10	10.78	84.72	91.47
3123.62	2525	80.1	28.15	433.1	4.23	2.31	25.87	1406	0.939	0.898	0.918	0.4891	U	16.856	0.437	2.923	20.32	10.88		
3123.35	2501	80.3	28.08	431.7	4.60	2.31	25.47	1408	0.939	0.895	0.918	0.4911	D	16.08	0.07	0.21	22.16	10.84	83.98	92.82
3123.59	2515	80.3	28.09	431.8	8.09	2.30	25.66	1383	0.841	0.861	0.918	0.4899	U	17.26	0.35	7.04	40.49	10.85		
3123.38	2489	80.3	27.46	430.5	8.19	2.25	25.41	1386	0.922	0.843	0.901	0.4839	D	16.19	0.08	0.19	40.85	10.53	77.14	97.30
3123.56	2555	80.4	28.10	439.1	11.44	2.25	25.89	1365	0.926	0.814	0.904	0.4825	U	17.48	0.34	5.98	60.37	10.74		
3123.41	2487	80.4	27.49	429.3	11.94	2.31	25.52	1355	0.926	0.810	0.905	0.4844	D	16.36	0.07	0.18	61.92	10.31	79.44	96.99
3123.53	2533	80.5	28.11	437.2	14.85	2.21	25.69	1342	0.929	0.785	0.908	0.4851	U	17.69	0.34	5.90	81.14	10.54		
3123.44	2484	80.3	27.54	428.1	15.22	2.35	25.42	1331	0.930	0.782	0.908	0.4857	D	16.44	0.08	0.18	81.77	10.99	76.47	96.95
3123.50	2527	80.3	28.10	436.9	17.81	2.24	25.70	1320	0.930	0.756	0.908	0.4871	U	17.42	0.36		100.80	10.67		
3123.47	2477	80.4	27.50	427.3	18.38	2.24	25.49	1309	0.930	0.751	0.909	0.4858	D	16.31	0.08	0.19	102.62	10.44	77.77	

*U = Upstream of catalytic converter; D = downstream of catalytic converter.
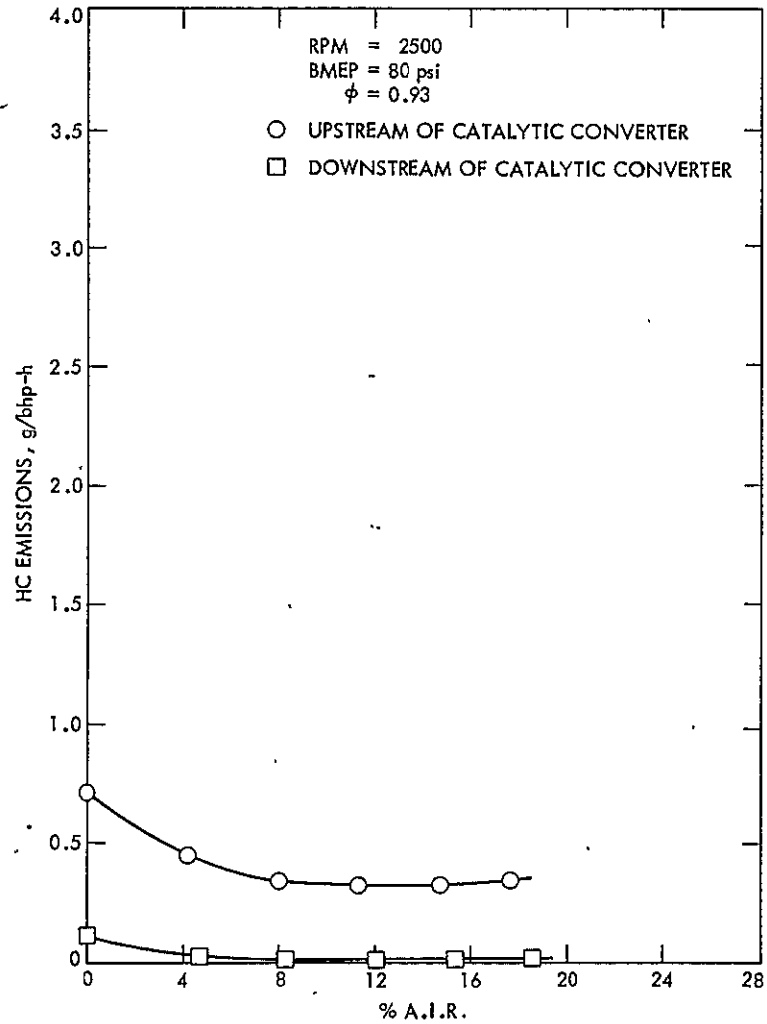
Figure F-13.   HC Emissions for A.I.R. Sensitivity
Tests —   RPM = 2500
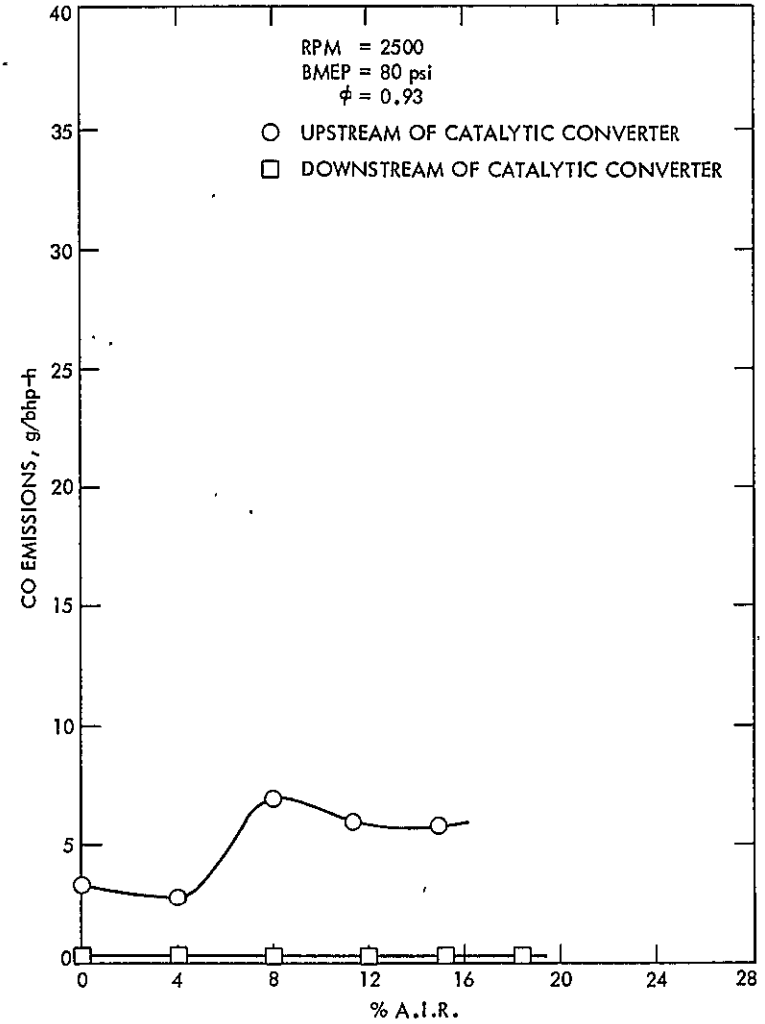BMEP = 80 psi
ϕ = 0.93

Figure F-14.   CO Emissions for A.I.R. Sensitivity
Tests —   RPM = 2500
BMEP = 80 psi
ϕ = 0.93

Table F-8. A.I.R. Sensitivity Test Results for RPM = 3000 and BMEP = 60 psi

Sequence No.	RPM	BMEP (psi)	$\dot{m}_{gaso}$ (lbm/h)	$\dot{m}_{air}$ (lbm/h)	% A.I.R.	% EGR	Spark Advance (°BTDC)	Average T_{exh} (°F)	ϕ	ϕ_A	ϕ_E	BSFC (lbm/bhp-h)	Emissions Data*	$BSNO_x$ (g/bhp-h)	BSHC (g/bhp-h)	BSCO (g/bhp-h)	$\dot{m}_{A.I.R.}$ (lbm/h)	$\dot{m}_{EGR}$ (lbm/h)	η_{HC}	η_{CO}
3132.01	3066	60.6	30.28	470.2	0.01	3.74	27.18	1492	0.930	0.932	0.895	0.5736	U	13.60	0.35	2.42	0.04	19.48		
3131.27	3045	60.6	29.59	464.5	0.01	4.08	27.42	1487	0.922	0.922	0.882	0.5643	D	13.88	0.08	0.26	0.04	20.97	77.14	89.26
3131.30	3025	60.7	29.59	462.0	2.27	3.75	27.48	1482	0.926	0.904	0.890	0.5664	D	14.05	·0.05	0.21	11.45	19.15		
3131.60	3077	60.4	30.26	470.7	4.06	3.83	27.19	1473	0.929	0.890	0.892	0.5744	U	13.56	0.22	1.86	21.15	19.93		
3131.33	3029	60.5	29.60	461.5	4.01	3.91	27.71	1474	0.927	0.889	0.890	0.5692	D	14.33	0.05	0.20	20.55	19.98	77.27	89.25
3131.57	3044	60.7	29.67	467.4	7.48	3.74	27.06	1456	0.917	0.846	0.882	0.5667	U	13.43	0.21	1.57	40.16	19.33		
3131.36	3000	60.6	29.63	459.6	7.92	3.72	27.77	1452	0.933	0.855	0.896	0.5736	D	14.13	0.05	0.19	42.05	18.88	76.19	87.90
3131.54	3030	60.8	29.62	466.9	10.87	3.67	26.95	1435	0.917	0.813	·0.882	0.5660	U	13.43	0.22	1.63	60.57	18.94		
3131.39	3007	60.5	29.67	460.8	11.15	3.76	27.66	1430	0.930	0̗.822	0.895	0.5734	D	14.28	0.05	0.19	61.53	19.16	77.27	88.34
3131.51	3117	60.5	30.76	485.1	16.25	3.23	27.22 ·	1411	0.917	0.761	0.886	0.5747	U	13.69	0.23	1.61	100.15	17.23		
3131.42	2976	60.5	29.60	457.0	17.11	3.71	27.72	1388	0.937	0.768	0.900	0.5795	D	14.10	0.06	·0.20	100.43	18.77	73.91	87.58
3131.48	3026	60.5	30.83	478.7 `	21.74	2.76	26.10 ·	1376	0.931	0.719	0.905	0.5919	U	13.56	0.24	1.59	141.61	14.47		
3131.45	3028	60.5	30.83	478.2	21.76	2.72	26.45	1379	0.932	0.720	0.906	0.5907	D	13.83	0.06	0.21	141.62	14.25	75.00	86.79

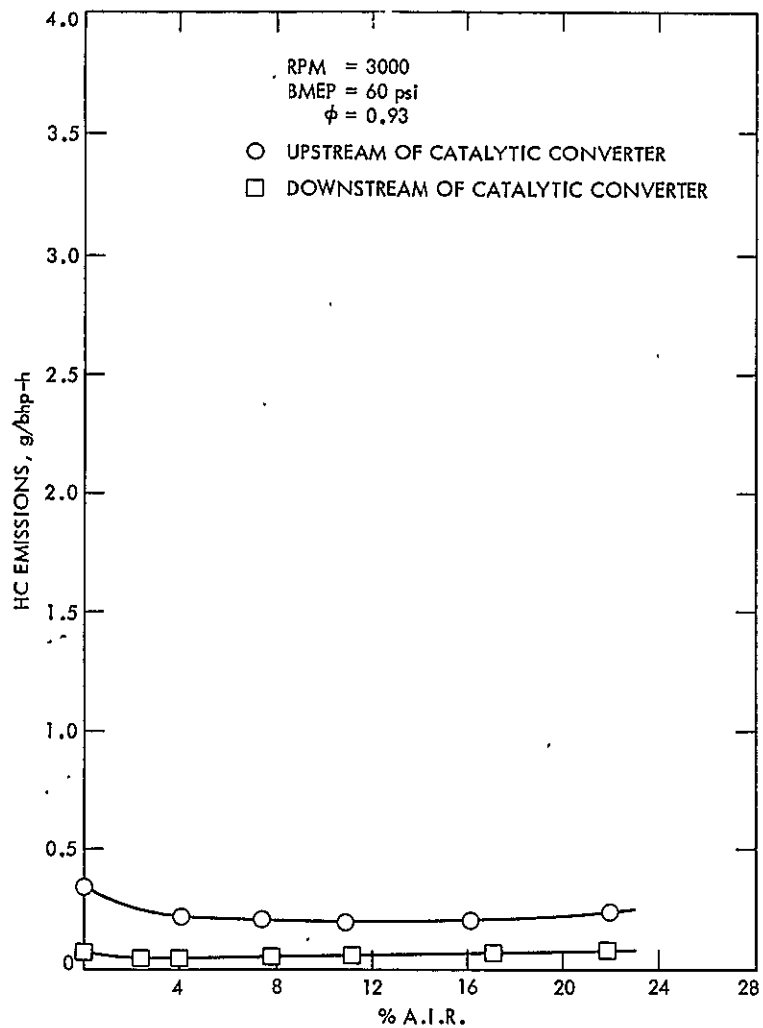*U = Upstream of catalytic converter; D = downstream of catalytic converter.

Figure F-15. HC Emissions for A.I.R. Sensitivity
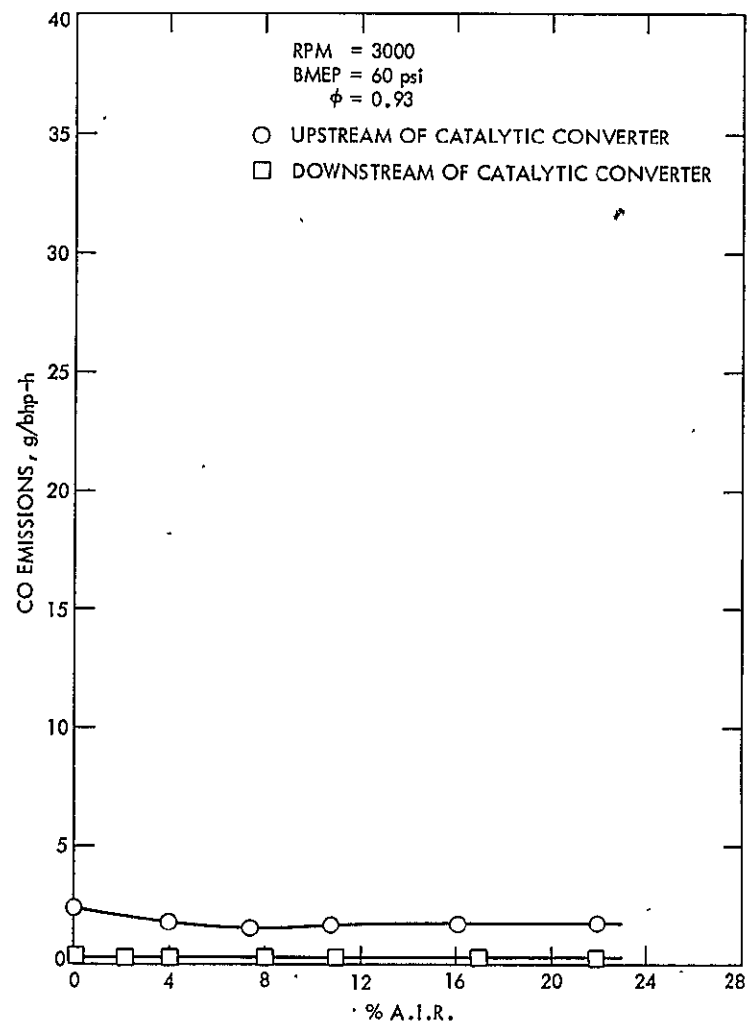Tests - RPM = 3000
BMEP = 60 psi
ϕ = 0.93

Figure F-16. CO Emissions for A.I.R. Sensitivity
Tests - RPM = 3000
BMEP = 60 psi
ϕ = 0.93